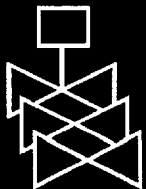
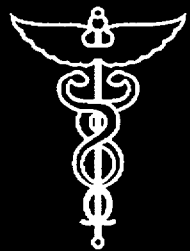
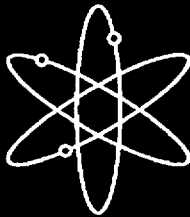


# Development of Technical Basis for Leak-Before-Break Evaluation Procedures

Battelle

U.S. Nuclear Regulatory Commission  
Office of Nuclear Regulatory Research  
Washington, DC 20555-0001



## AVAILABILITY OF REFERENCE MATERIALS IN NRC PUBLICATIONS

### NRC Reference Material

As of November 1999, you may electronically access NUREG-series publications and other NRC records at NRC's Public Electronic Reading Room at [www.nrc.gov/NRC/ADAMS/index.html](http://www.nrc.gov/NRC/ADAMS/index.html).

Publicly released records include, to name a few, NUREG-series publications; *Federal Register* notices; applicant, licensee, and vendor documents and correspondence; NRC correspondence and internal memoranda; bulletins and information notices; inspection and investigative reports; licensee event reports; and Commission papers and their attachments.

NRC publications in the NUREG series, NRC regulations, and *Title 10, Energy*, in the Code of *Federal Regulations* may also be purchased from one of these two sources.

1. The Superintendent of Documents  
U.S. Government Printing Office  
Mail Stop SSOP  
Washington, DC 20402-0001  
Internet: [bookstore.gpo.gov](http://bookstore.gpo.gov)  
Telephone: 202-512-1800  
Fax: 202-512-2250
2. The National Technical Information Service  
Springfield, VA 22161-0002  
[www.ntis.gov](http://www.ntis.gov)  
1-800-553-6847 or, locally, 703-605-6000

A single copy of each NRC draft report for comment is available free, to the extent of supply, upon written request as follows:

Address: Office of the Chief Information Officer,  
Reproduction and Distribution  
Services Section  
U.S. Nuclear Regulatory Commission  
Washington, DC 20555-0001

E-mail: [DISTRIBUTION@nrc.gov](mailto:DISTRIBUTION@nrc.gov)  
Facsimile: 301-415-2289

Some publications in the NUREG series that are posted at NRC's Web site address [www.nrc.gov/NRC/NUREGS/indexnum.html](http://www.nrc.gov/NRC/NUREGS/indexnum.html) are updated periodically and may differ from the last printed version. Although references to material found on a Web site bear the date the material was accessed, the material available on the date cited may subsequently be removed from the site.

### Non-NRC Reference Material

Documents available from public and special technical libraries include all open literature items, such as books, journal articles, and transactions, *Federal Register* notices, Federal and State legislation, and congressional reports. Such documents as theses, dissertations, foreign reports and translations, and non-NRC conference proceedings may be purchased from their sponsoring organization.

Copies of industry codes and standards used in a substantive manner in the NRC regulatory process are maintained at—

The NRC Technical Library  
Two White Flint North  
11545 Rockville Pike  
Rockville, MD 20852-2738

These standards are available in the library for reference use by the public. Codes and standards are usually copyrighted and may be purchased from the originating organization or, if they are American National Standards, from—

American National Standards Institute  
11 West 42<sup>nd</sup> Street  
New York, NY 10036-8002  
[www.ansi.org](http://www.ansi.org)  
212-642-4900

Legally binding regulatory requirements are stated only in laws; NRC regulations; licenses, including technical specifications; or orders, not in NUREG-series publications. The views expressed in contractor-prepared publications in this series are not necessarily those of the NRC.

The NUREG series comprises (1) technical and administrative reports and books prepared by the staff (NUREG-XXXX) or agency contractors (NUREG/CR-XXXX), (2) proceedings of conferences (NUREG/CP-XXXX), (3) reports resulting from international agreements (NUREG/IA-XXXX), (4) brochures (NUREG/BR-XXXX), and (5) compilations of legal decisions and orders of the Commission and Atomic and Safety Licensing Boards and of Directors' decisions under Section 2.206 of NRC's regulations (NUREG-0750).

**DISCLAIMER:** This report was prepared as an account of work sponsored by an agency of the U.S. Government. Neither the U.S. Government nor any agency thereof, nor any employee, makes any warranty, expressed or implied, or assumes any legal liability or responsibility for any third party's use, or the results of such use, of any information, apparatus, product, or process disclosed in this publication, or represents that its use by such third party would not infringe privately owned rights.

# Development of Technical Basis for Leak-Before-Break Evaluation Procedures

---

---

Manuscript Completed: October 2001

Date Published: May 2002

Prepared by

P. M. Scott<sup>1</sup>, R. J. Olson<sup>1</sup>

G. M. Wilkowski<sup>2</sup>

<sup>1</sup>Battelle

505 King Avenue

Columbus, OH 43201

Subcontractor:

<sup>2</sup>Engineering Mechanics Corporation of Columbus

3518 Riverside Drive

Suite 202

Columbus, OH 43221-1735

C. Santos, Jr., NRC Project Manager

Prepared for

Division of Engineering Technology

Office of Nuclear Regulatory Research

U.S. Nuclear Regulatory Commission

Washington, DC 20555-0001

NRC Job Code W6854



---

**NUREG/CR-6765, has been reproduced  
from the best available copy.**

---

## ABSTRACT

In the mid 1980's the USNRC began to accept LBB for large-diameter, high quality piping systems as a means of enhancing safety. To aide NRC staff in evaluating LBB submittals, a draft Standard Review Plan (SRP) entitled "Leak-Before-Break Evaluation Procedures" was published in 1987. Because of ongoing research, this draft SRP was never published in final form. Now that that research is nearly complete, the NRC has decided to develop and issue a LBB Regulatory Guide. A final version of SRP 3.6.3 will follow publication of the Regulatory Guide. These documents will address updated, acceptable LBB analyses. Consequently, in 1997 the NRC contracted with Battelle to conduct a study entitled "Technical

Support for Regulatory Guide on LBB Evaluation Procedures". During this study, a three-tiered approach to LBB was developed. Level 1 is the simplest level of assessment, designed to provide a conservative LBB evaluation. Level 2 is similar to the draft SRP procedures, except it incorporates enhancements in technology that have resulted from recent research. Level 3 is the most complex level of assessment, where nonlinear stress analyses are used to take advantage of margins that exist when one invokes elastic analysis on a nonlinear problem. Case studies of actual piping systems were conducted to ascertain the relative conservatism of the three levels of assessment.

# CONTENTS

	<i>Page</i>
Abstract.....	iii
Executive Summary.....	xv
Acknowledgments.....	xx
Nomenclature.....	xxi
Previous Reports in Series.....	xxvii
1 Introduction.....	1
2 Current Regulatory Requirements and Guidance Related to LBB.....	2
2.1 Regulations.....	2
2.2 Generic Issue A-2.....	2
2.3 Regulatory Guides.....	3
2.3.1 Regulatory Guide 1.45.....	3
2.4 Standard Review Plans.....	3
2.4.1 Draft SRP 3.6.2.....	4
2.4.2 Draft SRP 3.6.3.....	4
2.5 NUREG-1061 Volume 3.....	4
2.6 Industry Standards.....	5
2.7 Reference.....	5
3 Summary of Draft SRP 3.6.3 Procedures for Leak-Before-Break Evaluations.....	6
3.1 Applicability.....	6
3.2 Steps in an Acceptable SRP 3.6.3 LBB Analysis.....	7
3.2.1 Demonstrate Accuracy of Leak Rate and Fracture Mechanics Computational Methods.....	7
3.2.2 Identify Materials and Material Property Data.....	7
3.2.3 Specify Types and Magnitudes of Applied Loads.....	7

3.2.4	Postulate a Leaking Through-Wall Crack at the Critical Assessment Locations .....	7
3.2.5	Determine Critical Crack Size and Critical Crack Size Margin .....	8
3.2.6	Determine Applied Loads Margin .....	8
3.3	References.....	8
4	Lessons Learned from Reviews of Past LBB Applications.....	10
4.1	LBB Applications Purposes.....	10
4.2	Vendor LBB Methodology Examples .....	10
4.3	How Applications Evolved.....	10
4.4	Lines Typically Approved and Rejected for LBB .....	11
4.4.1	Lines Accepted for LBB in USNRC Applications .....	11
4.4.2	Lines Rejected for LBB in USNRC Applications .....	11
4.5	Material Property Aspects .....	11
4.5.1	Bimetallic Welds .....	12
4.5.2	Thermal Aging of Cast Stainless Steels.....	12
4.5.3	Thermal Aging of Stainless Steel Welds .....	13
4.5.4	HAZ or Fusion Line Toughness .....	14
4.5.5	Load-History Effects on Toughness .....	15
4.5.6	J-R Curve Limitations.....	16
4.5.7	Cracks at Nozzles .....	17
4.6	Leak-Rate Analysis Aspects.....	17
4.7	Fracture Mechanics Aspects .....	18
4.8	Stress and System Analysis Aspects.....	18
4.8.1	LBB Analysis Locations.....	18
4.8.2	Secondary Stresses.....	18
4.8.3	Torsional Stresses .....	21

4.9	References.....	21
5	Recent Research Results (1985 – 2001) .....	23
5.1	State-of-the-Art in Pipe Fracture Technology, Circa 1985.....	23
5.2	Summary of Major Research Programs Related to LBB .....	25
5.2.1	Battelle Programs.....	25
5.2.1.1	Battelle/EPRI Program on Circumferentially Cracked Stainless Steel Pipe.....	25
5.2.1.2	Battelle/EPRI Study on Two-Phase Flow Through IGSCC .....	25
5.2.1.3	Degraded Piping Program (Phases I and II: 1981 – 1989) .....	25
5.2.1.4	International Piping Integrity Research Group (IPIRG) programs .....	26
	(First and Second: 1986 – 1997)	
5.2.1.5	Short Cracks in Piping and Piping Welds Program (1990 – 1994) .....	27
5.2.1.6	Battelle Integrity of Nuclear Piping (BINP) Program .....	27
5.2.2	Research Programs Conducted at Argonne National Laboratories .....	27
5.2.2.1	Corrosion Fatigue .....	28
5.2.2.2	Thermal Aging Cast Stainless Steels .....	28
5.2.3	Foreign Programs.....	28
5.2.3.1	Japan .....	28
5.2.3.2	France .....	30
5.2.3.3	United Kingdom .....	30
5.2.3.4	Germany.....	30
5.2.4	Leak-Before-Break Conferences .....	31
5.3	Key Results from Recent Research Applicable to Leak-Before-Break.....	31
5.3.1	Leak-Rate Analysis.....	31
5.3.1.1	Leak-Rate Codes.....	31
5.3.1.2	Factors Influencing the Leakage Crack Size Predictions.....	32
5.3.1.3	Comparison of Postulated Leakage Crack Sizes for Various Leak-Rate.....	44
	Analysis Codes	

5.3.2 Subcritical Crack Growth Analysis .....	47
5.3.3 Material Issues .....	48
5.3.3.1 Source of Data .....	48
5.3.3.2 Cyclic Effects on Toughness .....	48
5.3.3.3 Dynamic Strain Aging Effects on Material Properties .....	52
5.3.3.4 Cracks in Welds .....	55
5.3.3.5 Thermal Aging Mechanisms.....	65
5.3.3.6 Fracture Toughness Properties of Stainless Steels with High Sulfur Contents .....	67
5.3.3.7 Effect of Toughness Anisotropy on LBB .....	69
5.3.3.8 J-Resistance Curve Extrapolation Techniques.....	71
5.3.3.9 Flow Stress Definitions.....	71
5.3.4 Stress Analysis.....	71
5.3.4.1 Additional Margins from Nonlinear Analysis .....	71
5.3.4.2 Effect on Secondary Stresses on Pipe Fracture.....	72
5.3.4.3 Effect of Torsional Stresses .....	74
5.3.5 Fracture/Stability Analyses.....	75
5.3.5.1 Limit-Load Analyses .....	75
5.3.5.2 Modified Limit-Load Analyses .....	75
5.3.5.3 Elastic-Plastic Fracture Mechanics (EPFM) Analyses .....	76
5.3.5.4 Stability Issues .....	82
5.3.5.5 Comparisons of Analysis Methodologies with Full-Scale..... Experimental Data and Finite Element Analyses Results	83
5.3.6 Probabilistic (Risk Informed) Analyses.....	83
5.4 References.....	89
6 Proposed Tiered Approach to LBB .....	93
6.1 General Screening Criteria for Proposed Tiered Approach to LBB .....	93

6.2	Extent of Assessment.....	93
6.3	Definition of Margins and Partial Safety Factors .....	94
6.4	Data Requirements.....	94
6.5	Subcritical Crack Growth Analysis .....	94
6.6	Level 1 Approach .....	95
6.7	Level 2 Approach .....	96
6.8	Level 3 Approach .....	97
6.9	Acceptance Criteria .....	97
6.10	References.....	98
7	Foreign Experience .....	99
7.1	France .....	99
7.2	Germany .....	100
7.3	Japan .....	102
7.3.1	Assumed Initial Surface Flaw.....	102
7.3.2	Applicable Damage Mechanisms Considered .....	104
7.3.3	Loads Used in Evaluation.....	104
7.3.4	Material Issues .....	104
7.3.5	Crack-Opening-Area and Leak-Rate Analyses.....	105
7.4	Republic of Korea.....	106
7.4.1	Dynamic Fracture Toughness Tests.....	106
7.4.2	Thermal Stratification Considerations .....	106
7.4.3	Thermal Striping in the Pressurizer Surge Line.....	106
7.4.4	Water/Steam Hammer in the Main Steam Line.....	106
7.4.5	Nozzle/Pipe Interface Considerations.....	107
7.4.6	Leak-Rate Detection Limit Capability.....	107

7.5	Russia.....	107
7.6	United Kingdom .....	108
7.6.1	Detectable Leakage Approach.....	108
7.6.2	Full Leak-Before-Break Approach.....	108
7.6.3	Crack Opening Area Analyses.....	109
7.6.4	Leak-Rate Calculations.....	110
7.7	Canada .....	110
7.8	Sweden.....	112
7.9	References.....	112
8	Summary and Conclusions .....	114
8.1	Summary of Level 1 Approach to LBB.....	114
8.2	Summary of Level 2 Approach to LBB.....	115
8.3	Summary of Level 3 Approach to LBB.....	116
8.4	Safety Factors to be Used in the Tiered Approach to LBB .....	117
8.5	References.....	117

### Appendices

Appendix A	Level 1 LBB Procedures .....	A-1
Appendix B	Level 2 LBB Procedures .....	B-1
Appendix C	Level 3 LBB Procedures .....	C-1
Appendix D	Evaluation of the Tiered Approach to LBB .....	D-1
Appendix E	The Development of a J-estimation Scheme for Circumferential and Axial..... Through-wall Cracked Elbows	E-1

### Figures

Figure 4.1	J-resistance curves of fusion-line specimens.....	14
Figure 4.2	Moment-rotation response for Experiment 1-1 from the Second IPIRG program.....	16

Figure 4.3 Moment-CMOD response for the BINP Task 2 experiment.....	16
Figure 4.4 Bar chart showing the effect of the different stress components on the fracture behavior ..... of the IPIRG-1 pipe-system experiments	20
Figure 5.1 Example J-R curve showing constant slope $dJ/da$ used in Tearing Modulus (T)..... determination	24
Figure 5.2 STA pipe system for dynamic flawed pipe tests .....	29
Figure 5.3 R6 failure assessment diagram (FAD) .....	30
Figure 5.4 Local and global surface roughness and number of turns .....	33
Figure 5.5 Crack morphology variables versus normalized COD .....	34
Figure 5.6 Photograph of fracture from aged cast stainless experiment (Experiment 1.3-7) .....	36
Figure 5.7 Net-Section-Collapse analyses predications, with and without considering induced ..... bending, as a function of the ratio of the through-wall crack length to pipe circumference	36
Figure 5.8 Normalized COD versus restraint length for two different sets of FE analyses.....	38
Figure 5.9 Calculated maximum loads for LBB, with and without restraint of the pressure-induced ..... bending, from the pipe system	39
Figure 5.10 Ratio of leak rates, with and without residual stresses, as a function of applied load.....	41
Figure 5.11 Calculated off-centered crack length for a 3.8 lpm (1 gpm) leak rate versus the angle ..... from the center of the off-centered crack to the bending plane	43
Figure 5.12 Comparison of maximum loads for 3.8 lpm (1 gpm) leaking cracks that were off-centered. .... during leakage but centered during the N+SSE loading versus the angle from the center of the off-centered crack to the bending plane	44
Figure 5.13 Moment versus rotation showing the effect of cyclic loading ( $R=0$ and $R=-1$ ) on stainless . .... steel through-wall-cracked pipe experiments at quasi-static loading rates	49
Figure 5.14 Moment versus rotation showing the effect of cyclic loading ( $R=0$ and $R=-1$ ) on carbon .... steel through-wall-cracked pipe experiments at quasi-static loading rates	50
Figure 5.15 Schematic of relationship between cyclic toughness degradation and stress ratio and ..... initial material toughness	50
Figure 5.16 Measured load versus load-line displacement for quasi-static, $R=0$ loading experiment .....	51
Figure 5.17 Crack-tip-opening angle data from IPIRG-1 Subtask 1.2 stainless steel through-wall-..... cracked pipe experiments (Reference 5.44)	51
Figure 5.18 Tensile properties at 288 C (550 F) versus strain rate for 16-inch diameter carbon steel..... pipe tested as part of IPIRG program	53

Figure 5.19 J-resistance curves for compact (tension) specimens tested at both quasi-static and dynamic loading rates at 288 C (550 F) for 16-inch diameter carbon steel pipe tested as part of the IPIRG program	54
Figure 5.20 J-resistance curves for compact (tension) specimens tested at both quasi-static and dynamic loading rates at 288 C (550 F) for carbon steel submerge-arc weld tested as part of the IPIRG program	54
Figure 5.21 Load-displacement record from a 28-inch diameter through-wall-cracked carbon steel pipe experiment illustrating the drops in load indicative of crack instabilities	55
Figure 5.22 Yield strength, ultimate strength, and Brinell hardness as a function of test temperature for five carbon steel pipe materials	57
Figure 5.23 J-resistance curves for carbon steel SAW and parent base metal material	58
Figure 5.24 J-resistance curves at 288 C (550 F) for stainless steel SAW and parent base metal material (Type 316) from Nine Mile Point plant	58
Figure 5.25 J-values at 1 mm and 2 mm (0.04 and 0.08 inch) of crack extension for bimetallic welds made with a stainless steel weld procedure	60
Figure 5.26 Crack propagation in stainless steel base metal, in the HAZ remote from fusion line, along the fusion line, and in the weld metal in SEN(T) specimens at 288 C (550 F)	64
Figure 5.27 Crack propagation along fusion line of a TP316 SAW in a 28-inch diameter pipe experiment even though initial starter notch was centered in the weld and the weld crown was ground off	64
Figure 5.28 Weld metal and fusion line J-R curve data for stainless steel SAW	65
Figure 5.29 J-resistance curves for two heats of pipe material A8 (A8I and A8II)	67
Figure 5.30 J-R curves for 7 heats of stainless steel extracted from PIFRAC showing the effect of sulfur content on the fracture resistance for wrought stainless steels	68
Figure 5.31 Predicated maximum moment normalized by the Net-Section Collapse moment as a function of sulfur content for the 7 heats of stainless steel extracted from the PIFRAC database	69
Figure 5.32 Photograph of the fractured pipe from Experiment 4111-1 from the Degraded Piping Program and a compact (tension) specimen from this same material	70
Figure 5.33 J-resistance curves for several different C(T) specimen orientations in Pipe DP2-F11 that was used in Experiment 4111-1 in the Degraded Piping Program	70
Figure 5.34 Comparison of the results from the IPIRG-1 pipe-system experiments with companion quasi-static, four-point bend experiments demonstrating how global secondary stresses, such as thermal expansion and seismic anchor motion stresses, contribute to fracture	73

Figure 5.35 Comparison of moment-time plots for IPIRG-1 Experiment 1.3-5 and BINP Task 2 experiment	74
Figure 5.36 Compiled data using simplified dimensionless-plastic-zone parameter and flow stress equal to average of yield and ultimate	77
Figure 5.37 Results of COD sensitivity study for 4.5-inch diameter TP304 stainless steel pipe with a 16-percent long circumferential TWC	78
Figure 5.38 Paris/Tada solutions from NRCPIPE for TP304 stainless steel pipes	79
Figure 5.39 Original GE/EPRI COD solutions for TP304 stainless steel pipe from the NRCPIPE code	79
Figure 5.40 Original GE/EPRI COD solutions from the NRCPIPE code for A516 Grade 70 pipe	80
Figure 5.41 Ovalization modes for through-wall cracks in elbows subjected to opening and closing bending moments	82
Figure 5.42 Comparison of SQUIRT predicted leak rate with experimental data obtained for a fatigue generated crack in a carbon steel girth weld loaded in 4-point bending	84
Figure 7.1 Flow diagram for German LBB analysis	103

### Tables

Table 5.1 Average surface roughness values from statistical analysis of fracture surfaces from NUREG/CR-6004	33
Table 5.2 Average number of 90-degree turns per inch of flow path (Ref. 5.23)	34
Table 5.3 Average values for global path deviation factor ( $K_G$ ) and local waviness path deviation factor ( $K_{G+L}$ )	35
Table 5.4 Differences in leakage flow sizes due to restraint of pressure-induced bending	38
Table 5.5 Comparison of total crack length at 38 lpm (10 gpm) using the 0.0076 mm (300-microinch) roughness and no turns as assumed by the applicant	45
Table 5.6 Crack morphology parameters relative to this LBB analysis	45
Table 5.7 LBB leakage flow sizes using Tada/Paris COD analysis	46
Table 5.8 LBB leakage flow sizes using Tada/Paris analysis and SQUIRT2 with different crack morphology parameters	46
Table 5.9 LBB leakage flow sizes using Tada/Paris COD analysis and applicants leak-rate code versus SQUIRT4 with NUREG/CR-6004 crack-morphology parameters	47
Table 5.10 Comparison of margins on crack length at 38 lpm (10 gpm) using Tada/Paris COD analysis and applicant's leak-rate code versus SQUIRT4 with NUREG/CR-6004 crack-	48

morphology parameters

Table 5.11 Mean values of maximum load ratios (experimental maximum load divided by predicated .. 78  
maximum load) for TWC pipe experiments

Table 5.12 Comparison of general deterministic analyses in probabilistic approaches and Level 2..... 86  
analysis procedures in this report

Table 5.13 Comparison of leakage-size crack deterministic analyses in probabilistic approaches and .... 87  
Level 2 analysis procedures in this report

Table 5.14 Comparison of leakage-size crack deterministic analyses in probabilistic approaches and .... 88  
Level 2 analysis procedures in this report

Table 6.1 Typical data requirements needed for the three levels of the proposed tiered approach to ..... 95  
LBB

## EXECUTIVE SUMMARY

In the mid 1980's the NRC began to accept the concept of leak-before-break (LBB) for large-diameter, high-quality piping systems as a means of enhancing the safety of nuclear power plants. The LBB concept permits removal, or non-installation, of many of the pipe-whip-restraint devices and jet-impingement shields originally designed to mitigate the dynamic effects of a postulated instantaneous pipe rupture. Furthermore, LBB enhances overall plant safety through increased knowledge of pipe loads and material data, and the increased access to critical systems for in-service inspection and monitoring.

As an aid to the NRC staff's review and evaluation of LBB submittals, a draft Standard Review Plan (SRP) 3.6.3 entitled "Leak-Before-Break Evaluation Procedures," was published in 1987. However, because of ongoing research in the area of piping integrity, and the expected conservatism associated with such LBB applications, the draft SRP was not to be published in final form until the ongoing research could be completed. Now that that research is coming to a close, and most of the outstanding technical issues have been addressed, the NRC has determined that action could be taken to update the draft SRP on LBB and to provide the technical basis for developing a Regulatory Guide on LBB for piping in operating plants (specifically PWRs) and possibly some of the advanced reactor designs. As a result, in late 1997, the NRC contracted with Battelle<sup>1</sup> to conduct a study entitled "Technical Support for Regulatory Guide on Leak-Before-Break (LBB) Evaluation Procedures". This report, which summarizes the key findings from this work, is broken down into eight sections, with five supporting appendices.

---

<sup>1</sup> Also eventually, Engineering Mechanics Corporation of Columbus (Emc<sup>2</sup>) as a subcontractor to Battelle.

**Section 1** of this report is the Introduction that provides some of the historical perspective behind the LBB approach.

**Section 2** provides a summary of current regulatory requirements and guidance related to LBB. Some of the pertinent Regulations, Generic Issues, Regulatory Guides, Standard Review Plans, and Industry Standards related to LBB are discussed.

The key regulation related to LBB is General Design Criterion-4 (GDC-4), "Environmental and Dynamic Effects Design Bases" in Appendix A of Part 50 of Title 10 of the Code of Federal Regulations (i.e., 10 CFR 50). Of particular interest to the subject of LBB is the stipulation in GDC-4 that allows the use of "analyses reviewed and approved by the Commission" to eliminate from the design basis the dynamic effects of pipe ruptures. The means of implementing this stipulation are applicable Regulatory Guides and Standard Review Plans.

Regulatory Guides provide guidance to licensees and applicants on implementing specific parts of the NRC's regulations, techniques used by the staff in evaluating specific problems or postulated accidents, and data needed by the staff in its review of applications for permits or licenses. A key Reg. Guide related to LBB is Regulatory Guide 1.45 – Reactor Coolant Pressure Boundary Leakage Detection Systems.

Standard Review Plans, on the other hand, are prepared for the guidance of the Office of Nuclear Reactor Regulation (NRR) staff responsible for the review of applications to construct and operate nuclear power plants. SRPs are not substitutes for Regulatory Guides or the Commission's regulations, and compliance with them is not mandatory. Two key Standard Review Plans related to LBB are:

- SRP 3.6.2 – Determination of Rupture Locations and Dynamic Effects Associated with the Postulated Rupture of Piping, and

- Draft SRP 3.6.3 – Leak-Before-Break Evaluation Procedures.

**Section 3** summarizes the existing draft SRP 3.6.3 on LBB. Both its applicability and the steps involved in applying an acceptable draft 3.6.3 LBB analysis are discussed. With regards to its applicability, draft SRP 3.6.3 is generally applicable to Class 1 and 2<sup>2</sup> piping systems with a few notable exceptions, e.g., it cannot be applied to discrete locations or individual welded joints, it cannot be applied to piping systems susceptible to stress corrosion cracking<sup>3</sup>, fatigue, creep damage, water hammer, or piping systems for which brittle fracture is a possibility. The concept being to eliminate cases where long surface cracks or unusually high (and unknown) stresses could occur. The steps involved in an acceptable draft SRP 3.6.3 analysis include:

- demonstrating the accuracy of the leak rate and fracture mechanics computational methods,
- identifying the pertinent materials and material property data to use,
- specifying the types and magnitudes of the applied loads (normal operating and transient),
- estimating the size of a readily detectable postulated leaking through-wall crack at the critical assessment locations,
- determining the critical crack size at the transient load condition and establishing the critical crack size margin, and
- determining the applied loads margin.

<sup>2</sup> Generally LBB is only applicable to Class 1 piping, but there has been some rare occasions where it has been applied to Class 2 piping, e.g., LBB was applied to the CE System 80+ steam lines inside containment.

<sup>3</sup> Stress corrosion cracking includes IGSCC that occurs in BWRs as well as the recent occurrence of PWSCC in Inconel 82/182 bimetallic welds in PWRs. No BWRs have been approved for LBB, and as of 2001 any new application for LBB for a PWR with an Inconel 82/182 bimetal weld is not being approved until there is a clearer understanding of PWSCC.

**Section 4** summarizes the lessons learned from the reviews of the past LBB applications. As part of this program, the NRC provided Battelle and its subcontractor, Engineering Mechanics Corporation of Columbus (Emc<sup>2</sup>), copies of the past LBB submittals. These applications were reviewed and a database compiled documenting the pertinent details of each application. A key outcome of this review process was an understanding of:

- the details of the specific approaches followed by the applicants;
- what piping systems had been approved and what piping systems had been rejected for LBB, and why those lines were rejected;
- how the applicants handled key material property issues, such as bimetallic welds, thermal aging of cast stainless steels, fusion line toughness concerns, load history effects on toughness, and J-R curve limitations;
- the details of the leak-rate analyses used in estimating the size of the postulated leaking through-wall crack;
- the details of the fracture analyses used to estimate the critical crack size for the transient load conditions and the crack stability of the postulated leakage size crack (with safety factor); and
- the details of the system and stress analysis, specifically how the locations for analysis were established, how secondary stresses were handled, and how torsional stresses were handled.

**Section 5**, which is the largest of the sections, summarizes some of the pertinent research that has been conducted since the initial publication of the draft SRP 3.6.3. This section begins with a discussion of the state-of-the-art of pipe fracture technology and leak-rate analyses at the time of the initial publication of the draft SRP 3.6.3 (mid 1980's). Next, the major research programs conducted since that time (e.g., the Degraded Piping program, the Short Cracks in Piping and Piping Welds program, the International Piping Integrity Research Group [IPIRG] programs, and the Battelle Integrity of Nuclear Piping (BINP) program) are discussed. Finally, the key results from these programs

pertinent to LBB are discussed. Research topics addressed in this discussion include the following:

**Leak-rate analyses** – Included here are discussions on some of the various leak-rate codes (e.g., PICEP and SQUIRT) as well as a discussion on factors that may influence the postulated leakage crack size analysis. These factors include: (1) the selection of the proper crack morphology parameters<sup>4</sup>, (2) the effect of the restraint of pressure-induced bending on the predicted crack-opening-displacements (COD)<sup>5</sup>, (3) the effect of weld residual stresses on the predicted COD, (4) the impact of the postulated leaking crack being oriented such that it is not coincident with the maximum bending plane for the transient load condition, and (5) the effect of other uncertainty issues on LBB, such as particulate plugging.

**Material issues** – Some of the key materials related research topics discussed at this point include:

- o cyclic load effects on material toughness,
- o dynamic strain aging effects on the strength and toughness of ferritic steels at light water reactor (LWR) temperatures,
- o cracks in welds, including bimetallic welds<sup>6</sup> and weld fusion line toughness concerns,

---

<sup>4</sup> As part of this program, a sensitivity study was conducted to compare the various leak-rate codes often used in an LBB assessment. It was concluded that the statistically determined crack morphology parameters in NUREG/CR-6004 should be used in the leak-rate analysis to estimate the size of the postulated leaking through-wall crack.

<sup>5</sup> The topics of the effects of restraint of pressure-induced bending and weld residual stresses on the COD predictions were addressed as part of the Battelle Integrity of Nuclear Piping (BINP) program.

<sup>6</sup> Bimetallic welds (82/182 weld materials) received recent attention due to the cracking experienced in a bimetallic weld joining the hot leg to the "A" reactor pressure vessel (RPV) nozzle at the Virgil C. Summer nuclear power plant. This primary water stress corrosion

- o thermal aging of cast stainless steels and stainless steel welds<sup>7</sup>,
- o toughness degradation of wrought stainless steels with high sulfur contents<sup>8</sup>,
- o anisotropy effects on the fracture toughness of ferritic piping and the impact such effects may have on piping systems subjected to torsional as well as bending stresses, and
- o J-R curve extrapolation techniques necessary for predicting large amounts of crack growth from small-scale specimens.

**Stress analysis issues** – Discussion topics here included (1) the additional margins one might realize in an LBB assessment by invoking a

---

cracking (PWSCC) phenomenon of Alloy 82/182 weld material in large-diameter primary piping systems is a potential concern from an LBB perspective since prior LBB evaluations assumed those systems to be free from any significant active degradation mechanism.

<sup>7</sup> Significant research has been conducted over the last 15 years on the subject of thermal aging of cast stainless steels. However, less is known about aging of stainless steel welds. Like cast stainless steels, these welds are duplex structures, and as such may be susceptible to aging-type phenomenon. As part of the reviews of the actual LBB submittals, it was found that one applicant did report a substantial reduction in fracture toughness (due to such an aging process) of one weld that had a relatively low toughness in the un-aged condition.

<sup>8</sup> As part of this program, a sensitivity study was conducted to examine the effect of sulfur content on the fracture toughness, and ultimately the load-carrying capacity, of cracked wrought stainless steel piping. It was found that sulfur content does have an impact on the fracture toughness of wrought stainless steel. The J-R curves for the high-sulfur wrought stainless steels ( $S > 0.015\%$ ) were about half the J-R curves for the low-sulfur wrought stainless steels ( $S < 0.015\%$ ). However, since the toughness values of the high-sulfur wrought stainless steels were sufficient that limit-load conditions still prevailed, the impact on load-carrying capacity was only about 15 to 20 percent, which was considered to be a second order effect in the overall evaluation.

nonlinear stress analysis, (2) the contribution secondary stresses make to pipe fracture, and (3) the potential impact of torsional stresses in an LBB assessment. For a PWR surge line, an analysis was conducted as part of this program that demonstrated that one might achieve an additional 20 to 30 percent in margin by incorporating nonlinear behavior into the piping system analysis and/or incorporating nonlinear crack behavior into the piping system model. This 20 to 30 percent additional margin might be all that is needed to demonstrate LBB for piping systems that are marginal from an LBB perspective when using a more traditional linear stress analysis.

**Fracture/stability analyses** – When the draft SRP 3.6.3 on LBB was first published, state-of-the-art pipe fracture analyses consisted of: (1) limit-load analyses for high toughness and/or small diameter pipe, or (2) either a modified limit-load analysis, using a Z-factor approach, or a very limited number of elastic-plastic fracture mechanics (EPFM) J-estimation schemes (e.g., Paris/Tada and GE/EPRI) for those piping systems for which limit-load conditions did not exist. For crack stability analyses, the tearing instability J/T approach was most often used. Since that time, considerable resources have been expended in developing, improving, expanding the realm of application, and validating new EPFM analysis methods with full-scale pipe tests and more detailed numerical solutions.

For LBB analyses, these J-estimation schemes are appropriate not only for estimating the critical crack size or crack stability under the transient load condition, but also for predicting the crack-opening-displacements (COD) under the normal operating loads needed for estimating the postulated leakage crack sizes. As part of this program, another sensitivity study was undertaken to examine the validity and conservatism of some of these J-estimation scheme based COD predictions by comparing their results with finite element analyses. From this assessment it was found that the Paris/Tada COD predictions were conservative, and in some situations excessively conservative, from an LBB perspective with respect to finite element

analyses. The original GE/EPRI COD predictions were more in agreement with the finite element results at the load levels more representative of normal operating conditions. Thus, it was concluded that one should use the original GE/EPRI COD methodology with the statistically determined crack morphology parameters recommended in NUREG/CR-6004 for determining the COD.

As part of the Battelle Integrity of Nuclear Piping (BINP) program, a new J-estimation scheme for through-wall cracks in elbows was developed in support of this program. The J-estimation scheme solutions developed were for both axially and circumferentially oriented through-wall cracks in elbows subjected to pure pressure, pure bending, and combined pressure and bending loading conditions.

**Probabilistic issues** – An option considered early in the development of the proposed LBB Regulatory Guide was to allow for the use of probabilistic analyses. Although a probabilistic approach was not included in this document, three existing probabilistic analyses were reviewed and the deterministic models in these three approaches were compared with the proposed Level 2 deterministic option for LBB proposed in this report. The three probabilistic approaches considered were the:

- pcPRAISE code,
- Westinghouse Structural Reliability and Risk Assessment (SRRA) code, and
- probabilistic codes in NUREG/CR-6004 (PSQUIRT and PROLBB).

**Chapter 6** presents the proposed three-tiered approach to LBB that was developed as part of this program. The simplest level of assessment is Level 1. Level 1 was designed to provide a conservative assessment of LBB acceptability, and yet be of sufficient accuracy that piping systems that readily passed the existing draft SRP 3.6.3 criteria (e.g., main coolant loop piping) can still pass this Level 1 criteria. The Level 1 criteria do not require the use of detailed leak-rate computer codes or fracture mechanics codes. Instead, Level 1 relies on a series of simple, empirically-derived algebraic

expressions or closed-form solutions from which one can estimate the postulated leaking crack size. Furthermore, instead of using one of the more sophisticated J-estimation schemes to calculate the critical crack size for the transient load conditions, the Level 1 fracture analysis will incorporate simple ASME Section XI modified (i.e., Z-Factor) limit-load type analysis.

Due to the simplicity of the analysis methods, there is Level 1 specific screening criteria to preclude using Level 1 in the following cases;

- (a) very tight cracks where the ratio of the COD to the surface roughness is less than approximately 2.5,
- (b) where the thermodynamic conditions of the water are not subcooled,
- (c) when the calculated postulated leakage crack length is greater than an eighth of the pipe circumference, and
- (d) where “thin-walled” pipe welds have not been stress relieved. The definition of “thin-wall” and “thick-wall” welds will be made as part of the BINP program.

The next level of complexity for LBB assessment will be the Level 2 methodology. The Level 2 methodology is similar in scope to the existing draft SRP 3.6.3 methodology except it incorporates enhancements in the technology that have resulted from the recent research. It is envisioned that this level of assessment would be used in the majority of future LBB applications. Enhancements in the technology that were considered in the development of this level of analysis were:

- o use of the best leak-rate code with appropriate crack morphology variables,
- o use of the most accurate fracture mechanics analyses,
- o accounting for the most recent developments in material property assessments, and
- o accounting for the effects of weld residual stresses and restraint of pressure-induced

bending on the COD for the postulated leakage crack size analysis.

The final level of analysis is the Level 3 methodology. The Level 3 methodology is the most complex of the three levels, requiring the greatest amount of information/data for its application. This level of analyses will be a very detailed deterministic analysis, involving nonlinear stress analysis, possibly incorporating a nonlinear spring representation of the crack. The nonlinear stress analyses will be used to take advantage of the inherent margins that exist when one invokes an elastic analysis on a nonlinear problem. This level of LBB assessment is expected to be used for those cases where LBB cannot be demonstrated using the simpler Level 1 or 2 methods.

**Chapter 7** summarizes the experience other countries have had in the area of LBB.

**Chapter 8** presents the conclusions drawn as a result of this effort. The key outcome of this program was the development of the proposed three-tiered approach to LBB, which we envision will form the basis for the development of a future NRC Regulatory Guide for LBB. In this section, the tiered approach was summarized along with a summary of some of the key conclusions supporting the development of this approach. The focus of this section is to synthesize the results and conclusions drawn as part of this program so that the reader has a clearer understanding of how this tiered approach is envisioned to be implemented and how it is an improvement over the existing draft SRP 3.6.3 approach.

**Appendices A, B, and C** present the details of the three levels of the proposed tiered approach to LBB while **Appendix D** presents an evaluation of this tiered approach. **Appendix E** documents the development of a J-estimation scheme for circumferential and axial through-wall-cracked elbows.

## ACKNOWLEDGMENTS

This work was supported by the United States Nuclear Regulatory Commission through the Materials Engineering Branch, Division of Engineering Technology of the Office of Nuclear Regulatory Research under Contract No. NRC-04-98-039. Ms. Louise Lund, Mr. Tanny Santos, and Mr. Chuck Hsu have been the NRC program managers throughout the course of this program.

We would also like to thank Mr. Keith Wickman and Mr. Matt Mitchell of the Office of Nuclear Reactor Regulation for their comments and directions during the course of this program.

We would also like to thank others at Battelle and Engineering Mechanics Corporation of Columbus. At Battelle we would like to thank

Dr. Fredrick (Bud) Brust for his efforts in developing the J-estimation scheme for through-wall cracks in elbows and Dr. Lee Fredette for his efforts in developing a correction factor for crack-opening displacement predictions for cracks subjected to weld residual stresses. At Engineering Mechanics Corporation, we would like to thank Mr. David Rudland for his assistance in performing a number of the Level 2 LBB calculations and Dr. Zhili Feng for his efforts in developing a correction factor to account for the effects of restraint of pressure induced bending on the crack-opening displacement predictions. Finally, we would like to thank Ms. Tracey Thomas, Ms. Nancy Schoen and Ms. Kelly VanDenBerge for their invaluable assistance in preparing this report.

# NOMENCLATURE

## 1. SYMBOLS

a	Crack size parameter
A	Leakage area
$a_f$	Final flaw depth
$a_i$	Initial flaw depth
$A_L$	Crack opening area for the detectable through-wall crack
$A_{TWC}$	Crack opening area of an elliptical through-wall crack
$B_2$	Stress index from ASME Section III
c	Half crack length
C	Empirically derived constant in DPZP analysis
C	Experimentally derived fatigue crack growth rate constant
$c_{crit}$	Half length of critical crack
$C_D$	Entrance loss coefficient
$c_{det}$	Half detectable flow length corresponding to detectable leak rate
$c_f$	Final half flaw length
$c_i$	Initial half flaw length
$c_L$	Half leakage crack from French A16 leakage crack size analysis
$c_{Leak}$	Half length of leakage size crack
$c_{LDS}$	Half length of detectable crack
$c_s$	Half length of a surface crack
$COD_{base}$	COD without accounting for weld residual stress effects
$COD_{cf}$	COD corrected for crack face pressure
$COD_{Residual}$	COD accounting for weld residual stress effects
$COD_{Restrained}$	Restrained axial tension component of COD
$COD_{Unrestrained}$	Unrestrained COD value
$COD_{wo}$	COD without accounting for crack face pressure
D	Diameter
$D_H$	Hydraulic diameter
E	Elastic modulus
$f_1$	Elastic F-function
$F_B$	Elastic F-function due to bending
$F_T$	Elastic F-function due to tension
$F_x$	Axial load on the pipe
FR	Flow rate per unit area
$FR_{Baseline}$	Baseline flow rate per unit area used in a Level 1 analysis
h	An elbow parameter ( $R_{ejt}/R_m^2$ )
$h_1$	Function in GE/EPRI method
$h_2$	Function in GE/EPRI method
$I_T$	Tensile compliance influence function
J	J-integral fracture parameter
$J_{AVG}$	Average J through the thickness from a finite element analysis
$J_D$	Deformation J
$J_e$	Elastic component of J
$J_i$	J at crack initiation
$J_I$	J at inside surface (node) in a finite element analysis
$J_{Ic}$	Plane strain J at crack initiation by ASTM813

$J_m$	Modified J
$J_M$	J at the mid surface (node) in a finite element analysis
$J_{\text{material}}$	J of the material
$J_O$	J at the outside surface (node) in a finite element analysis
$J_p$	Plastic component of J
$J_{\text{QS, cyc}}$	J for quasi-static, cyclic loading
$J_{\text{QS, mono}}$	J for quasi-static, monotonic loading
J-R	J-resistance
J/T	J/Tearing instability method
k	Fitted material constant
K	Stress intensity factor
$K_B$	Bending component of the stress intensity factor
$K_T$	Tension component of the stress intensity factor
$K_G$	Correction factor for global path deviation
$K_{G+L}$	Correction factor for global plus local path deviation
$K_I$	Mode I stress intensity factor
$K_{\text{max}}$	Maximum stress intensity factor
$K_{\text{min}}$	Minimum stress intensity factor
L	Restraint length
$L_1, L_2$	Restraint lengths on either side of crack
LR	Leak rate detection limit
m	Experimentally derived fatigue crack growth rate constant
M	Moment
M	Margin associated with load combination method
$M_b$	Bending moment
$M_{\text{EQ}}$	Equivalent moment
$M_{\text{Max}}$	Maximum moment
$M_{\text{NSC}}$	Net-Section-Collapse moment
$M_0$	Limit moment
$M_x$	Bending moment about x-axis
$M_y$	Bending moment about y-axis
n	Strain hardening exponent
N	Normal operating stress
$n_t$	Number of turns
$n_{tL}$	Local number of turns
p	Pressure
P	Applied load
$P_b$	Bending stress
$P_{cf}$	Pressure acting on the crack faces
$P_{\text{DPZP}}$	Predicted stress based on DPZP analysis
$P_e$	Thermal expansion stress
$P_f$	Pipe system pressure influence function in Level 1 analysis
$P_m$	Membrane stress
$P_{\text{NSC}}$	Net-Section-Collapse stress
$P_0$	Limit load
$Q_{\text{det}}$	Detectable leak rate
$Q_{\text{min}}$	Minimum detectable leak rate
R	Pipe radius
R	Stress ratio
r	Normalizing parameter used in J extrapolation method
$Re$	Reynolds Number

$R_{el}$	Bend radius of an elbow
$R_i$	Inside radius
$R_m$	Mean radius
$R_o$	Outside radius
$S$	Stress
$SI_{allowable}$	Allowable stress indices
$SI_{applied}$	Applied stress indices
$S_m$	ASME Code Design Stress
$ST_{345/20}$	Stratification stress due to normal operations of 345 C (653F) and stratification $\Delta T$ of 20C (36F)
$S_u$	Code specified ultimate strength
$S_y$	Code specified yield strength
$S_1$	Earthquake magnitude designator in Japan
$t$	Wall thickness
$T$	Tearing modulus
$T$	Temperature
$T$	Torque or torsion
$T$	Axial force at the end of an elbow
$T_{Applied}$	Applied tearing modulus
$t_f$	Pipe wall thickness influence function in Level 1 analysis
$T_f$	Water temperature influence function in Level 1 analysis
$T_{Mat}$	Tearing modulus of the material
$T_{Material}$	Tearing modulus of the material
$V$	Functions in GE/EPRI analysis for predicting COD
$V$	Fluid velocity
$Z$	ASME Section XI stress multipliers to account for low toughness
$\alpha$	Curve fitting parameter in Ramberg-Osgood relationship
$\alpha(\lambda)$	Bulging parameter used in shell-theory based COA analysis
$\beta$	Stress inversion angle in Net-Section-Collapse analysis
$\beta$	Plasticity correction factor
$\beta_1$	Plastic-zone size parameter
$\delta$	Crack opening displacement
$\delta^e$	Elastic component of COD
$\delta^p$	Plastic component of COD
$\Delta a$	Crack extension
$\Delta\sigma_b$	Cyclic bending stress
$\Delta\sigma_m$	Cyclic membrane stress
$\Delta K$	Change in stress intensity factor for fatigue crack growth analysis
$\Delta P$	Pressure difference across the crack
$\Delta T$	Change in temperature
$\epsilon$	Strain
$\epsilon^e$	Elastic component of strain
$\epsilon^p$	Plastic component of strain
$\epsilon_0$	Reference strain
$\lambda$	Function of rugosity and hydraulic diameter used in French A16 leak rate analysis
$\lambda$	Shell parameter
$\lambda$	Load ratio used in elbow J-estimation scheme analysis
$\lambda_1$	An elbow parameter ( $R_{el}t/R_m^2$ )
$\mu$	Dynamic viscosity of fluid

$\mu$	Surface roughness
$\mu_G$	Global surface roughness
$\mu_L$	Local surface roughness
$\rho$	Fluid density
$\sigma$	Stress
$\sigma_B$	Bending stress
$\sigma_{eff}$	Effective stress from combining bending and torsional stresses
$\sigma_f$	Flow stress
$\sigma_H$	Hoop stress
$\sigma_m$	Membrane stress
$\sigma_0$	Reference stress
$\sigma_T$	Nominal tensile stress
$\sigma_u$	Ultimate strength
$\sigma_y$	Yield strength
$\theta$	Half crack angle
$\theta_e$	Effective half crack angle accounting for plastic zone size
$\tau_T$	Torsional stress
$\nu$	Poisson's ratio
$\psi$	Bend angle of an elbow

## 2. ACRONYMS AND INITIALISMS

ANL	Argonne National Laboratories
ASME	American Society of Mechanical Engineers
ASTM	American Society for Testing and Materials
BHN	Brinell hardness number
BINP	Battelle Integrity of Nuclear Piping
BP	Break preclusion
BS	Basis safety
BWR	Boiling water reactor
B&W	Babcock and Wilcox
CE	Combustion Engineering
CEA	Commissariat A L'Energie Atomique (France)
CEGB	Central Electric Generating Board (United Kingdom)
CFR	Code of Federal Regulations
COA	Crack opening area
COD	Crack opening displacement
CRDM	Control rod drive mechanism
CRIEPI	Central Research Institute of Electric Power Industry (Japan)
CTOA	Crack tip opening angle
CTOA <sub>mono</sub>	Crack tip opening angle under monotonic loading
CUF	Cumulative usage factor
CVN	Charpy V-notch
C(T)	Compact (Tension) specimen
DEGB	Double ended guillotine break
DPZP	Dimensionless plastic zone parameter
DSA	Dynamic strain aging
DTRC	David Taylor Research Center
DW	Dead weight

Dyn	Dynamic
EAC	Environmental assisted cracking
ECCS	Emergency core cooling system
Emc <sup>2</sup>	Engineering Mechanics Corporation of Columbus
EPFM	Elastic plastic fracture mechanics
EPRI	Electric Power Research Institute
ET	Eddy current testing
ETEC	Energy Technology Engineering Center
E/C	Erosion/Corrosion
FAD	Failure assessment diagram
FEA	Finite element analysis
FEM	Finite element method
FORM	First order reliability method
FSAR	Final safety analysis report
GDC	General Design Criterion
GE	General Electric
GMAW	Gas-metal-arc weld
HAZ	Heat affected zone
IAEA	International Atomic Energy Agency
ID	Inside diameter
IGSCC	Intergranular stress corrosion cracking
IPIRG	International Piping Integrity Research Group
ISI	In-service inspection
JAERI	Japanese Atomic Energy Research Institute
KEPRI	Korea Electric Power Research Institute
KWU	Kraftwerk Union (Germany)
LBB	Leak-Before-Break
LLL	Lawrence Livermore Laboratory
LOCA	Loss of coolant accident
LWR	Light water reactor
MEA	Material Engineering Associates
MIG	Metal inert gas
MITI	Ministry of International Trade and Industry (Japan)
MPA	Staatliche Materialprüfungsanstalt (Germany)
NDE	Non-destructive examination
NRC	Nuclear Regulatory Commission
NPP	Nuclear power plant
NRR	Office of Nuclear Reactor Regulation (USNRC)
NSSS	Nuclear steam supply system
NUPEC	Nuclear Power Engineering Test Center (Japan)
OD	Outside diameter
ORNL	Oak Ridge National Laboratory
PICEP	PIpe Crack Evaluation Program
PIFRAC	PIping FRACTure mechanics material property database
PSI	Pre-service inspection
PWHT	Post-weld heat treatment
PWR	Primary water reactor
PWSCC	Primary water stress corrosion cracking
QS	Quasi-static
RCPB	Reactor coolant pressure boundary
RCS	Reactor coolant system

RHR	Residual heat removal
RPV	Reactor pressure vessel
SAM	Seismic anchor motion
SAR	Safety analysis report
SAW	Submerge-arc weld
SC	Surface crack
SEN(T)	Single-edge notch (tension)
SF	Safety factor
SG	Steam generator
SIS	Safety injection system
SKKU	Sungkyunkwan University (Korea)
SMAW	Shielded-metal-arc weld
SORM	Second order reliability method
SQUIRT	Seepage Quantification of Upsets in Reactor Tubes
SRP	Standard Review Plan
SRRA	Structural Reliability and Risk Assessment
SSE	Safe shutdown earthquake
STA	Science and Technology Agency (Japan)
TH	Thermal component of load
TIG	Tungsten-inert-gas weld
TWC	Through-wall crack
TWI	The Welding Institute (United Kingdom)
US	United States
USI	Unresolved Safety Issue
USNRC	United States Nuclear Regulatory Commission
UT	Ultrasonic testing
YGN	Yong Gwang Nuclear (Korea)

## **PREVIOUS REPORTS IN SERIES**

### **Reports from the IPIRG-2 Program**

“Summary of Results from the IPIRG-2 Round-Robin Analyses,” NUREG/CR-6337, BMI-2186, January 1996.

“IPIRG-2 Task 1 – Pipe System Experiments With Circumferential Cracks in Straight-Pipe Locations,” NUREG/CR-6389, BMI-2187, February 1997.

“The Effect of Cyclic and Dynamic Loads on Carbon Steel Pipe,” NUREG/CR-6438, BMI-2188, February 1996.

“Design of the IPIRG-2 Simulated Seismic Forcing Function,” NUREG/CR-6439, BMI-2189, February 1996.

“The Effect of Cyclic and Dynamic Loading on the Fracture Resistance of Nuclear Piping Steels,” NUREG/CR-6440, BMI-2190, December 1996.

“Deterministic and Probabilistic Evaluations for Uncertainty in Pipe Fracture Parameters in Leak-Before-Break and In-Service Flaw Evaluations,” NUREG/CR-6443, BMI-2191, June 1996.

“Fracture Behavior of Circumferentially Surface-Cracked Elbows,” NUREG/CR-6444, BMI-2192, December 1996.

“Development of a J-Estimation Scheme for Internal Circumferential and Axial Surface Cracks in Elbows,” NUREG/CR-6445, BMI-2193, June 1996.

“Fracture Toughness Evaluations of TP304 Stainless Steel Pipes,” NUREG/CR-6446, BMI-2194, February 1997.

“The Second International Piping Integrity Research Group (IPIRG-2) Program,” Final Report, October 1991 – April 1996, NUREG/CR-6452, BMI-2195, March 1997.

“State-of-the-Art Report on Piping Fracture Mechanics,” NUREG/CR-6540, BMI-2196, January 1998.

### **Reports from the IPIRG-1 Program**

“Evaluation and Refinement of Leak-Rate Estimation Models,” NUREG/CR-5128, BMI-2164, Revision 1, June 1994.

“Loading Rate Effects on Strength and Fracture Toughness of Pipe Steels Used in Task 1 of the IPIRG Program,” Topical Report, NUREG/CR-6098, BMI-2175, October 1993.

“Stability of Cracked Pipe Under Inertial Stresses,” NUREG/CR-6233, BMI-2177, Volume 1, August 1994.

"Stability of Cracked Pipe Under Seismic/Dynamic Displacement-Controlled Stresses," NUREG/CR-6233, BMI-2177, Vol. 2, June 1997.

"Cracked Stability in a Representative Piping System Under Combined Inertial and Seismic/Dynamic Displacement-Controlled Stresses," NUREG/CR-6233, BMI-2177, Vol. 3, June 1997.

"International Piping Integrity Research Group (IPIRG) Program," NUREG/CR-6233, BMI-2177, Vol. 4, June 1997.

#### **Previous Related Documents from NRC's Short Cracks in Piping and Piping Welds Program**

"Short Cracks in Piping and Piping Welds," First Semiannual Report, NUREG/CR-4599, BMI-2173, Vol. 1, No. 1, March 1991.

"Short Cracks in Piping and Piping Welds," Second Semiannual Report, NUREG/CR-4599, BMI-2173, Vol. 1, No. 2, April 1992.

"Short Cracks in Piping and Piping Welds," Third Semiannual Report, NUREG/CR-4599, BMI-2173, Vol. 2, No. 1, September 1992.

"Short Cracks in Piping and Piping Welds," Fourth Semiannual Report, NUREG/CR-4599, BMI-2173, Vol. 2, No. 2, February 1993.

"Short Cracks in Piping and Piping Welds," Fifth Semiannual Report, NUREG/CR-4599, BMI-2173, Vol. 3, No. 1, October 1993.

"Short Cracks in Piping and Piping Welds," Sixth Semiannual Report, NUREG/CR-4599, BMI-2173, Vol. 3, No. 2, March 1994.

"Short Cracks in Piping and Piping Welds," Progress Report, NUREG/CR-4599, BMI-2173, Vol. 4, No. 1, April 1995.

"Assessment of Short Through-Wall Circumferential Cracks in Pipes," NUREG/CR-6235, BMI-2178, April 1995.

"Fracture Behavior of Short Circumferential Short-Surface-Cracked Pipe," NUREG/CR-6298, BMI-2183, November 1995.

"Fracture Evaluations of Fusion Line Cracks in Nuclear Pipe Bimetallic Welds," NUREG/CR-6297, BMI-2182, April 1995.

"Effect of Dynamic Strain Aging on the Strength and Toughness of Nuclear Ferritic Piping at LWR Temperatures," NUREG/CR-6226, BMI-2176, October 1994.

"Effects of Toughness Anisotropy and Combined Loading on Fracture Behavior of Ferritic Nuclear Pipe," NUREG/CR-6299, BMI-2184, April 1995.

"Refinement and Evaluation of Crack-Opening Analyses for Circumferential Through-Wall Cracks in Pipes," NUREG/CR-6300, April 1995.

“Probabilistic Pipe Fracture Evaluations for Leak-Rate Detection Applications,” NUREG/CR-6004, BMI-2174, April 1995.

“Stainless Steel Submerged Arc Weld Fusion Line Toughness,” NUREG/CR-6251, BMI-2180, April 1995.

“Validity Limits in J-Resistance Curve Determination: Volume 1: An Assessment of the  $J_M$  Parameter,” NUREG/CR-6264, BMI-2181, Vol. 1, February 1995.

“Validity Limits in J-Resistance Curve Determinations: Volume 2: A Computational Approach to Ductile Crack Growth Under Large-Scale Yielding Condition,” NUREG/CR-6264, BMI-2181, Vol. 2, February 1995.

### **Previous Related Documents from NRC’s Degraded Piping Program - Phase I Reports**

“The Development of a Plan for the Assessment of Degraded Nuclear Piping by Experimentation and Tearing Instability Fracture Mechanics Analysis,” NUREG/CR-3142, Vols. 1 and 2, June 1983.

### **Previous Related Documents from NRC’s Degraded Piping Program - Phase II Reports**

“Degraded Piping Program - Phase II,” Semiannual Report, NUREG/CR-4082, BMI-2120, Vol. 1, Oct. 1984.

“Degraded Piping Program - Phase II,” Semiannual Report, NUREG/CR-4082, BMI-2120, Vol. 2, June 1985.

“Degraded Piping Program - Phase II,” Semiannual Report, NUREG/CR-4082, BMI-2120, Vol. 3, March 1986.

“Degraded Piping Program - Phase II,” Semiannual Report, NUREG/CR-4082, BMI-2120, Vol. 4, July 1986.

“Degraded Piping Program - Phase II,” Semiannual Report, NUREG/CR-4082, BMI-2120, Vol. 5, Dec. 1986.

“Degraded Piping Program - Phase II,” Semiannual Report, NUREG/CR-4082, BMI-2120, Vol. 6, April 1988.

“Degraded Piping Program - Phase II,” Semiannual Report, NUREG/CR-4082, BMI-2120, Vol. 7, March 1989.

“Degraded Piping Program - Phase II,” Semiannual Report, NUREG/CR-4082, BMI-2120, Vol. 8, March 1989.

“NRC Leak-Before-Break (LBB.NRC) Analysis Method for Circumferentially Through-Wall Cracked Pipes Under Axial Plus Bending Loads,” Topical Report, NUREG/CR-4572, BMI-2134, March 1986.

"Elastic-Plastic Finite Element Analysis of Crack Growth in Large Compact Tension and Circumferentially Through-Wall-Cracked Pipe Specimen--Results of the First Battelle/NRC Analysis Round Robin," Topical Report, NUREG/CR-4573, BMI-2135, September 1986.

"An Experimental and Analytical Assessment of Circumferential Through-Wall Cracked Pipes Under Pure Bending," Topical Report, NUREG/CR-4574, BMI-2136, June 1986.

"Predictions of J-R Curves With Large Crack Growth From Small Specimen Data," Topical Report, NUREG/CR-4575, BMI-2137, September 1986.

"An Assessment of Circumferentially Complex-Cracked Pipe Subjected to Bending," Topical Report, NUREG/CR-4687, BMI-2142, September 1986.

"Analysis of Cracks in Stainless Steel TIG Welds," Topical Report, NUREG/CR-4806, BMI-2144, November 1986.

"Approximate Methods for Fracture Analyses of Through-Wall Cracked Pipes," Topical Report, NUREG/CR-4853, BMI-2145, January 1987.

"Assessment of Design Basis for Load-Carrying Capacity of Weld-Overlay Repair," Topical Report, NUREG/CR-4877, BMI-2150, February 1987.

"Analysis of Experiments on Stainless Steel Flux Welds," Topical Report, NUREG/CR-4878, BMI-2151, February 1987.

"Experimental and Analytical Assessment of Circumferentially Surface-Cracked Pipes Under Bending," Topical Report, NUREG/CR-4872, BMI-2149, April 1987.

#### **Other Related Program Reports**

"Validation of Analysis Methods for Assessing Flawed Piping Subjected to Dynamic Loading," NUREG/CR-6234, ANL-94/22, BMI-2178, August 1994.

# 1 INTRODUCTION

As early as 1984, advances in technology had led the NRC staff to accept the concept of leak-before-break (LBB) for large-diameter, high-quality piping systems<sup>9</sup> as a means of enhancing the safety of nuclear power plants. The LBB concept permits removal, or non-installation, of many of the pipe-whip-restraint devices and jet-impingement shields, based on deterministic and probabilistic fracture mechanics analyses, originally designed to mitigate the dynamic effects of a postulated instantaneous pipe rupture. The safety benefit is realized through increased knowledge of pipe loads and material data, and the increased access to critical systems for in-service inspection and monitoring. However, 10 CFR 50, Appendix A, General Design Criterion-4 (GDC-4) did not permit the use of LBB, except by exemption. Rulemaking was therefore needed to accommodate these advances in the technology.

As a result, in 1987, a final rule was published amending GDC-4 to permit the use of LBB analyses in all qualified high-energy piping systems. Also, a draft Standard Review Plan (SRP) 3.6.3 entitled "Leak-Before-Break Evaluation Procedures" which provided review guidance for the implementation of the revised GDC-4, was published for public comment. This draft SRP, supplemented as necessary by NUREG-1061 Vol. 3 and other pertinent information available, formed the guidelines for NRC staff review of LBB submittals.

Because of ongoing research programs in the area of piping integrity and the expected conservatism associated with such LBB applications, the draft SRP 3.6.3 was not to be published in final form until the ongoing research could be completed. Now that the research is coming to a close, and most of the outstanding technical issues have been resolved, the NRC determined that action could be taken

---

<sup>9</sup> Such as that used in the main coolant loops of pressurized water reactors (PWRs)

to update the draft SRP on LBB and to provide the technical basis for developing a Regulatory Guide on LBB for the evaluation of piping in operating plants (specifically PWRs) and possibly some of the advanced reactor designs. As a result, in late 1997, the NRC contracted with Battelle (and Engineering Mechanics Corporation of Columbus [Emc<sup>2</sup>] through subcontract with Battelle) to conduct a study entitled "Technical Support for Regulatory Guide on Leak-Before-Break (LBB) Evaluation Procedures". The three main technical tasks<sup>10</sup> associated with this program were:

- Task 2 – Review Documentation of NRC Approval of Past LBB Applications,
- Task 3 – Review Relevant Research Results and Assess Their Significance on Past LBB Applications, and
- Task 5 – Identifying Alternatives and Revisions to the Draft Standard Review Plan 3.6.3 LBB Evaluation Method.

This report documents the findings of these technical tasks.

---

<sup>10</sup> Task 1 was to develop a detailed work plan and Task 4 was an optional effort that was not implemented.

## 2 CURRENT REGULATORY REQUIREMENTS AND GUIDANCE RELATED TO LBB

In this section, some of the current regulatory requirements that relate to Leak-Before-Break will be discussed.

### 2.1 Regulations

The governing section of the regulations related to LBB is General Design Criterion 4 (Environmental and Dynamic Effects Design Bases) in Appendix A of Part 50 (Domestic Licensing of Production and Utilization Facilities) of Title 10 (Energy) of the Code of Federal Regulations (10CFR50), Ref. 2.1. GDC-4 states that:

“Structures, systems, and components important to safety shall be designed to accommodate the effects of and to be compatible with the environmental conditions associated with normal operation, maintenance, testing, and postulated accidents, including loss-of-coolant accidents. These structures, systems, and components shall be appropriately protected against dynamic effects, including the effects of missiles, pipe whipping, and discharging fluids, that may result from equipment failures and from events and conditions outside the nuclear power unit. However, dynamic effects associated with postulated pipe ruptures in nuclear power units may be excluded from the design basis when analyses reviewed and approved by the Commission demonstrate that the probability of fluid system piping rupture is extremely low under conditions consistent with the design basis for the piping.”

Of particular interest to the subject of LBB, is the stipulation in GDC-4 that allows the use of “analyses reviewed and approved by the Commission” to eliminate from the design basis the dynamic effects of pipe ruptures.

Another specific reference in Appendix A of 10CFR50 that is particularly pertinent to LBB is the definition of a loss-of-coolant accident (LOCA):

“Loss of coolant accidents mean those postulated accidents that result from the loss of reactor coolant at a rate in excess of the capability of the reactor coolant makeup system from breaks in the reactor coolant pressure boundary, up to and including a break equivalent in size to the double-ended rupture of the largest pipe of the reactor coolant system<sup>11</sup>.”

The footnote to the definition of a loss-of-coolant accident warrants further discussion. Criteria relating to the type, size, and orientation of postulated breaks have been developed by the NRC staff, although not specifically promulgated in the regulations. These criteria have been published in the form of Regulatory Guides and Standard Review Plan (SRP) sections, both of which are described later in this section of the report.

### 2.2 Generic Issue A-2

Generic issues are issues or problems that are identified by the NRC that are common to a number of operating plants. One issue, or problem, of specific concern from an LBB perspective was due to the asymmetric blowdown loads on pressurized water reactor (PWR) primary systems. The problem of asymmetric blowdown loads on PWRs primary systems, initially identified to the NRC staff in 1975, was designated Unresolved Safety Issue (USI) A-2. This issue deals with safety concerns following a postulated major double-ended pipe break in the primary system. Previously unanalyzed loads on primary system components had the potential to alter primary system configurations or damage core-cooling equipment and contribute to core melt accidents. The resolution of this issue would have required some licensees for operating PWRs to add

---

<sup>11</sup> Further details relating to the type, size, and orientation of postulated breaks in specific components of the reactor coolant pressure boundary are under development.

massive piping restraints to address the consequences of these postulated large-pipe ruptures. Instead of resorting to these measures, this issue was resolved by the industry and the NRC staff by the adoption of the LBB approach utilizing advanced fracture mechanics techniques.

## 2.3 Regulatory Guides

The Regulatory Guide series provides guidance to licensees and applicants on implementing specific parts of the NRC's regulations, techniques used by the staff in evaluating specific problems or postulated accidents, and data needed by the staff in its review of applications for permits or licenses. With regard to LBB, one Regulatory Guide of specific interest, and referenced in SRP 3.6.3 on LBB Evaluation Procedures, is Regulatory Guide 1.45, Reactor Coolant Pressure Boundary Leakage Detection Systems (Ref. 2.2).<sup>12</sup>

### 2.3.1 Regulatory Guide 1.45 (Reactor Coolant Pressure Boundary Leakage Detection Systems)

General Design Criterion 30 (Quality of Reactor Coolant Pressure Boundary) of Appendix A to 10CFR50 requires, in part that, means be provided for detecting, and to the extent practical, identifying the location of the source of reactor coolant leakage.<sup>13</sup> Regulatory Guide

---

<sup>12</sup> At one time Regulatory Guide 1.46 (Protection Against Pipe Whip Inside Containment) was also pertinent to the subject, as evidenced by the reference made to it in NUREG-1061, Vol. 3. However, with the issuance of SRP 3.6.2 (Determination of Rupture Locations and Dynamic Effects Associated with Postulated Rupturing of Piping), which was thought to provide more current information concerning this subject, this Reg. Guide was withdrawn.

<sup>13</sup> GDC-30 states that "components which are part of the reactor coolant pressure boundary shall be designed, fabricated, erected, and tested to the highest quality standards practical. Means shall be provided for detecting and, to the extent practical, identifying the location of the source of reactor coolant leakage."

1.45 describes acceptable methods of implementing this requirement with regard to the selection of leakage detection systems for the reactor coolant pressure boundary. The position of Regulatory Guide 1.45 is that at least three different detection methods should be employed. Two of these methods should be; (1) sump level and flow monitoring and (2) airborne particulate radioactivity monitoring. The third method may involve either monitoring of condensate flow rate from air coolers or monitoring of airborne gaseous activity. The regulatory guide recommends that leak rates from identified and unidentified sources should be monitored separately, with the latter being monitored within an accuracy of 1 gallon per minute (gpm). Indicators and alarms for leak detection should be provided in the main control room. Other recommendations specified in Regulatory Guide 1.45 include:

- The sensitivity and response time of each leakage detection system should be adequate to detect an unidentified leakage of 3.8 lpm (1 gpm) in less than 1 hour.
- The leakage detection systems should be capable of performing their functions following a seismic event that does not require a plant shutdown.
- The leakage detection systems should be equipped with provisions to readily permit testing for operability and calibration during plant operations.

## 2.4 Standard Review Plans

Standard Review Plan (SRP) sections are prepared for the guidance of the Office of Nuclear Reactor Regulation (NRR) staff responsible for the review of applications to construct and operate nuclear power plants. The various SRP sections are incorporated in NUREG-0800, Standard Review Plan for the Review of Safety Analysis Reports for Nuclear Power Plants (Ref. 2.3). SRP sections are not substitutes for Regulatory Guides or the Commission's regulations, and compliance with them is not required. Two Standard Review Plan sections of prime interest to LBB are SRP 3.6.2, Determination of Rupture Locations and Dynamic Effects Associated with the Postulated

Rupture of Piping (Ref. 2.4), and draft SRP 3.6.3, Leak-Before-Break Evaluation Procedures (Ref. 2.5).

#### **2.4.1 SRP 3.6.2 (Determination of Rupture Locations and Dynamic Effects Associated with the Postulated Rupture of Piping)**

GDC-4 requires that structures, systems, and components important to safety shall be designed to accommodate the effects of postulated accidents, including appropriate protection against the dynamic and environmental effects of postulated pipe ruptures.

Information concerning break and crack location criteria and methods of analysis for evaluating the dynamic effects associated with postulated breaks and cracks in high- and moderate-energy fluid system piping inside and outside of containment should be provided in the applicant's safety analysis report (SAR). This information is reviewed by the NRC's Mechanical Engineering Branch in accordance with this SRP section (3.6.2), to confirm that requirements for the protection of structures, systems, and components relied upon for safe reactor shutdown, or for the mitigation of the consequences of a postulated pipe rupture, are met.

#### **2.4.2 Draft SRP 3.6.3 (Leak-Before-Break Evaluation Procedures)**

GDC-4 of Appendix A to 10CFR50 allows the use of analyses reviewed and approved by the Commission to eliminate from the design basis the dynamic effects of the pipe ruptures postulated, consistent with the guidance provided in SRP Section 3.6.2. The NRC staff reviews and approves each submittal to eliminate these dynamic effects. Approval of these LBB analyses by the NRC staff permits the case-by-case removal of protective hardware, such as pipe-whip restraints and jet impingement shield barriers, the redesign of pipe connected components, their supports, and their internals, and other related changes in operating plants.

This draft SRP section (3.6.3) is used by the NRC staff to evaluate all submittals from licensees and applicants dealing with the implementation of LBB technology. This draft SRP section has as its genesis the USNRC Piping Review Committee Report, NUREG-1061, Vol. 3, dated November 1984 (Ref. 2.6).

#### **2.5 NUREG-1061 Volume 3**

In the 1983/84 time frame, the Executive Director for Operations (EDO) of the USNRC requested that a comprehensive review be made of NRC requirements in the area of nuclear power plant piping. In response to this request, an NRC Piping Review Committee was formed. The activities of this review committee were divided into four tasks handled by appropriate task groups, namely:

- Pipe Crack Task Group
- Seismic Design Task Group
- Pipe Break Task Group
- Dynamic Load/Load Combination Task Group.

As a result of this Piping Review Committee, a five volume NUREG report (NUREG 1061) was published in 1984 and 1985. Volume 3 of this NUREG was the report prepared by the Pipe Break Task Group and dealt with the Evaluation of Potential for Pipe Breaks. Volume 3 summarizes a review of regulatory documents and contains the Task Group's recommendations for application of the leak-before-break (LBB) approach to the NRC's licensing process. Some of the key recommendations from NUREG-1061 Volume 3 that were later implemented into the draft SRP on LBB (3.6.3) include:

- A caveat on the use of LBB instead of the double-ended guillotine break (DEGB) criteria is the absence of excessive loads or cracking mechanisms that could adversely affect the accurate evaluation of flaws and loads. Specific examples include water hammer and water slugging, other large dynamic loads, intergranular stress corrosion cracking (IGSCC) and fatigue.

- Examination of leak detection systems in existing nuclear plants on a case-by-case basis to ensure that suitable detection margins exist so that the margin of detection for the largest postulated leakage size crack used in the fracture mechanics analyses is greater than a factor of ten on unidentified leakage.
- Postulate the existence of a through-wall flaw at the location(s) of the highest stresses coincident with the poorest material properties. The size of the flaw should be large enough so that the leakage is assured of detection with margin using the installed leak detection capability when the pipes are subjected to normal operating loads.
- Assume that a safe shutdown earthquake (SSE) occurs prior to detection of the leak to demonstrate that the postulated leakage flow is stable under normal operating plus SSE loads.
- Determine the flaw size margin by comparing the postulated leakage size flaw to the critical crack size. For normal plus SSE loads, demonstrate that there is a margin of at least 2 between the leakage size flaw and the critical crack size to account for the uncertainties inherent in the analyses and leak detection capabilities.
- Determine the margin in terms of applied loads by a crack stability analysis. Demonstrate that the leakage-size crack will not experience unstable crack growth even if larger loads (at least the  $\sqrt{2}$  times the normal plus SSE loads) are applied.
- The stipulation that LBB should only be applied to ASME Code Class 1 and 2 high-energy piping or equivalent. [In practice, LBB has typically only been approved for Class 1 piping systems. Only on rare occasions, such as the CE System 80+ steam lines, has it been applied to Class 2 piping.]
- The stipulation that piping susceptible to intergranular stress corrosion cracking (IGSCC) with any planar flaws in excess of those allowed by Article IWB 3514.3 of Section XI of the ASME Code would not be permitted to use LBB analyses.
- The stipulation that when dynamic effects of pipe rupture are eliminated from the design basis, current NRC criteria, and industry codes, such as ASME, may be required for calculating the seismic loads in the heavy component support redesign

## 2.6 Industry Standards

The industry standard of most interest to LBB is the ASME Boiler and Pressure Vessel Code (Ref. 2.7). There are several sections of the ASME Code that are referenced by the draft SRP 3.6.3 on LBB. Specific references to the ASME code within draft SRP 3.6.3 include:

## 2.7 References

- 2.1 "Environmental and Design Effects Design Bases," 10 CFR Part 50, Appendix A, General Design Criterion 4.
- 2.2 "Reactor Coolant Pressure Boundary Leakage Detection Systems," USNRC Regulatory Guide 1.45.
- 2.3 "Standard Review Plan for the Review of Safety Analysis Reports for Nuclear Power Plants," NUREG-0800, 1987.
- 2.4 "Determination of Rupture Locations and Dynamic Effects Associated with the Postulated Rupture of Piping," USNRC Standard Review Plan 3.6.2, Rev. 1, July 1981.
- 2.5 "Leak-Before-Break Evaluation Procedures," USNRC draft Standard Review Plan 3.6.3, August 1987.
- 2.6 "Report of the U.S. Nuclear Regulatory Commission Piping Review Committee - Evaluation of Potential for Pipe Breaks," NUREG-1061, Vol. 3, November 1984.
- 2.7 ASME Boiler and Pressure Vessel Code, 1995 Edition.

### 3 SUMMARY OF DRAFT SRP 3.6.3 PROCEDURES FOR LEAK-BEFORE-BREAK EVALUATIONS

In 1987, the USNRC first published for public comment draft Standard Review Plan (SRP) 3.6.3 (Ref. 3.1). The draft SRP was to be used by the NRC staff to evaluate all submittals made by licensees and applicants dealing with the implementation of leak-before-break (LBB) technology under the broad scope amendment to General Design Criterion 4 (GDC-4) of Appendix A to 10 CFR Part 50. Note that when LBB technology, as spelled out in draft SRP 3.6.3, is shown to be applicable, only the dynamic effects of postulated pipe ruptures may be eliminated. The requirements for containment design, emergency core cooling system performance, and environmental qualification of electrical and mechanical equipment are not affected.

#### 3.1 Applicability

When LBB technology is applied, all potential pipe rupture locations are examined. The examination is not limited to those postulated pipe rupture locations specified in SRP Section 3.6.2 (Ref. 3.2). Furthermore, the LBB evaluation should use design basis loads and as-built configurations for the piping system under consideration, as opposed to the design configuration. Correct locations for supports and their characteristics (such as gaps) should be verified, as well as weights and locations of components such as valves.

Draft Standard Review Plan 3.6.3 is generally applicable to ASME Code Class 1 piping with the following caveats:

- LBB cannot be applied to individual welded joints or other discrete locations. LBB is applicable only to an entire piping system or analyzable portion thereof. Analyzable portions are typically segments located between anchor points.
- LBB is typically not applicable to piping susceptible to intergranular-stress-corrosion cracking (IGSCC) or primary

water stress corrosion cracking (PWSCC). However, if the applicant can demonstrate to the NRC through analysis, data, or operational experience, that effective mitigation measures are in place to counteract these mechanisms, then LBB may be considered.

- Piping repaired by weld overlays cannot apply for LBB.
- LBB is not applicable to piping systems with a history of fatigue cracking. An evaluation should be performed to assure that the potential for pipe rupture due to thermal and mechanical induced fatigue is extremely low. Licensees and applicants must demonstrate that there is adequate mixing of low and high temperature fluids so that there is no potential for significant cyclic thermal stresses. In addition, it must also be demonstrated that there is no significant potential for vibration induced fatigue cracking or failure.
- LBB cannot be applied to piping supported by masonry block walls unless compliance with Multi-Plant Action B-59 is achieved.
- It must be demonstrated that for piping systems that may be degraded by corrosion, erosion, erosion/corrosion, and erosion/cavitation due to unfavorable flow conditions and water chemistries, that these mechanisms are not a potential source for pipe rupture.
- LBB is not applicable to piping systems for which pipe rupture due to water hammer is likely.
- LBB is not applicable to piping systems subject to creep mechanisms. Operation below 371C (700F) for ferritic steel piping and below 427C (800F) for austenitic steel piping can satisfy this concern with creep.
- LBB is not applicable to piping systems for which brittle fracture is a possibility. It must be demonstrated that the piping material is not susceptible to brittle cleavage-type failure over the full range of system operating temperatures, i.e., the

material is always operating on the upper shelf.

- An assessment of potential indirect sources of pipe rupture is required to demonstrate that indirect failure mechanisms defined in the plant FSAR are remote causes of pipe rupture. Indirect failure mechanisms include seismic events and system overpressurizations due to accidents resulting from human error, fires, or flooding which cause electrical and mechanical systems to malfunction.

### **3.2 Steps in an Acceptable SRP 3.6.3 LBB Analysis**

In demonstrating LBB following the draft SRP 3.6.3 methodology, the following steps should be adhered to:

#### **3.2.1 Demonstrate Accuracy of Leak Rate and Fracture Mechanics Computational Methods**

The first step in an acceptable LBB analysis is to demonstrate the accuracy of the leak rate and fracture mechanics computational methods to be used in the analysis by comparison with other acceptable computational procedures (e.g., finite element methods) or with experimental data, where available.

#### **3.2.2 Identify Materials and Material Property Data**

One of the stated safety benefits of applying LBB is the increased knowledge of the material data for the piping system under consideration. As part of any LBB analysis, one must identify the types of materials and material specifications used for the base metal, weldments, and safe ends for the piping system being analyzed. In addition, material property data, including toughness and tensile data, and long-term effects on these properties, such as thermal aging, must be specified.

Preferably the material data should be obtained using archival material for the piping system being evaluated. If archival material data are not available, then plant specific or industry wide

generic material databases can be used to define the required material tensile and toughness properties. Test material should include base and weld metals. To provide an acceptable level of reliability, plant specific generic databases must be reasonable lower bounds for compatible sets of material tensile and toughness properties associated with materials at the plant. Rules for ensuring the adequacy of these databases are included in the draft SRP.

#### **3.2.3 Specify Types and Magnitudes of Applied Loads**

Another stated safety benefit of applying LBB is the increased knowledge of the applied loads. For an LBB analysis, the type and magnitude of the applied loads (forces, bending and torsional moments), their source(s), and the method of combination must all be specified. Typically for the leak-rate analysis, the applied loads are combined algebraically while for the crack stability analysis, the applied loads are combined either absolutely or algebraically. If combined absolutely in the fracture analyses, then the margins on loads can be reduced from  $\sqrt{2}$  to 1.0 for the stability analysis. For each pipe size being analyzed, the location(s) that have the least favorable combination of stress and material properties (for the base metal, weldments, and safe ends), must be identified. Note, work from Reference 3.3 has shown that the worst combination of loads from a LBB perspective might be the combination of relative low normal operating stresses (resulting in a longer postulated leakage crack size) plus high faulted/seismic stresses (promoting crack instability).

#### **3.2.4 Postulate a Leaking Through-Wall Crack at the Critical Assessment Locations**

At the critical assessment locations identified above (worst case combination of stress and material data), a postulated leaking through-wall crack is assumed to exist. The size of the through-wall crack should be large enough so that the leakage is assured of detection with a specified margin when using the installed leak detection capability and when the pipes are subjected to the normal operating loads. When

prescribing the normal operating loads (i.e., deadweight, thermal expansion, and pressure) for estimating the leakage size flaw (i.e., the smallest flaw detectable by the leakage detection system with a margin of 10 on detection limit applied), the loads should be combined based on the algebraic sums of their individual values.

### 3.2.5 Determine Critical Crack Size and Critical Crack Size Margin

Using a fracture mechanics stability analysis, or a limit-load analysis (if appropriate), the critical crack size should be determined using the appropriate material data and normal operating plus safe-shutdown-earthquake (N+SSE) or other transient loads. An example of a transient load other than SSE is the thermal stratification stresses in a surge line during start up or shutdown<sup>14</sup>. The margin on crack size, i.e., the ratio of the critical crack size to the postulated leakage crack size, should be at least 2.0.

### 3.2.6 Determine Applied Loads Margin

The applicant should also determine the margin in terms of applied loads by a crack stability analysis. It should be demonstrated that the postulated leakage size crack (established above) will not experience unstable crack growth if 1.4 times the algebraic combination of the normal plus SSE loads are applied. It should be demonstrated that any crack growth is stable and the final crack is limited such that a double-ended-guillotine break (DEGB) will not occur. Note, that the margin of 1.4 can be reduced to 1.0 if the faulted loads (deadweight, thermal expansion, pressure, SSE (inertial) and seismic anchor motion [SAM]) are combined based on individual absolute values.

For these stability analyses, the piping materials toughness (i.e., J-R curve) and tensile properties (stress-strain curve) should be determined at temperatures near the upper range of normal

<sup>14</sup> Combining the SSE stresses with start up and shut down stratification stresses has been considered by the NRC staff as a very low probability event, and hence only the SSE or thermal transient stresses need be analyzed.

plant operations. The fracture toughness specimens (e.g., compact (tension) specimens) should be large enough to provide crack extensions up to an amount consistent with J/T conditions determined by analysis for the application. However, because practical specimen size limitations exist, the ability to obtain the desired amount of experimental crack extension may be restricted. In such cases, extrapolation techniques may be used as described in NUREG-1061 Volume 3 (Ref. 3.4) or in NUREG/CR-4575 (Ref. 3.5). The stress-strain curve should be obtained over the range from the proportional limit to the maximum load.

The generic use of limit-load analyses to evaluate leak-before-break conditions is somewhat limited in draft SRP 3.6.3. One of the fundamental conditions in any limit-load analysis is the assumption of fully-plastic conditions. As part of the Degraded Piping Program – Phase II (Ref. 3.6) a simple screening criterion was developed to identify when fully-plastic conditions existed and when they did not. This screening criterion was coined the Dimensionless-Plastic-Zone Parameter (DPZP) criterion (Ref. 3.7). Basically the DPZP criterion indicated that large-diameter piping systems fabricated from lower-toughness materials (e.g., carbon steels) would most likely not fail under limit-load conditions. Draft SRP 3.6.3 recognized this fact and limited the use of limit-load type analyses specifically to wrought stainless steel piping systems with relatively tough welds (TIG or GTAW) through the prescription of a modified limit-load analyses crafted like an ASME Section XI Appendix C flaw evaluation criteria (Ref. 3.8). The modification to the limit-load analyses is the introduction of the Z-factors that accounted for the possibility of cracks occurring in lower-toughness stainless steel flux welds, i.e., submerge-arc welds (SAW) and shielded-metal-arc-welds (SMAW).

### 3.3 References

- 3.1 "Leak-Before-Break Evaluation Procedures," USNRC draft Standard Review Plant 3.6.3, August 1987.

3.2 "Determination of Rupture Locations and Dynamic Effects Associated with the Postulated Rupture of Piping," USNRC Standard Review Plan 3.6.2, Rev. 1, July 1981.

3.3 Ghadiali, N., and others, "Deterministic and Probabilistic Evaluations for Uncertainty in Pipe Fracture Parameters in Leak-Before-Break and In-Service Flaw Evaluations," NUREG/CR-6443, June 1996.

3.4 "Report of the U.S. Nuclear Regulatory Commission Piping Review Committee. Evaluation of Potential for Pipe Breaks," NUREG-1061, Vol. 3, November 1984.

3.5 Papaspyropoulos, V, and others, "Predictions of J-R Curves with Large Crack Growth from Small Specimen Data," NUREG/CR-4575, September 1986.

3.6 Wilkowski, G. M., and others, "Degraded Piping Program – Phase II, Summary of Technical Results and Their Significance to Leak-Before-Break and In-Service Flaw Acceptance Criteria, March 1984 – January 1989," NUREG/CR-4082, Vol. 8, March 1989.

3.7 Wilkowski, G. M., and Scott, P. M., "A Statistical Based Circumferentially Cracked Pipe Fracture Mechanics Analysis for Design or Code Implementation," Nuclear Engineering and Design, Vol. 111, pp. 173-187, 1989.

3.8 ASME Boiler and Pressure Vessel Code, Section XI, Appendix C, 1998 Edition, July 1998.

## 4 LESSONS LEARNED FROM REVIEWS OF PAST LBB APPLICATIONS

One of the major technical tasks undertaken as part of the USNRC LBB Regulatory Guide program was a task in which past LBB applications were reviewed for lessons that could be learned from these past applications (Task 2). This section of the report summarizes some of the key findings uncovered as a result of those reviews of the actual LBB submittals.

### 4.1 LBB Applications Purposes

Generally LBB has been accepted for relief of General Design Criteria 4 (GDC-4) requirements for protection against dynamic effects. Some of the devices used that have been modified or eliminated as a result of LBB acceptance include:

1. Pipe whip restraints for asymmetric blowdown loads,
2. Pipe whip restraints after pipe replacement,
3. Jet impingement shields,
4. Refueling pool seals,
5. Steam generator and reactor coolant pump snubber requirements due to thrust loads, and
6. Flexible neutron absorbing water bags at the top of the vessel cavity.

As stipulated in draft SRP 3.6.3 (Ref. 4.1), LBB has not been accepted in the U.S. for modification of equipment environmental qualification, containment design, or emergency core cooling system (ECCS) requirements. However, in Europe and Russia, LBB has been applied to older Russian reactors where the ECCS was not sized for a full break of the primary piping. Furthermore, it is interesting to note that LBB has not been accepted in the U.S. for boiling water reactors (BWRs), but was first accepted in Japan for BWRs.

### 4.2 Vendor LBB Methodology Examples

The LBB methodologies used by different vendors have evolved over the years. Some specific examples are given below.

One vendor conducted very sophisticated dynamic analyses in the late 1970's and early 1980's. They considered seismic loading on a circumferentially cracked pipe, and performed dynamic analyses assuming there was a double-ended-guillotine-break (DEGB) or 2-dimensional axial pipe break opening. A crack was included in a finite element model of the whole pipe system, and dynamic analysis was conducted. Typically these analyses were for a stationary crack, and initially involved determining the driving force in terms of K rather than J. An aspect not considered in these analyses for axial cracks was that in a pipe system, the axial pipe break may result in a DEGB due to the fracture ringing off around the circumference of the pipe. This axial to circumferential crack growth behavior was experimentally observed in some of the EPRI/ETEC experiments (Ref. 4.2) and the Surrey erosion/corrosion (E/C) elbow failure. In latter applications, this vendor more closely followed the NRC draft SRP 3.6.3 type analyses.

Another vendor initially developed an LBB analysis for a representative "standard" nuclear plant. This "standard" plant was designed to bound all the conditions of their plants, thereby eliminating the need for plant specific analysis. Consequently, they only needed to demonstrate that the specific plant of concern was conservative by some amount with respect to this "standard" plant in all the critical LBB analysis parameters. This approach was initially followed for the main coolant piping, but specific analyses were later conducted for other piping systems.

Finally, two vendors addressed cracks in fittings, such as the body of elbows. However, there is no guidance for such analyses in draft SRP 3.6.3.

### 4.3 How Applications Evolved

LBB applications initially started with the NRC's Unresolved Safety Issue A-2 on

asymmetric blowdown loads. This dealt with the concern that if there was a major break in the main coolant lines, the pressure and thrust loads were hypothesized to be large enough to cause the reactor vessel to tip over or to damage the core internals, and hence insertibility of the vessel control rods would be lost. Obviously, this is a severe accident concern for safety purposes. Newer plants had pipe-whip restraints at the vessel biological shield wall to prevent the asymmetric loading concern, but older plants did not. The initial LBB work was a probabilistic approach by Lawrence Livermore Laboratory (LLL) with simple deterministic fracture models (Ref. 4.3).

At a later date, NUREG-1061 Volume 3 (Ref. 4.4) developed a more standardized procedure for LBB analysis that was based on the assessment of a circumferential through-wall crack in a straight pipe. From the NUREG-1061 Volume 3 approach, a draft Standard Review Plan (SRP) 3.6.3 (Ref. 4.1) was developed that has been followed in the more recent LBB applications.

#### **4.4 Lines Typically Approved and Rejected for LBB**

##### **4.4.1 Lines Accepted for LBB in USNRC Applications**

In reviewing the past LBB submittals supplied to Battelle and Emc<sup>2</sup> by the NRC, it was found that the following lines have been accepted for LBB by the USNRC. In some cases there were conditions imposed on the acceptance.

- Main coolant lines (28 to 42-inch diameter),
- Pressurizer surge lines (10 to 14-inch diameter),
- Residual heat removal (RHR) lines (10 to 12-inch diameter),
- Accumulator lines (12 to 14-inch diameter),
- Reactor coolant bypass lines (8-inch diameter),
- Safety injection system lines into cold legs (6-inch diameter),
- Safety injection system lines into hot legs (6-inch diameter),

- CE System 80+ direct vessel injection lines (12-inch diameter),
- CE System 80+ shutdown coolant line (16-inch diameter), and
- CE System 80+ main steam line inside containment (28-inch diameter).

##### **4.4.2 Lines Rejected for LBB in USNRC Applications**

The following lines have been rejected for LBB by the USNRC. Some of the reasons for their rejection are provided below.

- The CE System 80 main steam line was rejected due to water hammer history and lack of technical justification for the leak-rate analysis verification for steam leakage.
- Lines susceptible to thermal stratification where there was a lack of documentation or control of the temperature differentials.
- Auxiliary feedwater pump steam lines were rejected since the application sought relief from equipment qualification in the control room.
- A BWR isolation condenser pipe was rejected since the leak detection outside containment was insufficient, the pipe was deemed to still be susceptible to IGSCC, and the pipe was not analyzed completely from anchor to anchor. The latter two reasons for rejection were violations of the criteria set forth in draft SRP 3.6.3.
- AP600 feedwater lines because of the potential for water hammer.

#### **4.5 Material Property Aspects**

As a result of the reviews of the past LBB submittals, a number of interesting material property aspects are summarized below. In some cases these were aspects that were considered in the LBB applications, while in other cases these were aspects that perhaps should be considered in a future LBB Regulatory Guide based on more recent research efforts.

#### 4.5.1 Bimetallic Welds

Bimetallic welds occur at many locations in a plant. For example, in Westinghouse plants there is stainless steel main coolant piping that is welded to low alloy steel nozzles (i.e., A508 forgings) at the vessel and steam generators. In some plant designs, pump housings are made out of cast stainless steel and are joined to the main coolant ferritic piping using a bimetallic weld. Combustion Engineering (CE) surge lines in some cases are cast stainless steel and are welded to nozzles in the main coolant ferritic piping. There are also many smaller diameter lines that may be stainless steel that are teed off from larger diameter ferritic lines.

One of the concerns with a bimetallic weld is that if stainless steel weld metal is used, then there may be some carbon depletion in the HAZ. This has been found to cause a reduction of toughness in such welds (Ref. 4.5). On the other hand, it has been thought that welds made with Inconel weld metal, or welds where there is a buttering of the carbon steel weld bevel with Inconel, should not have a problem with carbon depletion. Note, however, that recent experience at the Virgil C. Summer plant in South Carolina and the Ringhals plant overseas indicate that there is a potential problem with pressurized water stress corrosion cracking (PWSCC) in these types of welds (i.e., Inconel 182/82 welds).

All newer plants that have been examined have bimetallic welds that were Inconel or were Inconel buttered welds. In some cases, a stainless steel buttering was applied to the nozzle, then the buttered area received a stress-relief treatment with the vessel. It is doubtful that such a stress-relief would correct the carbon depletion potential problem in the HAZ.

During the LBB submittal review process, a table was reviewed from the NRC that gave a listing of pressure vessel nozzle welds in one vendor's plants. From that table, Inconel welds or Inconel buttered welds were used on reactor vessel nozzles for 67 PWR plants. For these plants, there should be no concern with these bimetallic welds from a carbon depletion viewpoint. Stainless steel buttering was used on

20 PWR vessels and full stainless steel welds were used on six PWR vessels. If the stainless steel buttering weld rod was the same as used in typical stainless steel welds (i.e., TP308 or TP309 weld metal), then the stainless steel buttered welds would be susceptible to carbon depletion. This list provided by the NRC was further cross-checked against some of the LBB applications and the following was found.

- For one plant, the table indicated that a stainless steel weld process was used. In reviewing the LBB application, it was found that a stainless steel safe end was welded to the vessel nozzle with an Inconel weld metal. The cast stainless steel pipe was then field welded to the safe end. There should be no problem with carbon depletion in this case.
- For another plant, the table said there was a stainless steel buttering, however the LBB application showed a typical diagram of the vessel nozzle with an Inconel buttering. This buttering would overtake any carbon depletion concerns.
- For the rest of the reviews of the LBB applications, there is no recollection of a case where stainless steel buttering or a full stainless steel weld was made directly to the vessel low-alloy steel nozzle (i.e., A508 nozzle forging). Hence, there appears to be a number of inconsistencies between the NRC-provided table and the actual LBB applications. The NRC-provided table showed that 26 plants may have a potential concern with de-carbonization in the vessel bimetallic welds, but a more in-depth review of the actual LBB applications failed to confirm this. Stainless steel bimetallic welds may have been used at other locations in the main coolant pipe loop, i.e., steam generator welds that were reflected in the NRC-provided table but not in the actual LBB submittals.

#### 4.5.2 Thermal Aging of Cast Stainless Steels

Cast stainless steels are used in a number of vendor plants. Westinghouse uses cast stainless

steel in some of their main coolant loop piping. CE uses cast stainless steel for some of their surge lines. Cast stainless steel is also used in fabrication of pipe fittings, e.g., nozzles and elbows in some wrought stainless steel lines. Thermal aging of cast stainless steels has been investigated with great diligence for LBB applications. A significant amount of work was done in France (Ref. 4.6) and at Argonne for the USNRC (Ref. 4.7).

The concern with cast stainless steels is that in the duplex austenitic and ferritic microstructures in such steels, that the ferritic grains become embrittled with time. The chemistry of the steel, the ferrite number, the operating temperatures, and the time at temperature are all parameters that may impact the fracture toughness properties of such steels.

One applicant developed a program where they determined a "reference" heat of cast stainless steel. If a cast stainless steel passed certain screening criteria (composition, ferrite number, etc.,) then the reference heat toughness values were used in the LBB analysis. Since most steels were better than this reference heat, this was a conservative assumption for those applications. However, some cast stainless steel base metals failed this screening criterion, indicating that their toughness properties may not be bounded by the reference heat data. In those cases, a lower than "reference heat" alternative toughness methodology was used in these particular LBB applications.

A final comment with regard to thermal aging is that the thermal aging studies involved soaking the material at a temperature for some time period in an oven with no applied loads. It has been hypothesized that applied loads may affect the activation energy needed for thermal aging, so the aging may occur quicker in service than that observed in typical laboratory testing. However, since the long-term saturation level should be governed by the material chemistry and microstructure, and not the applied load, there should be no difference in the laboratory testing and in-service saturation levels. It is these saturation-level toughness values that are typically used in LBB analyses, in that they

represent more of a lower-bound toughness value. Consequently, the "no-load" thermal aging data that has been developed, and used in past applications, is probably adequate, i.e., conservative, for these type of LBB analyses.

#### 4.5.3 Thermal Aging of Stainless Steel Welds

Stainless steel welds also have a microstructure of ferrite and austenite. Submerged arc welds (SAWs) and shielded metal arc welds (SMAWs) typically have flux inclusions which result in a much lower toughness values than those for inert gas welds (i.e., MIG, TIG, and GMAW) or wrought stainless steel base metals. There is also a small amount of ferrite in the weld, which makes the weld duplex structures like casting stainless steel. Any one of these weld procedures might be used in a plant piping system, depending on the thickness of the pipe, and if it is a shop or field weld. A statistical analysis by Wilkowski and Ghadiali (Ref. 4.8) showed that there is effectively no difference between SAW and SMAW toughness values.

In the review of the LBB applications, applicants have tried to argue that thermal aging of stainless steel welds is negligible. However, it was noted that the Charpy energy values dropped from 54 to 32 J (40 to 24 ft-lb) due to aging. (The test temperature of the Charpy specimens was not given.) Although the percentage drop is lower for cast stainless steels, the drop in toughness for the stainless steel welds is in the low toughness range where the load-carrying capacity is very sensitive to any decrease in toughness. The toughness of typical submerged arc welds is around 87 kJ/m<sup>2</sup> (500 in-lb/in<sup>2</sup>) and the Charpy energy at temperature is typically around 68 J (50 ft-lb). The relationship between the Charpy energy and  $J_{Ic}$  developed for ferritic base metals is consistent with these values, i.e.,

$$J_{Ic} = 10 CVN \quad (4.1)$$

with  $J_{Ic}$  and Charpy energy having units of in-lb/in and ft-lb, respectively. Using this same relationship for the aged stainless steel SAW

results in a  $J_{Ic}$  value of only 42 kJ/m<sup>2</sup> (240 in-lb/in<sup>2</sup>).

The change in the slope of the J-R curve ( $T_{mat}$ ) is also related to the Charpy energy, at least for base metals. Westinghouse indicated in one of its reports that the slope of the aged weld metal J-R curve was higher than for the lower bound aged cast stainless steel base metal. This was the basis of their using the reference heat toughness for cast stainless steels rather than a weld metal toughness. However, the toughness change of the stainless steel welds with thermal aging would also be applicable to wrought stainless lines (surge lines, accumulators, and RHR), and perhaps Inconel bimetallic welds as well. Hence, thermal aging of the stainless steel welds may be an important factor to consider as part of the fracture analysis of an LBB assessment for a wrought stainless steel piping system, even if it is not a concern for cast stainless steel lines.

#### 4.5.4 HAZ or Fusion Line Toughness

Draft SRP 3.6.3 recommends the use of the worst case material properties at the highest stress location. LBB analyses typically involve analyses using either base metal toughness or toughness values at the center line of the weld. Frequently, however, cracks occur in the fusion line or HAZ areas of the welds. No fusion line or HAZ toughness values were cited in any of the LBB submittals reviewed.

An aspect of interest relative to this item is that in NUREG/CR-6251 (Ref. 4.9), it was found that for wrought stainless steel SAWs, the fusion lines had a flat J-R curve after 2 mm (0.08 inch) of crack extension, see Figure 4.1. Hence, the fusion-line toughness may be lower than the weld-metal center-line toughness typically referenced in the LBB submittals.

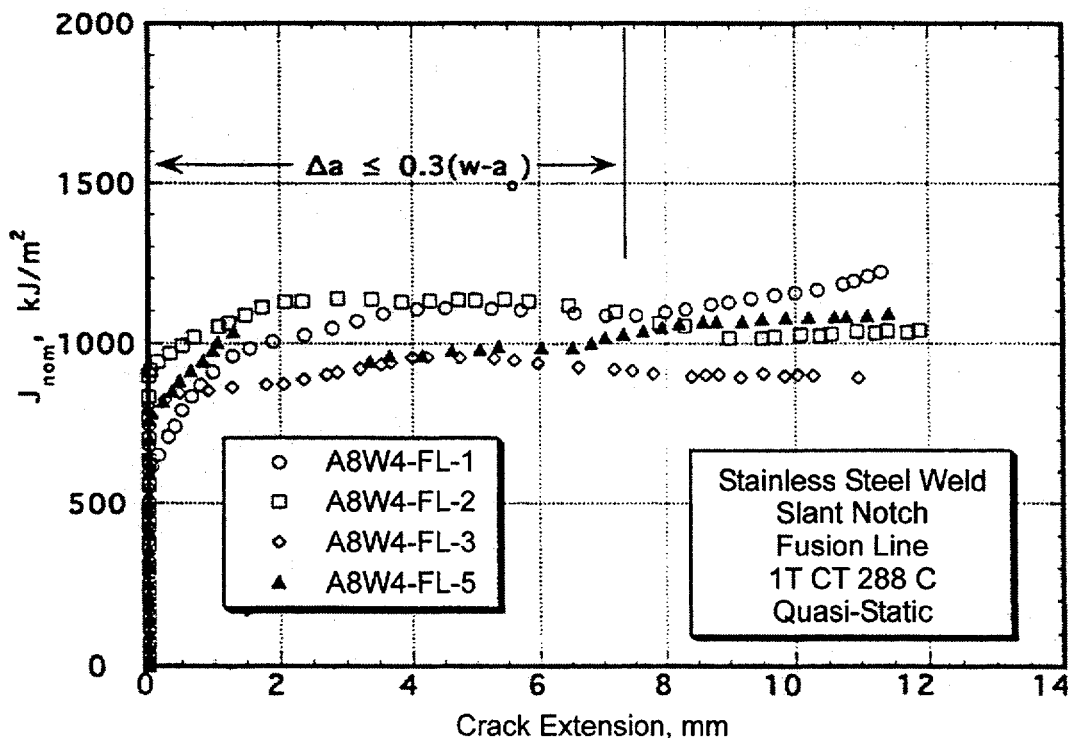


Figure 4.1 J-resistance curves of fusion-line specimens [limit on J-R curve data is  $\Delta a \leq 0.3(W-a)$ ], Ref. 4.9

#### 4.5.5 Load-History Effects on Toughness

Thermal aging effects account for the temperature history effects on the toughness of specific materials, i.e., either cast stainless steels or stainless steel welds. However, there are other history effects that were also found to be important during the course of the IPIRG programs (Refs. 4.10 and 4.11). These effects relate to seismic loading conditions, i.e., the dynamic, cyclic nature of the load history.

Seismic loading involves both dynamic loading rates and cyclic loading. It has been suggested that the loading rate can be approximated as the rate required to reach the maximum displacement of the large amplitude load cycle in a time equal to one-quarter of the period of the first natural frequency of the piping system involved. This is a loading rate that may be 10,000 times faster than that typically used for quasi-static testing in ASTM standard procedures. Quasi-static, monotonic-loaded specimens are typically tested to obtain a material's fracture resistance curve.

From the IPIRG program, it was determined that seismic loading rates generally increase the fracture toughness of austenitic base metals and welds (including cast stainless steels), but may be detrimental to ferritic steels (Ref. 4.10). The ferritic steel behavior is complicated by the susceptibility of most of these materials to dynamic strain aging<sup>15</sup> (Ref. 4.12). Virtually all carbon-steel piping grades that were tested in the IPIRG and other NRC programs had some pipe lengths that were susceptible to dynamic strain aging. The worst case resulted in the toughness being reduced by slightly more than a factor of two. A dynamic strain aging screening criterion was developed in the NRC's Short Cracks in Piping and Piping Welds Program (Ref. 4.12).

---

<sup>15</sup> Dynamic strain aging not only effects the fracture toughness properties of ferritic steels, but it also has been shown to effect the ultimate tensile strength and percent elongation. At elevated temperature, the ultimate strength of many ferritic steels has been found to decrease significantly at the higher loading rates.

Cyclic loads will also occur during a seismic event. These loads will be superimposed on the static loads. The ratio of the minimum to maximum loads is typically referred to as the stress ratio (R). A stress ratio of -1.0 is fully reversed loading. Work in the IPIRG programs showed that cyclic load effects may only be important in some subset of seismic load histories. In the worst case, cyclic loading was found to reduce the toughness of piping steels by a factor of four, however, in many cases the effect was negligible. Furthermore, the manner of the cyclic loading build-up to the maximum load was found to be an important parameter that is currently hard to quantify for a seismic event. During the BINP program an additional pipe-system experiment was conducted with a seismic load history having a more gradual cyclic build-up than that used in the Second IPIRG program (Ref. 4.13). In comparing the results from these two seismically-loaded pipe-system experiments, see Figures 4.2 and 4.3, it appears that the more gradual build-up of the loading cycles in the BINP experiment was more damaging than the initial single large amplitude cycle that occurred in the IPIRG experiment (Ref. 4.14).

For the most part, there does not seem to have been any consideration of these dynamic or cyclic effects in any of the LBB applications reviewed, at least in the past U.S. applications (However, it should be noted that in general most prior domestic LBB submittals, did not involve ferritic materials.) The Koreans, however, are considering dynamic effects on toughness for ferritic pipe due to dynamic strain aging in some of their plants currently under construction. In addition, at one time CE used a safety factor of four on the J-R curve, even for ferritic steels. This was probably sufficient to account for the combination of the dynamic and cyclic loading rate effects for seismic type events. However, as noted, for the most part no evidence has been found during the reviews of the past LBB applications that consideration for these effects has been taken.

### 4.5.6 J-R Curve Limitations

In NUREG-1061 (Ref. 4.4), there was a recommendation on how the J-R curve of a material could be extrapolated. This involved plotting the J-R curve in J-T space, and then linearly extrapolating the curve once  $T_{mat}$  was equal to 50. Considering that ASTM typically has a validity range that limits the maximum amount of crack growth to 10-percent of the ligament, this results in a very conservative extrapolation procedure.

Work during the Degraded Piping Program showed that when using the deformation plasticity based J-R curve ( $J_D-R$ ), Ref. 4.15, the J-R curve with crack growth up to 30-percent of the ligament could be used. Furthermore, making a power-law extrapolation of the  $J_D-R$  gave conservative results compared with J-R curves from larger C(T) specimens with the same thickness.

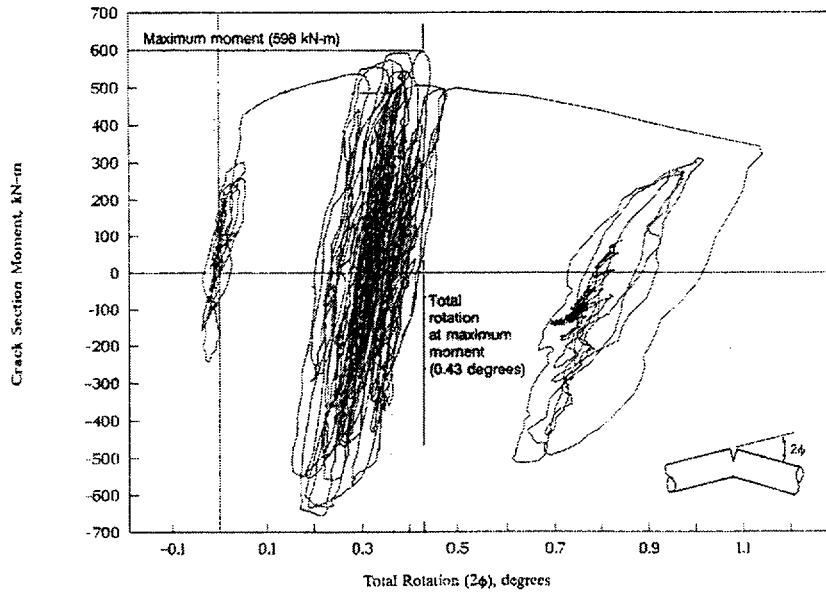


Figure 4.2 Moment-rotation response for Experiment 1-1 from the Second IPIRG program

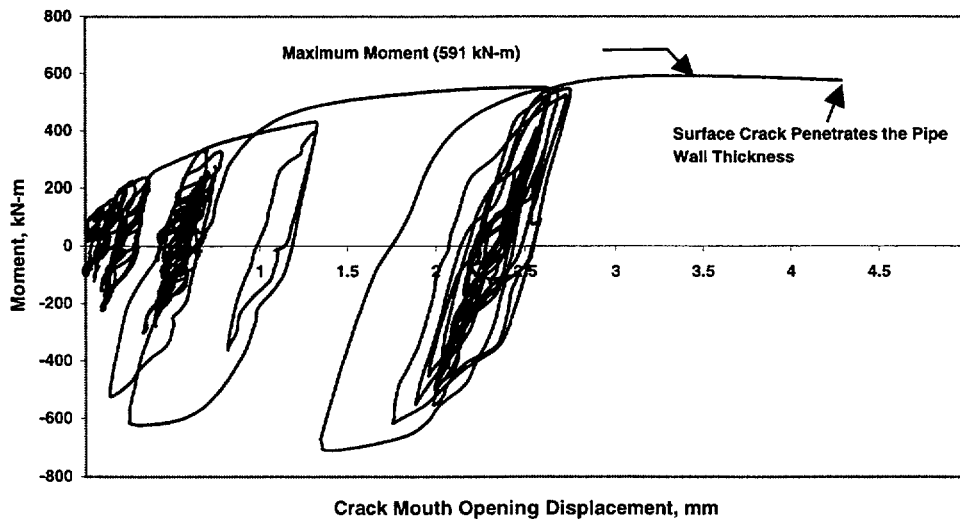


Figure 4.3 Moment-CMOD response for the BINP Task 2 experiment

Furthermore, it was found from the various programs at Battelle (and subsequently validated in French programs), that the Modified J-R curve ( $J_{M-R}$ ) gave a much better prediction of large crack growth and load-displacement records in pipe tests. The  $J_{M-R}$  curve is linearly extrapolated using the crack growth data between 10 and 30-percent of the ligament. It was not uncommon to accurately predict load-displacement behavior for crack growth in through-wall-cracked pipe tests with over 235 mm (9.25-inches) of crack extension at each crack tip when using results from the linearly extrapolated  $J_{M-R}$  of a 1T C(T) specimen. This was an extrapolation of the  $J_{M-R}$  curve maximum crack growth in the 1T C(T) specimen by a factor of 30.

In some of the earlier LBB evaluations, the NRC staff limited the J-R curve of aged cast stainless steels to a maximum J value of 525 kJ/m<sup>2</sup> (3,000 in-lb/in<sup>2</sup>). That was because the highest value J from a laboratory specimen J-R curve was 525 kJ/m<sup>2</sup> (3,000 in-lb/in<sup>2</sup>) for the data available at that time. Current knowledge of J-R curve extrapolation methods and full-scale behavior would allow a more accurate extrapolation procedure that might offer more relief than what was used in the past.

#### 4.5.7 Cracks at Nozzles

Nozzles are frequently analyzed since the high stress locations are typically at nozzle and fitting locations. Frequently these analyses consider the weld and safe end material, but not the nozzle material. Data on the toughness of nozzle materials has been generated at Oak Ridge National Laboratory (ORNL). Such material systems may also involve a bimetallic weld.

In the LBB application reviews, a few cases were found where the nozzle thickness was accounted for in the crack-opening-area analysis for leak-rate considerations by using the greater thickness on the side of the nozzle weld. In one case the weld thickness at the nozzle was less than the nozzle or pipe side due to counter

boring, and the small thickness was used in the fracture analysis.

#### 4.6 Leak-Rate Analysis Aspects

Interestingly, the normal operating loads that determine the postulated crack length for a given leak rate were found to be more important in an LBB analysis than are the magnitude of the faulted (N+SSE) loads (Ref. 4.16). Consequently, close attention should be paid to factors that affect the leak-rate.

In reviewing the various LBB submittals, it was found that one applicant developed their own leak-rate model, which was stated to give comparable results to the PICEP program (Ref. 4.17). However, in examining the surface roughness value they used, this value appeared to be much lower than values statistically determined in NUREG/CR-6004 (Ref. 4.18), i.e., this applicant used a roughness of 0.0076 mm (300 microinch) versus the 0.034 to 0.040 mm (1,325 to 1,595 microinch) roughness values typical of air fatigue and corrosion-fatigue cracks cited in NUREG/CR-6004. Furthermore, this applicant did not use any number of turns in their analysis such as are frequently used in other leak rate codes, like PICEP and SQUIRT (Ref. 4.19). Consequently, the applicant's leak-rate code with their surface roughness values gives smaller cracks for the same leak rate than if the SQUIRT default values were used. Calculations carried out as part of this program showed in an LBB submittal case, the difference in the calculated crack lengths was a factor of 2. This is a non-conservative aspect associated with this applicant's approach.

Another applicant found in a pipe-system analysis of a main coolant pipe system, with a circumferential crack 50 percent of the pipe circumference in length, that the crack opening due to pressure loads was much less (by a factor of 3.8) than when conducting the crack-opening analysis as a simple end-capped vessel. Hence, they recognized what has been recently been called restraint of pressure-induced bending on

the COD for LBB analyses (Ref. 4.16). This is a topic of current research being studied as part of the Battelle Integrity of Nuclear Piping (BINP) program.

#### 4.7 Fracture Mechanics Aspects

In draft SRP 3.6.3 there is guidance for conducting LBB analyses that suggests that only circumferential cracks in the piping welds need to be considered. However, the reviews showed that the high stress regions were either at nozzle locations or at pipe fittings, e.g., elbows. There was no evidence in any of the applications indicating that a straight-pipe to straight-pipe girth weld location was the limiting case, unless there was a cast stainless steel pipe susceptible to significant thermal aging in a straight pipe run.

One applicant considered axial cracks in the body of a pipe elbow. Axial cracks in straight pipe were also considered in this work, although if an axial crack did occur, experimental evidence suggests that it would turn in the circumferential direction and result in a DEGB. Fortunately, axial cracks (other than across girth welds) have not been a problem in nuclear piping. The axial cracks across girth welds are much shorter than the critical crack size, and those due to SCC arrested in the base metal.

In reviewing the actual LBB submittals supplied by the NRC, the Z-factor approach was used in some EPFM fracture analyses. This approach is a simplified EPFM analysis where the Z-factor is simply the ratio of the limit-load solution to the EPFM value. The ASME Z-factors were developed using the crack length (approximately 30 percent of the circumference) that would give a maximum value for a pipe geometry and set of material properties. In LBB applications, large diameter pipe typically would have much smaller crack lengths, so the Z-factors developed for the ASME Section XI flaw acceptance criterion would be conservative. The definition of the flow stress in the ASME Section XI criterion (flow stress equals  $2.4S_m$ ) is also conservative compared to recent results on statistically determining the flow stress for

ferritic pipe (Ref. 4.8). Statistically, the flow stress for both ferritic and austenitic pipe could be defined as either  $1.25(S_y+S_u)/2$  or  $(\sigma_y+\sigma_u)/2$ . For austenitic pipe, the ASME Code had different Z-factor equations for SAW than SMAW welds. However, more recently it has been statistically shown that there is no difference in the toughness of stainless steel SAW and SMAW welds. Hence, the Z-factors for SMAW's should be equal to those for SAW's.

#### 4.8 Stress and System Analysis Aspects

There are many stress analysis and pipe system considerations that affect LBB analyses. Some of those from the LBB reviews are given below.

##### 4.8.1 LBB Analysis Locations

The number of locations analyzed and the method to determine the locations to be analyzed varied considerably in the LBB submittals reviewed. In many cases, the assumed worst case that was analyzed might have had the highest N+SSE stresses, but the second highest N+SSE stress location may have had much lower normal operating stresses, which would result in a longer postulated leakage crack size. In one analysis, the maximum stress value used in the LBB analysis was  $3.56 S_m$  at the hot leg to vessel nozzle weld. However, this was virtually all-normal operating stresses, with trivial SSE loading. Consequently, it is highly doubtful that this was the limiting case for this piping system from a LBB perspective.

The lower normal operating stresses will drive the LBB acceptance more so than having high N+SSE stresses. On the other hand, if the normal operating stresses are very low, then the propensity to develop a crack at that location is much smaller, at least in the absence of residual stresses. Hence, better guidance on what locations should be considered in an LBB analysis is needed.

##### 4.8.2 Secondary Stresses

Thermal expansion and seismic anchor motion stresses (SAM) are typically classified as

secondary stresses. Other classes of secondary stresses are weld residual stresses or thermal gradients through the thickness. For piping fracture on the upper shelf, there is no experimental evidence that says that weld residual stresses should be considered. However, weld residual stresses can play a key role in the crack-opening displacement analyses, important in the determination of the postulated leakage crack size for LBB analyses. On the other hand, thermal expansion and SAM stresses are global secondary stresses and can be more important from a fracture perspective.

Thermal expansion and seismic anchor motion stresses have been found in the IPIRG programs to be important, particularly when the crack size is large enough that the maximum load is close to or below the yield strength of the pipe material, as reflects in Figure 4.4 (Ref. 4.13). Figure 4.4 is a stacked bar chart showing the effect of the different stress components (i.e., primary membrane, primary bending, secondary thermal expansion, and secondary seismic anchor motion) on the fracture behavior of the IPIRG-1 pipe-system experiments. As can be seen in Figure 4.4, the total normalized failure stresses<sup>16</sup> (including both the primary and secondary stress components) for the pipe-system experiments agree closely with the normalized failure stresses for the companion quasi-static, monotonic pipe experiments. If the secondary stresses were ignored, then the normalized failure stresses for the IPIRG-1 pipe-system experiments would have only been a fraction of the normalized failure stresses for the quasi-static pipe experiments. This supports the contention that these types of secondary stresses (thermal expansion and seismic anchor motion) can contribute just as much to the fracture process as do the primary stresses.

During the development of the recent ASME Code Case N-597, it was found that a screening criterion could be developed so that if the failure stress at the flawed pipe section is below yield, then the secondary stresses should be considered

as a primary stress. This is consistent with the local overstrain design requirements in ASME B31.3 and Section III of the ASME Boiler and Pressure Vessel Code for Class 2 and 3 piping. On the other hand, for large diameter pipe in LBB submittals, the crack size is small enough so that failure is typically predicted to be well above yield. For those cases, the pipe would be less sensitive to thermal expansion stresses. However, larger postulated cracks such as in surge lines and smaller diameter pipe systems, may require secondary stresses to be treated as primary stresses. There is also some transition region between very large cracks and small cracks where the secondary stress importance decays nonlinearly with the flaw size, pipe system geometry, and material strain hardening characteristics. This is another aspect being examined as part of the BINP program. If a complete (anchor to anchor) dynamic elastic-plastic pipe system analysis, with the crack properly modeled, is properly conducted, then the significance of secondary stresses is automatically included in a technically correct manner.

---

<sup>16</sup> Normalized by the Net-Section-Collapse stress to account for differences in crack size, etc. between experiments.

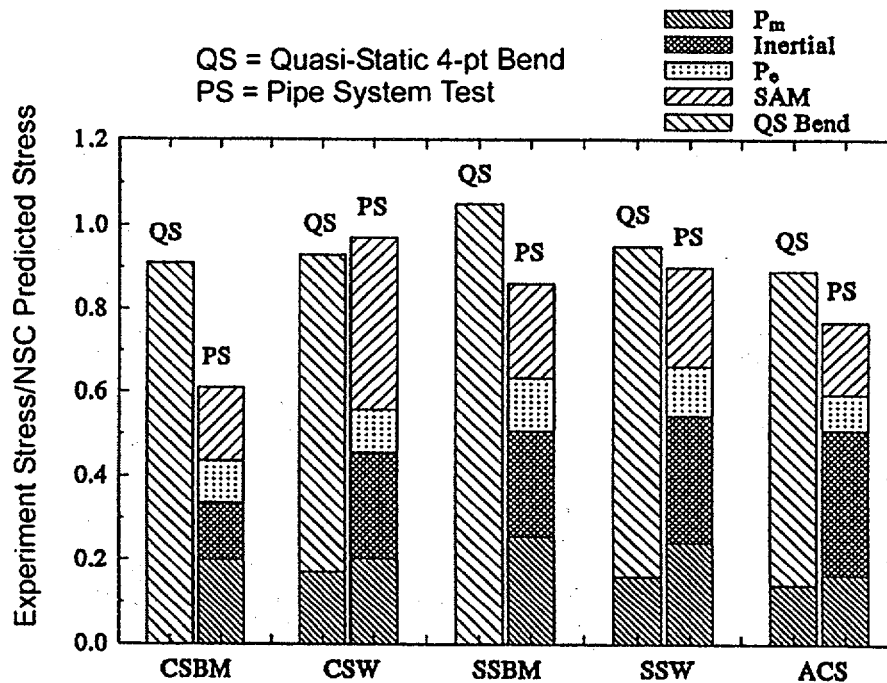


**Figure 4.4** Bar chart showing the effect of the different stress components (i.e., primary membrane, primary bending, secondary thermal expansion, and secondary seismic anchor motion) on the fracture behavior of the IPIRG-1 pipe-system experiments

SAM stresses are dynamic secondary stresses, that, as is the case for thermal expansion stresses, are generally considered less significant than primary stresses. However, as is the case for thermal expansion stresses, SAM stresses do often contribute to fracture, just as their primary stress counterparts do, see Figure 4.4. In reviewing the LBB applications, it is not clear if the SAM stresses were typically considered in these LBB applications. Some examples are:

- One vendor included the SAM stresses with inertial stresses for piping inside containment. SAM stresses were determined by assuming 180-degree out-of-phase behavior of major components in the containment building. This was a worst case assumption. The SAM stresses were ignored in other buildings.
- Another vendor did not explicitly state that it used SAM stresses in most of its submittals, but a few of the more recent

submittals noted that the SAM stresses were considered with the SSE stresses.

Note for some older plants, designed to B31.1 standards, it may not be possible to extract the seismic anchor motion stresses from the stress report. For these cases, the NRC may have to provide some default values in the Regulatory Guide that the applicant can use. Alternately, the applicant may have to go back and do additional analysis. For surge line analysis, the applicant can get by without these seismic anchor motion stresses since the faulted condition for the surge line typically does not consider SSE type loadings.

It is also of note that this discussion of the inclusion of secondary stresses is inconsistent with certain sections of the ASME Code. For Section III Level C and D analysis, one does not have to consider secondary stresses. For Section XI, secondary stresses are considered, but with reduced margins.

Also, draft SRP 3.6.3 did consider them, with full margin, for the case of submerge-arc and shielded-metal-arc welds, but draft SRP 3.6.3 was not always applied consistently.

#### 4.8.3 Torsional Stresses

Torsional stresses were seldom considered in LBB submittals. In one case, it was shown that the torsional stresses were lower than the bending stresses. This was then used as a justification for not including the torsional stresses in the analysis. This is considered to be poor justification for totally excluding the torsional stresses. NUREG/CR-6299 (Ref. 4.20) showed that a Von Mises combination of the torsional and bending stresses gives an equivalent bending stress that will give the same J or COD values as if a full bending and torsional FEM analysis was conducted. Hence, a methodology already exists for handling torsional stresses in a simple manner for LBB analyses of circumferential through-wall cracks.

#### 4.9 References

- 4.1 "Leak-Before-Break Evaluation Procedures," draft Standard Review Plant 3.6.3, August 1987.
- 4.2 "Piping and Fitting Dynamic Reliability Program – Program Summary," EPRI TR-102792, Vols. 1-5, 1995.
- 4.3 "Probability of Pipe Fracture in the Primary Coolant Loop of a PWR Plant," NUREG/CR-2189, Vols. 1-9, September 1981.
- 4.4 "Report of the U.S. Nuclear Regulatory Commission Piping Review Committee. Evaluation of Potential for Pipe Breaks," NUREG-1061, Vol. 3, November 1984.
- 4.5 Scott, P. M., and others, "Fracture Evaluations of Fusion Line Cracks in Nuclear Pipe Bimetallic Welds," NUREG/CR-6297, April 1995.
- 4.6 Bonnet, S., and others, "Relationship Between Evolution of Mechanical Properties of Various Cast Duplex Stainless Steels and Metallurgical and Aging Parameters: An Overview of Current EDF Programmes," *Material Science Technology*, Vol. 6, pp 221-229, 1990.
- 4.7 Chopra, O., and others, "Long-Term Embrittlement of Cast Duplex Stainless Steels in LWR Systems," NUREG/CR-4744, Vol. 4, No. 2, June 1991.
- 4.8 Krishnaswamy, P., and others, "Fracture Behavior of Short Circumferentially Surface-Cracked Pipe," NUREG/CR-6298, November 1995.
- 4.9 Rosenfield, A. R., and others, "Stainless Steel Submerge Arc Weld Fusion Line Toughness," NUREG/CR-6251, April 1995.
- 4.10 Marschall, C. W., and others, "Loading Rate Effects on Strength and Fracture Toughness of Pipe Steels Used in Task 1 of the IPIRG Program," NUREG/CR-6098, October 1993.
- 4.11 Rudland, D. L., and others, "The Effects of Cyclic and Dynamic Loading on the Fracture Resistance of Nuclear Piping Steels," NUREG/CR-6440, December 1996.
- 4.12 Marschall, C. W., and others, "Effect of Dynamic Strain Aging on the Strength and Toughness of Nuclear Ferritic Piping at LWR Temperatures," NUREG/CR-6226, October 1994.
- 4.13 Scott, P. M., and others, "IPIRG-2 Task 1 – Pipe System Experiments with Circumferential Cracks in Straight-Pipe Locations," NUREG/CR-6389, February 1997.
- 4.14 Olson, R., and others, "Effect of Cyclic Loads on the Fracture Behavior of Stainless Steel Pipes with High and Low Sulfur Contents," to be published in *16<sup>th</sup> International Conference on Structural Mechanics in Reactor Technology*, Paper No. 1759, Division G, August, 2001.
- 4.15 Papaspyropoulos, V., and others, "Predictions of J-R Curves with Large Crack

Growth from Small Specimen Data,”  
NUREG/CR-4575, September 1986.

4.16 Ghadiali, N., and others, “Deterministic and Probabilistic Evaluations for Uncertainty in Pipe Fracture Parameters in Leak-Before-Break and In-Service Flaw Evaluations,” NUREG/CR-6443, June 1996.

4.17 Norris, D., and others, “PICEP: Pipe Crack Evaluation Program,” EPRI Report NP-3596-SR, 1984.

4.18 Rahman, S., and others, “Probabilistic Pipe Fracture Evaluations for Leak-Rate-Detection Applications,” NUREG/CR-6004, April 1995.

4.19 Paul, D. D., and others, “Evaluation and Refinement of Leak-Rate Estimation Models,” NUREG/CR-5128, Rev. 1, June 1994.

4.20 Mohan, R., and others, “Effects of Toughness Anisotropy and Combined Tension, Torsion, and Bending Loads on Fracture Behavior of Ferritic Nuclear Pipe,” NUREG/CR-6299, January 1995.

## 5 RECENT RESEARCH RESULTS (1985 – 2001)

When draft SRP 3.6.3 was published in 1987, there were research activities underway that had the potential to improve the final form of this SRP section. It was decided at that time that the final SRP 3.6.3 would not be issued until those research activities were completed. Now that research is coming to a close, it was deemed appropriate to review that research and how it would impact LBB. The state-of-the-art in pipe fracture technology at the time of the 1987 publication of draft SRP 3.6.3 will first be discussed in Section 5.1. Then, a summary of the major research programs related to LBB will be presented in Section 5.2. Finally, some of the key results from these programs as they relate to LBB will be presented in Section 5.3.

### 5.1 State-of-the-Art in Pipe Fracture Technology, Circa 1985

When draft SRP 3.6.3 was published in 1987, research in the area of pipe fracture technology was at a crossroads. While some early studies had been completed, the major research initiatives were just beginning. In 1985, the PICEP (Pipe Crack Evaluation Program) leak rate code was just coming on the scene (Ref. 5.1). The thermal-hydraulics model in PICEP, like SQUIRT that was developed later as part of the IPIRG programs, is based on the Henry-Fauske model for two-phase flow through long channels (Ref. 5.2). PICEP was capable of predicting both the leak-rate through a crack, as well as the crack-opening-displacements (COD) needed for estimating the length of the postulated leakage crack size for an LBB analysis. For the PICEP code, the original GE/EPRI analysis functions (Ref. 5.3) used to predict COD.

Part of the validation of the PICEP Code was based on a Battelle research program from the early 1980's for the Electric Power Research Institute (EPRI) that studied the two-phase flow through intergranular stress corrosion cracks (IGSCC), Ref. 5.4. As part of this program, extensive experimental data were developed that

were used in the validation of the PICEP code. In the first phase of this program, leak-rate experiments were conducted in which the flow characteristics through slits and simulated cracks were studied. In the second phase, the focus was on the flow characteristics through actual stress-corrosion cracks. In addition, as part of this program, the resulting acoustic-emission signatures for these leaking through-wall cracks were analyzed as an assessment of the feasibility of using acoustic-emission technology as a leak-detection system for nuclear power plant piping systems. In addition to PICEP, there were other proprietary leak-rate codes being used by applicants for LBB submittals.

In 1985, the J/T tearing instability approach (Ref. 5.5) was the generally preferred method for pipe flaw evaluation instability predictions. Tearing instability theory states that a crack in a ductile material will tear in a stable manner when it is loaded beyond the point where the applied J value exceeds the  $J_{Ic}$  of the material and the applied tearing modulus ( $T_{applied}$ ) is less than the tearing modulus of the material ( $T_{material}$ ). Conversely, a crack in a ductile material will tear in an unstable manner when it is loaded beyond the point where the applied J value exceeds the  $J_{Ic}$  of the material and  $T_{applied}$  is greater than  $T_{material}$ . In this approach, the slope of the J-R curve ( $dJ/da$ ) was initially considered to be constant beyond the point of crack initiation ( $J_{Ic}$ ), see Figure 5.1, and was normalized by the elastic modulus and the flow stress of the material such that the tearing modulus (T) is defined as:

$$T = \frac{dJ}{da} \times \frac{E}{\sigma_f^2} \quad (5.1)$$

where,

T = tearing modulus,  
E = elastic modulus,  
 $dJ/da$  = slope of the J-R curve,  
 $\sigma_f$  = flow stress =  $(\sigma_y + \sigma_u)/2$ ,  
 $\sigma_y$  = yield strength, and

$\sigma_u$  = ultimate strength.

the applied and material curves was used to determine the instability.

Later, it was recognized that the  $J_{\text{material}}-T_{\text{material}}$  curve could be nonlinear, and a graph of  $J/T$  for

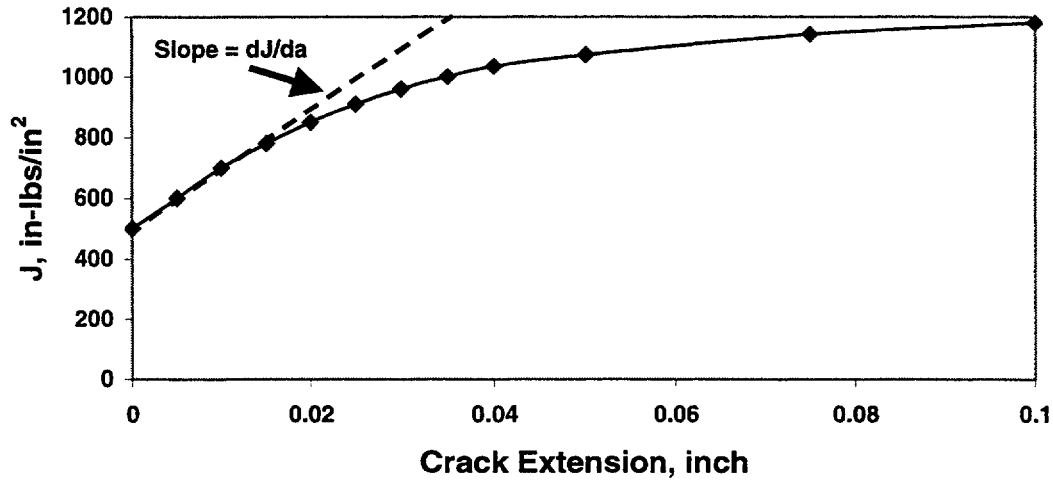


Figure 5.1 Example J-R curve showing constant slope  $dJ/da$  used in Tearing Modulus (T) determination

In 1985, the GE/EPRI handbook (Ref. 5.3) was under development and was being used to estimate applied J values for cracked structures. In estimating J, the elastic and plastic components are determined separately and then added together.

$$J = J_e + J_p \quad (5.2)$$

where,

$J_e$  = elastic component of J and  
 $J_p$  = plastic component of J.

For the case of bending, the elastic component of J is a function of the bending moment (M), the elastic modulus (E), and the elastic F-function ( $f_1$ ), Ref. 5.6.

$$J_e = f_1 \frac{M^2}{E} \quad (5.3)$$

The plastic component of J is a function of crack size (c) or remaining ligament ( $\pi R - c$ ), the applied load or moment (P or M), the limit load

or moment ( $P_0$  or  $M_0$ ), the stress strain characteristics of the material as defined by the Ramberg-Osgood relationship, and an influence function  $h_1$  that is a function of the crack size, R/t ratio, and strain hardening exponent (n) of the material.

$$J_p = \alpha \sigma_0 \epsilon_0 (\pi R - c) h_1 \left( \frac{P}{P_0} \right)^{n+1} \quad (5.4)$$

where, the Ramberg-Osgood stress strain relationship is defined as:

$$\frac{\epsilon}{\epsilon_0} = \frac{\sigma}{\sigma_0} + \alpha \left( \frac{\sigma}{\sigma_0} \right)^n \quad (5.5)$$

where,

- $\sigma$  = stress
- $\epsilon$  = strain
- $\sigma_0$  = reference stress (typically the yield strength)
- $\epsilon_0$  = reference strain =  $\sigma_0/E$
- $\alpha$  = curve fitting parameter, and

$n$  = strain hardening exponent.

In 1985, tabulated solutions for the influence function  $h_1$  existed for through-wall-cracked pipe in the GE/EPRI handbook as a function of crack size,  $R/t$ , and  $n$ . Note, since the initial publication of this handbook, these functions have been updated extensively. In addition, since that time, numerous other J-estimation scheme methods have been developed (Refs. 5.7 through 5.9).

In addition to J-based tearing instability theory, limit-load solutions such as the Net-Section-Collapse analysis method were also available for predicting the critical crack size of a cracked piping system. Unlike the J-based solutions, the limit-load analyses do not require knowledge of the fracture toughness of the material. They depend solely on a knowledge of the strength, as measured in terms of flow stress, in their prediction of the critical crack size. Obviously, this independence of toughness required a screening criterion to define its limits of applicability. In the draft SRP 3.6.3, the use of the limit-load equations was limited to stainless steel piping (with its inherent high toughness). Furthermore, for cracks in lower toughness welds (e.g., submerge-arc welds (SAW) and shielded-metal-arc welds [SMAW]) in stainless steel pipe, a stress multiplier factor (i.e., Z-factor) was applied to account for the crack being postulated in the lower toughness material. This Z-factor is a function of the pipe diameter, which is another key factor in determining whether a cracked pipe will reach fully plastic conditions.

Such was the state-of-the-art in LBB technology at the time of the publication of the draft SRP 3.6.3 on leak-before-break. Extensive research on the subject has been carried out since that time.

## **5.2 Summary of Major Research Programs Related to LBB**

In this section some of the major research programs related to LBB are summarized. Details of the key results are presented in Section 5.3 below.

### **5.2.1 Battelle Programs**

The key Battelle Programs are:

**5.2.1.1 Battelle/EPRI Program on Circumferentially Cracked Stainless Steel Pipe** – In the 1970's Battelle conducted a program for EPRI aimed at developing analysis methods for predicting the load-carrying capacity of circumferential cracks in stainless steel piping (Ref. 5.10). One of the key outcomes of this program was the development of the Net-Section-Collapse (NSC) limit-load analysis. This NSC analysis still serves as the technical basis for the limit-load analysis embodied in the draft SRP 3.6.3 methodology.

**5.2.1.2 Battelle/EPRI Study on Two-Phase Flow Through IGSCC** – In the late 1970's and early 1980's Battelle conducted another program for EPRI. This program focused on developing and validating models for predicting the two-phase flow characteristics through cracks (Ref. 5.4). The first phase of this program examined the flow characteristics through slits and simulated cracks while the second phase looked at the flow characteristics through actual stress-corrosion cracks. Extensive leak-rate data were developed for use in the validation and extension of a leak-rate analysis first established in an NRC study on cold-leg integrity (Ref. 5.11). In addition, acoustic emission technology was studied as a possible means of detecting leaking cracks in service. One of the inadvertent observations pertinent to LBB that came out of this work was the effect of particulate plugging on the leak rate through tight cracks. At times, crud in the test system would temporarily shut off the flow of fluid through the crack. Typically the potential impact of this crud on the leakage flaw size predictions is not addressed in modern day LBB analysis.

**5.2.1.3 Degraded Piping Program (Phases I and II: 1981 - 1989)** – The Degraded Piping Program (Phases I and II), Refs. 5.12 and 5.13 were the first in a series of major research initiatives funded by the USNRC with a focus of developing the tools for predicting the fracture behavior of cracked nuclear power plant piping systems. The program had both analytical and

experimental aspects. A number of sophisticated (at least at the time) analysis routines were developed for predicting the fracture behavior of circumferentially cracked pipe. In addition, numerous full-scale pipe experiments were conducted to validate these analysis routines. Some of the key technical topics examined as part of these programs that are applicable to LBB include:

- An extrapolation method for predicting large scale crack growth from small scale fracture toughness specimens (Ref. 5.14) was developed. This work documented in NUREG/CR-4575 was referenced specifically in the draft SRP 3.6.3.
- Cracks in welds (TIG and SAW/SMAW) were assessed (Ref. 5.15).
- J-estimation scheme analyses for circumferentially oriented through-wall cracks were developed. Such J-based analyses most likely will form the basis of the critical crack size analyses used in future LBB applications.
- A screening criterion for assessing the adequacy of limit-load analyses was developed (Ref. 5.16).
- The fracture behavior of complex cracks, i.e., long circumferential part through surface cracks that penetrate the pipe wall thickness for a relatively short extent, representative of the IGSCC cracks discovered in the Duane Arnold plant, was assessed (Ref. 5.17). Analysis and experiments clearly demonstrated the low tearing resistance of such a crack, supporting the draft SRP position of excluding lines susceptible to IGSCC from LBB considerations.
- Dynamic strain aging was identified as a potential degradation mechanism for ferritic nuclear pipe steels (Ref. 5.18) at LWR temperatures. Dynamic strain aging causes both a lowering of the ultimate strength and fracture toughness at elevated temperatures when these materials are loaded at dynamic loading rates. In addition, some of the crack instabilities, i.e., crack jumps, that were observed in some of the carbon steel

through-wall-cracked pipe experiments were attributed to dynamic strain aging.

#### **5.2.1.4 International Piping Integrity Research Group (IPIRG) programs (First and Second: 1986 - 1997) –**

One of the outcomes of the Degraded Piping Program Phase II was the development of the IPIRG organization. This was a group of 12 to 15 international organizations who shared a common interest in the subject of nuclear pipe fracture technology. One of the major advantages of IPIRG was that of cost sharing. (Another advantage was the sharing of ideas and information between the members of the group.) Organizations could pool their resources such that some very large (i.e., costly) experiments that would have been difficult, if not impossible, for a single entity to fund, could be conducted. Some of the key technical topics pertinent to LBB that came out of these programs included:

- The SQUIRT leak-rate code was developed and validated (Ref. 5.19). The SQUIRT code is a two-phase leak-rate code based on the Henry-Fauske flow model that includes a number of separate modules for predicting leak rates and crack-opening-displacements, both of which are necessary for LBB analyses.
- The effects of cyclic loading during ductile tearing on the fracture toughness of nuclear piping steels were investigated (Ref. 5.20),
- The effect of sulfur content on the fracture toughness properties of stainless steel pipes was examined (Ref. 5.21),
- Pure inertially loaded pipe tests were conducted that showed unstable crack growth within four cycles of reaching maximum load,
- Pipe-system experiments were conducted with combined pressure, thermal expansion, inertial, and seismic anchor motion stresses. These experiments showed that for large cracks the secondary stresses acted as primary stresses, and
- A special purpose cracked-pipe element was developed for pipe-system analysis that allowed for the prediction of surface flaw penetration and resulting through-wall crack

growth in a time-history analysis. This procedure was initially used to design the pipe-system experiments, and later was used to assess margins when using elastic uncracked pipe analyses.

**5.2.1.5 Short Cracks in Piping and Piping Welds Program (1990 – 1994)** – The Short Cracks in Piping and Piping Welds program was a 5-year program funded solely by the USNRC whose main focus was to extend the work developed earlier as part of the Degraded Piping and First IPIRG programs by focusing attention on crack sizes more typically considered in LBB or pragmatic in-service flaw evaluations. Some of the key aspects of this program that are pertinent to LBB include:

- The effects of off-centered cracks on LBB was studied (Ref. 5.22),
- Two probabilistic analyses (PSQUIRT and PROLBB) that could be used in LBB analyses were developed (Ref. 5.23),
- Some enhancements to J-estimation scheme analyses for circumferentially oriented through-wall cracks in pipe were developed (Ref. 5.9),
- Various aspects to more accurately predict the crack-opening-area (COA) for through-wall cracks were developed (Ref. 5.24),
- Statistically-based crack morphology parameters to be used in leak-rate analyses were developed (Ref. 5.23),
- A more detailed study on the effects of dynamic strain aging on the material properties of ferritic nuclear piping steels was conducted (Ref. 5.25),
- A study of the fracture behavior of bimetallic welds (Ref. 5.26) with Inconel 182 weld metal showed the carbon steel to inconel fusion line had similar fracture resistance as the A516 Grade 70 steel,
- The impact of the fusion line toughness values on the stability of through-wall cracks in stainless steel welds was examined (Ref. 5.27), and
- A methodology was developed for assessing the effects of toughness anisotropy on the fracture behavior of circumferentially oriented through-wall cracks in ferritic

nuclear piping (Ref. 5.28). Toughness anisotropy becomes an especially important consideration when the piping system is subjected to high torsional stresses.

**5.2.1.6 Battelle Integrity of Nuclear Piping (BINP) Program** – At the end of the Second IPIRG program, Battelle was charged with the responsibility of identifying any holes remaining in the technology that may still need to be addressed in the area of pipe fracture technology. The results of this analysis were documented in NUREG/CR-6443 (Ref. 5.22). At about the same time, the USNRC held a series of piping review meetings with knowledgeable organizations to solicit their feedback as to what additional research may be needed in this area. As a result of the Battelle study and the NRC's piping review committee meetings, a prioritized list of potential research topics was identified. The BINP program was developed to address the most pressing of those topics. Some of the key outcomes from the BINP program, which is still ongoing, that are pertinent to LBB will include:

- An assessment of the effects of secondary stresses on pipe fracture,
- An assessment of the additional margins that might be realized through the use of nonlinear analysis,
- An assessment of the effects of the restraint-of-pressure-induced bending on the crack-opening displacements (COD) for LBB analyses, and
- An assessment of the effects of weld residual stresses on the COD for LBB analyses.

## **5.2.2 Research Programs Conducted at Argonne National Laboratories**

The two research initiatives pertinent to LBB that were conducted at Argonne National Laboratories (ANL) were their work in the areas of corrosion fatigue and thermal aging of cast stainless steels.

### 5.2.2.1 Corrosion Fatigue

In the early 1990's, researchers at ANL reviewed the data in the literature with the aim of developing new fatigue design curves for carbon, low-alloy, and austenitic stainless steels in light water reactor (LWR) environments, Ref. 5.29. The existing ASME Section III Appendix I design curves were based on air data at moderate to lower temperatures, i.e., less than 700 F for carbon steels and 800 F for austenitic steels. Environmentally assisted-cracking (EAC) data from a number of sources were analyzed statistically by ANL in the development of these new design curves. In addition, the design curves were extended for lives between  $10^6$  to  $10^8$  cycles in that systems can accumulate cycles far in excess of the existing  $10^6$  limit due to turbulent mixing of hot and cold fluid streams or flow-induced vibrations. These EAC interim design curves may effect a new LBB methodology with regard to satisfying restrictions such as that imposed by the draft SRP 3.6.3 that "an evaluation be performed to assure that the potential for pipe rupture due to thermal and mechanical induced fatigue is extremely low."

### 5.2.2.2 Thermal Aging Cast Stainless Steels

Argonne National Laboratories conducted a ten-year program from the fall of 1982 to the fall of 1992 for the USNRC aimed at understanding the effects of long-term embrittlement of cast duplex stainless steels in light water reactor (LWR) systems (Refs. 5.30 through 5.33). The scope of this investigation included the following goals: (1) characterize and correlate the microstructure of in-service reactor components and laboratory-aged material with loss of fracture toughness to establish the mechanism of aging and validate the simulation of in-reactor degradation by accelerated aging, (2) establish the effects of key compositional and metallurgical variables on the kinetics and extent of thermal embrittlement, and (3) develop the methodology and correlations necessary for predicting the toughness loss suffered by cast stainless steel components during the normal and extended life of LWRs.

### 5.2.3 Foreign Programs

At the same time as all this work was going on in the United States, other countries had their own ongoing programs in the area of pipe fracture technology. The Japanese (Ref. 5.34) and French (Ref. 5.35) were developing their own LBB procedures (see Section 7), and were developing an extensive database of pipe experiments for validation purposes. In the sections that follow some of the work conducted in Japan, France, England, and Germany are briefly summarized. Note, that other countries were also conducting research in this area, but for the sake of brevity, this discussion will be limited to these four major contributors. For a more detailed discussion of the types of ongoing overseas research activities, the reader is referred to Section 1 of the "State-of-the-Art Report on Piping Fracture Mechanics" (Ref. 5.36).

#### 5.2.3.1 Japan

The Japanese have always been one of the leaders in the area of piping integrity research. Some, although not all, of the programs related to LBB that they have been involved with are discussed below.

One of the early programs conducted in Japan was the NUPEC/MITI TP304 pipe fracture instability program (Ref. 5.37). This program, completed in 1981, examined pipe instability of circumferential through-wall and surface flaws under compliant axial tension loading. The compliant loading refers to the fact that there were springs in series with the pipe specimen to simulate the elastic energy that would be available in an actual piping system due to having a much longer pipe system than available in the length of the test pipe.

Later in Japan, JAERI, which was funded by the Science and Technology Agency (STA), conducted a series of 6-inch and 16-inch diameter pipe experiments using both TP304 stainless steel and STS42 carbon steel pipe samples (Ref. 5.38). These tests were four-point bend tests, generally without pressure, and typically at room temperature, sometimes with

higher compliance for instability evaluations, and with either circumferential through-wall or surface cracks.

In the late 1980's, JAERI again was funded by STA to conduct a series of 4- and 6-inch diameter pipe-system experiments (Ref. 5.39). A sketch of the pipe system used in these experiments is shown in Figure 5.2. Pressurized, room temperature tests were conducted, with and without initial flaws. The loading consisted of constant amplitude

sinusoidal blocks at 8 Hz for 10 seconds, or a seismic load history of similar duration. In one of the long circumferential surface crack experiments, a complete break occurred in approximately 4 to 7 cycles after the surface crack penetrated the pipe wall thickness. These experiments, which involved a more complicated (but smaller) pipe system than the IPIRG pipe system, showed that inertial stresses can cause a complete failure of the cracked-pipe section.

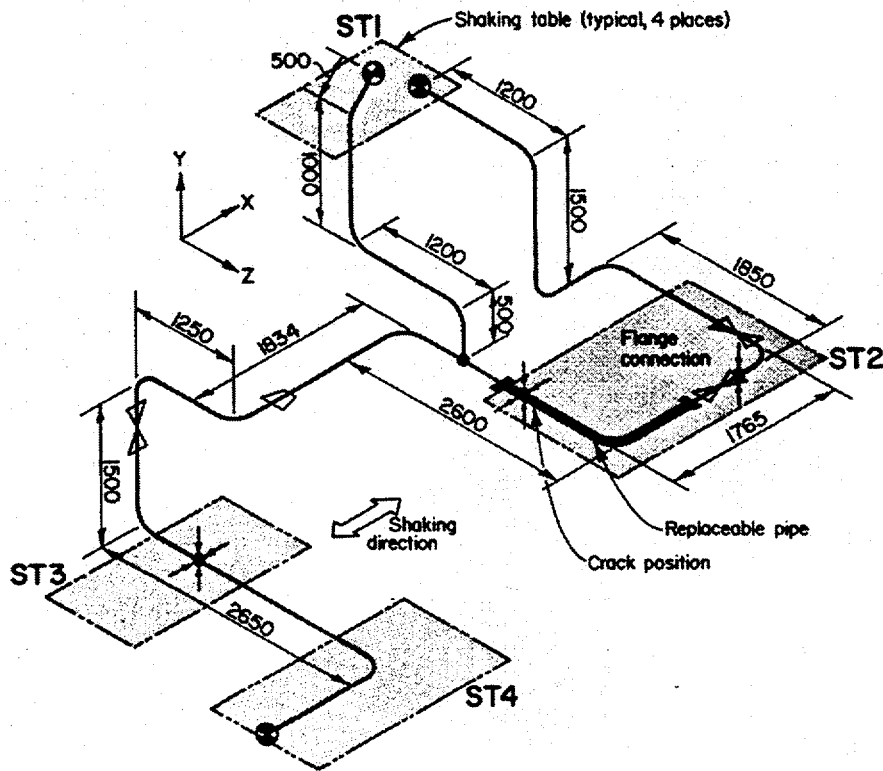


Figure 5.2 STA pipe system for dynamic flawed pipe tests

Somewhat related to the piping fracture work were various studies on jet forces, thrust loads, and pipe whip from DEGB failures. Significant efforts in this area were conducted at JAERI (Refs. 5.40 and 5.41).

In 1990, the Japanese completed a program on carbon steel pipe fracture at NUPEC (Ref. 5.42). These tests were quasi-statically loaded pipe tests on 6-inch and 16-inch diameter pipe. Related to this effort, two 30-inch diameter

Schedule 80 pipe experiments were conducted at Battelle on Japanese carbon steel pipe under pressure and bending at 300 C (572 F) as part of the IPIRG-1 program. The pipes tested generally had sufficient toughness to fail at limit-load conditions.

Additional carbon steel pipe tests (Ref. 5.43) were conducted in Japan in the mid 1990's to evaluate whether Japanese carbon steel piping was susceptible to the dynamic and cyclic

degradation observed in the IPIRG-1 program (Ref. 5.44).

### 5.2.3.2 France

Researchers in France conducted considerable research in the area of structural integrity of nuclear power plant piping systems. Their work covered a variety of topics. One of the most significant pieces of work that they conducted was some work in the area of the effects of aging on cast stainless steels (Ref. 5.45).

### 5.2.3.3 United Kingdom

The R6 analysis method was developed originally by the Central Electric Generating Board (CEGB) in the United Kingdom (Ref. 5.46). It has become one of the most widely used fracture analysis programs used in the world. The current R6 Revision 3 method was published in 1986 with several different optional analysis levels. The general approach was to predict crack initiation and fracture loads

through the use of a dimensionless failure assessment diagram, or FAD curve, see Figure 5.3. Assessment points falling inside the FAD curve are deemed safe while points outside the curve are not necessarily unsafe, but at least require additional scrutiny. In all cases, the ratio of the applied load to the limit load is plotted on the abscissa, and the ratio of linear elastic stress intensity to material toughness is plotted on the ordinate. In this methodology, there is an interpolation between linear elastic (brittle) failure and limit-load (or plastic collapse) failure. The simplest option uses a fixed FAD curve when the stress-strain curve of the material is unknown. The second option uses a fixed formula for incorporating the material's stress-strain curve in the shape of the FAD curve, but does not account for geometry effects. The last option, essentially allows the user to use any more sophisticated analysis method (e.g., FEM, GE/EPRI J-estimation scheme) to account for material and geometry effects, and puts these analyses in the format of a FAD curve.

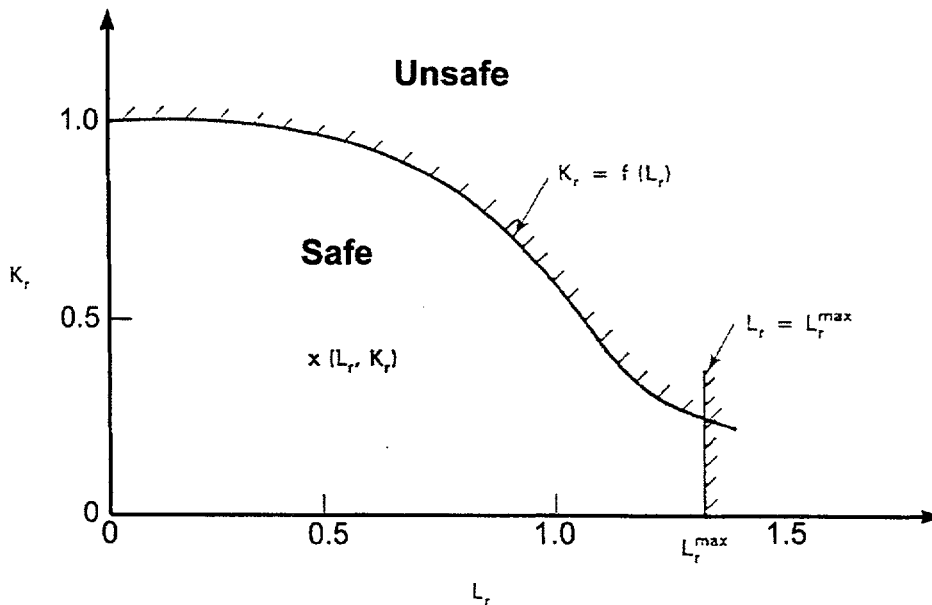


Figure 5.3 R6 failure assessment diagram (FAD)

### 5.2.3.4 Germany

MPA-Stuttgart in Germany undertook several programs for the German government on the

burst strength of German pipe. The "Phänomenologische Behälterberstversuche - Phase I" report was completed in 1985 (Ref. 5.47). This report concentrated on axial cracks

and a few circumferentially cracked pipes at operating temperatures under pressure loads. Such flaws cause very dynamic crack openings and are very energetic. Interesting data on dynamic depressurization, opening area, and velocities of severed pieces of pipes (end capped and pressurized to failure) were developed. The MPA Phase II effort was completed in 1987 (Ref. 5.48). This effort took a closer look at large-diameter low-alloy-steel pipe with circumferential flaws tested at LWR pressures and temperatures. These German projects led to the development of their "Basis Safety Approach" (Ref. 5.49) for LBB. (See Section 7 of this report for additional details.) As part of this approach, they postulated that the instantaneous DEGB design criteria could be replaced with a criterion that said that the crack-opening area would be at most 10 percent of the pipe cross-sectional area.

#### 5.2.4 Leak-Before-Break Conferences

Between 1984 and 1995, six international Leak-Before-Break Conferences were held throughout the world so that individuals working in the area of LBB could come together to discuss LBB related issues. Proceedings of the papers presented at these conferences were published (Refs 5.50 through 5.55). The locations and dates of these conferences were:

- Monterey, California – September 1983
- Columbus, Ohio – October 1985
- Tokyo, Japan – May 1987
- Taipei, Taiwan – May 1989
- Toronto, Canada – October 1989
- Lyon, France – October 1995.

### 5.3 Key Results from Recent Research Applicable to Leak-Before-Break

In this section of the report, some of the key results from the recent research (since 1985) that are applicable to LBB will be discussed. The presentation of these results will be broken out by the major elements associated with an LBB analysis, i.e.,

- Leak-rate analyses for determining postulated leakage crack size,
- Subcritical crack growth analysis,
- Material issues,
- Stress analyses,
- Fracture and stability analyses, and
- Probabilistic analyses.

#### 5.3.1 Leak-Rate Analyses

**5.3.1.1 Leak-Rate Codes** – A number of leak-rate codes have been developed and validated for use in determining the postulated leakage crack size used in an LBB analysis. Two of these codes, PICEP and SQUIRT, have undergone an informal peer-review process and the details of their technical bases are fairly well known in that they have been documented in the literature. These codes and have been used fairly extensively by a number of different organizations. A third proprietary code, that has been used in a number of actual past LBB applications, is not as well understood due to its proprietary nature. There are also some international codes, i.e., Daftcat from Nuclear Electric in England and FLORA from Siemens in Germany.

The thermal hydraulics models in both PICEP and SQUIRT have as their basis the Henry-Fauske model (Ref. 5.2) for two-phase flow through long channels<sup>17</sup>. Some of the key parameters contributing to the mass flow equation of Henry-Fauske are the:

- quality of the fluid,
- pipe diameter,
- flow path length,
- pressure losses due to entrance effects,
- pressure losses due to friction effects,
- pressure losses due to crack flow path losses,
- pressure losses due to the acceleration of the fluid, and

---

<sup>17</sup>The PICEP code is currently able to handle single-phase flow conditions and the SQUIRT code is currently being upgraded so that it can also handle single-phase flow conditions.

- pressure losses due to the crack cross section area changes.

Some of the factors that affect these pressure loss terms are the:

- hydraulic diameter, which is a function of the COD,
- surface roughness, and
- number of turns that the fluid has to take as it transverses along the flow path.

Both PICEP and SQUIRT are equipped to predict the crack-opening-displacements needed to estimate the leakage size crack for a given leak-rate detection capability. PICEP uses the original GE/EPRI solutions while SQUIRT has the option of using either the GE/EPRI method as modified by Battelle (Ref. 5.9), the LBB.ENG2 method (Ref. 5.8), or the original GE/EPRI method (Ref. 5.3). The GE/EPRI solutions for pure bending and pure tension are widely used and documented, but for combined loading the solutions are not well documented. Consequently, a sensitivity study was conducted to compare the center COD values for combined loading using the SQUIRT, PICEP, and 3D FEM solutions for various pipe diameters, crack lengths, and materials (carbon versus stainless steel). These results are presented in Section 5.3.5.3. Nevertheless, all these solutions assume the pipe is an end-capped vessel where the ends are free to rotate due to induced bending at the crack plane. This induced bending is assumed to be independent of the applied bending, which is strictly not correct. This effect of pipe system boundary conditions on the induced-bending is discussed in Section 5.3.1.2.

**5.3.1.2 Factors Influencing the Leakage Crack Size Predictions** – There are a number of factors that influence the leakage crack size predictions. These include the:

- crack morphology parameters,
- restraint of pressure induced bending on the crack-opening displacements,
- effect of weld residual stresses on the crack-opening displacements,
- effect of crack-face pressure on the crack-opening displacements,
- effect of the crack being centered off the maximum bending plane, and
- uncertainty issues such as particulate plugging.

**Crack Morphology Parameters** – The key crack morphology parameters which impact the leak rate through a crack are; (1) the surface roughness, (2) the number of turns in the leakage path, (3) the entrance loss coefficients, and (4) the ratio of the actual crack path length to the pipe thickness.

In Reference 5.23, a statistical analysis of surface roughness values was conducted for IGSCC and fatigue cracks (air environment) for stainless steel pipe materials and fatigue cracks (corrosion and air environment) for carbon steel pipe materials. Both global ( $\mu_G$ ) and local ( $\mu_L$ ) roughness values were considered, see Figure 5.4. Table 5.1 summaries the results from this statistical analysis.

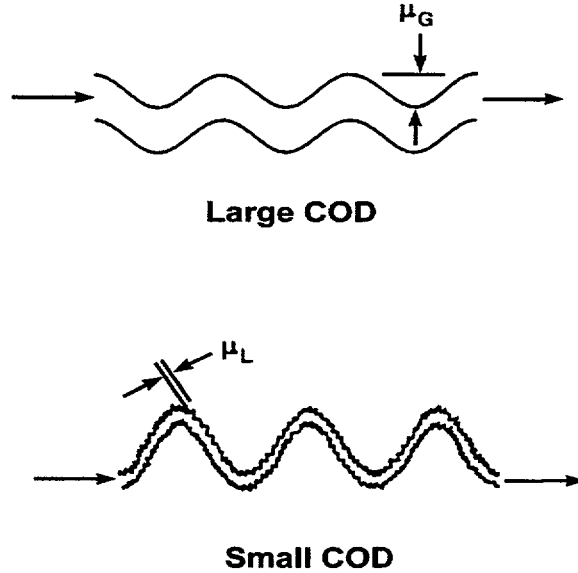


**Figure 5.4** Local and global surface roughness and number of turns  
(Statistically averaged values of  $\mu_G$  and  $\mu_L$  are shown in Table 5.1)

**Table 5.1** Average surface roughness values from statistical  
analysis of fracture surfaces from NUREG/CR-6004

Material and Cracking Mechanism	Local Roughness, mm ( $\mu$ inch)	Global Roughness, mm ( $\mu$ inch)
Stainless Steel IGSCC	0.0047 (185)	0.080 (3,150)
Stainless Steel Fatigue Cracks in Air	0.0080 (317)	0.034 (1,325)
Carbon Steel Fatigue Cracks in Air	0.0065 (257)	0.034 (1,325)
Carbon Steel Corrosion Fatigue Cracks	0.0088 (347)	0.040 (1,595)

In addition, from an examination of photomicrographs of a number of fracture surfaces, another statistical analysis was made of the number of 90-degree turns per inch of thickness of flow path. Table 5.2 shows the results from that statistical analysis. As can be seen from Table 5.2, the number of turns per inch of flow path is much larger for IGSCC in stainless steels than it is for air fatigue cracks. Similarly, the number of turns per inch for a

corrosion fatigue crack in carbon steel is much higher than it is for an air fatigue crack. The bottom line is that the flow path the fluid must transverse is much more tortuous for IGSCC and corrosion fatigue cracks than it is for air fatigue cracks both from a global surface roughness and number of turns perspective. As such, the pressure loss term for these types of cracks will be greater than those for air fatigue cracks.

**Table 5.2 Average number of 90-degree turns per inch of flow path (Ref. 5.23)**

Material and Crack Mechanism	Number of 90-degree Turns, mm <sup>-1</sup> (inch <sup>-1</sup> )
Stainless Steel IGSCC	28.2 (717)
Stainless Steel Fatigue Cracks in Air	2.52 (64)
Carbon Steel Fatigue Cracks in Air	2.01 (51)
Carbon Steel Corrosion Fatigue Cracks	6.73 (171)

The leak-rate analysis methodology in NUREG/CR-6004 noted that there was a COD-dependence on the surface roughness and number of turns. In Reference 5.23, the overall effective surface roughness ( $\mu$ ) was defined in terms of the local roughness ( $\mu_L$ ), global roughness ( $\mu_G$ ), and center crack COD ( $\delta$ ) using the expression

$$\mu = \begin{cases} \mu_L, & 0.0 < \frac{\delta}{\mu_G} < 0.1 \\ \mu_L + \frac{\mu_G - \mu_L}{9.9} \left[ \frac{\delta}{\mu_G} - 0.1 \right], & 0.1 < \frac{\delta}{\mu_G} < 10 \\ \mu_G, & \frac{\delta}{\mu_G} > 10 \end{cases} \quad (5.6)$$

Similarly the number of turns ( $n_t$ ) was found to be larger for tight cracks than for cracks with larger CODs for which the turns contribute to the surface roughness. From Reference 5.23, the

COD-dependent number of turns to be used in a leak rate analysis is:

$$n_t = \begin{cases} n_{tL}, & 0.0 < \frac{\delta}{\mu_G} < 0.1 \\ n_{tL} - \frac{n_{tL}}{11} \left[ \frac{\delta}{\mu_G} - 0.1 \right], & 0.1 < \frac{\delta}{\mu_G} < 10 \\ 0.1n_{tL}, & \frac{\delta}{\mu_G} > 10 \end{cases} \quad (5.7)$$

This interpolative method for estimating the surface roughness and number of turns is illustrated in Figure 5.5.

The remaining two crack morphology parameters of interest are the entrance loss coefficient ( $C_D$ ) and the ratio of the actual crack

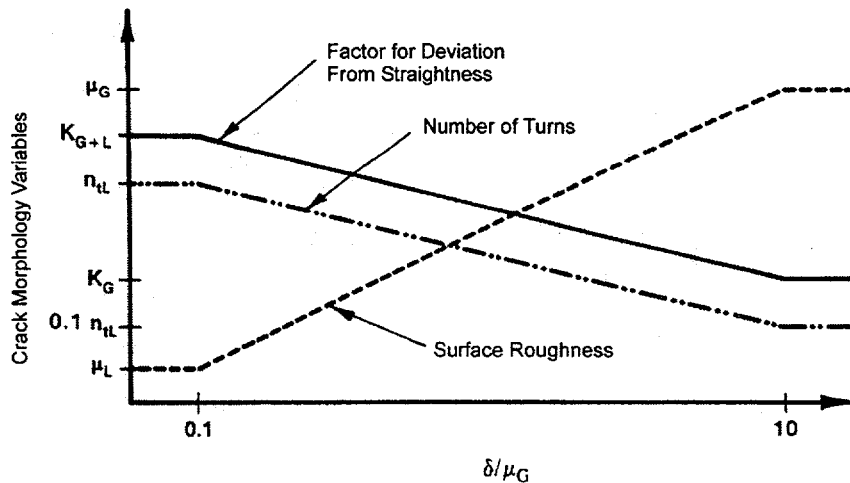


**Figure 5.5 Crack morphology variables versus normalized COD**

path length to pipe thickness ( $K_G$ ). For the entrance loss coefficient, if the entrance edges have a radius of 1/6 of the COD or larger, then

they are considered as rounded and the value of  $C_D$  is set at 0.62. In review of the fracture surfaces as part of Ref. 5.23, it appears that

fatigue and corrosion fatigue cracks typically initiate at small pits with some surface corrosion to round the edges. Consequently, a  $C_D$  value of 0.62 is appropriate for such cracks. Conversely, IGSCC often results in sharp edges, with no pitting or corrosion to round the edges, so a  $C_D$  value of 0.95 is more appropriate for tight cracks, i.e.,  $COD < 0.15$  mm (0.006 inch).

There are two aspects of interest with regard to the ratio of the actual crack path length to the pipe thickness ( $K_G$ ). One is a global path deviation from straight through the pipe wall thickness,  $K_G$ . If a crack follows the fusion line of a single-vee weld, then this ratio is  $1/\cos(37 \text{ degrees}) = 1.25$ , assuming that the weld prep geometry is a 37 degree bevel. Furthermore, Reference 5.23 showed that  $K_G = 1.05$  for thermal fatigue cracks in feedwater piping.

The second aspect causing the flow path to be longer than the pipe thickness is the local waviness of the fracture surface. If the COD is small compared with the global roughness, then the local waviness will cause an increase in the flow path length. If the COD is small compared with the global roughness, then the local surface roughness should be used with this local plus global waviness flow-path multiplication factor,  $K_{G+L}$ , as well as the pressure drop from the number of turns. Statistically averaged measured values of  $K_G$  and  $K_{G+L}$  from typical cracks in stainless and carbon steels are presented in Table 5.3. In general, these values are larger for IGSCC cracks in stainless steel than for corrosion fatigue cracks in carbon steel.

**Table 5.3 Average values for global path deviation factor ( $K_G$ ) and local waviness path deviation factor ( $K_{G+L}$ )**

Material and Cracking Mechanism	Global Path Deviation Factor, $K_{G+L}$	Local Waviness Path Deviation Factor, $K_G$
Stainless Steel IGSCC	1.33	1.07
Carbon Steel Corrosion Fatigue	1.06	1.02

**Restraint of Pressure-Induced Bending on Crack-Opening Displacements for LBB Analyses** – At the end of the Second International Piping Integrity Research Group (IPIRG-2) Program, a study was commissioned to assess the factors that are most critical to leak-before-break (LBB) and in-service flaw evaluation methods (Ref. 5.22). One factor identified that will potentially affect LBB analyses is an effect called *restraint of pressure-induced bending on crack-opening displacement*. The common analysis practice for past LBB applications is to determine the center crack-opening displacement (COD) by using the solution for an end-capped vessel. The so-called end-capped vessel model, although relatively simple to analyze, allows the ends of the vessel to freely rotate. Furthermore, it

ignores the ovalization restraint at the crack plane from any boundary conditions. Therefore, the end-capped vessel model may over-estimate the crack-opening displacement more than if the pipe is not allowed to rotate.

**Background** - In Experiment 1.3-7 from the First IPIRG program (Ref. 5.56), it was experimentally determined that a guillotine break did not occur until the growing through-wall crack was 95 percent around the pipe circumference, see Figure 5.6. From pressure loads alone, it was expected that a break would occur once the crack reached 65 percent of the circumference. The crack length of 95-percent of the pipe circumference corresponded to the pressure-induced failure for full restraint of the induced bending moment, see Figure 5.7.

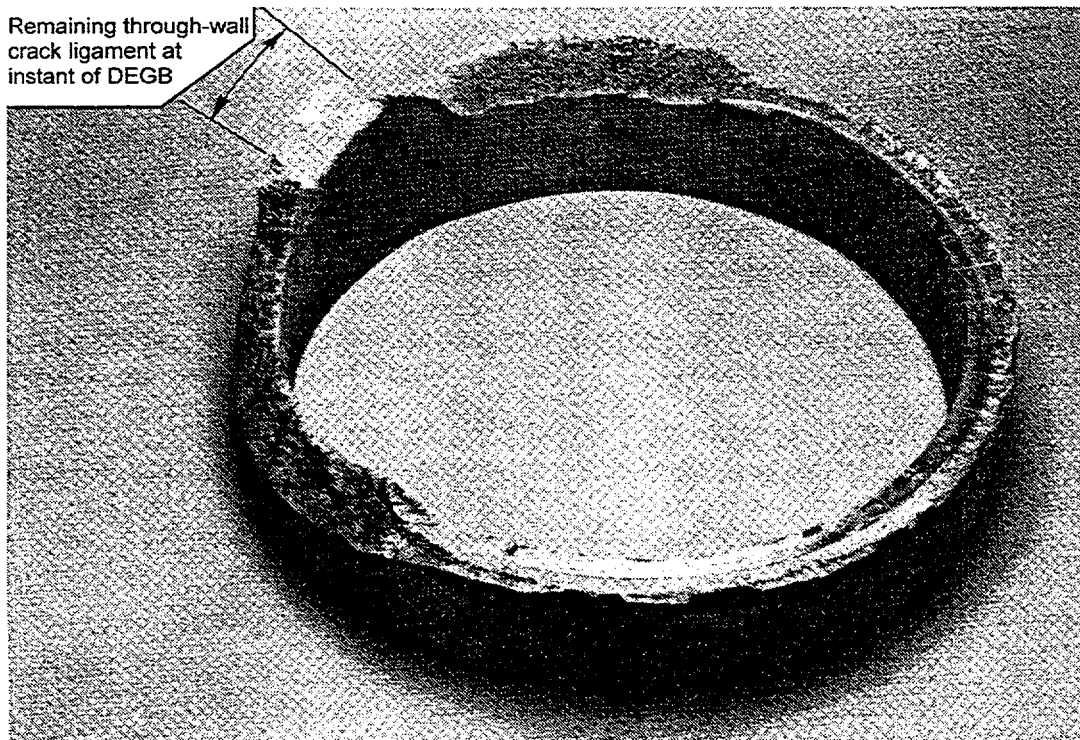


**Figure 5.6** Photograph of fracture from aged cast stainless experiment (Experiment 1.3-7)

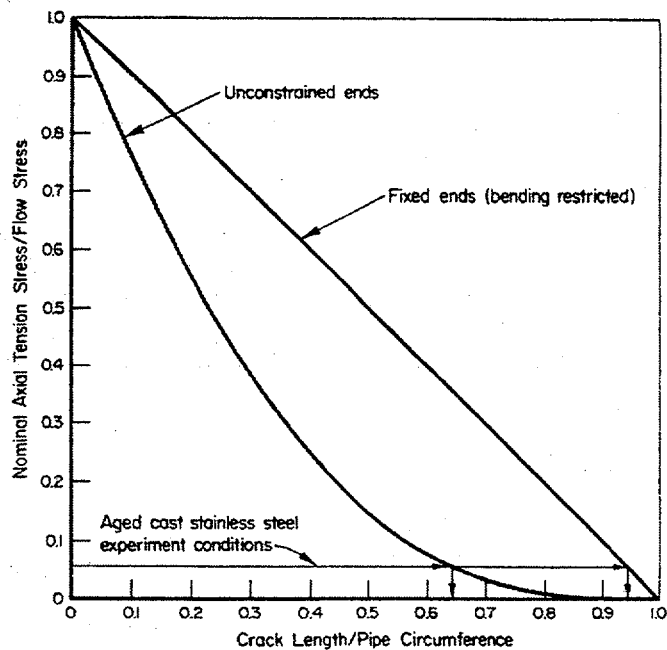


**Figure 5.7** Net-Section-Collapse analyses predictions, with and without considering induced bending, as a function of the ratio of the through-wall crack length to pipe circumference

The results from this experiment, with the crack located 3.4 pipe diameters from an elbow,

provide strong evidence that pipe-system boundary conditions restrain pressure-induced

bending and that this effect increases the load-carrying capacity of the cracked pipe. Furthermore, virtually all fracture analyses assume that the pipe is free to rotate due to the pressure-induced bending. Consequently, the contemporary fracture methods will tend to inaccurately predict the propensity for crack instability because they ignore the restraint that the pipe-system boundary conditions provide.

It was later noted, however, that if the failure loads are increased, then the driving force is reduced, so that the crack-opening displacement in the pipe system will be less than what is typically calculated using current crack-opening-displacement analyses. Hence, the increased load-carrying capacity that is beneficial to LBB has a corresponding decrease in crack-opening displacement that is detrimental to LBB. Because the trade-offs between these two effects were not well understood, some selected case studies were undertaken in Reference 5.22.

Calculations were initially done for a 28-inch diameter pipe with a mean pipe radius to wall thickness ratio ( $R_m/t$ ) of 10. Only elastic analyses were conducted. At various distances from the circumferential crack plane, the pipe rotation and ovalization were restricted in the FE analyses. This distance from the crack to the restraining boundary conditions was called the restraint length. The restraint length was normalized by the pipe diameter for making non-dimensional plots with COD values for different pipe diameters.

In these initial analyses, the crack length was either 12.5 or 25 percent of the pipe circumference, and the normalized restraint lengths considered were 1, 5, 10, and 20. A calculation was also done that would allow free rotation and no ovalization restrictions. This is

representative of the fully unrestrained conditions (the end-capped vessel assumption) used in all the COD estimation procedures. Since this was an elastic analysis, the COD of the restrained boundary condition analyses could be normalized by the unrestrained COD for any load level. Subsequently, similar analyses were conducted for a 4-inch nominal diameter pipe with an  $R_m/t$  of 6. In addition, another crack length of  $1/2$  of the pipe diameter was added for both pipe diameters. Figure 5.8 shows the results of the both of these analyses together.

An additional LBB sensitivity study was conducted in Reference 5.22 using the above restrained COD trends. This LBB analysis was based on the following conditions:

- a leak rate of 1.89 liters/min (0.5 gpm),
- IGSCC crack morphology parameters,
- a pressure of 15.5 MPa (2,250 psi), and
- a bending stress chosen to give a total pressure plus bending stress of 50 percent of the Service Level A maximum allowable stress from ASME Section III Article NB-3650 for TP304 stainless steel pipe.

The resulting leakage-size cracks were calculated using the SQUIRT Version 2.4 computer code. These results are shown in Table 5.4. For the restrained condition,  $L/D$  was set to 1.0. For these conditions, the large-diameter pipe is basically unaffected by the restraint condition while the small-diameter pipe is very much affected. The effect of restraint on the COD is strongly controlled by the crack length even though it appears to manifest itself as a pipe diameter effect, since a shorter normalized crack length (normalized by pipe circumference, i.e.,  $\theta/\pi$ ) is needed in larger-diameter pipe for LBB to be satisfied.

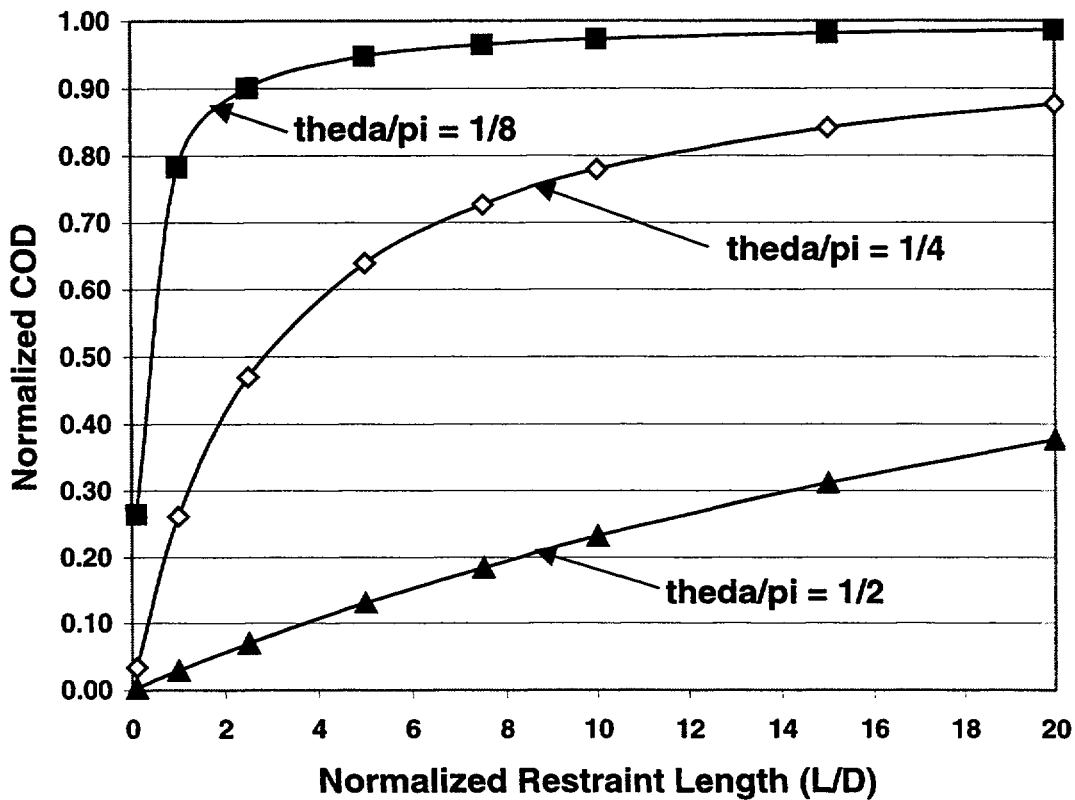


Figure 5.8 Normalized COD versus restraint length for two different sets of FE analyses

Table 5.4 Differences in leakage flow sizes due to restraint of pressure-induced bending

Outside Pipe Diameter inches	Leakage Crack Length, $\theta/\pi$	
	Restrained	Unrestrained
4.5	0.7250	0.2360
28.0	0.0219	0.0219

The corresponding LBB fracture loads for these postulated leakage crack lengths were evaluated under the following conditions:

- the crack was centered on the bending plane,
- the average stress-strain curve properties for TP304 stainless steel base metal were used, and
- the crack was assumed to be in the center of the weld, hence the mean minus one

standard deviation J-R curve for a stainless steel SAW weld was used.

Using the LBB.ENG2 (Ref. 5.8) analysis, modified to eliminate the induced bending from the tension component of the axial stress component, the ratios of the unrestrained to restrained failures loads are shown in Figure 5.9. This result shows that the effects of the restraint of pipe-system boundary conditions are negligible for the 28-inch diameter pipe. This

was because for this leak rate, the crack size was a small percent of the circumference, and hence the beneficial effects on fracture and detrimental effects on COD were negligible. However, the effect on the 4-inch nominal diameter pipe was very large. The unrestrained load is a factor of nine larger than the restrained load. This was a more significant effect than any possible effect from toughness considerations. The reason this occurred was that for this leak rate, under this loading, the crack in the small-diameter pipe for the restrained condition had to be very large when compared with the larger-diameter pipe. The crack, in fact, became so large from this effect, that any benefits on fracture loads were small, especially considering that the additional loads to fracture were all bending loads, not increases in pressure loads. Also, like any LBB analysis, the calculations were made up to maximum load, and were not an actual determination of a DEGB.

The effect seen in this sample calculation suggests that LBB applications need to be assessed carefully for cases where large normalized crack sizes ( $\theta/\pi$ ) may occur, i.e., small-diameter pipe, or steam-line applications. It also suggests that there may be some concern with LBB applications to intermediate pipe diameters. Fortunately, for large-diameter pipe, where LBB is of greatest benefit, there are no detrimental effects from this phenomenon.

Of practical importance is the fact that the past Battelle analysis assumes symmetric boundary conditions either side of the crack. This would probably never occur in practice. Hence to make any analysis for this effect a practical tool, one would have to account for the different pipe bending stiffnesses on either side of the LBB postulated crack locations.

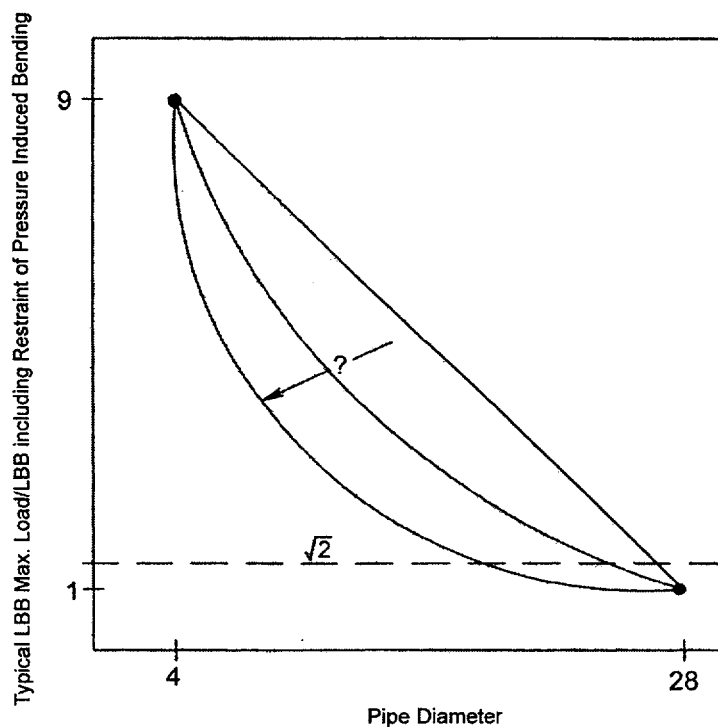


**Figure 5.9 Calculated maximum loads for LBB, with and without restraint of the pressure-induced bending, from the pipe system**

**Round Robin Analyses** – In the Battelle Integrity of Nuclear Piping (BINP) program, six

organizations from three countries participated in a finite element round-robin analysis to study

this effect. The objective of this round-robin analysis was to check the past calculations from Reference 5.22, as well as compare and evaluate the results and modeling approaches from the different participants. Each participant was then assigned some additional problems to solve. This resulted in a large matrix of FE results, which were subsequently used in the BINP program in the development of a closed-form analytical expression for this effect.

The round-robin analysis was coordinated by Engineering Mechanics Corporation of Columbus (Emc<sup>2</sup>). The other five participating organizations were: Battelle, Central Research Institute of Electric Power Industry of Japan (CRIEPI), Korea Electric Power Research Institute (KEPRI), Sungkyunkwan University of Korea (SKKU), and the U.S. Nuclear Regulatory Commission (USNRC).

The round-robin participants were to perform linear-elastic finite element analyses to determine the center crack-opening displacement (COD) at the mid-thickness of a through-wall circumferentially-cracked straight pipe restrained at both ends. The basic variables investigated in the round robin included the pipe outside diameter (OD), pipe mean radius to thickness ratio ( $R_m/t$ ), crack length ( $\theta/\pi$ ), and the distance between the restraint planes to the crack plane ( $L_1, L_2$ ).

A total of 144 cases were included in the analysis matrix of the round robin. It covered a wide range of pipe diameters and  $R_m/t$  ratios. The effects of different restraint lengths on the two sides of a crack plane (the asymmetric restraint condition) were considered also. The analysis matrix also included the cases that were analyzed earlier to evaluate the validity of the prior calculations.

Some of the key findings from these round-robin analyses include:

- The normalizing procedure accounted for the pipe diameter effects.
- As the  $R_m/t$  ratio increases, the restraint effect increases, resulting in lower normalized COD.

- As the difference in the restraint lengths from the two sides of the crack increases, the asymmetric restraint effect on the normalized COD increases. The effect becomes significant once one of the restraint lengths is reduced to  $L/D=1$ , or the crack length was the longest ( $\theta=\pi/2$ ).

#### ***Development of a Closed-Form Analytical Expression to Account for Restraint of Pressure Induced Bending Effects –***

Subsequent to the above round-robin analyses, a task was undertaken as part of the BINP program to develop closed form analytical expressions that could be used in a Level 2 type LBB analysis to account for the effects of restraint of pressure induced bending. At the time of this writing, this effort is still ongoing.

#### ***Effect of Weld Residual Stresses on Crack-Opening Displacements for LBB Analyses –***

In the IPIRG-2 program, several efforts were undertaken that dealt with the effect of weld residual stresses on LBB analyses. One effort involved a set of calculations from an IPIRG-2 round-robin analysis involving SAQ and Battelle (Ref. 5.57). In these analyses, two weld residual stress analysis fields were assumed, one for “thick pipe” and one for “thin pipe”. The “thin pipe” results showed that the weld residual stresses could have a significant effect on crack-opening behavior at operating stresses less than 50-percent of the maximum Service Level A allowable stresses. In this case, the residual stresses were tensile-to-compressive through the thickness, which caused the crack faces to rotate. At these lower operating stresses, the applied crack-opening displacements may be small enough that the crack may partially or fully close on the outside surface, hence reducing the leakage (which is undesirable from a LBB perspective). For “thick pipe”, the effect of weld residual stresses on crack-opening behavior was negligible, except at unrealistically low operating stresses. In terms of the resultant leak rates, Figure 5.10 shows the ratios of leak rates, with and without residual stresses, as a function of applied load for both “thin” and “thick” wall pipe. More recent work by Battelle, using a more sophisticated thermo-plastic finite element approach, has further demonstrated that weld

residual stresses can significantly affect the crack-opening behavior, including:

- crack-face closure due to the through-wall bending residual stresses (thin-wall pipes),

- non-elliptical opening (in part, contributed to by the presence of yield-magnitude hoop residual stresses on the crack face), and
- through-wall residual stress distribution being a function of weld preparation geometry, total number of passes, start-stop locations, and the bulk heat input.

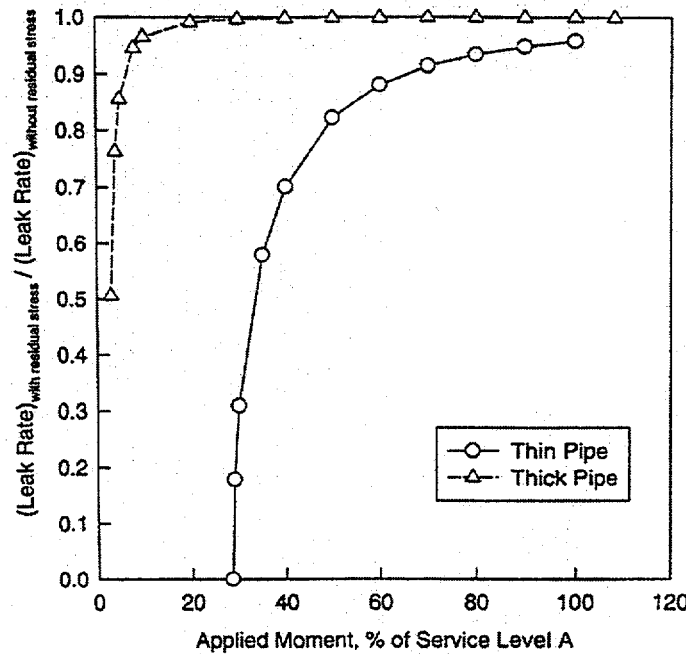


Figure 5.10 Ratio of leak rates, with and without residual stresses, as a function of applied load

One point of note with regards to the effect of weld residual stresses on “thin pipe” is that these thin pipes are more often exempt from post-weld-heat-treatment (PWHT) residual stress relieving. For example, welds joining A106 Grade B pipe (P-No. 1 in ASME nomenclature) in materials less than 38 mm (1 ½ inches) thick are not required to be stress relieved according to Table NB-4622.7(b)-1 of ASME Section III.

At the time of the writing of this NUREG/CR report there is on-going research being conducted at Battelle examining the effect of weld residual stresses on the crack-opening behavior for LBB analyses. At this time it is envisioned that a correction factor to the GE/EPRI V-Functions, used to estimate the crack-opening-displacement, will be developed

as part of the BINP program to address the effect of weld residual stresses on COD predictions for LBB analysis.

**Crack-Face Pressure Effects on Crack-Opening Displacements** – One effect not accounted for to date is the effect of the crack-face pressure on the CODs for a LBB analysis. Even though there are no plans to quantify this effect at this time, ignoring it should result in a conservative assessment because the pressure on the crack faces should tend to open the postulated leaking crack, resulting in a shorter postulated leaking crack length for a prescribed leak-rate detection capability. Consequently, consideration of this effect will make it easier to satisfy LBB, hence the applicant can ignore it and still be acceptable from a regulatory sense.

This effect is probably only significant if the crack length is longer than a prescribed percent of the pipe circumference. This effect may compensate for some of the restraint of pressure induced bending effects discussed previously. Thus, this may be an effect an applicant may want to consider in the future if a difficulty arises in qualifying a particular line for LBB. The pressure on the crack faces will depend on the pressure drop along the flow path, hence, the full internal pressure should not be applied to the crack faces. One question of interest is whether the benefits from considering crack-face pressure compensates for other detrimental effects (i.e., residual stresses) so that the LBB approach could be simplified by ignoring both factors.

One possible means of accounting for this effect in an LBB assessment is:

1. Determine the exit plane fluid pressure (Pressure at throat in PICEP or exit plane pressure in SQUIRT).
2. Assume the pressure distribution is linear through the thickness from the inside pressure to the exit plane (outside diameter).
3. Calculate the applied bending moment and axial tension forces on the pipe by integrating the pressure along the crack faces.
4. Add those moments and axial tension forces to the applied normal operating loads. Calculate the new leak rate. Check the pressure distribution through the thickness from the leak-rate code and iterate until there is convergence for that crack length.
5. Change the crack length and iterate through Step 1 of this section until the target leak rate is determined.

Obviously, a validated technical basis for accounting for the benefits of such an effect would have to be developed.

It should be noted, however, that while crack face pressure may result in a beneficial effect on the postulated leakage size crack, the impact of this effect on the crack driving force for the critical crack size assessment is unknown and

should be assessed prior to one taking credit for this effect on the leakage crack size.

***Effect of the Crack Being Centered Off the Maximum Bending Plane*** – The question was addressed as part of Reference 5.22 as to what would happen if the leaking crack was not centered on the maximum bending plane during normal operating conditions, but was centered on the maximum bending plane for the N+SSE bending plane. The cracks could occur off the center of the bending plane during normal operations due to random locations of workmanship flaws.

The deterministic calculations from Reference 5.22 involved the off-center crack COD calculational procedure described in Reference 5.19. Here it was assumed that there was a 1 gpm leaking crack, but the center of the crack was at various angles to the bending plane. It was assumed that the crack could not extend below the neutral axis of the bending plane, that is, the crack wouldn't grow if the applied bending loads were compressive. (This is logical, except in the presence of high axial stresses and/or residual stresses.) These calculations also assumed:

- The SQUIRT Version 2.4 default leak-rate parameters for an IGSCC crack,
- Outside pipe diameter of 14 inches with an  $R_m/t$  ratio of 10,
- A pressure of 15.5 MPa (2,250 psi) and a temperature of 288 C (550 F), and
- A bending stress to give a total pressure and bending stress of 50 percent of the Service Level A maximum allowable stress from ASME Section III Article NB-3650 for TP304 stainless steel pipe.

The resulting crack lengths are shown in Figure 5.11 as a function of the angle of the off-centered crack. This shows that there was not a very large difference in the crack lengths until the center of the crack was more than 50 degrees off the center of the bending plane.

To see the effect on the entire LBB analysis procedure, fracture calculations were then made assuming the following conditions.

- It was assumed, for N+SSE loading, that the crack was centered on the bending plane.
- The Net-Section-Collapse, LBB.NRC, and GE/EPRI analysis methods were all used to calculate the maximum loads.
- The average stress-strain curve properties for TP304 stainless steel base metal were used from the statistical analysis in Appendix B of Reference 5.23, i.e.,

$$\frac{\epsilon}{\epsilon_0} = \frac{\sigma}{\sigma_0} + \alpha \left( \frac{\sigma}{\sigma_0} \right)^n \quad (5.8)$$

where

$\sigma_0/\epsilon_0 = E = 183 \text{ GPa (26,500 ksi)}$ ,  
 $\sigma_0 = \sigma_y = 15.5 \text{ MPa (22.5 ksi)}$ ,  
 $\alpha = 8.073$ , and  
 $n = 3.80$ .

- The mean minus one standard deviation J-R curve for a stainless steel SAW weld from data in the PIFRAC data base (Ref. 5.58) was used. The mean minus one standard deviation J-R curve is

$$J = 0.419 + 0.477(\Delta a/r)^{0.643} \quad (5.9)$$

where

J is in units of in-kips/in<sup>2</sup>,  
 $\Delta a$  is in units of inches,  
 and r has a value of 1 mm (0.0394 inch).

The change in the maximum load-carrying capacity was calculated relative to the centered leaking crack case, see Figure 5.12. These results show that the maximum load of the off-centered crack (under normal operating conditions) was less than 10 percent from the centered crack maximum load when the middle of the off-centered crack was 50-degrees off the bending plane. This 10 percent difference is considered insignificant.

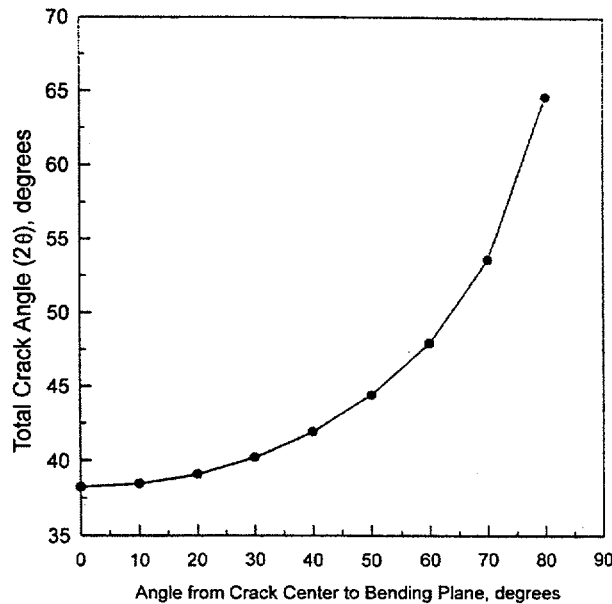


**Figure 5.11** Calculated off-centered crack length for a 3.8 lpm (1 gpm) leak rate versus the angle from the center of the off-centered crack to the bending plane

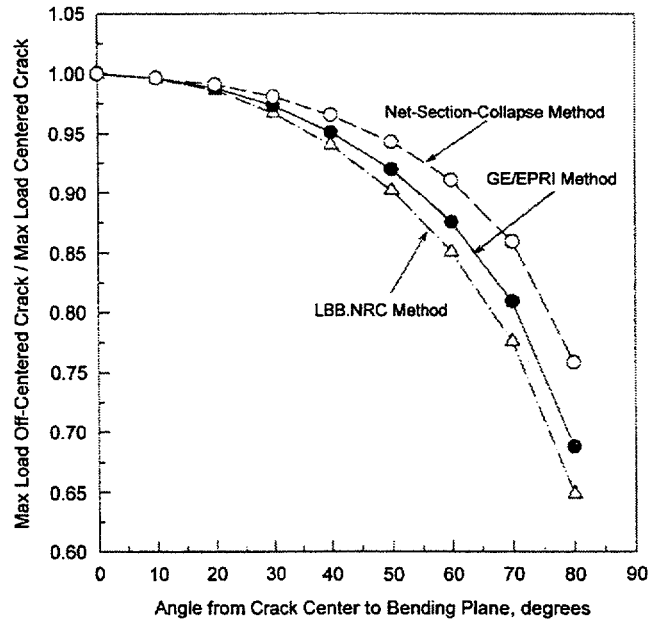


**Figure 5.12 Comparison of maximum loads for 3.8 lpm (1 gpm) leaking cracks that were off-centered during leakage but centered during the N+SSE loading versus the angle from the center of the off-centered crack to the bending plane**

**Uncertainty Issues such as Particulate**

**Plugging** – Particulates from pipe mill scale, corrosion products, or other sources can collect between the crack faces of tight cracks, and cause the flow through the crack to be reduced significantly. This phenomenon was observed during the leak-rate experiments conducted as part of Reference 5.4. During these experiments, flow through the actual stress corrosion cracks was temporarily choked off as particulates accumulated in the flow path. Typically the flow would be re-established once the particulates cleared themselves. However, any leak detection system that counted on an accumulation of leakage, such as sump level monitoring, would be directly affected by these temporary reductions in flow due to particulate plugging. The net effect on LBB would be that the postulated leakage crack size would be longer than predicted based on existing leak-rate estimation models. At this time, the means of accounting for this non-conservative aspect of the analysis is through the applied safety factor on leak rate, i.e., the existing safety factor of 10 on leak-rate detection capability.

**5.3.1.3 Comparison of Postulated Leakage Crack Sizes for Various Leak-Rate Analysis Codes**

– In comparing the postulated leakage crack sizes for the various leak-rate codes (i.e., SQUIRT, PICEP, and the proprietary code developed by one of the applicants) it was necessary to perform the SQUIRT and PICEP calculations for the same cases evaluated by the applicant since the applicant’s proprietary code was not directly available. As a first comparison, the total postulated leakage crack size was calculated assuming a 3.8 lpm (1.0 gpm) leakage detection capability (with a safety factor of 10) and using the applicant’s assumed surface roughness of 0.0076 mm (300 microinches) and no number of turns. The applicant’s calculated crack lengths were based on using the Tada/Paris COD analysis (Ref. 5.59) while SQUIRT and PICEP used the GE/EPRI COD analysis (Ref. 5.3). The results of this comparative analysis are shown in Table 5.5.

**Table 5.5 Comparison of total crack length at 38 lpm (10 gpm) using the 0.0076 mm (300-microinch) roughness and no turns as assumed by the applicant**

Location	Total crack length for 38 lpm (10 gpm) leak rate, mm (inch)		
	Using applicant's leak-rate code with Tada/Paris COD analysis	Using SQUIRT with GE/EPRI COD analysis	Using PICEP with GE/EPRI COD analysis
Location A	76.2 (3.00)	79.6 (3.14)	72.4 (2.85)
Location B	109 (4.30)	135 (5.31)	124 (4.88)

The agreement was fairly good for the Location A case, i.e., the applicant's result was bracketed by the PICEP and SQUIRT results with about a  $\pm 5$  percent difference. For the Location B case, both the SQUIRT and PICEP crack lengths were larger than the applicant's analysis. The differences in the crack lengths were 13.5 to 23.5 percent. For both locations, the calculated crack lengths using the SQUIRT code were about 10 percent longer than when the PICEP code was used. Thus, SQUIRT results in a slightly more conservative assessment of the leakage size crack than does PICEP for the same input parameters.

The above analysis assumed a surface roughness value of 0.0076 mm (300 microinches) with no number of turns. This surface roughness is quite a bit lower (i.e., smoother) than the statistically determined values from NUREG/CR-6004 (Ref. 5.23) reported earlier in Tables 5.1 and 5.2 for corrosion fatigue cracks, i.e., 0.040 mm (1,595 microinches) global roughness, 0.0088 mm (347 microinches) local roughness, and 6.73 90-degree turns per mm (171 90-degree turns per

inch) of flow path. Note that NUREG/CR-6004 states that this global roughness value and corresponding number of turns should only be used if the COD is 10 times greater than the surface roughness. If the COD is less than 10 times the global roughness, then the interpolative methods outlined in Equations 5.6 and 5.7, and as illustrated in Figure 5.5, should be used to establish the surface roughness and number of turn values to be used in the leak rate analysis. Using the crack lengths calculated by the applicant, see Table 5.5, the calculated COD using the Tada/Paris method (method also used by the applicant) from NRCPIPE was 0.131 mm (0.00517 inch) for Location A and 0.118 mm (0.00466 inch) for Location B. Thus, the average COD-to-global roughness ratio is about 3.08 in this case. Hence, the NUREG/CR-6004 interpolation method between global-to-local crack morphology values should be used.

Table 5.6 gives the global, local, and interpolated values to be used in this case for corrosion fatigue cracks.

**Table 5.6 Crack morphology parameters relative to this LBB analysis**

	Global	Local	Calculated value for this case using interpolative method from Figure 5.5
<b>Roughness, mm (microinch)</b>	0.040 (1,595)	0.0088 (347)	0.018 (723)
<b>Number of turns per mm (inch) of flow path</b>	0.67 (17.1)	6.73 (171)	4.92 (125)
<b>Flow path/thickness</b>	1.017	1.06	1.047

For comparison with the applicant's calculated leakage size flaws, the COD and crack lengths values for Locations A and B were calculated for a 38 lpm (10 gpm) leak rate using the interpolated crack morphology parameters from Table 5.6 and an iterative scheme using the NRCPIPE (Version 3) and the SQUIRT

(Version 2.4) codes. This analysis used the Tada/Paris method in NRCPIPE for calculating the COD and assumed an elliptical crack opening shape with a discharge coefficient of 0.6 for a sharp crack. The results are given in Table 5.7.

**Table 5.7 LBB leakage flaw sizes using Tada-Paris COD analysis**

Location	Total crack length for 38 lpm (10-gpm) leak rate, mm (inch)	
	SQUIRT2 with NUREG/CR-6004 crack morphology	Applicant's LBB report with 0.0076 mm (300 μinch) roughness
A	210 (8.65)	76.2 (3.00)
B	265 (10.45)	109 (4.3)

Table 5.7 shows that the SQUIRT2 crack length was about *2.5 times larger* than the applicant's crack length. The SQUIRT code with the larger crack morphology values was expected to give a greater crack length, *but this was a very large difference*.

done using only the SQUIRT code with the Tada/Paris COD analysis. This was done with both the 0.0076 mm (300 microinch) roughness and the NUREG/CR-6004 roughness with a discharge coefficient of 0.6 for a sharp-edge crack. These results are shown in Table 5.8.

To clarify the surface roughness aspect further, the calculations for Locations A and B were

**Table 5.8 LBB leakage flaw sizes using Tada/Paris analysis and SQUIRT2 with different crack morphology parameters**

Location	Total crack length for 38 lpm (10-gpm) leak rate, mm (inch)	
	0.0076 mm (300 μinch) roughness	NUREG/CR-6004 crack morphology
A	126 (4.98)	210 (8.65)
B	163 (6.43)	265 (10.45)

In Table 5.8 it can be seen that using the same analysis procedure and the different roughness values resulted in a change in the crack length of about 60 to 75 percent for this case. Hence, specifying the surface-roughness value to be used was deemed to be very important.

GE/EPRI COD analysis and NUREG/CR-6004 crack morphology parameters) in Table 5.9. This comparison shows that the applicant's LBB analysis gave a shorter crack length than the proposed analysis by a factor of 1.7 to 1.8. This difference was due to the larger amount of non-conservatism of using their leak-rate code with a roughness of 0.0076 mm (300 microinches) and no turns compared with the amount of conservatism they gained by using the Tada/Paris COD analysis.

As a final comparison, the applicant's calculated postulated crack lengths (using the Tada/Paris COD analysis with their leak-rate code and 0.0076 mm (300 microinch) roughness) are compared with the recommended leak-rate analysis procedure (SQUIRT with Original

**Table 5.9 LBB leakage flaw sizes using Tada/Paris COD analysis and applicants leak-rate code versus SQUIRT4 with NUREG/CR-6004 crack-morphology parameters**

Location	Total crack length for 38 lpm (10-gpm) leak rate, mm (inch)	
	Applicant's analysis with Tada/Paris and 0.0076 mm (300 μinch) surface roughness	SQUIRT analysis with GE/EPRI COD analysis and NUREG/CR-6004 crack morphology parameters
A	76.2 (3.0)	131 (5.14)
B	109 (4.3)	199 (7.84)

The ratio of the leakage crack size to the transient load<sup>18</sup> critical crack size is given in Table 5.10 for Locations A and B for both the applicant's leak-rate code and the SQUIRT leak-rate code. The critical crack lengths are those reported by the applicant. When SQUIRT, with the NUREG/CR-6004 average crack-morphology values, were used, Location A barely passed the crack-length margin requirement of two (and only if actual strength properties were used), and Location B did not pass, even when actual properties were used. Conversely, the applicant reported that both locations passed LBB if actual properties were used in the critical crack-size analyses.

### 5.3.2 Subcritical Crack Growth Analysis

Since the draft SRP 3.6.3 procedures start by postulating the existence of leaking through-wall crack, there is no need to conduct a flaw growth analysis of a part-through surface crack due to fatigue or stress corrosion cracking. However, as will be seen later in Section 7 of this report (Foreign Experience), procedures in other countries often do account for the growth of a part-through surface crack. Furthermore, there is no guarantee that the new Regulatory Guide procedures will not incorporate this facet of the analysis; at least maybe for fatigue, if not stress corrosion cracking. It is doubtful that the new procedures would account for crack growth due to stress corrosion cracking since piping systems that are susceptible to stress corrosion cracking (either IGSCC or PWSCC) are typically

excluded from LBB consideration due to the fact that stress corrosion cracks often are very long, thus making LBB more difficult to demonstrate.

From a fatigue perspective, one possible means of accounting for fatigue crack growth is to follow the example of Section XI (1995 Edition) of the ASME Boiler and Pressure Vessel Code. In the in-service flaw evaluation procedures in Section XI, guidance is provided as to how to conduct a fatigue crack growth analysis. For both ferritic and austenitic piping, the Paris-Law expression is used:

$$\frac{da}{dN} = C_0 (\Delta K_I)^n \quad (5.10)$$

where,

- da/dN = fatigue crack growth rate,
- $\Delta K_I$  = range of the applied stress intensity factor,
- n = slope of the log(da/dN) versus log( $\Delta K_I$ ) curve, and
- C<sub>0</sub> = a scaling constant.

<sup>18</sup> Transient loading for the surge line was used rather than N+SSE in this case.

**Table 5.10 Comparison of margins on crack length at 38 lpm (10 gpm) using Tada/Paris COD analysis and applicant's leak-rate code versus SQUIRT4 with NUREG/CR-6004 crack-morphology parameters**

Location	Critical crack length, mm (inch)	Margin on leakage size crack	
		Applicant's Code	SQUIRT4
A	252 (9.93)	3.31	1.93 (2.19) <sup>(b)</sup>
B	202 (7.95)	1.85 (2.1) <sup>(a)</sup>	1.01 (1.15) <sup>(b)</sup>

(a) Margin was 2.1 with actual strength properties.

(b) Using actual properties with 2.1/1.85 scaling to get the "actual" margin.

The terms "n" and "C<sub>0</sub>" are functions of the material, load history, and environment. ASME Section XI (1995 Edition) stipulates that the crack growth rate data from which these parameters are derived should be obtained from specimens of the actual material and product form, considering material variability, environment (including temperature), test frequency, and other variables that affect the data. However, recognizing that archival material may not always be available, and the expense of generating such data, Section XI provides reference fatigue crack growth rate expressions for both ferritic and austenitic materials in Appendices A and C, respectively, that can be used in lieu of actually generating fatigue crack growth rate data. The parameter "n" is provided as a function of the material, environment (air or water), and for ferritic steels in a water environment, in terms of the regime of the crack growth rate, i.e., either high or low  $\Delta K_I$  values. The parameter "C<sub>0</sub>", in turn, is a function of material, stress ratio (R), and for austenitic steels, in terms of temperature.

Finally, determining the progression of a fatigue crack as it grows through the wall of a pipe is a matter of integrating the Paris Law expression in Equation 5.10 using the design transients prescribed for the piping system. A number of K solutions exist in the literature; with the Newman and Raju solutions (Ref. 5.60) probably being the most widely used. The Newman and Raju solutions were derived for flat plates, and as such, may require a curvature correction for cracks in pipes.

### 5.3.3 Material Issues

Some of the key material issues related to the subject of LBB are discussed in the following sections.

**5.3.3.1 Source of Data** – One of the recurring problems that faces those attempting to apply LBB is estimating the material properties to use in the analyses. Ideally one would like to test samples machined from archival material for the piping system under consideration. Frankly, though, such material usually does not exist. As such, databases are often used to extract data from. The questions here are; (1) are such data truly representative of the actual piping system material, and (2) should one use mean or lower-bound data in the analyses. Typically, in reviewing the actual LBB submittals supplied by the NRC, the applicant's used mean material property data for the leakage crack size analysis and lower-bound data for the crack stability and critical crack size analyses. Then, the question needs asked as how confident are you that the so-called lower-bound data truly represents a lower bound. In reviewing a number of the LBB submittals supplied by the NRC the so-called lower bound values were not lower bounds. Data existed in the literature that clearly refuted this claim.

**5.3.3.2 Cyclic Effects on Toughness** – During the IPIRG programs numerous cyclic C(T) fracture toughness tests and cyclically-loaded pipe fracture experiments were conducted (Refs. 5.20 and 5.44) using both stainless steels and carbon steels, and both base metals and weld metals.

From this work it was found that cyclic loading does lower the material's fracture resistance. The extent of this reduction is a function of a number of parameters, including the:

- stress ratio ( $R$ ), i.e., the ratio of the minimum applied stress to the maximum applied stress for the load cycle,
- material, and
- increment of plastic displacement between load cycles.

From Reference 5.44, the effect of cyclic loads for  $R = 0$  load histories was small for both the stainless steel and carbon steels evaluated at

quasi-static loading rates. For the fully reversed load case ( $R = -1.0$ ), the maximum load and moment-rotation curves for the pipe experiments were significantly lowered for both the Type 304 stainless and A106 Grade B carbon steels, see Figures 5.13 and 5.14. At the intermediate stress ratios tested, e.g.,  $R = -0.3$ , the carbon steel material tested was more affected by the cyclic loading than the stainless steel material tested, i.e., at  $R = -0.3$  there was no effect on the stainless steel material, but the A106 Grade B material tested showed a significant lowering of the load-displacement record.

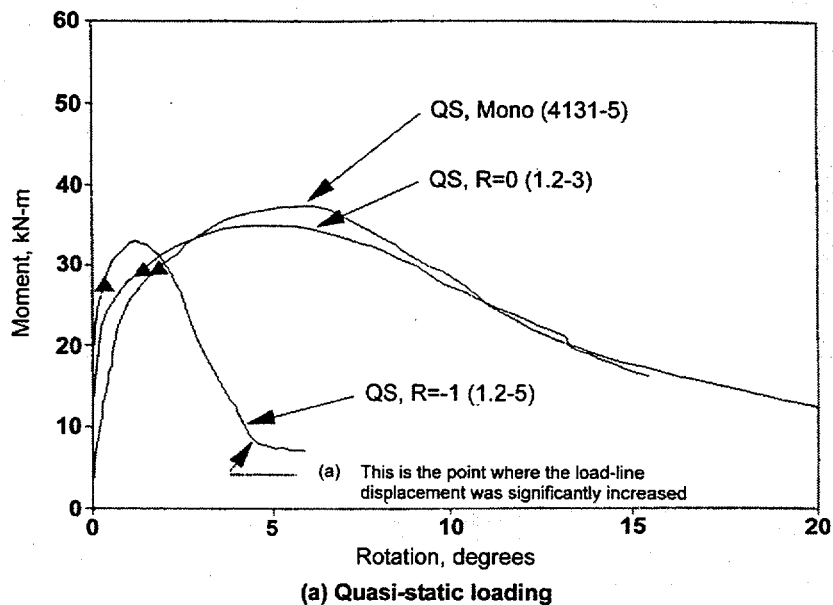


**Figure 5.13** Moment versus rotation showing the effect of cyclic loading ( $R=0$  and  $R=-1$ ) on stainless steel through-wall-cracked pipe experiments at quasi-static loading rates

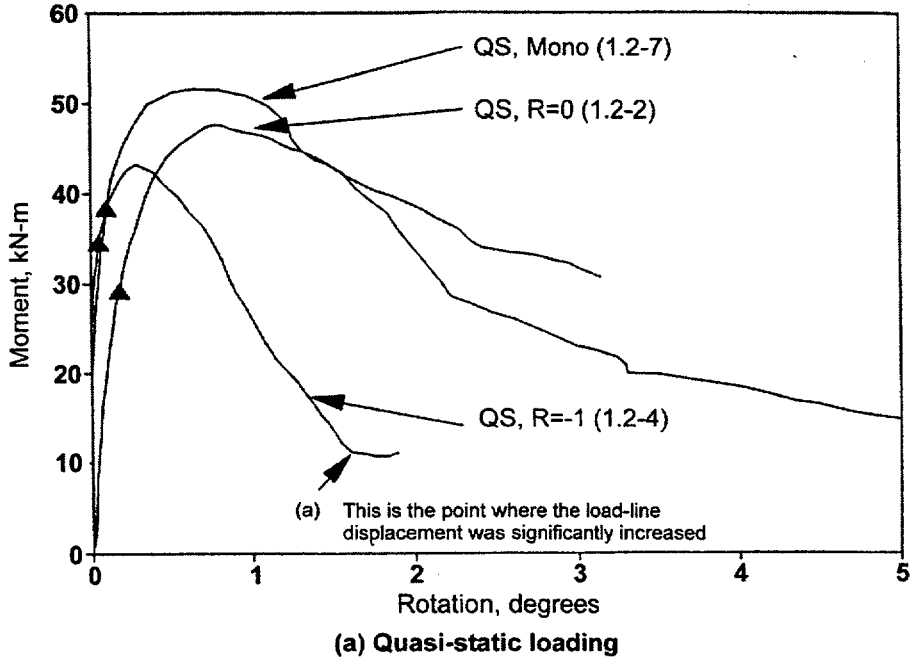


**Figure 5.14** Moment versus rotation showing the effect of cyclic loading ( $R=0$  and  $R=-1$ ) on carbon steel through-wall-cracked pipe experiments at quasi-static loading rates

This dependency of toughness due to cyclic loading on the stress ratio,  $R$ , and material (specifically the initial material toughness) is shown schematically in Figure 5.15. The trends

are such that lower toughness materials are more affected by cyclic loading, and more negative stress ratios will increase the amount of degradation.

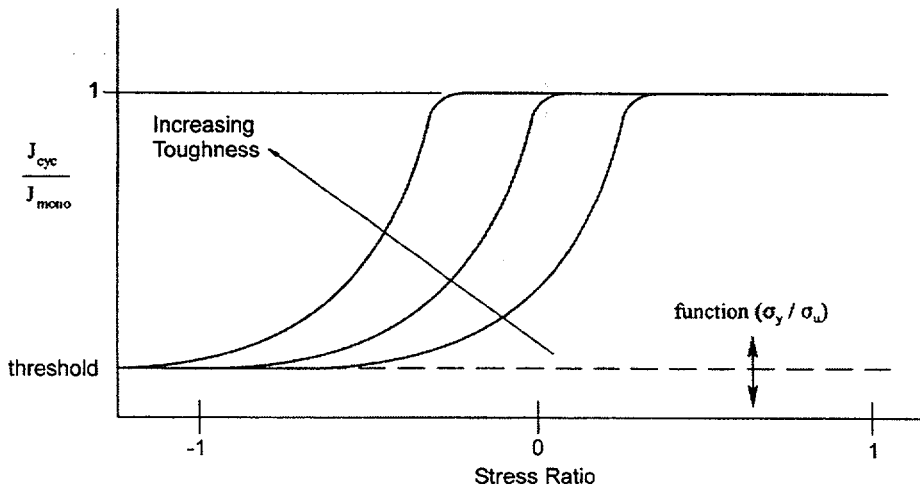


**Figure 5.15** Schematic of relationship between cyclic toughness degradation and stress ratio and initial material toughness

In Reference 5.44, the effect of the plastic displacement increment between load cycles was

assessed in several stainless steel pipe experiments. This was accomplished by

changing the cyclic spacing as shown in Figure 5.16. The effect of plastic-displacement increment versus the experimentally measured crack-tip-opening angle (CTOA), a measure of fracture toughness, is shown in Figure 5.17 for the stainless steel through-wall-cracked pipe experiments conducted as part of Reference 5.44. Both the CTOA and plastic displacement increment data have been normalized by the data

from a companion quasi-static monotonic pipe experiment (Experiment 4131-5). The results from Figure 5.17 indicate that decreasing the plastic displacement increment (denominator of the x-axis in Figure 5.17), lowers the CTOA. Hence, the magnitude of this plastic-displacement increment, as well as the stress ratio (R), can affect the apparent fracture resistance of the material.

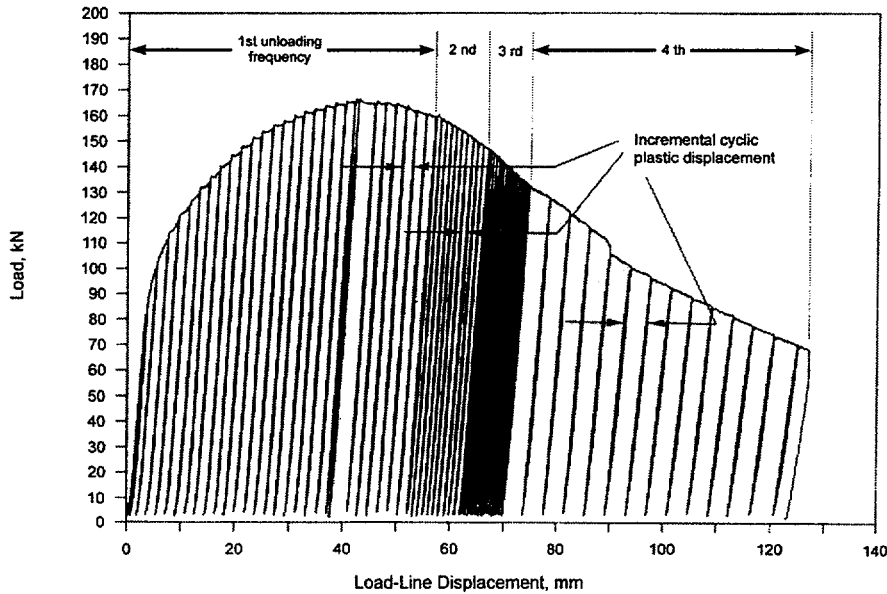


**Figure 5.16 Measured load versus load-line displacement for quasi-static, R=0 loading experiment (Experiment 1.2-3 from Reference 5.44)**

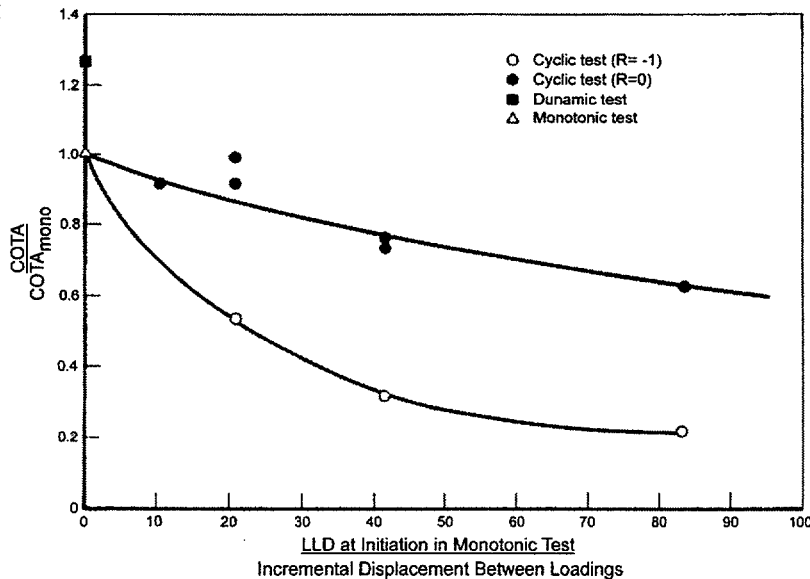


**Figure 5.17 Crack-tip-opening angle data from IPIRG-1 Subtask 1.2 stainless steel through-wall-cracked pipe experiments (Reference 5.44)**

Crack-tip sharpening was observed to be one of the main mechanisms in the cyclic degradation process, both for the stainless steel and the carbon steel. This sharpening acts to increase the crack-tip stress intensity and promote crack extension, thus lowering the apparent fracture resistance of the material. Because of the more ductile nature of the stainless steel, its tendency toward more pronounced crack-tip blunting resulted in less severe crack-tip sharpening than in the carbon steel. Because the carbon steel has a lower toughness and less-pronounced crack-tip blunting than stainless steel, it may take less compressive load to sharpen the crack tip. This may partially explain why the carbon steel tested was more affected by the intermediate stress ratios (e.g.,  $R = -0.3$ ) than the stainless steel.

Void sharpening also appeared to be an important mechanism in the cyclic degradation process, but only the carbon steel material tested experienced substantial void sharpening. Sharp voids tend to enhance void coalescence and lower the apparent fracture toughness. The rationale for this mechanism is similar to the one made for crack-tip sharpening; the higher the material toughness, the larger the compressive load needed to promote void sharpening. Crack-tip sharpening and void sharpening can work together in degrading a material's fracture resistance under cyclic loading.

From an LBB perspective, based on the above discussion, cyclic loads, potentially from a seismic event, could affect the material toughness, and thus the stability analysis and critical crack size analysis of an LBB assessment. The extent of the degradation will be somewhat probabilistic in nature, depending somewhat on how the cyclic load history builds up. From the IPIRG-2 simulated-seismic pipe experiments (Ref. 5.61), it was found that the way the time history evolves could significantly affect the results. If the seismic time history involves elastic cyclic loading, followed by a large amplitude cyclic load, then the seismic load history will act like a monotonic dynamic load history, with minimal cyclic damage. (See the results for Experiment 1-1 from IPIRG-2 in Reference 5.61.) Seismic histories like the

Northridge and Kobe earthquakes tended to have a sudden large amplitude loading of this type. On the other hand, if the amplitude gradually builds up, then there would be more cyclic damage at the crack tip. (See the results from the BINP Task 2 experiment in Reference 5.21.)

For an LBB assessment, cyclic loadings can reduce the fracture resistance of the material and thus the resultant stability of the through-wall crack, but the extent of that degradation is only important if there are large compressive stresses applied, i.e., a significantly negative stress ratio. Furthermore, the magnitude of the stress ratio will be biased towards a more positive value due to the tensile membrane stress due to the internal pipe pressure, thus somewhat mitigating the detrimental effects of the cyclic loading.

In summary, although cyclic loads can be detrimental to fracture resistance, there is no clear way as to how to account for them. Perhaps the best way would be to conduct a probabilistic study on seismic load functions, and use that to assess the magnitude of the degradation effect versus frequency of occurrence. One could then establish a cyclic toughness correction based on the mean result of that study.

#### **5.3.3.3 Dynamic Strain Aging Effects on Material Properties**

– In the First IPIRG program it was observed that both the ultimate strength and fracture toughness of many ferritic pipe steels decreased with increasing strain rate when the tests were conducted at light water reactor (LWR) temperatures (Ref. 5.19), see Figures 5.18 and 5.19. (Conversely, one ferritic weld showed a significant increase in toughness at the higher loading rate, see Figure 5.20.) In addition to the natural concern over this decrease in material properties, there was also a concern over the occurrence of unstable crack jumps in these materials at these temperatures, and the potential effect of these crack instabilities on LBB. Figure 5.21 shows the load versus displacement curve for a 28-inch diameter pipe test conducted as part of the Degraded Piping Program showing the sharp drops in loads indicative of the crack instabilities that occurred

during this experiment. These observations of lowering of the material's strength and toughness and crack instabilities were attributed to dynamic strain aging. As a result, during the Short Cracks in Piping and Piping Welds

program, a more detailed study was undertaken to examine the effect of dynamic strain aging (DSA) on the fracture behavior of carbon steel pipe (Ref. 5.25).

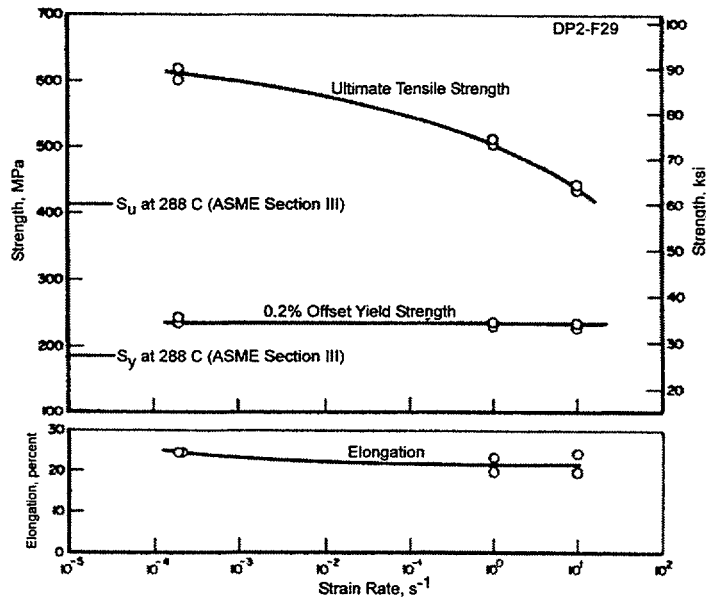


**Figure 5.18 Tensile properties at 288 C (550 F) versus strain rate for 16-inch diameter carbon steel pipe tested as part of IPIRG program**

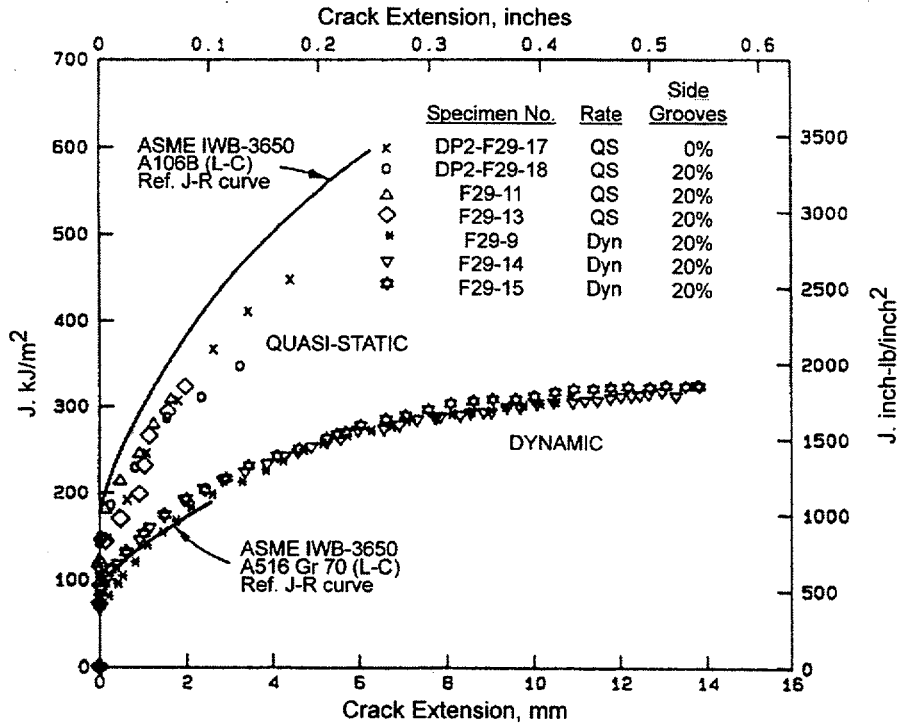


Figure 5.19 J-resistance curves for compact (tension) specimens tested at both quasi-static and dynamic loading rates at 288 C (550 F) for 16-inch diameter carbon steel pipe tested as part of the IPIRG program

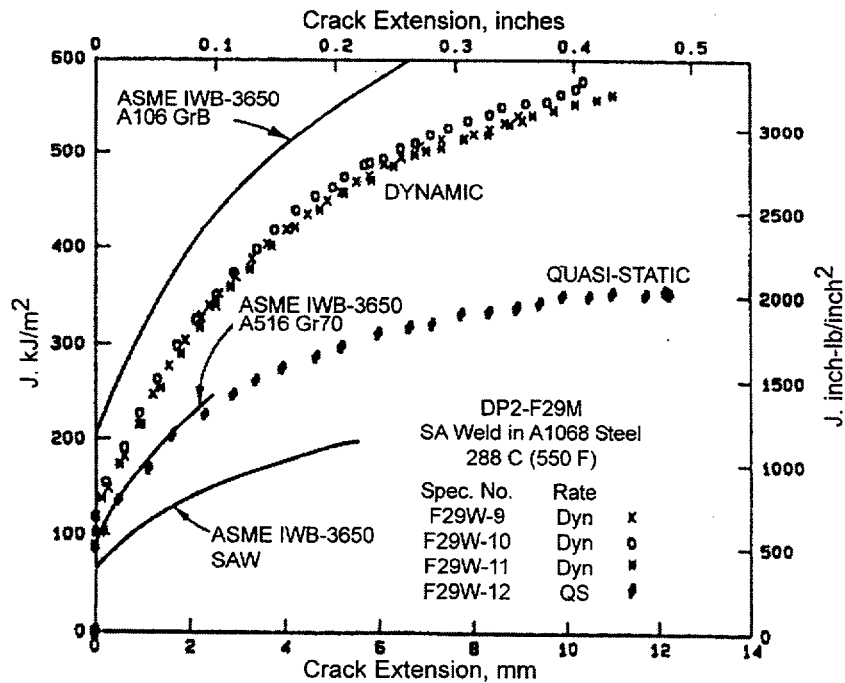
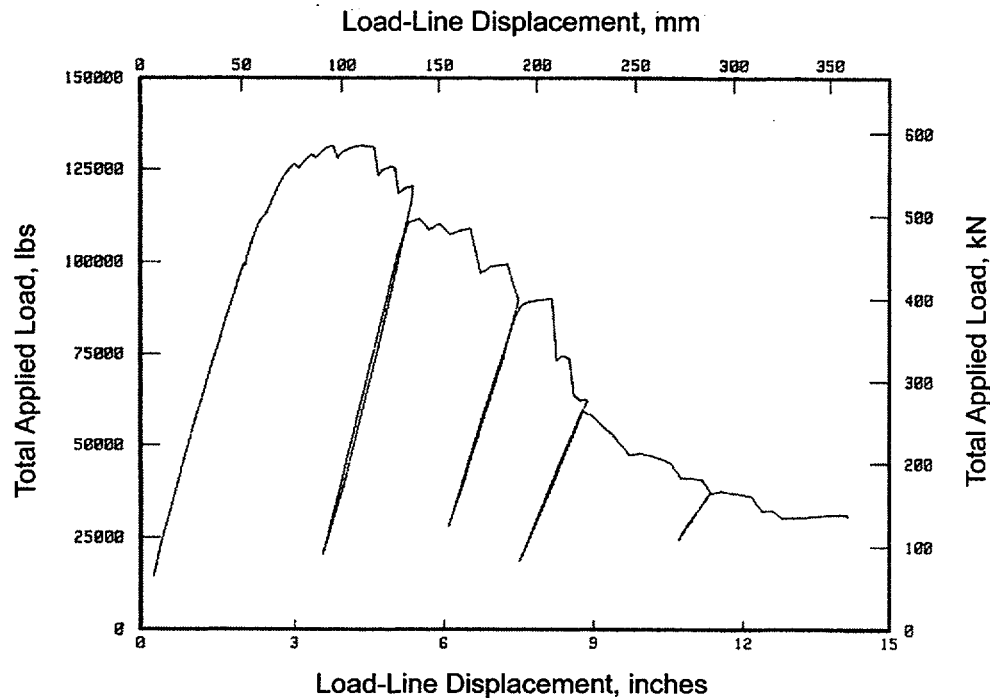


Figure 5.20 J-resistance curves for compact (tension) specimens tested at both quasi-static and dynamic loading rates at 288 C (550 F) for carbon steel submerge-arc weld tested as part of the IPIRG program



**Figure 5.21 Load-displacement record from a 28-inch diameter through-wall-cracked carbon steel pipe experiment illustrating the drops in load indicative of crack instabilities**

The overall objective of this task in the Short Cracks program was to develop the tools in order that one could predict the occurrence of and evaluate the effects of these ductile crack instabilities. Dynamic strain aging is a phenomenon observed in many carbon steels at light water reactor temperatures. It involves interactions between highly mobile nitrogen and carbon atoms dissolved in the steel and moving dislocations associated with plastic strains. At certain combinations of strain rate and temperature, these interactions can lower the crack-growth resistance and can cause a stably growing crack to become temporarily unstable, i.e., to jump. Specific objectives of this study were to: (1) establish a simple screening criterion to predict which ferritic steels may be susceptible to crack jumps, and (2) evaluate the ability of current J-based analysis methodologies to assess the effect of crack instabilities on the fracture behavior of ferritic steel pipe.

Laboratory tests on a number of nuclear grade carbon steel pipe materials revealed that materials susceptible to DSA exhibited a peak in both the ultimate tensile strength and the Brinell

hardness number (BHN) at temperatures near the operating temperatures of light water reactors, see Figure 5.22. It was believed that the ratio of the maximum to minimum values of strength or hardness could provide a useful, though maybe not totally reliable, measure of a steel's propensity for crack jumps. Examination of both the laboratory specimen fracture test data and the full-scale pipe test data indicated that the DSA-induced crack jumps are random in nature. As such, the prediction of the occurrence of DSA-induced crack jumps and their effect on toughness in pipe tests from simpler laboratory tests will require the accumulation of more extensive data than are now available.

**5.3.3.4 Cracks in Welds** – Numerous tests have been conducted in all of the recent Battelle programs looking at the behavior of cracks that occur in welds, which is where cracks most naturally occur. One finding common to all of these efforts, regardless of weld type, is that for the analysis of cracks in welds, one should use the tensile properties of the base metal and the fracture toughness properties of the weld as part of the fracture analysis.

***Submerge-Arc and Shielded-Metal-Arc Welds (SAW and SMAW)*** – Numerous tests, both laboratory specimen and full-scale pipe, have been conducted where the crack was centered in a submerge-arc or shielded-metal arc weld. Both carbon and stainless steel weld procedures have been evaluated. Both SAW weld procedures were obtained from nuclear plant vendors in the United States. Figures 5.23 and 5.24 show J-R curves from C(T) specimen tests for these welds. Also shown for comparison are the J-R curves for the parent base metal material. As can be seen in these figures, the J-R curves for the welds are considerably lower than the

J-R curves for the base metals, at least at the quasi-static loading rates. This lowering of the fracture toughness is reflected in the ASME Section XI flaw evaluation criteria, as well as in the draft SRP 3.6.3 limit-load analysis, through the inclusion of the Z-factors to account for the fact that the crack is in a lower toughness material. At the dynamic loading rates, the J-R curve for the carbon weld metal is higher than the J-R curve for the carbon steel base metal, see Figure 5.23. This has been attributed to dynamic strain aging effects that were discussed in the previous section.

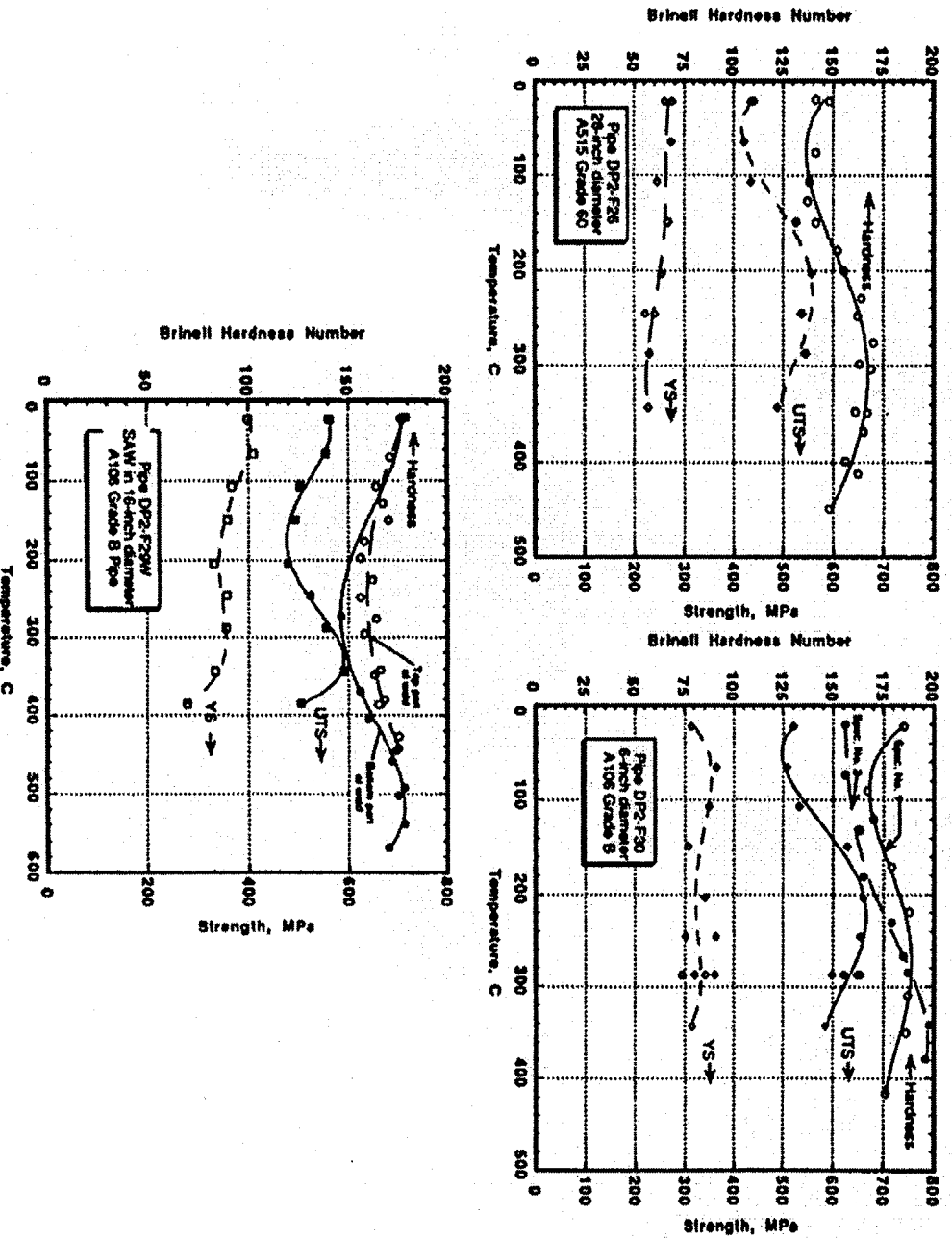
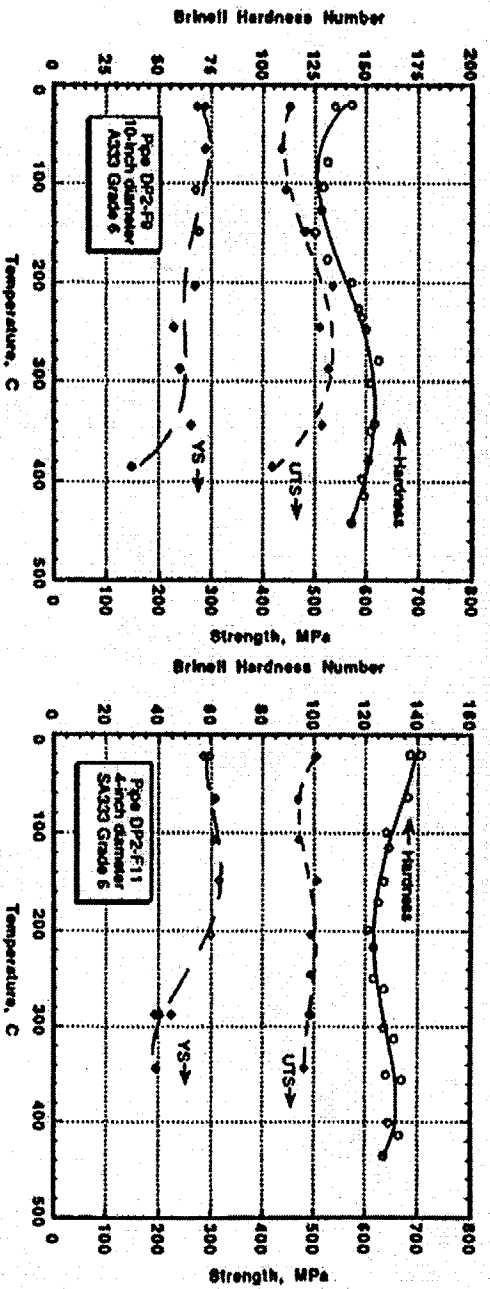


Figure 5.22 Yield strength, ultimate strength, and Brinell hardness as a function of test temperature for five carbon steel pipe materials

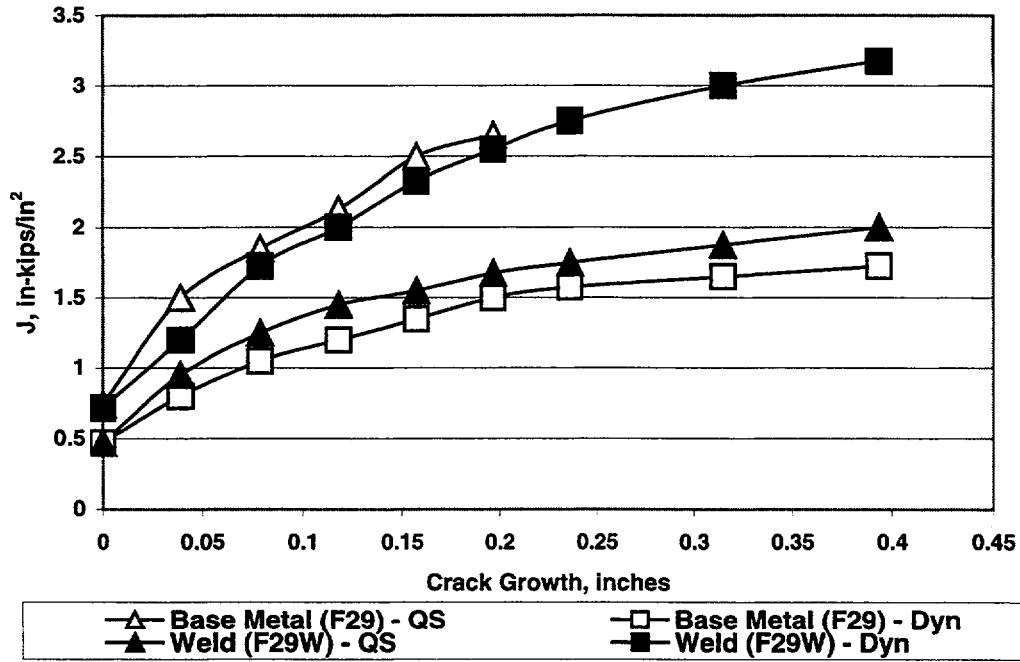


Figure 5.23 J-resistance curves for carbon steel SAW and parent base metal material

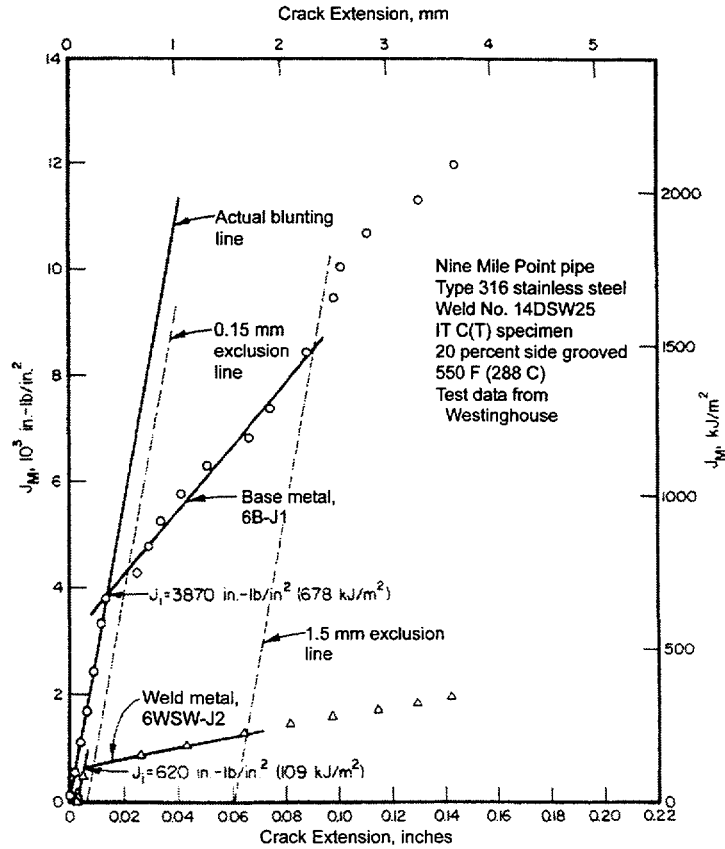


Figure 5.24 J-resistance curves at 288 C (550 F) for stainless steel SAW and parent base metal material (Type 316) from Nine Mile Point plant

**Tungsten-Inert-Gas (TIG) Welds** – Unlike their submerge-arc and shielded-metal-arc weld counterparts, tungsten-inert-gas (TIG) welds in stainless steels have toughness values comparable or in some cases higher than the parent base metal materials (Ref. 5.15). This is reflected in the ASME Section XI flaw evaluation criteria in which limit load conditions are assumed to exist, and the same evaluation criteria are used for TIG welds as are used for the stainless steel base metals, i.e., no stress reduction factor (Z-factor) is required for the analysis of cracks in these types of welds.

**Bimetallic Welds** – In both BWRs and PWRs there are many locations where carbon steel pipes or components are joined to austenitic pipes or components with a bimetallic weld. Examples from Westinghouse reactors include welds joining the hot and cold legs to the reactor pressure vessel and steam generators. In Combustion Engineering (CE) and Babcock and Wilcox (B&W) reactors, such welds include ferritic piping to cast stainless steel pump housings.

The bimetallic welds evaluated in the Degraded Piping and Short Cracks programs were obtained from a cancelled Combustion Engineering plant. The welds joined sections of the carbon steel cold leg piping system to stainless steel safe ends that were to be welded to the stainless steel pump housings. The carbon steel material was A516 Grade 70. The safe ends were fabricated from SA182 F316 stainless steel (forged TP316 stainless steel). The welds were fabricated by first buttering the beveled end of the carbon steel pipe with an ENiCrFe-3 (Inconel 182) electrode. The welds joining the buttered pipes to the stainless steel safe ends were then completed using a shielded-metal-arc weld process, using Inconel 182 weld rod. Several such welds in the nominal 36-inch diameter by 76 mm (3.0 inch) thick pipe were available for testing.

Both laboratory specimen tests (tensile and fracture toughness) and a full-scale through-wall-cracked pipe test were conducted as part of Reference 5.26. The initial cracks in the C(T) fracture toughness tests were positioned in the;

(1) carbon steel base pipe material, (2) the stainless steel forging material, and (3) along the carbon to stainless steel fusion line. The crack tips for the full-scale through-wall-cracked pipe test were along the fusion line. The major conclusion reached as a result of this effort was that the fracture behavior of the bimetallic fusion line pipe test could be predicted with reasonable accuracy using the strength and toughness properties of the carbon steel pipe material in conjunction with conventional elastic-plastic fracture mechanics analyses. This is believed to be due to; (1) the fusion line toughness, evaluated in the C(T) specimen tests, was slightly higher than the carbon steel base metal, (2) the Inconel weld metal was stronger than the carbon steel base metal, which coupled with the higher fusion line toughness, caused the crack to grow more in the carbon steel than in the Inconel 182 weld metal, and (3) the higher strength Inconel 182 weld metal may have shielded some of the plastic strains between the cracked section and the lower strength stainless steel safe end.

One point that should be emphasized is that the conclusions reached in Reference 5.26 are applicable to only this one class of bimetallic welds, i.e., a low strength carbon steel pipe welded to a stainless steel safe end using an Inconel weld procedure. The fracture behavior of other classes of bimetallic welds, made up of different material systems, may not be the same. For instance, for bimetallic welds associated with low alloy ferritic steel nozzle forgings, the strength and toughness properties of the various materials may be such that the crack will tend to grow in the weldment. In addition, if the bimetallic weld was made with stainless steel buttering rather than Inconel, then the crack may grow into a softer, carbon-depleted region near the heat-affected-zone of the carbon steel material. The resultant fracture toughness properties of such bimetallic welds can be significantly less than those measured as part of Reference 5.26. Figure 5.25 shows the measured J values at 1 and 2 mm (0.04 and 0.08 inch) of crack extension for a bimetallic weld fabricated using a stainless steel weld procedure. From Figure 5.25 it can be seen that the fusion line and heat-affected zone fracture toughness values for this stainless steel weld procedure

were a factor of almost four less than the fusion line toughness measured for the Inconel weld procedure in Reference. 5.26. For such welds, the fracture moments may be less than would be predicted using the carbon steel pipe properties in conjunction with conventional elastic-plastic

fracture mechanics analysis methods. (Furthermore, to our knowledge, the effects of thermal aging on the strength and toughness of bimetal welds have not been investigated to date.)

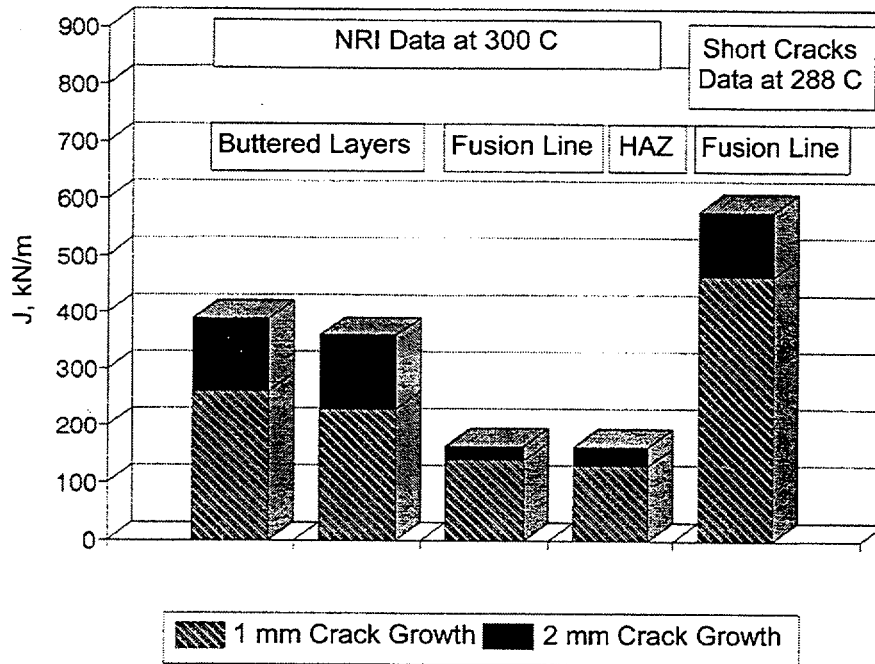


**Figure 5.25 J-values at 1 mm and 2 mm (0.04 and 0.08 inch) of crack extension for bimetallic welds made with a stainless steel weld procedure (data from Reference 5.26 for an Inconel weld are shown for comparison purposes)**

It should be noted though that in a review of some of the actual LBB submittals supplied by the NRC as part of this program, it was found that the vast majority of the bimetallic welds were fabricated using an Inconel weld procedure. Even so, recent experience with the Virgil C. Summer crack problem indicates that residual stresses associated with bimetallic welds may be a contributor to crack initiation and subcritical crack growth. This more recent service history has indicated the potential for the occurrence of primary water stress corrosion cracking (PWSCC) at bimetallic welds in PWR environments. In the past, PWSCC has been identified with Inconel 600, a high nickel alloy, used in the manufacturing of steam generator (SG) tubing. Steam generator service experience has shown that when Inconel 600 is

exposed to a high temperature, high purity water environment, in the presence of tensile residual stresses, intergranular PWSCC may occur. In 1986, leaks were first reported in Alloy 600 pressurizer instrument nozzles at both domestic and foreign reactors from several different NSSS vendors. The NRC staff identified PWSCC as an emerging technical issue to the Commission in 1989, after cracking was noted in Alloy 600 pressurizer heater sleeve penetrations at a domestic PWR facility. In September 1991, PWSCC cracks were first observed in Alloy 600 vessel head penetrations in the reactor head of a French PWR (Ref. 5.62).

On October 7, 2000, the licensee for V. C. Summer identified a large quantity of boron on the floor and protruding from the air boot around

the "A" loop RCS hot leg pipe. Ultrasonic testing (UT) and eddy current testing (ET) identified an axial crack-like indication approximately 69 mm (2.7 inches) long in the first weld between the reactor vessel nozzle and the "A" loop hot leg piping. The "A" loop hot leg weld was cut out and destructively examined. The 69 mm (2.7-inch) long indication was determined to be an axial crack approximately 63 mm (2.5 inches) long and almost through wall that was caused by PWSCC. High tensile residual stresses were present in the weld as a result of extensive weld repairs during original construction, and these stresses were considered a contributing cause for the PWSCC. The extensive weld repairs also complicated previous in-service inspections of the weld because weld roughness made it difficult to perform UT on portions of the weld. The destructive examination of the "A" loop hot-leg weld confirmed that a number of ET indications were also PWSCC cracks. The licensee also identified ET indications in four of the other five reactor coolant system nozzle to pipe welds. Although the cracking observed in this event was limited in extent, it confirmed that an active degradation mechanism was present in the primary system piping previously believed to be unaffected by known cracking mechanisms (Ref. 5.62 through 5.64).

Recent experience with Alloy 82/182 PWSCC in piping welds has not been limited to the V. C. Summer plant. Foreign reactors (Ringhals Units 3 and 4 in Sweden) have reported PWSCC of Alloy 82/182 weldments in main coolant loop piping.

Additional recent experience with Inconel 82/182 weld cracking has arisen as a result of inspections of RPV Control Rod Drive Mechanism (CRDM) penetrations. On February 18, 2001, a visual examination of the Oconee Nuclear Station Unit 3 (ONS3) RPV head identified boric acid deposits around nine CRDM nozzles (Numbers 3, 7, 11, 23, 28, 34, 50, 56, and 63), as described in LER 287/2001-001, Revision 0, dated April 18, 2001.

Eddy Current (EC) examinations of the nine leaking CRDM nozzles and nine non-leaking

CRDM nozzles (Numbers 4, 8, 10, 14, 19, 22, 47, 64, and 65) indicated clusters of shallow axial type cracks located above and below the weld. Nozzles 50 and 56 exhibited "non-typical clusters" above the weld; these clusters were later determined to be associated with through-wall circumferential cracks extending approximately 165 degrees around the nozzles. Six of the leaking nozzles (Numbers 11, 23, 28, 50, 56 and 63) had deep axial indications, and Nozzles 50 and 56 had circumferential indications below the weld.

Ultrasonic testing (UT) examinations were performed on the nine leaking CRDM nozzles and the same nine non-leaking CRDM nozzles examined with EC. The nine non-leaking nozzles did not have any crack-like axial or circumferential indications. The nine leaking nozzles had a total of 36 axial indications, nine circumferential indications below the weld and three circumferential indications above the weld. CRDM Nozzle 23 was identified with two circumferential indications below the weld and one circumferential indication above the weld. The latter was discovered through a third party review of the data.

Penetrant testing (PT) examinations of the nine leaking CRDM nozzles covered an area 3 inches in diameter from the nozzle, including the J-groove weld surface, the fillet weld cap and part of the vessel head cladding, and extended 1 inch down the OD of the nozzle from the weld to nozzle interface. For all nine nozzles, the PT examination revealed multiple rejectable indications. Post-repair PT examinations of Nozzles 50 and 56 identified through-wall circumferential cracks extending approximately 165 degrees around the nozzles.

The leaking CRDM nozzles were repaired using manual repair methods, using Alloy 690 filler materials (Alloy 152). A protective Alloy 690 weld pad was applied to the repairs to protect and isolate any remaining original Alloy 600 from the reactor water environment.

On November 12, 2001, a visual examination of the ONS3 RPV head identified boric acid deposits around seven CRDM nozzles (Numbers

2, 10, 26, 39, 46, 49, and 51), as described in LER 287/2001-003, Revision 0, dated January 9, 2002. The inspection was performed as part of the planned surveillance activity during ONS3 refueling outage 19. The licensee classified four CRDM nozzles (Numbers 26, 39, 49, and 51) as having a high probability of leakage through the pressure boundary as evidenced by the boric acid deposits on the reactor vessel head. The licensee characterized the remaining three CRDM nozzles (Numbers 2, 10, and 46) as masked by boron from an external source (i.e. flange leakage). All seven nozzles were identified as requiring further inspections.

The licensee elected not to perform EC examinations for any of the leaking or suspected leaking nozzles due to radiation dose considerations. However, the licensee performed PT and UT examinations as described below.

UT examinations were performed on the seven leaking and suspect CRDM nozzles plus an additional two nozzles (Numbers 29 and 31). The two additional nozzles were examined for extent of condition since their CRDM's had to be removed to allow access for repair equipment. Two nozzles (Numbers 29 and 46) had no UT indications. Five nozzles (Numbers 2, 26, 39, 49, and 51) all had indications that extended from below the weld to above the weld, indicating a leak path in addition to various other ID and OD indications. One of these five nozzles (Nozzle Number 2) had a circumferential crack in the nozzle above the J-groove weld. Identification of the circumferential crack above the J-groove weld in Nozzle Number 2 is significant since the nozzle is near the top of the reactor vessel head. All previous circumferential cracks above the J-groove weld have been identified in nozzles on the periphery of the reactor vessel head, which is the expected location due to higher stresses. As mentioned, Nozzle Number 2 was characterized as masked by boron from an external source, and had also been masked during the February 2001 outage. Therefore, the licensee concluded that the CRDM nozzle had most likely been leaking for years prior to the discovery of the circumferential crack during the November 2001

outage. Nozzle Numbers 10 and 31 contained several OD indications located below the weld and extending slightly into the weld, but showed no leak path.

PT examinations were performed on Nozzle Numbers 10, 31, and 46. Nozzle Number 10 had previously been identified as masked, and Nozzle Numbers 10 and 31 had UT results showing several OD indications located below the weld. As mentioned, Nozzle Number 46 had no UT indications. PT results for Nozzle Numbers 10 and 31 showed small nozzle OD flaws that ran up to the J-groove weld region at the weld to nozzle wall interface. No PT indications were found for Nozzle Number 46.

The five leaking CRDM nozzles and two non-leaking nozzles (Numbers 10 and 31) were repaired utilizing a process similar to the method used for the ONS-2 CRDM nozzle repairs performed in May 2001 (LER 270/2001-002). The decision to repair the additional two nozzles was primarily based on the axial indications on the OD nozzle surface and the comparison of this data to previous ONS nozzle inspections that showed that these types of active PWSCC flaws could eventually result in a leakage pathway. The protruding portions of the nozzles and a length about 5 inches into the RV Head bore were removed by machining. A new pressure boundary weld was installed within the bore, inspected and surface conditioned with a water jet peening process to complete the repair.

As a result of the circumferential flaw found on Nozzle 2, an extended scope inspection was performed. The scope of the inspection involved the 43 remaining nozzles that, historically, had neither been previously repaired nor volumetrically inspected. Circumferential blade probes were used to inspect the nozzle area from one inch above the top of the J-groove weld to one inch below the bottom of the J-groove weld. Thirty-six of the nozzles were inspected with 100 percent of the coverage area being examined. There were seven nozzles where 100 percent inspection of the coverage area could not be achieved due to limited access inside the nozzle annulus. The inspection coverage on these 7 nozzles ranged from 75% to

99%. Overall results revealed no indications within the nozzle material for the 43 nozzles inspected.

The licensee used the NRC crack growth methodology from the generic technical assessment dated November 2001 to conclude that if circumferential cracks existed in the uninspected areas of these 7 nozzles, these cracks would not grow to the extent that they would present a safety concern prior to the next planned outage in 18 months. The licensee has also concluded that ONS3 will be restarting with no known leakage, and this is in compliance with applicable technical specification requirements.

Both the V. C. Summer main coolant loop and Oconee Unit 3 CRDM weld cracking events serve to illustrate that PWSCC of Inconel 82/182 material has the potential to seriously affect the integrity of structural welds in a PWR environment. Conditions of the environment (temperature, oxygen content, etc.) as well as characteristics of a specific weld (number/severity of repair welds, residual stresses, fabrication flaws, etc.) may affect the sensitivity of a weld to PWSCC. All of these factors, therefore, must be accounted for when assessing the potential for PWSCC to influence pipe-rupture probabilities.

From an LBB perspective, this occurrence of PWSCC in the primary piping systems of PWRs is certainly problematic. While as shown, the use of the Inconel 82/182 weld procedure is advantageous from a fracture toughness viewpoint, its use does appear to introduce a potential new degradation mechanism. Obviously, the existence of this new degradation mechanism is in conflict with the requirements spelled out in draft SRP 3.6.3 for LBB acceptance. This is especially problematic since most of these piping systems have already been approved for LBB, based at least partially on the fact that there were no known degradation mechanisms associated with these piping systems at the time LBB was applied for. With

this recent experience with PWSCC in Inconel 82/182 weldments (used extensively in the fabrication of bimetallic welds in many of these systems), the contention of no known degradation mechanisms is clearly brought into question.

Currently there is ongoing work at Battelle sponsored by the NRC as part of the BINP program aimed at modeling the residual stress state around one of these RPV/hot leg repair welds. Data from this residual stress analysis will then be used to make an assessment of the impact that these repair welds have on PWSCC.

*Fusion Line Toughness* – Early in the Degraded Piping Program a series of four single-edge notch (tension), SEN(T), specimen tests were conducted in which the initial notches were introduced; (1) in the base metal, (2) in the heat-affected zone (HAZ), (3), along the fusion line, and (4) in the weld metal. Post-test photographs of cross sections of these SEN(T) specimens are shown in Figure 5.26, illustrating the differences in the crack-tip-opening angle (CTOA) for the four crack locations. From Figure 5.26, it can be seen that the CTOA, which is a measure of fracture toughness, for the fusion line is a factor of 6 less than the CTOA for the base metal and HAZ, and a factor of 3 less than the weld metal. Higher CTOA values are indicative of higher toughness materials. Consequently, from this figure it appears that the fracture resistance for the fusion line is considerably less than it is for the other locations.

Later in the Degraded Piping, IPIRG, and Short Cracks programs it was observed that the cracks in the stainless steel weld pipe experiments tended to grow along the fusion line after a small amount of crack growth, even though the initial crack was located in the center of the weld, see Figure 5.27. The explanation for this observation was the lower apparent fracture toughness of the fusion line when compared with the weld metal or base metal as evident in Figure 5.26.

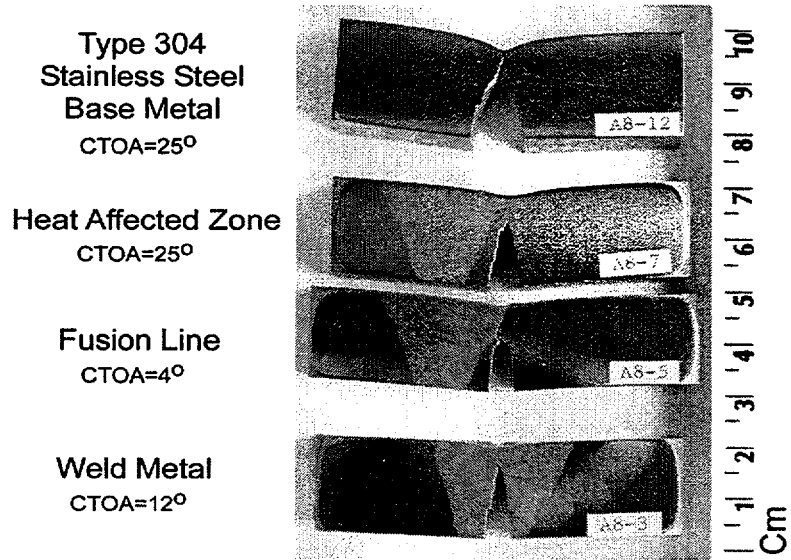


**Figure 5.26 Crack propagation in stainless steel base metal, in the HAZ remote from fusion line, along the fusion line, and in the weld metal in SEN(T) specimens at 288 C (550 F)**

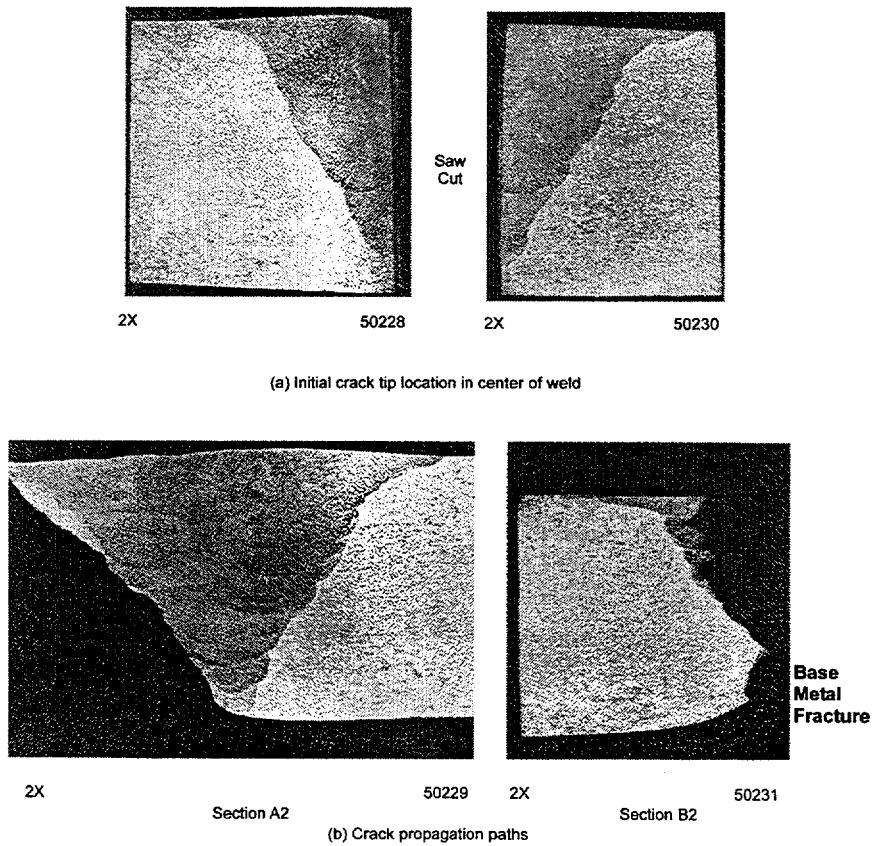


**Figure 5.27 Crack propagation along fusion line of a TP316 SAW in a 28-inch diameter pipe experiment even though initial starter notch was centered in the weld and the weld crown was ground off**

As a result, as part of the Short Cracks program, a study was undertaken to examine in detail the weld fusion-line toughness of stainless steel submerge-arc welds (Ref. 5.27). As part of this study, it was found that while the  $J_{Ic}$  for the fusion line was much higher than that for the submerge-arc weld, the crack growth resistance (measured in terms of the J-R curve) of the fusion line reached a steady-state value, while the SAW metal had a continually increasing J-R

curve, see Figure 5.28. This explains why the cracks eventually turned and grew along the fusion line in the pipe experiments. A method of incorporating these results into an LBB assessment would be to use the weld metal J-R curve up to the fusion-line steady-state J-value, and then use the steady-state portion of the fusion-line J-R curve for the remainder of the crack growth, see Figure 5.28.

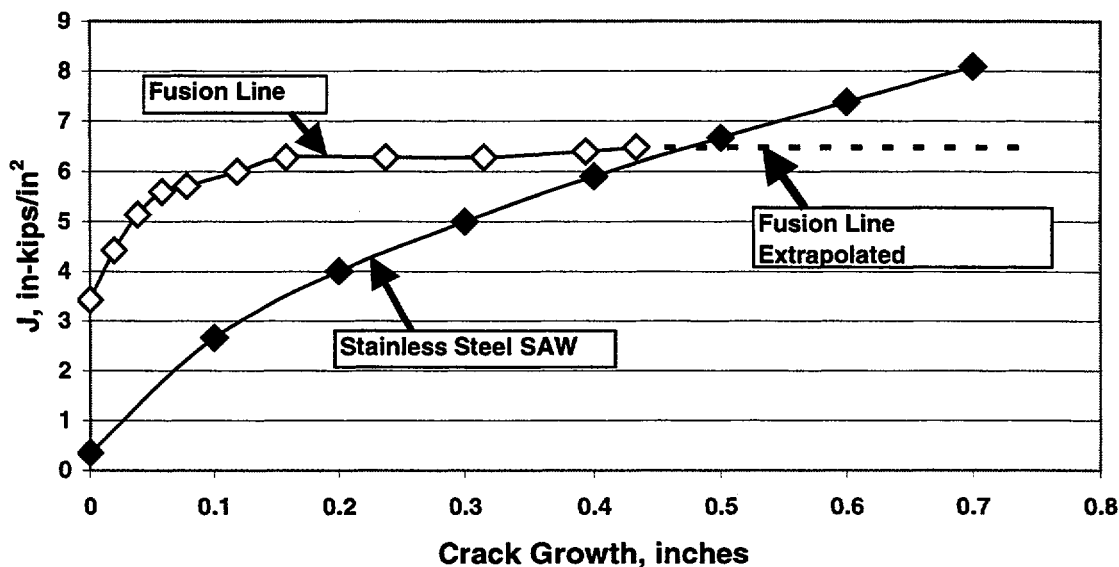


Figure 5.28 Weld metal and fusion line J-R curve data for stainless steel SAW

**5.3.3.5 Thermal Aging Mechanisms** – Cast stainless steels, that are often used in Westinghouse primary piping (hot, cold and crossover legs of the main coolant loops), surge lines, and some elbows, are well known to be susceptible to fracture toughness degradation due to thermal aging. In addition, some stainless steel weldments are suspected of being susceptible to the same type of fracture toughness degradation mechanism.

**Cast Stainless Steels** – Investigations at Argonne National Laboratories (ANL), Refs. 5.30 through 5.33, and elsewhere have shown that thermal aging of cast stainless steel components can occur during the reactor design

lifetime of 40 years. Thermal aging at reactor temperatures increases the hardness and tensile strength and decreases the ductility, impact energy and fracture toughness of the steels. The Charpy transition curve shifts to higher temperatures. Different heats exhibit different degrees of thermal embrittlement. The low carbon CF3 steels are the most resistant and the Mo-bearing high carbon CF8M steels the least resistant to thermal embrittlement.

At Argonne, micro-structural and mechanical property data have been obtained on 25 experimental heats [static-cast keel blocks and slabs) and 6 commercial heats [centrifugally cast pipes, a static-cast pump impeller, and a static-

cast pump casing ring), as well as on reactor-aged material of CF3, CF8, and CF8M grades of cast stainless steel. The ferrite content of the cast materials ranges from 3 to 30 percent.

As part of the Argonne work, it was found that embrittlement of cast stainless steels results in brittle fracture associated with either cleavage of the ferrite or separation of the ferrite/austenite phase boundary. Predominantly brittle failure occurs when either the ferrite phase is continuous (e.g., in cast materials with a large ferrite content) or when the ferrite/austenite phase boundary provides an easy path for crack propagation (e.g., in high carbon grades of cast steel with large phase-boundary carbides). Consequently, the amount, size, and distribution of the ferrite phase in the duplex structure and the presence of phase-boundary carbides are all important parameters in controlling the degree or extent of thermal embrittlement.

The ANL work resulted in procedures and correlations for estimating Charpy-impact energy, tensile properties, fracture toughness J-R curves, and  $J_{Ic}$  values of aged cast stainless steels from known material data. For example,

- The extent of degree of thermal embrittlement at "saturation", i.e., the minimum impact energy that can be achieved for a material after long-term aging, is determined from the chemical composition of the steel. Charpy-impact energy as a function of the time and temperature of reactor service can be estimated from the kinetics of thermal embrittlement, which is also determined from the chemical composition. The impact energy of the unaged steel is required for these estimates.
- The tensile properties of aged cast stainless steel are estimated from information that is readily available from certified material test records for the component, i.e., chemical composition and the initial tensile strength of the unaged material. Tensile yield and flow stresses, and Ramberg-Osgood parameters for tensile strain hardening, can be estimated from the flow stress of the unaged material and the kinetics of embrittlement.
- The fracture toughness J-R curve for the material can be obtained by correlating room temperature Charpy-impact energy with fracture toughness parameters. Alternatively, in Reference 5.33, a common "predicted lower bound" J-R curve for cast stainless steels with unknown chemical composition is defined for a given grade of steel, range of ferrite contents, and temperatures.
- The values of  $J_{Ic}$  are estimated from the estimated J-R curve and flow stress.

**Stainless Steel Welds** – There are limited data on the subject of the effect of thermal aging of stainless steel welds on their toughness levels. As such, this effect has not been considered to date in LBB evaluations. However, in reviewing the various LBB submittals, one applicant did cite that the Charpy energy of one weld (at least in one case) decreased from 54 to 32 J (40 to 24 ft-lbs) as a result of an aging process. The applicant did not say at what temperature the Charpy testing was conducted, but assuming that this was upper-shelf behavior, this represents a toughness drop of 40 percent. In the low toughness regime, this is a significant decrease. For instance the  $J_{Ic}$  value of an unaged stainless steel submerge-arc weld is typically around 87 kJ/m<sup>2</sup> (500 in-lbs/in<sup>2</sup>). With the Charpy energy being proportional to  $J_{Ic}$  in this regime, the aged weld toughness would be approximately 52 kJ/m<sup>2</sup> (300 in-lbs/in<sup>2</sup>). This is a toughness regime where the load-carrying capacity is very sensitive to such toughness changes. As such, the aging of welds in stainless steel pipes (surge lines, accumulator lines, etc.) can be a very important factor to consider. Additional data in this area are needed. In addition, a sensitivity study to examine the significance of this effect on the load-carrying capacity should be conducted to see if this effect is negligible or not. It may be found that if the rest of the J-R curve is lowered in addition to the  $J_{Ic}$  value, it may be worthwhile to conduct a small sensitivity study to examine the magnitude of this effect. It is difficult to say if this effect is significant or not at this time.

**5.3.3.6 Fracture Toughness Properties of Stainless Steels with High Sulfur Contents –** At the end of the Second IPIRG program it was discovered that a group of 16-inch diameter Schedule 100 stainless steel pipes that had been used in numerous pipe experiments in the Degraded Piping and IPIRG programs, and which were thought to be all of the same heat, were actually from two distinct heats. Furthermore, the fracture toughness properties

for the two heats (designated as A8I and A8II) were dramatically different, see Figure 5.29. In reviewing the chemistry data for the two heats, it was found that for the most part, the chemical composition of the two heats were very similar, except that A8II had a much higher sulfur content than A8I, i.e., 0.019 percent versus 0.002 percent.

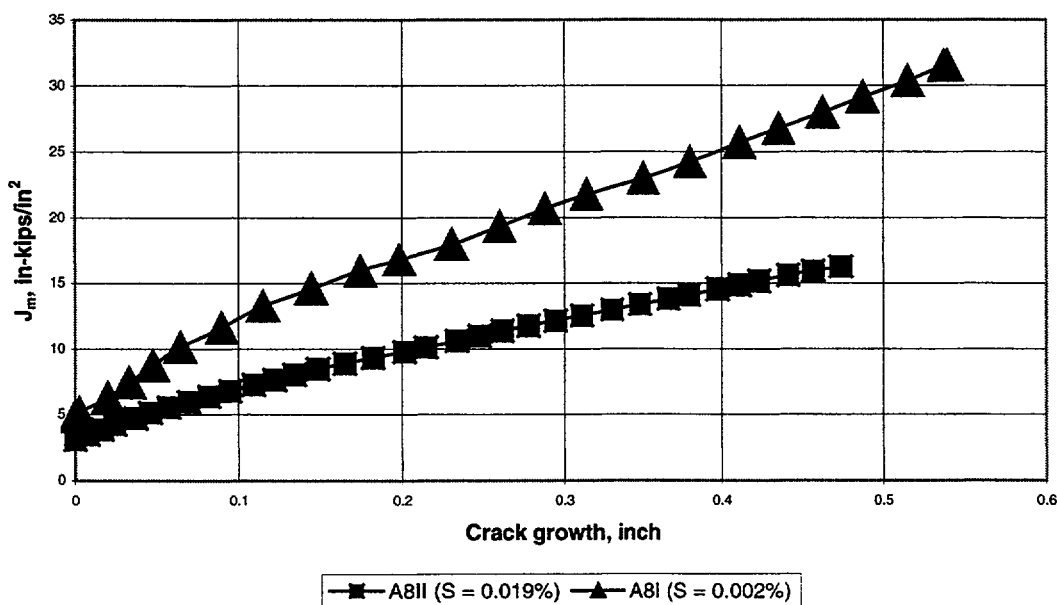


**Figure 5.29 J-resistance curves for two heats of pipe material A8 (A8I and A8II)**

As a result, as part of the NRC LBB Regulatory Guide program conducted at Battelle, a sensitivity study was under taken to look at the effect of sulfur content on the load-carrying capacity of cracked stainless steel pipes<sup>19</sup>. As part of this study, the PIFRAC database (Ref. 5.58) was exercised and the J-R curves for 7 heats of stainless steels with varying amounts of sulfur were extracted. Figure 5.30 shows the J-R curves for these heats of steel. From Figure 5.30 it can be seen that the J-R curves are

grouped together in terms of sulfur content. The J-R curves for those heats with sulfur contents less than about 0.011 percent were about twice as high as the J-R curves for those heats with sulfur contents greater than about 0.018 percent. Furthermore, it appears that the J-R curves tend to saturate since increasing the sulfur content above 0.018 percent did not appreciably lower the J-R curves further. Note, one material, A52-5, whose J-R curve is shown in Figure 5.30, contained the maximum sulfur content, 0.30 percent, allowed by the applicable ASTM standard.

<sup>19</sup> There are other inclusion causing impurities in stainless steel, e.g., phosphorous, that may cause a similar reduction in toughness, but as part of this small sensitivity study, only the effect of sulfur content was examined.

Using the data in Figure 5.30, a number of NRCPIPE type calculations were made to predict the maximum load-carrying capacity of

through-wall-cracked stainless steel pipe as a function of the sulfur content. Sample pipe diameters from 6 to 36 inch were assumed in these sample calculations. From these calculations it was predicted that the higher sulfur content pipes would have about a 15 to 20 percent lower maximum load-carrying capacity than the lower sulfur stainless steels, see Figure 5.31. While draft SRP 3.6.3 assumes that

stainless steel base metals would always fail under limit-load conditions, this result indicates that this may not necessarily be the case. However, this effect was still considered a second order effect, since the analysis procedures used tended to be conservative by about 10 percent and in light of the safety factors imposed in a draft SRP 3.6.3 LBB analysis.

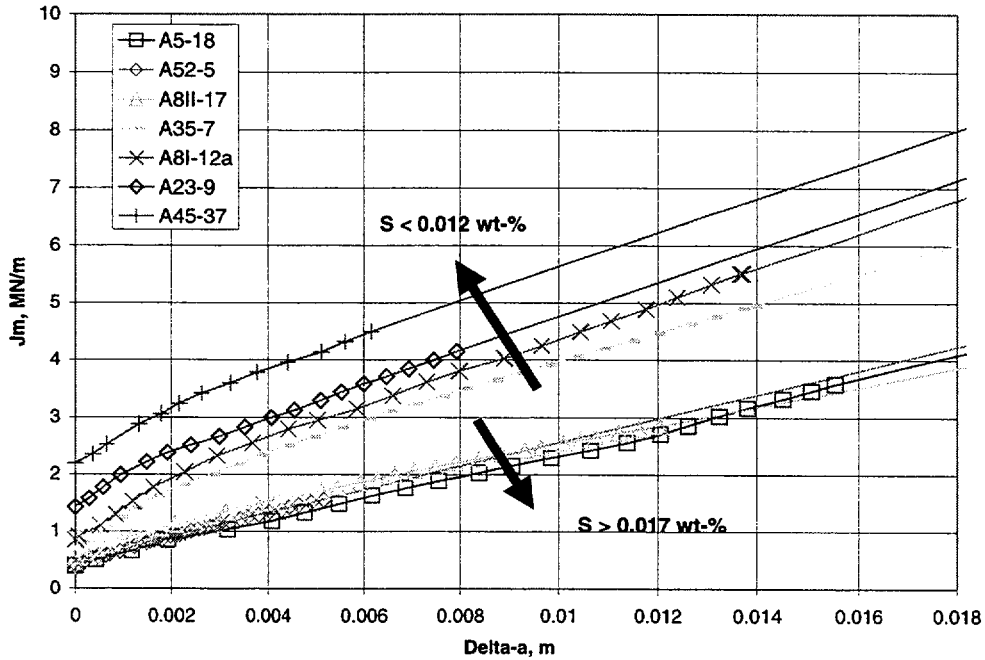


**Figure 5.30 J-R curves for 7 heats of stainless steel extracted from PIFRAC showing the effect of sulfur content on the fracture resistance for wrought stainless steels**

**Maximum Moment for Battelle Tested Specimens  
(Through Crack, 36 x 3.25 Pipe)**

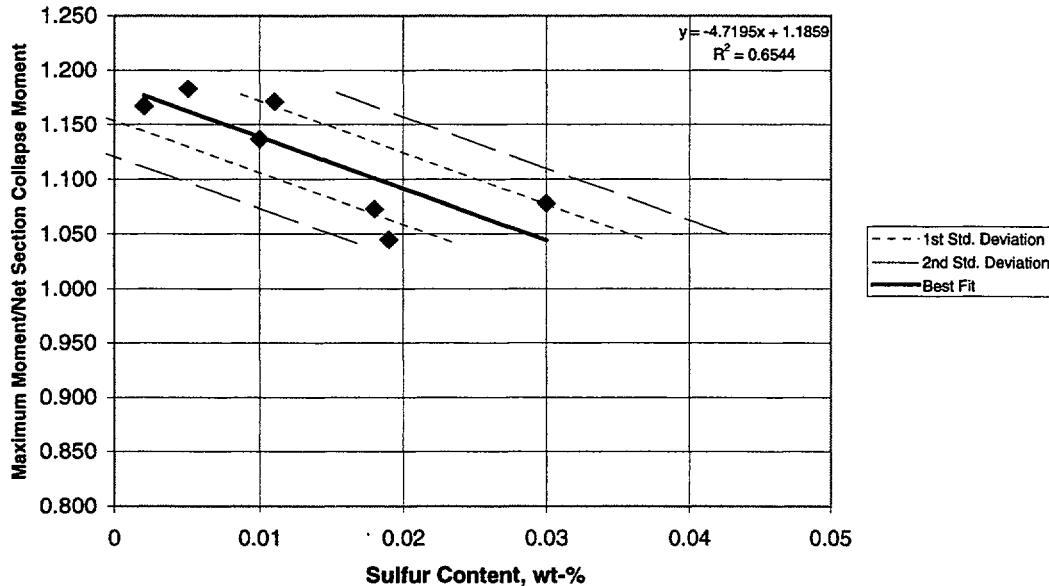


**Figure 5.31 Predicted maximum moment normalized by the Net-Section Collapse moment as a function of sulfur content for the 7 heats of stainless steel extracted from the PIFRAC database**

**5.3.3.7 Effect of Toughness Anisotropy on LBB** – In some of the early carbon steel through-wall-cracked pipe experiments in the Degraded Piping Program it was observed that the crack turned out of the circumferential plane, which was the direction of maximum crack-driving force, and grew in a helical direction with respect to the circumferential plane. This same angled crack growth was observed in some laboratory C(T) specimen tests which were machined without side grooves, see Figure 5.32. Later in the Degraded Piping Program it was found that this angled crack growth was caused by the fracture resistance in the helical direction being less than in the circumferential direction. C(T) specimens were machined from a 4-inch diameter pipe with the cracks oriented in the circumferential direction, the axial or longitudinal direction, and at 45 and 66 degree angles with respect to the circumferential crack plane. Figure 5.33 shows the J-R curves for the different orientations. As can be seen in this

figure, the circumferential direction had the highest crack-growth resistance while the specimens machined with the crack oriented helically with respect to the circumferential plane had the lowest crack growth resistance. Subsequent metallographic sections revealed that the inclusions in this pipe material were aligned in the helical direction. From an LBB perspective this is of highest concern when the piping system is subjected to high torsional stresses. In such cases, the principal stress direction may be aligned with the direction of least crack growth resistance. Note, that this helical crack growth was only observed for carbon steel pipes. None of the stainless steel pipe experiments exhibited such behavior. The fact that the carbon steels exhibited this behavior and the stainless steels did not has been attributed to the pipe manufacturing process used in fabricating carbon steel pipe.

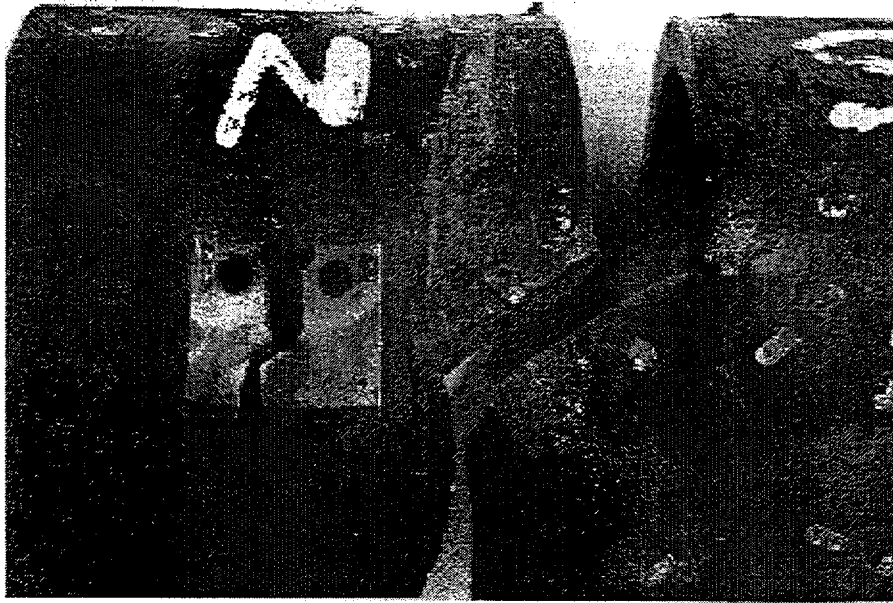


**Figure 5.32** Photograph of the fractured pipe from Experiment 4111-1 from the Degraded Piping Program and a compact (tension) specimen from this same material

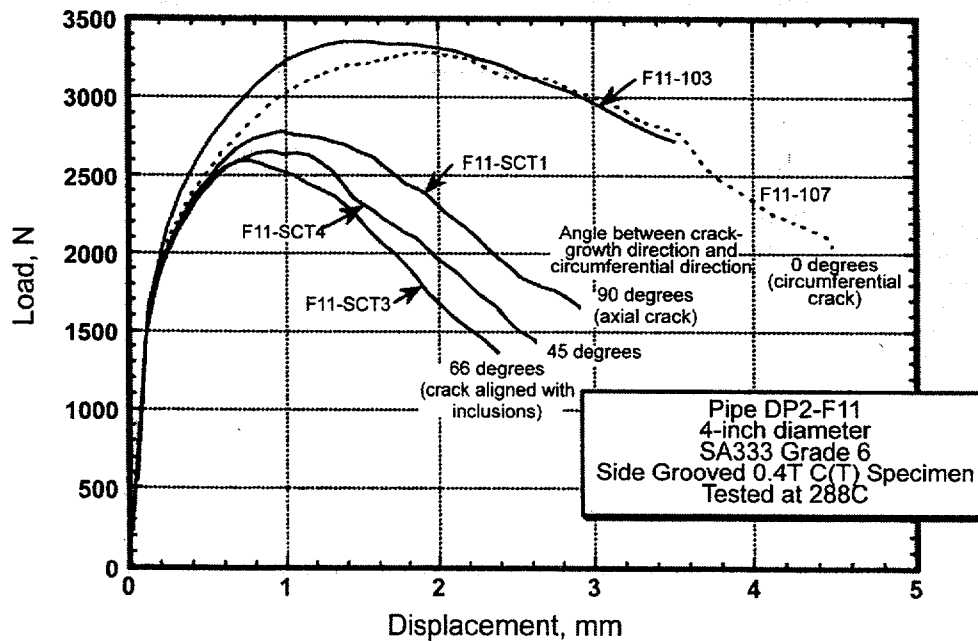


**Figure 5.33** J-resistance curves for several different C(T) specimen orientations in Pipe DP2-F11 that was used in Experiment 4111-1 in the Degraded Piping Program

**5.3.3.8 J-Resistance Curve Extrapolation Techniques** – To make predictions of the fracture behavior of through-wall cracks in large-diameter pipe for LBB analyses, one needs a J-R curve with a large amount of crack growth. Unfortunately, most J-R curves are obtained from laboratory-size C(T) specimens and the amount of valid crack growth one can obtain is typically very limited, oftentimes less than 6.3 mm (0.25 inches). In order to predict the relatively large amount of through-wall-crack growth that might occur up to the point of maximum load, one needs some means of extrapolating the laboratory-size C(T) specimen data to larger amounts of crack growth. In the Degraded Piping Program, a study involving a combined experimental and analytical approach was undertaken to address this need (Ref. 5.14). The experimental effort included tests of 25.4-mm (1.0-inch) thick compact (tension) specimens of 1T, 3T, and 10T planar dimensions. Both side-grooved and nonside-grooved specimens, machined from both Type 304 stainless steel plate and A516 Grade 70 carbon steel plate, were tested at 288 C (550 F). The data were analyzed using both deformation theory J ( $J_D$ ) and modified J ( $J_M$ ) estimation schemes to develop resistance curves. Also, elastic-plastic finite element analyses were performed of the 1T, 3T, and 10T stainless steel nonside-grooved specimen data. The results of these analyses were then used to assess the extrapolation procedures.

It was found as a result of this study that using small-specimen  $J_D$ -resistance curves to generate large-crack-growth  $J_D$ -resistance curves is either not possible or can result in gross underestimates of both  $J_{Material}$  and  $dJ_{Material}/da$  for large crack growth, i.e., a conservative assessment from an LBB crack stability viewpoint. Attempts were made to apply the NUREG-1061 (Ref. 5.65) approach for extrapolating small-specimen data to large amounts of crack extension. Since the  $J_D$  values for the stainless steel material exceeded the maximum permissible values, even at crack initiation, the NUREG-1061 approach could not be used for this material. When applied to the carbon steel data, the NUREG-1061 approach resulted in large underestimates

(conservative) of  $J_D$ , and could be applied only to the 1T C(T) specimen data. Therefore, the NUREG-1061 extrapolation method was of little value for the materials examined. As an alternative, an empirical approach for extrapolating small-specimen data was used. This method involves use of the modified J ( $J_M$ ) and suggests that the  $J_M$ -versus- $dJ_M/da$  curve can be represented by a hyperbola.

**5.3.3.9 Flow Stress Definitions** – For the flaw stability or critical-crack-size analyses associated with an LBB assessment, the flow stress is an often used parameter to define the strength characteristics of the material. The flow stress of the material can be defined in a number of ways. If actual tensile data exist from archival material, the definition oftentimes used is the average of the yield and ultimate strengths. Lacking actual data from archival material, one can either rely on lower-bound database properties or code properties. For flaw evaluation criteria, ASME Section XI initially defined the flow stress in terms of the Code Design Stress ( $S_m$ ), either  $3S_m$  for austenitic materials or  $2.4 S_m$  for ferritic materials. The 2001 revised ASME Section XI Appendix C for austenitic and ferritic pipe uses the average of the Code yield and ultimate strengths or actual strength values, if known. The draft SRP 3.6.3 also uses Code minimum values at temperature for its definition of flow stress.

### 5.3.4 Stress Analysis

The stresses used in an LBB analysis are typically based on linear-elastic analysis using a response spectrum type analysis that only provides peak loads. No consideration is made of the additional margins one might achieve by considering nonlinear plasticity effects, or the coupled nature of the stress and fracture analyses.

**5.3.4.1 Additional Margins from Nonlinear Analysis** – The 19 to 38 lpm (5 or 10 gpm) postulated leakage size flaw (depending on the capability of the leakage detection system and accounting for the factor of safety of 10 on leakage detection capability) in a large or

medium size piping system is a relatively small percentage of the pipe circumference. As a result, the loads and stresses in the uncracked pipe necessary to drive the crack most likely will exceed the yield strength of the material, maybe by a considerable margin. As a result, for crack extension to occur, the uncracked pipe will undergo plastic deformation, and thus, crack-driving energy will be absorbed. In addition, the crack itself behaves in a nonlinear manner, and as such, acts as another sink for energy absorption. This crack-driving energy absorption due to the presence of the crack and the nonlinear behavior of the uncracked pipe is not accounted for in traditional LBB analyses. As such there are potential additional sources of margin if one wants to consider nonlinear behavior. This additional source of margin is the basis for the proposed Level 3 analysis in the Tiered Approach to LBB discussed in Section 6. Level 3 offers the applicant the option of pursuing this additional margin due to nonlinear behavior if LBB cannot be satisfied using the more traditional Level 2 methodology. As part of the Task 3 efforts conducted as part of the LBB Regulatory Guide program, it was demonstrated that one may be able to achieve an additional margin on the moments at the crack plane of 20 to 30 percent for the cases examined, by invoking nonlinear behavior in their analysis. (See Appendix D where the relative accuracies of the various levels of analyses of the tiered approach are compared.) This may be just enough to demonstrate LBB for some piping systems that could not pass a Level 2 type analysis.

**5.3.4.2 Effect of Secondary Stresses on Pipe Fracture** – Currently, the flaw evaluation procedures embodied in ASME Section XI specify different safety factors for global secondary stresses, such as thermal expansion and seismic anchor motion (SAM) stresses, than they do for primary stresses, such as primary membrane or primary bending stresses. For cracks in ferritic materials (base metals and welds) and austenitic flux welds (SAW and SMAW), the Section XI procedures indicate that the thermal expansion stresses should be included, but with a safety factor of only 1.0. Furthermore, for cracks in wrought stainless

steel base metals and austenitic TIG welds, the ASME Code indicates that thermal expansion stress need not be considered at all.

In a similar vein, the LBB procedures specified in draft SRP 3.6.3 have an option that allows the thermal expansion stresses to be considered in the stability analysis of cracks in austenitic submerge-arc and shielded-metal-arc welds, but not in the stability analysis of cracks in austenitic wrought base metals and TIG welds. For ferritic steels, this option was not given so that secondary and primary stresses were combined.

The results from the IPIRG pipe-system experiments (Ref. 5.56) indicated that for large surface cracks, where the failure stresses are below the general yield strength of the uncracked pipe, the thermal expansion and SAM stresses contributed just as much to the fracture process as did the primary stresses, see Figure 5.34. (Similar analysis of the experimental results from the through-wall cracked pipe-system and quasi-static bend experiments from IPIRG-2 yielded a similar conclusion. In addition, finite element analysis of a through-wall cracked pipe system, conducted as part of the margin assessment task in BINP (Task 3) yielded a similar conclusion.) Figure 5.34 shows a plot of the maximum experimental stress normalized by the Net-Section-Collapse (NSC) stress for five quasi-static bend and five pipe-system experiments conducted as part of the IPIRG and related programs (Refs. 5.13 and 5.56). The crack sizes in each of these experiments were relatively large, such that the failure moments were low enough that plasticity was restricted to the crack section. The maximum experimental stresses have been normalized by the NSC stress to account for slight differences in pipe size and crack size. For each experiment, the maximum stress has been broken down into its various stress components, i.e., primary membrane, primary bending (inertial), secondary seismic anchor motion, and secondary thermal expansion. (For the quasi-static bend companion experiments, the only stress components applicable are primary membrane and primary bending [quasi-static bending].) From Figure 5.34, it can be

seen that if the thermal expansion and seismic anchor motion stresses are ignored in the stress terms for the pipe-system experiments, then the normalized failure stresses for the pipe-system experiments would only be 40 to 60 percent of the normalized failure stresses for the quasi-static bend experiments. Consequently, it appears that secondary stresses do contribute to fracture, at least for the case of large surface cracks where plasticity is limited.

This phenomenon was studied further as part of Task 1 of the Battelle Integrity of Nuclear Piping (BINP) program, in which a stainless steel SAW pipe-system experiment was conducted in which the actuator at the start of the test was intentionally offset to simulate a larger thermal stress component. From this experiment there are a couple of points of note which support the findings from the IPIRG-1 program. For one, the maximum moment from this experiment was about the same as that for a companion stainless steel weld experiment (with nominal thermal expansion) from IPIRG-1, see Figure 5.35. Secondly, the crack actually initiated while initially offsetting the actuator to simulate the larger thermal expansion stress. Both of these findings support the contention that the thermal expansion stresses (secondary stresses) are not less detrimental than the primary stresses, at least for these test conditions

for which the stresses at failure for the uncracked pipe were less than the yield strength.

For such conditions, there is the potential for elastic follow-up. Section III of the ASME Code recognizes this potential in its local overstrain criteria in paragraph NC-3672.6(b). This paragraph implies that global secondary stresses, such as thermal expansion and seismic anchor motion stresses, can act as primary stresses under certain conditions, such as when the weaker or higher stressed portions of the piping system are subjected to strain concentrations due to elastic follow-up of the stiffer or lower stressed portions. One such obvious example of this is the IPIRG pipe system in which a large crack is introduced into a weaker material (lower yield strength) than the surrounding materials. Consequently, the resultant stresses for the uncracked pipe sections were less than the yield strength at the time of failure of the cracked section. The implication is that the safety factor for secondary stresses may be a function of the ratio of the failure stress to yield strength. If the failure/yield stress ratio is less than 1.0, then global secondary stresses should probably be treated the same as primary stresses for fracture in the stability/critical crack size analysis. If the opposite holds true, then the global secondary stresses may become less important with some nonlinear function.

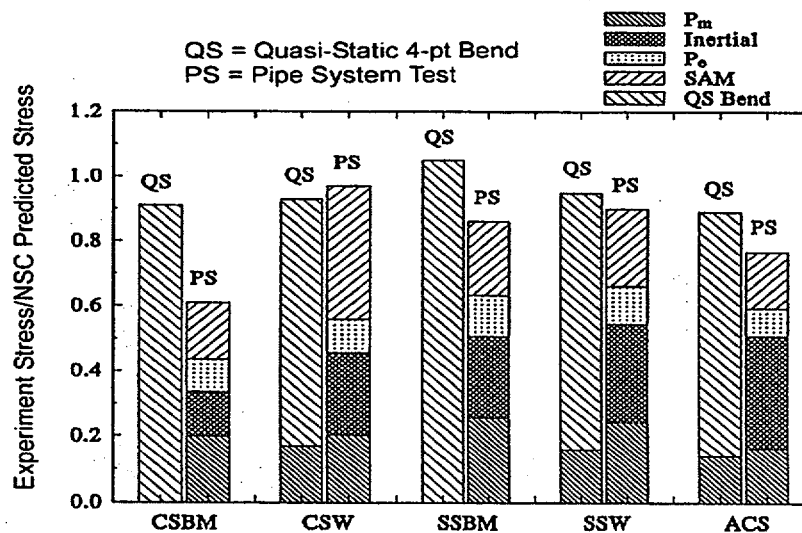


Figure 5.34 Comparison of the results from the IPIRG-1 pipe-system experiments with companion quasi-static, four-point bend experiments demonstrating how global secondary stresses, such as thermal expansion and seismic anchor motion stresses, contribute to fracture

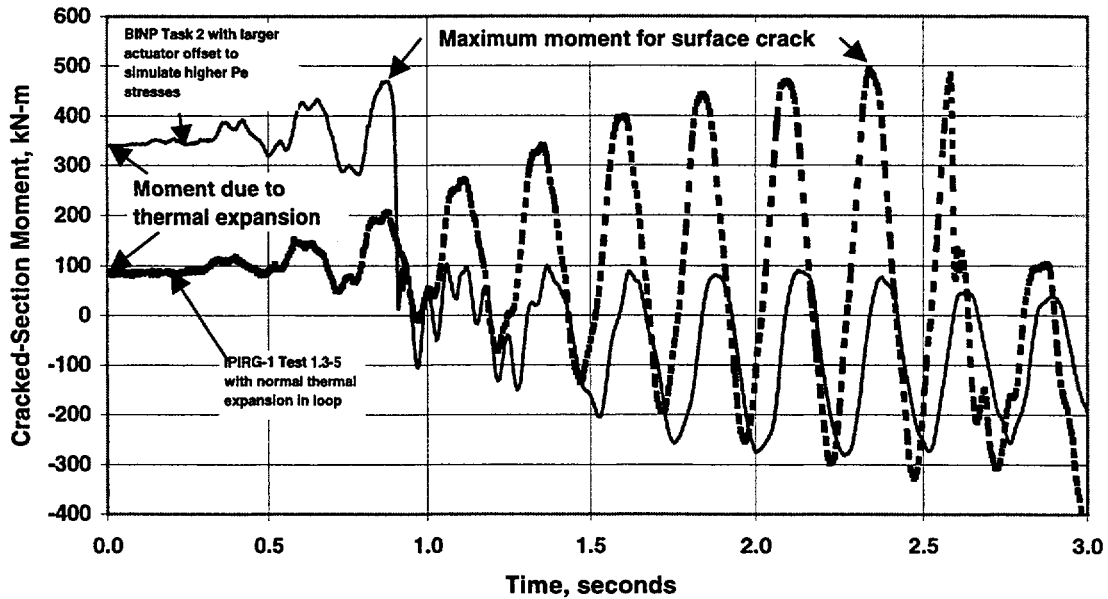


Figure 5.35 Comparison of moment-time plots for IPIRG-1 Experiment 1.3-5 and BINP Task 2 experiment

**5.3.4.3 Effect of Torsional Stresses** – One of the objectives of Reference 5.28 was to assess the fracture behavior of pipes subjected to torsional stresses in addition to bending and tension stresses from internal pipe pressure. Prior to starting this analysis, a survey of piping stress analyses results from various organizations was undertaken. This survey showed that bending moment-to-torque ratios of 3.0 were common, and occasionally this ratio was as low as 1.0. Analyses were then conducted using both of these ratios. It was found that an effective bending moment could be defined in at least four different ways to account for torsional and bending moments. By adopting the Von Mises relation to define the effective bending stress,  $\sigma_{eff}$ , in terms of the applied bending stress,  $\sigma_B$ , and the torsional stress,  $\tau_T$

$$\sigma_{eff} = \left[ \sigma_B^2 + 3\tau_T^2 \right]^{0.5} \quad (5.11)$$

it was seen that the finite element solutions obtained for the crack-driving force and crack-

opening displacements under bending conditions may be used in evaluating the corresponding quantities for cracked pipes subjected to combined bending and torsion. The finite element results demonstrated the validity of this approach for a straight circumferential through-wall crack as well as for an angled circumferential through-wall crack with a crack-tip angle of 45 degrees. This significant conclusion enables the use of simple engineering estimation schemes of through-wall-cracked pipes under bending to be used to determine fracture parameters when combined loading with torsion occurs. The limitation to this approach, however, is that the analyses conducted to date were restricted to very small amounts of angular crack growth. For large crack growth at an angle, there may be some deviations from the results obtained to date. For instance, the ratio of the J-R curves at different orientations do not seem to be constant with crack growth, and the ratio of the  $J_{applied}$  values with crack-tip angle for a growing crack is unknown. Also, crack growth analyses for the straight growing crack were not conducted to examine the validity of

the effective moment concept, but it is anticipated that this approach would work. Nevertheless, the conclusion of using this effective bending stress for combined loads involving torsion is valid for all leak-rate calculations of concern to LBB analyses and for determining loads up to crack initiation.

### 5.3.5 Fracture/Stability Analyses

The existing LBB methodology embodied in draft SRP 3.6.3 specifies that one must determine the margin in terms of applied loads using a crack stability analysis in which one demonstrates that the leakage size crack will not experience unstable crack growth if 1.4 times the normal plus SSE loads are applied. In draft SRP 3.6.3, this stability analysis is based on a through-wall crack limit-load analysis. In the future (i.e., future Level 2 type analyses), this stability analysis may be based on more sophisticated J-estimation scheme analyses or finite element analyses.

**5.3.5.1 Limit-Load Analyses –** Limit-load analyses are the simplest and most straightforward methods for evaluating the fracture behavior of circumferentially cracked pipe. Typically they involve simple closed-form equations. Equations 5.12 and 5.13 are the limit-load equations for a through-wall-cracked pipe in bending according to the Net-Section-Collapse analysis (Ref. 5.10).

$$M_{NSC} = 2\sigma_f R_m^2 t (2 \sin(\beta) - \sin(\theta)) \quad (5.12)$$

where,

$M_{NSC}$  = Net-Section-Collapse predicted moment,

$\sigma_f$  = flow stress,

$R_m$  = mean pipe radius,

$t$  = pipe wall thickness,

$\theta$  = half crack angle, and

$\beta$  = stress inversion angle, where

$$\beta = \frac{\pi - \theta}{2} - \frac{\pi R_i^2 p}{4 R_m t \sigma_f} \quad (5.13)$$

$p$  = internal pipe pressure, and

$R_i$  = inside pipe radius.

The problem with such limit-load analyses is that they have limited applicability. One of the basic assumptions embodied in such analyses is that the cracked-pipe section reaches fully plastic conditions. Such is only the case for smaller diameter pipe and/or higher toughness materials.

**5.3.5.2 Modified Limit-Load Analyses –** Draft Standard Review Plan 3.6.3 precludes the generic use of limit-load analyses to evaluate leak-before-break conditions for eliminating pipe restraints. As indicated above, the problem with limit-load analyses is that they have limited applicability. As part of the Degraded Piping Program, a screening criterion was developed to sort out those cases where limit-load analyses were applicable from those that are not. This screening criterion, known as the Dimensionless Plastic Zone Parameter, DPZP, (Ref. 5.16) is essentially the ratio of the calculated plastic-zone size to the remaining tensile ligament. In its simplified form, this parameter is:

$$DPZP = \frac{2EJ_i}{\pi^2 \sigma_f^2 D} \quad (5.14)$$

where,

$E$  = elastic modulus,

$J_i$  = value of  $J$  at crack initiation from a C(T) type laboratory test,

$\sigma_f$  = flow stress (average of yield and ultimate), and

$D$  = pipe diameter.

If this ratio is greater than 1.0, then fully plastic conditions are assumed to exist and the use of the limit-load analyses is assumed to be appropriate. As part of Reference 5.66, this approach was extended by empirically modifying the NSC analysis by multiplying the NSC predicted stress by a DPZP-dependent factor to account for the fact that fully plastic conditions do not exist.

$$P_{DPZP} = P_{NSC} \left( \frac{2}{\pi} \right) \arccos(e^{-C(DPZP)}) \quad (5.15)$$

where,

$P_{DPZP}$  = Predicted stress based on DPZP analysis,

$P_{NSC}$  = Net-Section-Collapse predicted stress,

DPZP = Dimensionless plastic zone parameter, and

C = empirically derived constant = 4.62 (best fit) for through-wall cracks or 3.0 (95 percent confidence level fit).<sup>20</sup>

Figure 5.36 illustrates this DPZP analysis with a large amount of full-scale pipe experimental data that was used for the empirical derivation of the constant C.

At about the same time that the DPZP analysis was under development, the ASME Section XI Pipe Flaw Evaluation Working Group was developing their own modification to the limit-load analyses. Like the DPZP analysis, the Section XI Z-factor modification is dependent on fracture toughness and pipe diameter. For cracks in lower toughness austenitic flux welds (i.e., SAW and SMAW), the Section XI Z-factors are:

$$Z = 1.15 [1 + 0.013 (D - 4)] \quad \text{for SMAW} \quad (5.16)$$

$$Z = 1.30 [1 + 0.010 (D - 4)] \quad \text{for SAW} \quad (5.17)$$

Even though draft SRP 3.6.3 does not allow for the generic use of limit-load analyses to evaluate leak-before-break conditions for eliminating pipe restraints, it does allow for the use of modified limit-load analysis for austenitic steel piping demonstrating acceptable margins. The

<sup>20</sup> As part of Reference 5.67 the “best fit” curve for the through-wall cracked pipe data were updated based on additional data in the CIRCUMCK pipe fracture database; C = 18.3 for “best fit” of data.

equations in the draft SRP are the same equations as found in ASME Section XI, i.e., Equations 5.16 and 5.17.

### 5.3.5.3 Elastic-Plastic Fracture Mechanics (EPFM) Analyses –

Due to the known limitations with limit-load analyses, more detailed EPFM-based analyses have been developed. These include finite element as well as J-estimation scheme analyses.

**Finite Element Analyses** – Finite element analyses (FEA) are often used for the analysis of special cases for which applicable analysis routines, such as J-estimation schemes, do not exist. For example, prior to the development of the analysis routine for through-wall cracks in elbows as part of the LBB Regulatory Guide program, the only way in which to make such an assessment would be through FEA. In addition, many of the analysis routines used for pipe fracture analyses are based on curve fitting of FEA results. Examples of such analysis routines that are applicable to LBB assessments include:

- the h-functions used in the GE/EPRI J-estimation schemes for predicting the load-carrying capacity of through-wall cracks in straight pipe that are a function of  $R_m/t$  ratio, strain-hardening exponent (n), crack size ( $\theta/\pi$ ), and applied load; and
- the V functions in the GE/EPRI method for predicting the crack-opening displacements for an LBB assessment.

**J-estimation Schemes** – Numerous J-based estimation schemes have been developed over the past 15 years. For through-wall cracks of interest in LBB analyses, these include:

- several versions of the GE/EPRI methodology (Refs. 5.3, 5.9, and 5.66),
- the Tada/Paris approach (Ref. 5.59),
- LBB.NRC (Ref. 5.7),
- LBB.ENG2 (Ref. 5.8), and
- LBB.ENG3 (Ref. 5.9).

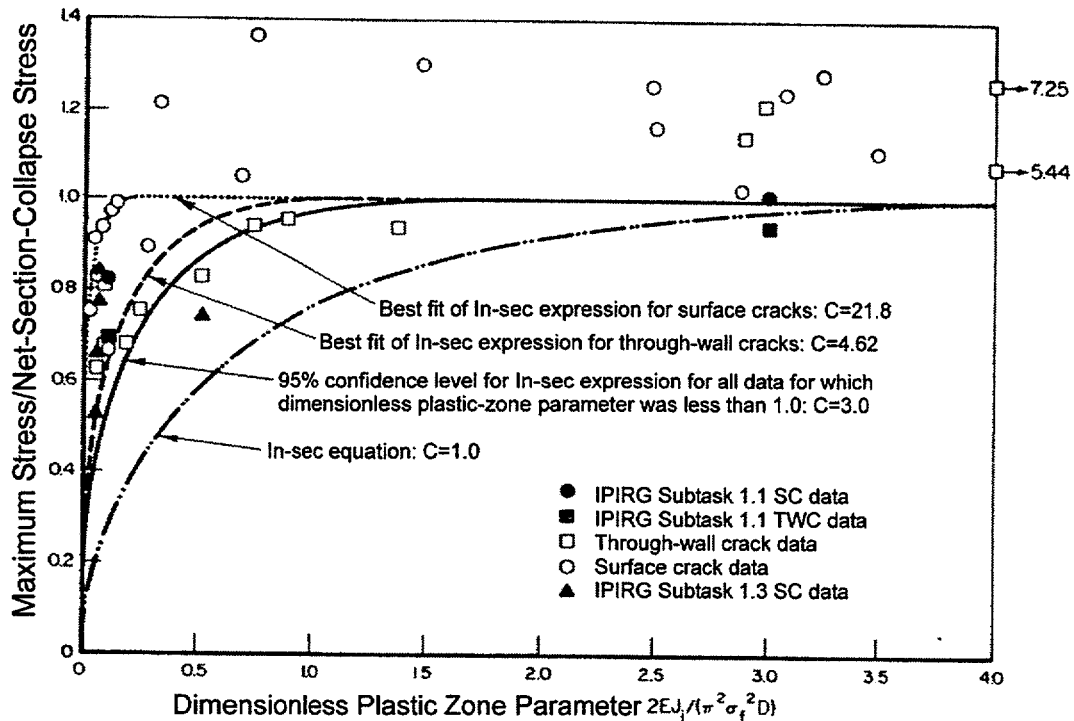


**Figure 5.36** Compiled data using simplified dimensionless-plastic-zone parameter and flow stress equal to average of yield and ultimate

In addition, there is the R6 method developed in England (Ref. 5.46). Most of these methods can be used to predict not only the load-displacement relationship but also the crack-opening-displacements needed for the leakage crack size determinations for an LBB analysis. To facilitate their use, a special purpose Windows®-based computer code has been developed (NRCPIPE) which allows one to simply input pipe/crack geometry and material data, and the computer code automatically outputs the loads (moments), displacements (rotations), and crack-opening displacements.

Sensitivity studies have been conducted to ascertain the relative accuracy of each of these approaches. In predicting the maximum load-carrying capacity of a through-wall-cracked pipe, each method does reasonably well, see Table 5.11. The GE/EPRI method tends to be

the most conservative while the Tada/Paris approach was the most likely to give a non-conservative result. All of the methods tend to be a bit more conservative for the case of combined loading, i.e., bending plus tension.

With regards to the accuracy of the crack-opening displacement predictions, as part of this study for the LBB Regulatory Guide program, it was found that the Tada/Paris solutions, as prescribed in the NRCPIPE code, were very conservative (small predicted COD values that result in long predicted leakage size flaws for a prescribed leak-rate detection capability) with respect to finite element analyses, especially at the higher applied load levels, see Figures 5.37 and 5.38 for TP304 stainless steel pipe. Similar trend curves were developed for carbon steel pipe.

**Table 5.11 Mean values of maximum load ratios (experimental maximum load divided by predicted maximum load) for TWC pipe experiments**

Fracture Analysis Method	All TWC Experiments Under Bending (12 Tests)	Short TWC Experiments Under Bending (5 Tests)	TWC Welded Pipe Experiments Under Bending (4 Tests)	All TWC Experiments Under Bending and Tension (6 Tests)
LBB.ENG2	1.04	0.96	1.08	1.18
LBB.NRC	1.01	1.02	0.94	1.17
LBB.GE	1.01	0.98	0.98	--
GE/EPRI-1A	1.15	1.12	1.18	1.31
Tada/Paris	0.96	0.91	0.87	1.03
LBB.ENG3	1.00	0.90	1.02	1.18

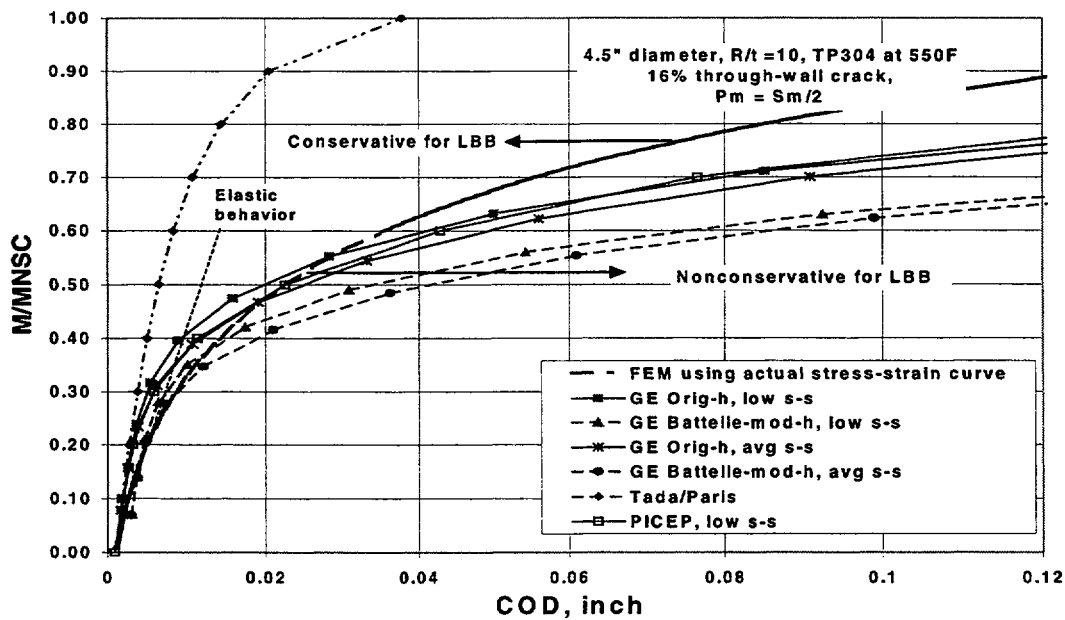


**Figure 5.37 Results of COD sensitivity study for 4.5-inch diameter TP304 stainless steel pipe with a 16-percent long circumferential TWC**

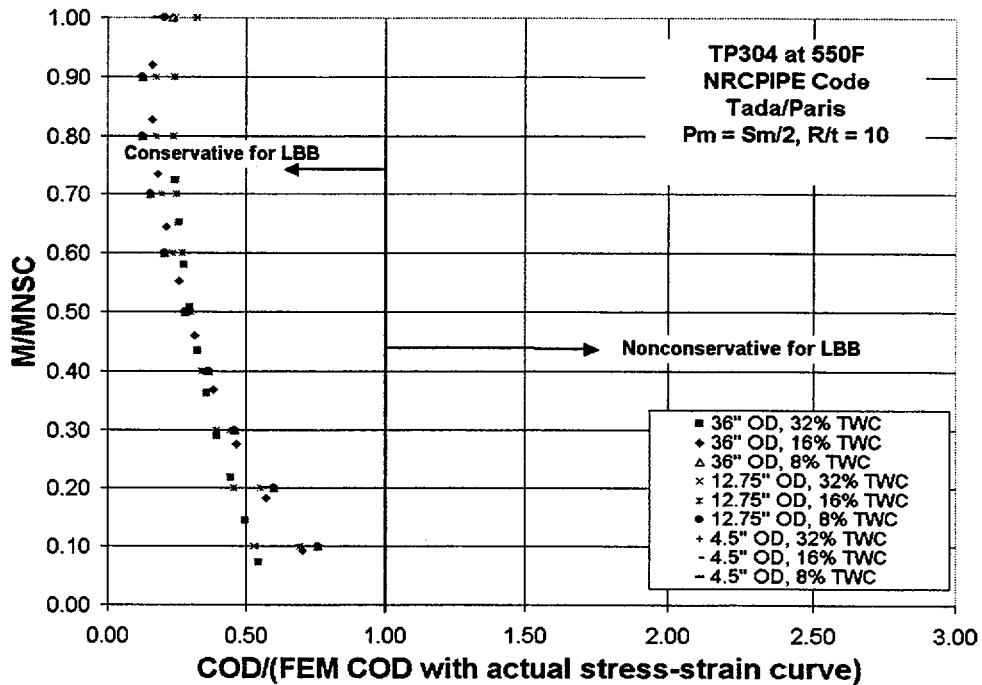


Figure 5.38 Paris/Tada solutions from NRCPIPE for TP304 stainless steel pipes

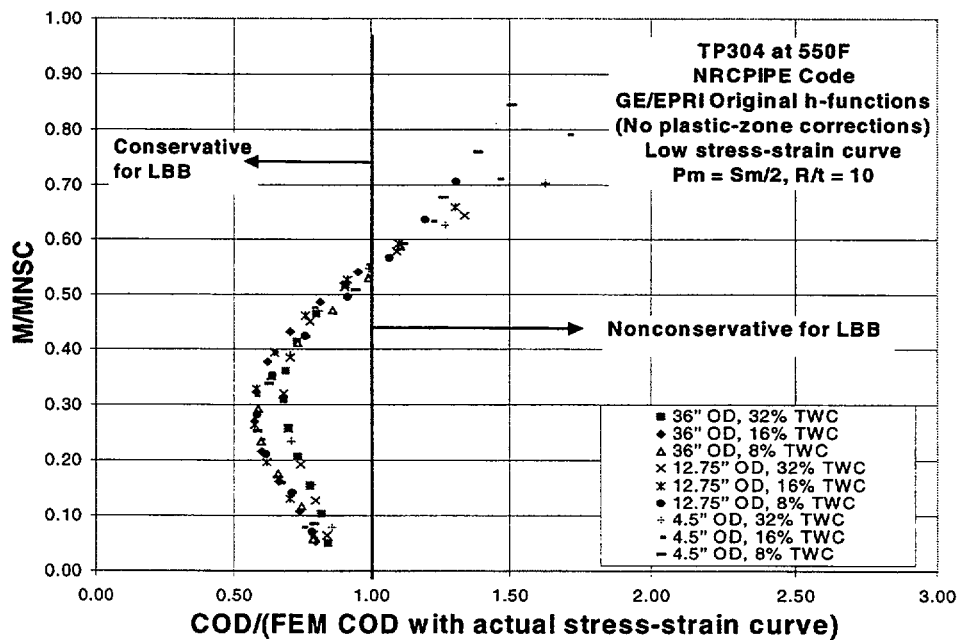
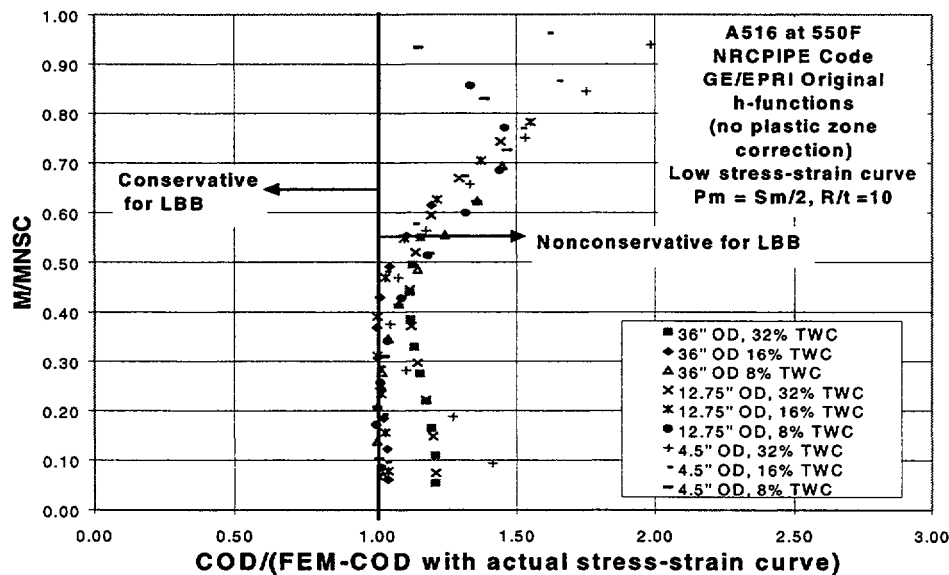


Figure 5.39 Original GE/EPRI COD solutions for TP304 stainless steel pipe from the NRCPIPE code



**Figure 5.40 Original GE/EPRI COD solutions from the NRCPIPE code for A516 Grade 70 pipe**

Conversely, while the Tada/Paris approach is consistently conservative for COD leakage calculations for TP304 stainless steel, the GE/EPRI method was found to be conservative at the lower load levels (less than half of the NSC load), and nonconservative at the higher load levels, see Figure 5.39. For the carbon steel test case considered, the GE/EPRI method in the NRCPIPE code was in exact agreement with the FE analysis for the shorter cracks considered (8 and 16 percent of the pipe circumference) at load levels less than 50-percent of the limit-load and nonconservative for the crack lengths of 32-percent of the pipe circumference, see Figure 5.40. The amount of disagreement within the NRCPIPE-GE/EPRI solutions would be amply covered by the safety factor of 10 on leak rate.

**Elbow Through-Wall Crack Analysis** – Prior to this program there were few methodologies for predicting either the maximum loads or CODs for through-wall-cracked elbows. A simplified criterion had been developed for surface-cracked elbows as part of the Second IPIRG program (Ref. 5.68), but no such methodology existed for through-wall cracks. The main objective of the development activity conducted, as part of the

LBB Regulatory Guide program was to develop a new estimation scheme for through-wall cracks in elbows (both axially and circumferentially oriented cracks). A secondary issue considered the assessment of the feasibility of using simple influence functions (in conjunction with existing straight-pipe solutions) to predict LBB for elbows. Prior to this development work, the only mechanism for making a fracture assessment of a through-wall crack in an elbow was through finite element analysis (FEA) on a case-by-case basis.

The J-estimation scheme solutions developed here were for both axially and circumferentially oriented through-wall cracks in elbows subjected to pure pressure, pure bending, and combined pressure and bending loading conditions. The axial cracks were located along the flank of the elbow while the circumferential cracks were along the extrados of the elbow. Solutions were developed for a variety of R/t ratios (5, 10, and 20), crack lengths (45 and 90 degree circumferential cracks and 15 and 30 degree axial cracks), and strain-hardening exponents ( $n = 3, 5, 7, \text{ and } 10$ ). Influence functions were developed for both J (crack-driving force) and

were developed for both elastic and plastic loadings. For the axially cracked case, solutions for COD were developed for both the inside and outside pipe surfaces.

One of the key points considered in the development of these solutions was the effect of ovalization on elbows when subjected to bending loads. During the course of this effort, it was found that ovalization had an important effect on both J and COD, especially for the axially cracked case.

For circumferential cracks, an elbow closing moment causes an oblate ovalization pattern; see Figure 5.41, that adds additional compression stresses or loads at the circumferential crack plane, especially for high R/t ratio elbows. For these higher R/t ratio elbows (i.e., R/t = 20), this oblate ovalization is significant enough to fully close off the crack while for the lower R/t ratio elbows (i.e., R/t = 5), the crack remains open, but with a reduced J value. The elbow opening moment (elbow straightening moment) causes a prolate ovalization pattern, see Figure 5.41, that results in an increase in the crack opening which tends to counteract the effect on crack opening caused by the global bending moment (crack closing). This results in a modest crack opening for smaller crack sizes.

For the axial flank crack case, the effect of ovalization on crack opening is even more important. The elbow opening/straightening moment causes a tensile opening stress along the crack flank. Such a moment also causes rotation of the crack faces such that there is a pinching of the outer crack surface that may impede leaking, and hence LBB considerations. Because of this crack-face rotation phenomenon, COD influence functions were compiled for both the inner and outer surfaces for the axial flank crack case. In an actual elbow in service, which is subjected to combined bending and pressure, the competition between the pressure, which causes opening CODs at both the ID and OD, and the bending, which tends to close the crack on the OD, will ultimately determine the service loading profile. As a result, the ovalization induced from elbow bending must be considered in the COD predictions that are used in the leak-rate

calculations conducted as part of an LBB assessment. One possible means of accounting for these crack face rotations is to use the minimum COD values for the OD surface in the leak rate codes, but that may result in a very conservative assessment.

Using the results from these finite element analyses and this estimation scheme, a sensitivity study was conducted to examine the effect of applying LBB to elbows. The objective of this evaluation was to determine if a simplified analysis could be established for axial and circumferential through-wall cracks in elbows under combined pressure and bending. This was assessed by using the elbow finite element analyses developed as part of this effort with a hoop stress loading of  $1.0 S_m$  for typical nuclear piping steels. The approach undertaken was to compare the ratio of the moments for the same size crack in an elbow and straight-pipe at the same applied J values. This was similar to efforts done for circumferential surface flaws in elbows in the IPIRG-2 program. The following conclusions came from this analysis.

- The results of the analysis showed that a circumferential through-wall crack centered on the extrados of an elbow had the same crack-driving force under plastic conditions as a circumferential through-wall crack in a straight pipe. Hence, for the LBB Regulatory Guide, the simple straight-pipe solutions could be used for the fracture analysis of a circumferential through-wall crack in an elbow.
- The results of the analysis showed that an axial crack on the flank of an elbow had a higher crack-driving force under plastic conditions than a circumferential through-wall crack in a straight pipe. A conservative approach would be to use the straight-pipe solution, but divide the straight-pipe moment by the elbow  $B_2$  index. This could readily be done in the new LBB Regulatory Guide for the fracture analysis of an axial flank through-wall crack in an elbow in a Level 1 or Level 2 analysis.
- The COD evaluations were not conducted in this effort. Caution should be used in applying this same approach for the COD

values since the COD should be for elastic loading where the constant moment ratio

that occurs under plastic conditions does not exist.

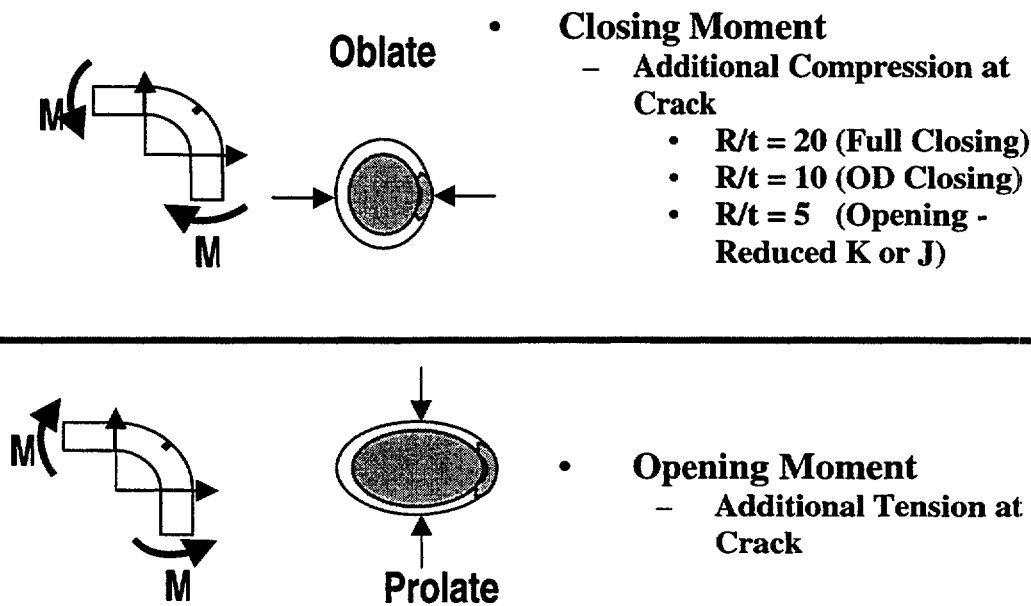


**Figure 5.41** Ovalization modes for through-wall cracks in elbows subjected to opening and closing bending moments.

**5.3.5.4 Stability Issues** – One of the key elements of the draft SRP 3.6.3 approach is the determination of the critical crack size for the normal plus SSE loads using a fracture mechanics stability analysis. For LBB to be satisfied, it is necessary to demonstrate that there is a margin of at least 2.0 between the postulated leakage crack size and the calculated critical crack size. In addition, the margins in terms of load need to be determined through stability analysis by demonstrating that the leakage size crack will not experience unstable crack growth if loads 1.4 times the normal plus SSE loads are applied.

In the past, this sort of stability analysis has been performed using a tearing instability ( $J/T$ ) approach. The vast majority of the LBB submittals reviewed included some sort of  $J/T$  type analysis. In the future, such analyses may be conducted using a J-estimation scheme analysis, which will probably be more accurate and easier to apply.

With regards to crack stability, one experimental observation from the Degraded Piping Program of particular note with regards to LBB is the result from Experiment 4115-6. This was 6-inch diameter, stainless steel, surface-cracked-pipe experiment, with a long (360 degree) internal surface crack. The loading conditions for the experiment were pure four-point bending. During this experiment, once maximum load was achieved, and the surface crack penetrated the pipe wall thickness, the resultant through-wall crack grew unstably until the two halves of the pipe completely severed. This was the one experiment for which this occurred. This unstable crack growth was attributed to the lower crack growth resistance for the complex-crack geometry, i.e., a long internal surface crack that penetrates the pipe wall thickness over a short distance (Ref. 5.17). This observation demonstrates the wisdom in the draft SRP procedures that precludes the application of LBB technology to piping systems susceptible to IGSCC type cracking. Due to the sometimes uniform nature of weld residual stresses, which tend to act as the crack-driving force for IGSCC, often times IGSCC cracks grow around a

significant portion of the pipe circumference, sometimes all the way around, such that the resultant resistance to a crack instability is minimal.

### 5.3.5.5 Comparisons of Analysis Methodologies with Full-Scale Experimental Data and Finite Element Analyses Results –

Each of the pipe fracture research initiatives undertaken by Battelle over the past 15 to 20 years had a number of full-scale pipe experiments associated with them. The scope of these experiments differed between programs. The focus of the Degraded Piping Program experiments was to generate full-scale data for a wide variety of pipe sizes, materials, and crack types, at quasi-static load histories. The focus of the IPIRG programs was on dynamic and cyclic loading, and the focus on the Short Cracks program was on smaller crack sizes, more typical of in-service conditions, than previously evaluated as part of the Degraded Piping or IPIRG programs.

The data from these experiments was used to validate many of the fracture analysis methodologies that were being developed. For the most part, as can be seen in Table 5.11, these analysis methodologies have been found to be generally conservative, although not overly so, at least with respect to their prediction of the load-carrying capacity of a through-wall-cracked pipe. The only exception to this is when these analysis routines are applied in such a manner that one of the fundamental assumptions embodied in the analysis routine is violated, e.g., applying the Net-Section-Collapse limit-load analyses to a case where fully plastic conditions do not exist, i.e., where failure is governed by EPFM and not limit-load conditions.

The fidelity of the COD predictions for combined pressure and bending is not so high. As shown previously, the Tada/Paris approach for stainless steel pipe is very conservative (smaller COD values than the FEA COD values, which corresponds to longer crack lengths for a given leak-rate detection capability) at all load levels, but especially at the higher load levels. Conversely, for stainless steel pipes, the original GE/EPRI method in the NRCPIPE code is

conservative (although less so than for the Tada/Paris approach) at the lower load levels, but is nonconservative at the higher load levels<sup>21</sup>. For carbon steel pipes, the GE/EPRI method in the NRCPIPE code is nonconservative at higher load levels and longer cracks, but quite accurate at the lower load levels. The magnitude of the error in the NRCPIPE-GE/EPRI COD analysis is amply covered by the factor of 10 on leak rate.

Finally, with respect to the leak-rate prediction models, predictions based on the SQUIRT code were found to agree well with the experimental data developed as part of Reference 5.17. Figure 5.42 shows a comparison of the SQUIRT predicted leak rates with experimental data obtained for a fatigue-generated crack in a girth weld. For this experiment, the through-wall-cracked pipe sample was loaded in 4-point bending such that there was combined pressure and bending load on the crack. The temperature of the water inside the pipe was nominally 288 C (550 F).

### 5.3.6 Probabilistic (Risk Informed) Analyses

An option that was considered early in the development of the proposed LBB Regulatory Guide was to allow for the use of partial safety factors or a probabilistic analysis. Since the LBB procedures suggested have different safety factors on leakage as well as on crack lengths, this is already a partial safety factor approach. Although a probabilistic option is not included in this document, the following section discusses some probabilistic analyses. The Level 2 deterministic option suggested in this report is compared with the deterministic relationships used in several existing probabilistic codes. This review is not intended to be an in-depth review of all details in these probabilistic approaches, but rather to point out similarities

---

<sup>21</sup> For stainless steel pipe with a 10 percent long circumferential through-wall crack subjected to a pure bending loading condition, the applied stress at which the GE/EPRI method transitions from being conservative to non-conservative is approximately 1.6 times the code design stress intensity ( $S_m$ ).

and differences. The three different probabilistic approaches used in this comparison are the;

- pcPRAISE code,

- Westinghouse Structural Reliability and Risk Assessment (SRRA) code, and
- probabilistic codes in NUREG/CR-6004 (PSQUIRT and PROLBB).

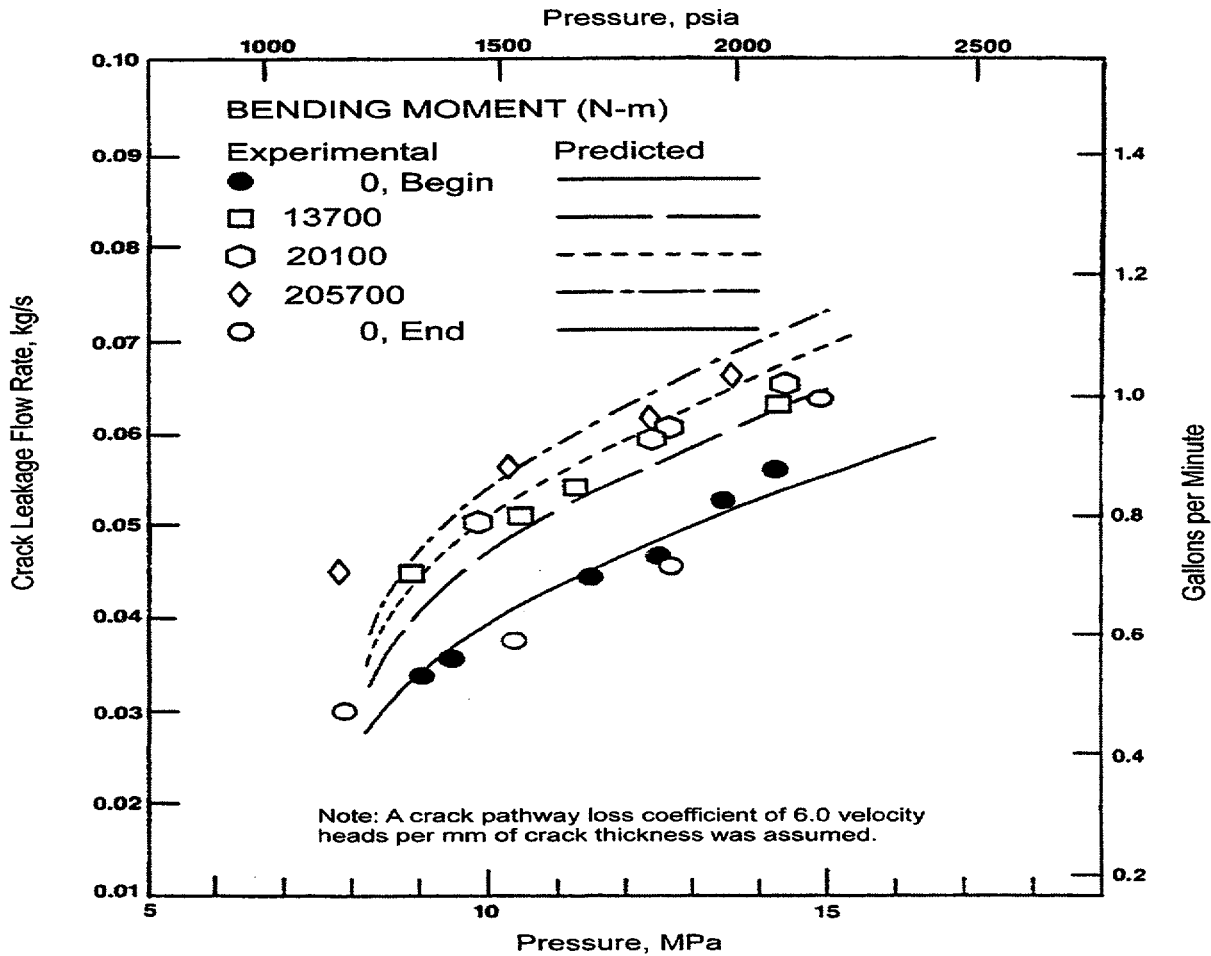


**Figure 5.42 Comparison of SQUIRT predicted leak rates with experimental data obtained for a fatigue generated crack in a carbon steel girth weld loaded in 4-point bending**

The PRAISE code was developed in the earlier investigations for LBB applications for nuclear power plant piping (Ref. 5.69). That code involved a probabilistic determination of fatigue crack growth. Later, in 1986, it was expanded for initiation and growth of stress-corrosion cracks (Ref. 5.70). A personal computer version of the code (pcPRAISE) was developed for more economical use in 1992 (Ref. 5.71). Finally, in 2000 a modification of the code (pcPRAISE 4.2) was made to account for initiation and growth of

cracks in ferritic steels under corrosion-fatigue conditions, where crack initiation and growth can be accelerated due to environmental and loading-rate conditions (Ref. 5.72). Thus, considerable developments have been made to the PRAISE code in the area of subcritical crack growth analyses, as well as some leak-rate and fracture prediction capabilities. However, for consistency with the NRC LBB procedure, the PRAISE code subcritical crack growth procedure would have to be bypassed so that

only the leak-rate and fracture analyses are conducted. Alternatively, one could conduct a full probabilistic analysis to determine the probability of either a leak, or a large leak (small-break LOCA), or a large break occurring from the beginning of plant life to the end-of-design life. The contribution to overall plant risk (core damage) from piping failures should be maintained at an extremely low level. In order to achieve this, piping failure probabilities of less than  $10^{-6}$  per reactor-year of operation, have typically been considered to be acceptable. The objectives of the risk-informed inspection criteria are to assign priorities of where inspection resources could be best spent.

Another probabilistic computer code is the Westinghouse Structural Reliability and Risk Assessment (SRRA) model (Ref. 5.73). This model was developed for the risk-informed in-service-inspection (RI-ISI) activities for the ASME Code. Subcritical crack growth, leakage, and fracture analyses are conducted in the SRRA code, and were also compared with the pcPRAISE code.

Another probabilistic LBB approach was developed in NUREG/CR-6004 (Ref. 5.23). This analysis was along the lines of the more classical NRC LBB procedure. That is, rather than conducting subcritical crack growth analyses and final probabilities of failure, conditional probabilities of failure were calculated for a crack distribution coming from a given leak-rate, and the elastic-plastic analyses are conducted to determine if that crack is stable at some transient loading (i.e., Service Levels C or D stresses). No safety factors on leak-rate or crack length were used in these analyses. Also in this approach, the leaking crack and the transient (i.e., seismic) loads are assumed to occur with a probability of 1. Hence, the absolute failure probabilities would be less than the values calculated in that report.

A brief comparison of these three approaches is given in Tables 5.12 through 5.14, although there are many fine details that would require additional review. These comparisons are made relative to the deterministic model used in a Level 2 LBB approach in this document.

Further comparisons for each of the general analysis steps are given in Tables 5.13 and 5.14. Since subcritical crack growth analysis aspects are not included in the proposed Level 2 analysis or in the NUREG/CR-6004 approach, a comparison is not given for subcritical crack growth aspects. Table 5.13 compares some of the leak-rate analyses aspects. The leak-rate considerations include crack-opening area (COA) and thermal-hydraulic considerations. Table 5.14 compares some of the fracture mechanics analyses aspects.

It should be noted that there are a number of differences in the deterministic analyses between the available probabilistic methods and the Level 2 option that is suggested in this report. Consequently, some modification of the probabilistic approaches would be needed prior to assessing their probabilistic analysis capabilities.

**Table 5.12 Comparison of general deterministic analyses in probabilistic approaches and Level 2 analysis procedures in this report**

Analysis conditions	Analysis Procedures			
	Level 2 Analysis	Pc-PRAISE (Ref. 5.71)	SRRA (Ref. 5.73)	NUREG/CR-6004 (Ref. 5.23)
Subcritical crack growth analyses	No	Yes - fatigue, corrosion fatigue, and IGSCC No - PWSCC	Yes - fatigue, corrosion fatigue, FAC, and IGSCC No - PWSCC	No
Leak-rate analyses	Yes - with detailed crack-opening area considerations	Yes - with simplified crack-opening area and leak-rate procedures	Yes - with simplified crack-opening area and leak-rate analyses	Yes - but not as detailed as the Level 2 analyses
Fracture analyses	Yes - with elastic-plastic fracture mechanics analyses	Yes - generally with limit-load analyses	Yes - with limit-load analyses	Yes - with elastic-plastic fracture mechanics analyses

There is a separate effort by the USNRC and US industry to assess if the emergency core cooling requirements can be redefined based on risk-based analyses. This desire came about from some of the risk-based inspection efforts that showed the probability of a large-break LOCA was quite small. Redefining the ECCS requirements, however, is a more significant safety aspect than redefining where inspections should be done. That is because if some unknown cracking mechanism occurred that was not considered in the risk-based inspection models, then if a large break occurred at a non-inspected area, the ECCS was still in place to protect the reactor from a core meltdown. Hence, changing the ECCS requirement may require more than just using the current LBB analysis procedures and modeling the failure modes from the past history of pipe cracking incidents. Recall that the LBB approach in this document is really a flaw tolerance approach for a hypothetical flaw. One example of where additional considerations might be needed is in the fact that the circumferential flaw is assumed to be centered on the bending axis in an LBB

analysis, which probably would not occur in reality. This is conservative assumption for fracture, but not in the determination of the leakage flow size. Reference 5.23 showed that the leakage flow size determination is more important for LBB failure probabilities than the fracture mechanics consideration. Additionally, the large-break LOCA from a pipe crack is also a surrogate for other failure mechanisms such as a loss of a manway on a steam generator or bolting on a valve bonnet. Hence the probabilities of these other failure modes would also have to be considered. Finally, if ECCS requirements were to be changed, then one also needs to account for other potential failure modes in the future. An example is PWSCC, which just recently became an active mechanism for primary pipe cracking in PWRs. Although the PWSCC cracks that have occurred to date have been primarily axial in bimetallic welds, it is not clear that a circumferential crack could not occur in the welds with different welding residual stress conditions. PWSCC is not a mechanism that was considered in the recent risk-based inspection analysis.

**Table 5.13 Comparison of leakage-size crack deterministic analyses in probabilistic approaches and Level 2 analysis procedures in this report**

Analysis conditions	Analysis Procedures			
	Level 2 Analysis	Pc-PRAISE	SRRA	NUREG/CR-6004
COA – estimation procedure	Either GE-EPRI or Tada-Paris analysis procedures can be used. Versions in PICEP and NRCPIPE have been validated against matrix of FE analyses. Use average stress-strain curve.	Closed-form equation of COD for a crack in an infinite plate (conservative for small cracks, but may not be conservative for larger cracks, i.e., a 12-inch crack in an infinite plate may have a specific leak rate, but in a 4.5-inch pipe it would be a DEGB) (Eq. 6-3 in NUREG/CR-5864)	GE-EPRI estimation scheme (not stated how combined pressure and bending loads are accounted for)	Used GE-EPRI method that was coded in SQUIRT 2.2 code.
COA- additional considerations	Effects of pipe-system boundary conditions on induced bending of cracked pipe from axial loads, and effects of residual stresses on crack-face rotation included. Account for thickness changes at a nozzle.	None.	None.	Following factors mentioned but not included; pipe-system boundary conditions on induced bending from axial loads, residual stresses, and off-centered cracks.
Thermal hydraulic code	SQUIRT or PICEP acceptable, as well as any benchmarked code	Closed-form equation relating leak rate and center COD; applicable only for PWR condition, 15.5 MPa (2250 psi) and 288 C (550F) (Eq. 6-4 in NUREG/CR-5864)	Ref. 5.73 stated that a simplified correlations used to relate crack size to pressure, and thickness. SQUIRT believed to be used in a more recent version of SRRA.	Probabilistic version of SQUIRT 2.2 that includes below factors. This version of the SQUIRT code is only good for two-phase flow.
Additional thermal-hydraulic considerations	Roughness, number of turns, actual flow path length parameters are COD dependant and depend on crack mechanism	Leak-rate analysis independent of cracking mechanism.	Leak-rate analysis independent of cracking mechanism.	Roughness, number of turns, actual flow path length parameters are COD dependant and depend on crack mechanism

**Table 5.14 Comparison of leakage-size crack deterministic analyses in probabilistic approaches and Level 2 analysis procedures in this report**

Analysis conditions	Analysis Procedures			
	Level 2 Analysis	Pc-PRAISE	SRRA	NUREG/CR-6004
Fracture mechanics procedure	Either GE-EPRI or LBB.ENG2 analysis procedures can be used. Versions in NRCPIPE have been validated against pipe tests.	User can select either a limit-load or tearing modulus analysis; J-integral is calculated by a method similar to the GE/EPRI method; J-R curve is linear. (NUREG/CR-5864)	Uses limit-load.	Used LBB.ENG2 analysis method (most accurate of J-estimation schemes in the NRCPIPE code).
Additional considerations	Uses primary and secondary stresses, as well as transient stresses (i.e., seismic or thermal stratification at start-up). Weld residual stresses not needed in fracture analyses – based on experimental results.	Uses primary and secondary stresses, as well as transient stresses (i.e., seismic or thermal stratification at start-up). Weld residual stresses can be included, but probably only for subcritical crack growth. (NUREG/CR-5864)		Uses primary and secondary stresses, as well as transient stresses (i.e., seismic or thermal stratification at start-up). Weld residual stresses not needed in fracture analyses – based on experimental results.
Input	Use lower-bound stress-strain curve, fracture toughness (including weld metal HAZ, aging effects on cast stainless steels and welds, rate effects due to dynamic strain aging on ferritic steels.)	Statistical variation of material properties (flow stress only), crack size, and residual stresses. (NUREG/CR-5864)	Statistical variation of strength.	Statistical variation of material properties (correlated stress-strain and J-R curve parameters), crack size, and crack morphology parameters; aging effects on cast stainless steels.

## 5.4 References

- 5.1 Norris, D., and others, "PICEP: Pipe Crack Evaluation Program," EPRI Report NP-3596-SR, 1984.
- 5.2 Henry, R. E., and Fauske, H. K., "Two-Phase Critical Flow at Low Qualities," *Nuclear Science and Engineering*, Vol. 41, pp. 79-98, 1970.
- 5.3 Kumar, V., and others, "An Engineering Approach for Elastic-Plastic Fracture Analysis," EPRI Report NP-1931, July 1981.
- 5.4 Collier, R. P., and others, "Two-Phase Flow Through Intergranular Stress Corrosion Cracks and Resulting Acoustic Emission," EPRI Report No. NP-3540-LD, 1984.
- 5.5 Paris, P. C., and others, "The Theory of Instability of the Tearing Mode of Elastic-Plastic Crack Growth," *Elastic-Plastic Fracture*, ASTM STP 668, pp. 5-36, 1979.
- 5.6 Sanders, J. L., Jr., "Circumferential Through-Cracks in a Cylindrical Shell Under Combined Bending and Tension," *Journal of Applied Mechanics*, Vol. 50, March 1983.
- 5.7 Klecker, R., and others, "NRC Leak-Before-Break (LBB.NRC) Analysis Method for Circumferentially Through-Wall-Cracked Pipes Under Axial Plus Bending Loads," NUREG/CR-4572, May 1986.
- 5.8 Gilles, P. and Brust, F., "Approximate Fracture Methods for Pipes – Part I: Theory," *Nuclear Engineering and Design*, Vol. 127, pp. 1-27, 1991.
- 5.9 Brust, F. W., and others, "Assessment of Short Through-Wall Circumferential Cracks in Pipes," NUREG/CR-6235, April 1995.
- 5.10 Kanninen, M. F., and others, "Mechanical Fracture Predictions for Sensitized Stainless Steel Piping with Circumferential Cracks," Final Report, EPRI NP-192, September 1976.
- 5.11 Mayfield, M. E., and others, "Cold Leg Integrity Evaluation – Final Report," NUREG/CR-1319, February 1980.
- 5.12 Kanninen, M. F., and others, "The Development of a Plan for the Assessment of Degraded Nuclear Piping by Experimentation and Tearing Instability Fracture Mechanics Analysis," NUREG/CR-3142, June 1983.
- 5.13 Wilkowski, G. M., and others, "Degraded Piping Program – Phase II, Summary of Technical Results and Their Significance to Leak-Before-Break and In-Service Flow Acceptance Criteria, March 1984 – January 1989," NUREG/CR-4082, Vol. 8, March 1989.
- 5.14 Papaspyropoulos, V., and others, "Predictions of J-R Curves with Large Crack Growth from Small Specimen Data," NUREG/CR-4575, September 1986.
- 5.15 Nakagaki, M., and others, "Analysis of Cracks in Stainless Steel TIG Welds," NUREG/CR-4806, December 1986.
- 5.16 Wilkowski, G. M., and Scott, P. M., "A Statistical Based Circumferentially Cracked Pipe Fracture Mechanics Analysis for Design or Code Implementation," *Nuclear Engineering and Design*, Vol. 111, pp. 173-187, 1989.
- 5.17 Kramer, G., and Papaspyropoulos, V., "An Assessment of Circumferentially Complex-Cracked Pipe Subjected to Bending," NUREG/CR-4687, October 1986.
- 5.18 Marschall, C. W., and others, "Loading Rate Effects on Strength and Fracture Toughness of Pipe Steels Used in Task 1 of the IPIRG Program," NUREG/CR-6098, October 1993.
- 5.19 Paul, D. D., and others, "Evaluation and Refinement of Leak-Rate Estimation Models," NUREG/CR-5128, Rev. 1, June 1994.
- 5.20 Rudland, D. L., and others, "The Effects of Cyclic and Dynamic Loading on the Fracture Resistance of Nuclear Piping Steels," NUREG/CR-6440, December 1996.

5.21 Olson, R., and others, "Effect of Cyclic Loads on the Fracture Behavior of Stainless Steel Pipes with High and Low Sulfur Contents," *16<sup>th</sup> International Conference on Structural Mechanics in Reactor Technology*, Paper No. 1759, Division G, August, 2001.

5.22 Ghadiali, N., and others, "Deterministic and Probabilistic Evaluations for Uncertainty in Pipe Fracture Parameters in Leak-Before-Break and In-Service Flaw Evaluations," NUREG/CR-6443, June 1996.

5.23 Rahman, S., and others, "Probabilistic Pipe Fracture Evaluations for Leak-Rate-Detection Applications," NUREG/CR-6004, April 1995.

5.24 Rahman, S., and others, "Refinement and Evaluation of Crack-Opening-Area Analyses for Circumferential Through-Wall Cracks in Pipes," NUREG/CR-6300, April 1995.

5.25 Marschall, C. W., and others, "Effect of Dynamic Strain Aging on the Strength and Toughness of Nuclear Ferritic Piping at LWR Temperatures," NUREG/CR-6226, October 1994.

5.26 Scott, P. M., and others, "Fracture Evaluations of Fusion Line Cracks in Nuclear Pipe Bimetallic Welds," NUREG/CR-6297, April 1995.

5.27 Rosenfield, A. R., and others, "Stainless Steel Submerge Arc Weld Fusion Line Toughness," NUREG/CR-6251, April 1995.

5.28 Mohan, R., and others, "Effects of Toughness Anisotropy and Combined Tension, Torsion, and Bending Loads on Fracture Behavior of Ferritic Nuclear Pipe," NUREG/CR-6299, January 1995.

5.29 Majumdar, S., and others, "Interim Fatigue Design Curves for Carbon, Low-Alloy, and Austenitic Stainless Steels in LWR Environments," NUREG/CR-5999, April 1993.

5.30 Chopra, O., and others, "Long-Term Embrittlement of Cast Duplex Stainless Steels in LWR Systems," Annual Report October 1982-September 1983, NUREG/CR-3857, August 1984.

5.31 Chopra, O., and others, "Long-Term Embrittlement of Cast Duplex Stainless Steels in LWR Systems," Annual Report October 1983-September 1984, NUREG/CR-4204, March 1985.

5.32 Chopra, O., and others, "Long-Term Embrittlement of Cast Duplex Stainless Steels in LWR Systems," Annual Report October 1984-September 1985, NUREG/CR-4503, January 1986.

5.33 Chopra, O., "Long-Term Embrittlement of Cast Duplex Stainless Steels in LWR Systems," NUREG/CR-4744, Vol. 1, No. 1 thru Vol. 7, No. 2, July 1993.

5.34 Kyokai, N. D., and Bukai, G. S., "Technical Guidelines for Protection Design Against Postulated Piping Failures in Nuclear Power Plants," JEAG 4613-1998, December 1998.

5.35 "A16: Guide for Defect Assessment and Leak Before Break Analysis," DMT 96.096, third draft, December 1995.

5.36 Wilkowski, G. M., and others, "State-of-the-Art Report on Piping Fracture Mechanics," NUREG/CR-6540, January 1998.

5.37 Yagawa, G., and others, "Stable Growth and Instability of Circumferential Cracks in Type 304 Stainless Steel Pipes Under Tensile Load," *Journal of Pressure Vessel Technology*, Vol. 106, pp 405-411, November 1984.

5.38 Shibata, K., and others, "Evaluation of JAERI's Ductile Fracture Test Results on Stainless Steel and Carbon Steel Piping," *Nuclear Engineering and Design*, Vol. 111, pp 135-146, 1989.

5.39 Ogawa, N., "Experimental Study of Piping Stability Under Strong Earthquake," ASME

PVP special publication PVP 150, pp 69-80, July 1988.

5.40 Kurihara, R., and others, "Experimental Studies of 4-inch Pipe Whip Test Under BWR LOCA Conditions," *Nuclear Engineering and Design*, Vol. 76, pp 23-33, 1983.

5.41 Isozaki, T., and Miyazono, S., "Experimental Study of Jet Discharge Test Results Under BWR and PWR Loss of Coolant Accident Conditions," *Nuclear Engineering and Design*, Vol. 96, pp 1-9, 1986.

5.42 Takumi, K., "Results of the Japanese Carbon Steel Pipe Fracture Program, "NUREG/CP-0109, *Leak-Before-Break: Further Development in Regulatory Policies and Supporting Research*, Taipei, Taiwan, pp 13-31, February 1990.

5.43 Fujioka, T., and others, "A Fracture Strength Evaluation Method for Carbon Steel Pipes Subjected to Dynamic/Cyclic Loadings: Evaluation of Dynamic/Cyclic Pipe Fracture Tests at Elevated Temperatures," *ASME PVP* Vol. 304, pp 191-197, 1995.

5.44 Kramer, G., and others, "Stability of Cracked Pipe Under Seismic/Dynamic Displacement-Controlled Stresses," *NUREG/CR-6233*, Vol. 2, June 1997.

5.45 Bonnet, S., and others, "Relationship Between Evolution and Mechanical Properties of Various Cast Duplex Stainless Steels and Metallurgical and Aging Parameters: An Overview of Current EDF Programmes," *Material Science Technology*, Vol. 6, pp 221-229, 1990.

5.46 Milne, I., and others, "Assessment of the Integrity of Structures Containing Defects, CEBG Report R/H/R6 – Revision 3," January 1987.

5.47 Kußmaul, K., and others, "Phänomenologische Behälterberstversuche – Phase I," BMFT Report BMFT-TB-150 279, by MPA-Stuttgart, July 1985.

5.48 Sturm, D., and others, "Phänomenologische Behälterberstversuche – Phase II," BMFT Report BMFT-TB-1500 279, by MPA-Stuttgart, December 1987.

5.49 Bartholome, Gunther, "German Leak-Before-Break Concept – Description of German LBB Procedures, Practices, and Applications," *International Journal of Pressure Vessel and Piping*, Vol. 71, pp 139-146, 1997.

5.50 "Proceedings of the CNSI Specialist Meeting on Leak-Before-Break in Nuclear Reactor Piping," Proceedings of a Seminar Held in Monterey, California, NUREG/CP-0051, August 1984.

5.51 "Leak-Before-Break: International Policies and Supporting Research," Proceedings of a Seminar Held in Columbus, Ohio on October 28-30 1985, NUREG/CP-0077, June 1986.

5.52 "Leak-Before-Break: Progress in Regulatory Policies and Supporting Research," Proceedings of a Seminar held in Tokyo, Japan on May 14-15, 1987, NUREG/CP-0092, March 1988.

5.53 "Leak-Before-Break: Further Developments in Regulatory Policies and Supporting Research," Proceedings of a Seminar in Taipei, Taiwan on May 11-12, 1989, NUREG/CP-0109, February 1990.

5.54 "Leak-Before-Break in Water Reactor Piping and Vessels," C. E. Coleman Editor, held on October 24-27, 1989, in Toronto, Canada, reprinted from *The International Journal of Pressure Vessels and Piping*, Vol. 43, Nos. 1-3, 1990.

5.55 "Proceedings of the Seminar on Leak Before Break in Reactor Piping and Vessels," Proceedings of a Seminar Held in Lyon, France on October 9-11, 1995, NUREG/CP-0155, April 1997.

5.56 Scott, P., and others, "Crack Stability in a Representative Piping System Under Combined

Inertial and Seismic/Displacement-Controlled Stresses," NUREG/CR-6233, Vol. 3, June 1997.

5.57 Rahman, S., and others, "Summary of Results from the IPIRG-2 Round-Robin Analyses," NUREG/CR-6337, February 1996.

5.58 Hiser, A. L., and Callahan, G. M., "A User's Guide to the NRC's Piping Fracture Mechanics Database (PIFRAC)," NUREG/CR-4894, May 1987.

5.59 Paris, P. C., and Tada, H., "The Application of Fracture Proof Design Methods Using Tearing Instability Theory to Nuclear Piping Postulating Circumferential Through-Wall Cracks," NUREG/CR-3464, September 1983.

5.60 Newman, J.C., and Raju, I.S. "An Empirical Stress-Intensity Factor Equation for the Surface Crack," *Engineering Fracture Mechanics*, Vol. 15, No. 1-2, pp. 185-192, 1981.

5.61 Scott, P., and others, "IPIRG-2 Task 1 - Pipe System Experiments with Circumferential Cracks in Straight-Pipe Locations," NUREG/CR-6389, February 1997.

5.62 NRC Generic Letter 97-01: Degradation of Control Rod Drive Mechanism Nozzle and Other Vessel Closure Head Penetrations.

5.63 NRC Information Notice 2000-17: Crack in Weld Area of Reactor Coolant System Hot Leg Piping at V. C. Summer.

5.64 NRC Information Notice 2000-17, Supplement 1: Crack in Weld Area of Reactor Coolant System Hot Leg Piping at V. C. Summer.

5.65 "Report of the U.S. Nuclear Regulatory Commission Piping Review Committee. Evaluation of Potential for Pipe Breaks," NUREG-1061, Vol. 3, November 1984.

5.66 Krishnaswamy, P., and others, "Fracture Behavior of Short Circumferentially Surface-Cracked Pipe," NUREG/CR-6298, November 1995.

5.67 Scott, P. M., and Wilkowski, G. M., "Development and Application of a Database of Pipe Fracture Experiments," PVP Vol. 323, Fatigue and Fracture, Vol. 1, July 1996.

5.68 Kilinski, T., and others, "Fracture Behavior of Circumferentially Surface-Cracked Elbows," NUREG/CR-6444, December 1996.

5.69 Harris, D. O., E. Y. Lim, and D. D. Dedhia, "Probability of pipe Fracture in the Primary Coolant Loop of a PWR Plant - Volume 5: Probabilistic Fracture Mechanics Analysis," NUREG/CR-2189, Vol. 5, 1981.

5.70 Harris, D. O., Dedhia, D. a., Easton, E. D., and Patterson, S. P., "Probability of Failure in BWR Piping," NUREG/CR-4792, Vol. 3, 1986.

5.71 Harris, D. O., and D. Dedhia. 1992. A Probabilistic Fracture Mechanics Code for Piping Reliability, Analysis (pc-PRAISE code), NUREG/CR-5864, U.S. Nuclear Regulatory

5.72 Kaheel, M. A., Simonen, F. A., Phanh. K., Harris, D. O., and Dedhia, D., "Fatigue Analysis of Components for 60-year Plant Life," NUREG/CR-6674, June 2000.

5.73 Bishop, B. A., "Westinghouse Structural Reliability and Risk Assessment (SRRA) Model for Piping Risk Informed Inservice Inspection," WCAP-14572 Revision 1, Supplement 1, October 1997.

## 6 PROPOSED TIERED APPROACH TO LBB

As part of Task 3 of the LBB Regulatory Guide program a three-tiered approach to LBB was proposed. Details of the three levels for this tiered approach to LBB (i.e., Levels 1, 2, and 3) are provided in Appendices A, B and C, respectively.

### 6.1 General Screening Criteria for Proposed Tiered Approach to LBB

Prior to applying any of the three levels of the proposed tiered LBB assessment methodology, there needs to be a **general screening criteria** to preclude its application to cases for which LBB is not applicable, e.g.,

- piping systems susceptible to corrosion, flow-accelerated erosion-corrosion, stress corrosion cracking, creep, or water hammer,
- piping systems for which there is a significant probability of degradation from indirect sources, such as fires, missiles, and damage from equipment failures (e.g. cranes), and failures of systems or components in close proximity.
- piping systems that may experience significant cyclic stresses,
- piping supported by masonry block walls, and
- piping materials operating at temperatures that would make them susceptible to brittle-cleavage type fracture.

If the general screening criteria are met, any of the three levels of analysis may be selected to demonstrate LBB, with the Level 1 approach being the simplest requiring the least knowledge of the piping system and the Level 3 approach being the most complex. It is envisioned that the Level 2 approach will be the "standard" level of assessment, most often used for LBB assessments. These three levels of assessment will be summarized later in this section of this report.

### 6.2 Extent of Assessment

LBB is applicable only to an entire piping system, or an analyzable portion thereof. Analyzable portions are typically segments located between anchor points. LBB cannot be applied to individual welded joints or other discrete locations. When LBB technology is applied, all potential pipe rupture locations along the piping system, or analyzable portion thereof, are to be considered. In making such a consideration, it is necessary to make assessments at a number of critical locations along the piping system. At a minimum, one should postulate the existence of a flaw at each of the following locations:

- (a) The location which has the highest stresses coincident with the most limiting material properties for the piping base metal, weldments, and safe ends (per the requirements of NUREG-1061 Vol. 3),
- (b) The location with the highest normal operating stresses (this is the location where a crack is more likely to start),
- (c) The location with the lowest normal operating stress (this is the location where the postulated leakage crack size will be the largest),
- (d) The location with the highest transient stresses, i.e., safe shutdown earthquake (SSE) or transient thermal expansion stresses, at start-up or shut-down,
- (e) The locations with the highest ratios of the normal operating plus transient stresses (N+SSE) to the normal operating stresses (N), and
- (f) Any other location that has a J-R curve that is less than 75 percent of the J-R curve for the above material locations.

Postulated cracks can be in the straight pipes, girth welds, or fittings. For fittings, the most common type of fitting to develop cracks is an elbow. Elbow cracks can be either circumferential cracks on the extrados (closing moment applied), especially in thicker walled

elbows, or axial cracks on the flank of the elbow, especially in thinner walled elbows.

### 6.3 Definition of Margins and Partial Safety Factors

For an existing draft SRP 3.6.3 LBB assessment (Ref. 6.1), two separate margins are applied during the analysis. First, a margin of 10 on leak rate detection limit capability is applied for the postulated leakage crack size analysis. In addition, a margin of 2 between the critical crack size and the postulated leakage crack size must be shown to exist. In a similar vein, it must be demonstrated that the leakage size crack will not experience unstable crack growth if 1.4 times the normal plus SSE loads are applied.<sup>22</sup> For the higher levels of the proposed tiered approach (Levels 2 and 3), these margins may be different due to the increased fidelity in the analyses. (For the Level 1 analysis, the prescribed safety factors may be left as is or may be increased or decreased. That decision will be left to the NRC (with possible guidance from its contractors), as will be all decisions related to safety margins. In addition, it may be desirable to invoke a partial safety factor approach. Partial safety factors are probabilistic-based variable-specific safety factors, i.e., there might be different safety factors on strength, toughness, leak-rate detection capability, loads, etc., established ahead of time through probabilistic type analyses.

### 6.4 Data Requirements

The data typically required for the three levels of the proposed tiered approach to LBB are shown in Table 6.1. As can be seen in Table 6.1, more detailed data are required for the higher levels of analysis, i.e., the Level 2 and 3 approaches.

For advanced reactor designs, which may be constructed under a provisional license, the current thought is that if a certain line is

---

<sup>22</sup> The margin of 1.4 can be reduced to 1.0 if the deadweight, thermal expansion, SSE (inertial), and seismic anchor motion (SAM) loads are combined based on individual absolute values instead of combining them algebraically.

generically approved for LBB and the applicant can demonstrate that if certain input parameters for their plant specific application, e.g., actual wall thicknesses, loads, etc., are within some pre-established bounds, then LBB is acceptable. It is currently envisioned that the NRC will specify in the Regulatory Guide, the process of how one is to develop these input parameters and the bounds on their acceptable values.

### 6.5 Subcritical Crack Growth Analysis

One of the elements of a NUREG-1061 Vol. 3 type LBB assessment (Ref. 6.2) is a fatigue crack growth analysis of a postulated part-through surface flaw at the location or locations which exhibit the highest stresses coincident with the poorest material properties for the base metals, weldments, and safe ends<sup>23</sup>. The size of that postulated part-through surface flaw should be no less than that which would be permitted by the acceptance criteria of the appropriate subsections of Section XI of the ASME Boiler and Pressure Vessel Code (Ref. 6.3). The purpose of the NUREG-1061 Vol. 3 required fatigue crack growth analysis is to demonstrate that a flaw permitted by the acceptance criteria of Section XI of the ASME Code would not grow significantly during service. Specifically, that such a flaw will not result in a leak nor grow to a critical size during the remaining lifetime of the plant. The fatigue crack growth analysis should be performed in accordance with the rules of Appendix A (ferritic materials) and Appendix C (austenitic materials) of Section XI of the ASME Boiler and Pressure Vessel Code.

---

<sup>23</sup> Draft SRP 3.6.3 is not as specific as NUREG-1061 Vol. 3 in this regard in that the draft SRP only specifies that the applicant must demonstrate that there is "no potential for significant cyclic thermal stresses" or "no significant potential for vibration induced fatigue cracking or failure".

**Table 6.1 Typical data requirements needed for the three levels of the proposed tiered approach to LBB**

<b>Level 1 requirements</b>	<b>Level 2 requirements</b>	<b>Level 3 requirements</b>
Physical dimensions - Pipe diameter - Wall thickness	Same as Level 1	Same as Level 2
Thermo-hydraulic conditions - Temperature - Pressure	Same as Level 1	Same as Level 2
Material property data - Code or actual yield and ultimate strength values	Material property data - Code or actual yield and ultimate strength values - Stress-strain data - J-R curve data - Leakage flaw type Surface roughness Number of turns	Same as Level 2
Specialized computer codes required - None	Specialized computer codes required - Leak-rate code, e.g., SQUIRT, PICEP, - Fracture mechanics code, e.g., NRCPIPE or FEM analyses	Same as Level 2, except also need a finite element code for dynamic pipe system evaluations, e.g., ANSYS, ABAQUS, etc.
Stresses - Normal operating and transient stresses (i.e., SSE or transient thermal expansion) from the stress report	Same as Level 1	Stresses - Nonlinear finite element analysis
Elastic-plastic fracture analysis - Simplified procedures	Elastic-plastic fracture analysis - J-estimation schemes, or - FEM analyses	- Same as Level 2

This fatigue crack growth requirement in NUREG-1061 Vol. 3 is somewhat redundant with the postulated leakage crack size analysis embedded in each of the levels of the proposed tiered approach to LBB. The fatigue crack growth analysis is used to demonstrate that if a postulated part-through surface flaw, of size that it would pass the acceptance criteria of Section XI, did exist, then that part-through surface crack would not grow to the extent that it would leak (i.e., grow through the remaining wall thickness) nor grow to a critical size during the remaining lifetime of the plant. On the other hand, the postulated leakage crack size analysis (and associated critical crack size analysis) embedded in each of the levels of the proposed tiered approach, demonstrate that if such a part-

through crack did in fact grow through the pipe wall, then the leakage from that flaw could be detected by the plant's leakage detection system, and actions taken to shutdown the plant, prior to the flaw growing in further extent that it would be at risk of reaching a critical size when subjected to severe transient load conditions, e.g., a safe-shutdown-earthquake. Thus, according to NUREG-1061 Vol. 3, one must pass two somewhat sequential "gates" in order to demonstrate LBB.

### 6.6 Level 1 Approach

The **simplest** of the three levels (Level 1) was designed to provide a **conservative assessment** of LBB acceptability, and yet be of sufficient

accuracy that piping systems that readily pass the existing draft Standard Review Plan (SRP) 3.6.3 criteria (e.g., main coolant loop piping) can still pass this Level 1 criteria. Details of this Level 1 analysis methodology are provided in Appendix A. The Level 1 criterion does not require the use of detailed leak-rate computer codes or fracture mechanics codes. It relies on a series of simple, empirically-derived algebraic expressions or closed-form solutions from which one can estimate the postulated leakage crack size. In addition, instead of having to use more sophisticated J-estimation schemes to calculate the allowable stresses for the postulated crack lengths, the Level 1 fracture analysis is the simple ASME Section XI limit-load type analysis, modified possibly by the ASME Section XI Z-factors to account for the postulated crack being located in a lower toughness material, e.g., a low-toughness stainless steel flux weld. The input data requirements for the Level 1 approach are also simpler than that typically required for an existing draft SRP 3.6.3-type assessment. The only material data required are the yield and ultimate strengths. The Level 1 type assessment does not require a full-stress strain relationship or J-R curve as might be necessary if one were using a J-estimation scheme, like GE/EPRI, to calculate the crack-opening displacements for the leakage crack size determination or the critical crack size for a stability type analysis.

To account for the simplicity in input data, the empirically derived influence functions that are used in the Level 1 leak-rate assessment were derived so as to result in a conservative assessment of the postulated leakage crack size.

In addition, there is a **specific Level 1 screening criteria** to preclude the use of the Level 1 methodology for cases outside its realm of validity, e.g., small diameter pipe that may be influenced by pressure-induced bending effects or thin-wall piping that may be influenced by weld residual stress effects. If a piping system fails to pass the Level 1 screening criteria or Level 1 assessment criteria, Level 2 or Level 3 analysis must be used to demonstrate LBB. Furthermore, the investment in resources in

applying the failed Level 1 analysis should not be so great as to be a burden on the applicant.

## 6.7 Level 2 Approach

The next level of complexity for LBB assessment will be the Level 2 methodology. Details of the Level 2 methodology are provided in Appendix B. The Level 2 methodology is similar in scope to the existing draft SRP 3.6.3 methodology except it incorporates some of the **recent enhancements in the technology** that have resulted from the recent research results. It is envisioned that this level of assessment is the type of approach that would be **used in the majority of future LBB applications**. The level of complexity associated with the input parameters for this Level 2 analysis methodology will be similar to that that might be required for an existing draft SRP 3.6.3-type analyses, i.e., full-stress strain curve representation of the material strength data and lower bound fracture toughness data. In addition the margins associated with the Level 2 criteria may be different than those used in the existing draft SRP 3.6.3 criteria, e.g., 10 on leak-rate detection capability and 2.0 on crack size.

The main difference between the Level 2 criteria and the existing draft SRP 3.6.3 criteria is the enhancements in the technology that have arisen as a result of the recent NRC-funded research that are incorporated as part of this Level 2 criteria. Some of the enhancements in the technology which were considered in the development of this level of analysis are:

- Use of the best leak-rate code with most appropriate crack morphology variables,
- Use of the most accurate fracture mechanics analyses,
- Accounting for the most recent material property information, including the effect of dynamic and/or cyclic loading, weld/fusion line toughness data, and current J-R curve extrapolation techniques,
- Accounting for the effects of weld residual stresses on the crack-opening

displacements for the leak-rate analyses<sup>24</sup>, and

- Accounting for the effects of restraint of pressure induced bending on the crack-opening displacements for the leak-rate analyses. Note, preliminary analyses as part of Task 3 of the LBB Regulatory Guide program, based on results from an ongoing effort in the BINP program, showed that the effect of restraint of pressure induced bending was minor for the case of a 14-inch diameter surge line. However, for a smaller 6-inch diameter safety injection system line, the effect was much larger, especially for the case where the physical restraint was close to the postulated crack plane. For the particular 6-inch diameter line analyzed, the postulated leakage size crack for the restrained case was 42 percent longer than for the unrestrained case. (See Test Case 3 in Table D.3.)

If one cannot demonstrate LBB for a piping system using this Level 2 approach, then a Level 3-type analysis, which is the most complex and accurate of the three levels would be required.

### 6.8 Level 3 Approach

The Level 3 approach is the **most complex** of the three levels of deterministic analyses, requiring the greatest amount of information/data for its application. Details of this Level 3 methodology are provided in Appendix C. This level of analysis will be a very detailed deterministic analysis, involving **nonlinear stress analyses**, possibly incorporating a **nonlinear spring representation of the crack section**, and possibly incorporating **partial safety factors** previously determined from probabilistic type analyses. The nonlinear stress analyses will be used to take advantage of the inherent margins that exist when one invokes an elastic analysis on a nonlinear problem. (This topic of additional margin due to nonlinear behavior is the subject of an ongoing task in the BINP

---

<sup>24</sup> This is the subject of an ongoing task in the BINP program.

program.) By incorporating plasticity into the modeling, energy that would have otherwise gone into driving the crack will be absorbed in plastically deforming the surrounding uncracked pipe material. This level of analysis should only be used for those cases where LBB cannot be demonstrated using the simpler Level 1 or 2 methods. As part of Task 3 of the LBB Regulatory Guide program, additional margins of 20 to 30 percent on crack size over a Level 2 assessment were demonstrated during a case study analysis of a PWR surge line.

### 6.9 Acceptance Criteria

The existing LBB acceptance criteria embodied in NUREG-1061 Vol. 3 and the draft SRP 3.6.3 specify that one must satisfy the following requirements in order to demonstrate LBB:

- the sub-critical crack growth analysis for a postulated Section XI-acceptable, part-through surface crack at the location or locations along the piping system with the highest stresses coincident with the poorest material properties for the base metal, weldments, and safe ends,
- the critical crack size at the faulted load conditions is at least a factor of 2 longer than the postulated leakage size crack for the normal operating stresses, and
- the postulated leakage size crack will not demonstrate unstable crack growth if 1.4 times the normal plus SSE loads are applied<sup>25</sup>.

For the proposed tiered approach to LBB, it is envisioned that the same sort of criteria will be applied although the magnitudes of some of the applied safety factors may differ depending on the level of analysis invoked.

---

<sup>25</sup> The 1.4 margin can be reduced to 1.0 if the deadweight, thermal expansion, pressure, SSE (inertial), and seismic anchor motion (SAM) loads are combined based on individual absolute values instead of combining them algebraically.

## **6.10 References**

6.1 "Leak-Before-Break Evaluation Procedures," draft Standard Review Plant 3.6.3, August 1987.

6.2 "Report of the U.S. Nuclear Regulatory Commission Piping Review Committee. Evaluation of Potential for Pipe Breaks," NUREG-1061, Vol. 3, November 1984.

6.3 ASME Boiler and Pressure Vessel Code, 1998 Edition.

## 7 FOREIGN EXPERIENCE

A number of other countries have developed, or are in the process of developing, their own LBB procedures. Some of the countries that have or are developing LBB procedures include:

- France,
- Germany,
- Japan,
- Korea,
- Russia,
- United Kingdom,
- Canada, and
- Sweden.

Like the NRC's LBB procedures, many of these foreign procedures are still in draft form. For the most part, the procedures in these other countries are very similar to those in the United States. However, one striking difference is that they oftentimes start by postulating the existence of a part-through surface flaw, instead of a postulated through-wall crack, and then conduct a fatigue crack growth analysis of that postulated surface flaw up to the instant of surface crack penetration. Some of the other differences will be discussed in the sections that follow.

### 7.1 France

Chapter 4 of the draft French A16 Report (Ref. 7.1), prepared by the Commissariat A L'Energie Atomique (CEA), the NRC's Office of Research counterpart in France, provides a set of draft procedures for conducting LBB analyses. The purpose of such an LBB analysis is to determine if it is possible to detect, under in-service conditions, a leak in a fluid-filled structure prior to the associated flaw causing a rupture of the structure. Procedures are provided in Reference 7.1 for both the case where creep damage would not be expected and for the case where the potential for creep damage is deemed significant.

The key steps in the procedures are:

- The highest stressed regions need to be selected.
- The initial surface flaw, including the position, orientation, shape, and dimensions, needs to be defined. Typically a semi-elliptical initial flaw of size  $a_i$  and  $2c_i$  is assumed.
- The fatigue crack growth of the initial semi-elliptical flaw ( $a_i, 2c_i$ ) under normal operating conditions and the analysis of the avoidance of a fast rupture or instability of the final semi-elliptical flaw ( $a_f, 2c_f$ ) need to be analyzed, for both the normal operating and normal operating plus faulted load conditions.
- The evolution of the semi-elliptical flaw size ( $a_f, 2c_f$ ) under cyclic loading up to a detectable through thickness flaw ( $2c_{det}$ ) corresponding to a detectable leak rate ( $Q_{det}$ ) needs to be calculated. The evolution of the flaw can be determined in two stages: up to the instant the surface flaw penetrates the pipe wall thickness, and up to the situation where the length of the through-wall flaw on the external surface reaches a value equal to the detectable flaw length ( $2c_{det}$ ).
- Analysis needs to be conducted to demonstrate the avoidance of a fast rupture or instability of the detectable flaw ( $2c_{det}$ ) under the normal plus faulted conditions.

In calculating the evolutionary crack size ( $a, c$ ) as a result of the cyclic loading, and the length of the associated through-wall crack at the instant of surface-crack penetration, an approach is presented in Reference 7.1 to estimate the relationship between the length of the surface crack ( $c_s$ ) and the wall thickness ( $t$ ). For this approach, the ratio of  $c_s/t$  is a function of the ratio of the cyclic bending stress to the cyclic membrane stress, i.e.,  $\Delta\sigma_b/\Delta\sigma_m$ . From this

approach, it can be seen that pure tension loadings result in relatively short cracks while pure bending loadings result in relatively long cracks.

Chapter 4 provides a series of closed-form equations to calculate the detectable flow length ( $2c_{det}$ ) from the detectable leak rate ( $Q_{det}$ ). First, the crack-opening area ( $A_L$ ) for the detectable through-wall crack is calculated from the detectable leak rate ( $Q_{det}$ ) and the fluid velocity ( $V$ ) through the crack.

$$A_L = \frac{Q_{det}}{V} \quad (7.1)$$

where, the detectable leak rate ( $Q_{det}$ ) is equal to the minimum detectable leak rate ( $Q_{min}$ ) with a safety of factor of 10 applied, i.e.,

$$Q_{det} = 10Q_{min} \quad (7.2)$$

The crack-opening area of an elliptically-shaped through-wall crack is:

$$A_{TWC} = \frac{\pi\delta c}{2} \quad (7.3)$$

where the crack-opening displacement ( $\delta$ ) is a function of the applied stress, crack length ( $2c$ ), and the dimensions of the component under consideration, i.e., mean radius ( $R_m$ ) and wall thickness ( $t$ ). In the third draft version of this document, it was indicated that a simplified expression for  $\delta$  was forthcoming.

Two equations are provided for the fluid velocity ( $V$ ) depending on whether the fluid flow is in the laminar (Reynolds Number,  $Re$ ,  $< 2300$ ) or turbulent ( $Re > 2300$ ) flow regime.

For laminar flow,

$$V = \frac{\Delta P(D_H^2)}{48\mu t} \quad (7.4)$$

where,

- $\Delta P$  = pressure difference across the crack, i.e., typically internal pipe pressure,
- $D_H$  = hydraulic diameter, approximated in Chapter 4 as  $\pi\delta/2$  for an elliptical crack,
- $\mu$  = dynamic viscosity of the fluid at the temperature under consideration, and
- $t$  = pipe wall thickness.

For turbulent flow,

$$V = \left( \frac{2\Delta P}{\rho \left( 1.5 + \frac{\lambda t}{D_H} \right)} \right)^{1/2} \quad (7.5)$$

where,

- $\rho$  = fluid density at the temperature and pressure under consideration, and
- $\lambda$  = a function of the rugosity and hydraulic diameter.

Rearranging Equations 7.1 and 7.3,

$$c_L \delta V = \frac{2Q_{det}}{\pi} \quad (7.6)$$

The three terms in the left hand side of Equation 7.6 ( $c_L$ ,  $\delta$ , and  $V$ ) are all functions of the crack length ( $c$ ), thus Equation 7.6 has to be solved iteratively.

In order to demonstrate the avoidance of a fast rupture or a crack instability, both limit-load and elastic-plastic J-based analysis routines are provided in Reference 7.1 for both surface cracks and through-wall cracks.

## 7.2 Germany

In Germany, LBB is applied for many of the same reasons as it is applied in other countries, i.e., to justify the elimination of the design requirements that account for the dynamic effects during a pipe rupture. The elimination of these design requirements allows for the elimination of hardware, such as pipe whip restraints and jet impingement shields. This

hardware can impede accessibility to pipes for inspections and increases radiation exposure during maintenance operations. As with other countries, to demonstrate LBB in Germany, it has to be shown that any crack will lead to a leak, and that this leak will be detected long before it could possibly grow to a critical size that it would grow unstably at the faulted load conditions.

In Germany, the LBB procedures are part of the break-preclusion (BP) or basis safely (BS) concept. There are two main prerequisites of the BP (or BS) concept: basic safety and independent redundancies (Refs. 7.2 and 7.3). The independent redundancies required for break preclusion are: (1) in-service inspection, (2) load monitoring, and (3) leak-detection systems. The process of demonstrating that a break will not occur is based on the following points:

1. Stress corrosion cracking, thermal fatigue, and water hammer need to be shown that they are not relevant failure mechanisms for the piping system under consideration. Thus, the only failure mechanism that needs to be considered is potential ductile failure resulting from a large load (emergency and faulted conditions, e.g., earthquake).
2. The fracture resistant material properties used in the fabrication of the piping system make a rupture of the piping system highly unlikely.
3. The pre-service and in-service inspections will detect any flaws. If a flaw goes undetected, its growth over the life of the plant will be insignificant, i.e., no mechanisms exist to develop a through-wall crack.
4. If an unlimited number of plant lives are assumed, a theoretical through-wall crack may develop, but that through-wall crack will not become unstable under the worst case loading conditions.
5. This stable through-wall crack will leak at a rate such that the leak can be detected by the plant's leakage detection equipment, and the plant subsequently

shutdown, so that the appropriate repairs completed.

Fracture mechanics principles and criteria are used to demonstrate LBB behavior, according to the last three steps above (Steps 3 through 5 above). The initial flaw (or reference flaw) used in the fatigue crack growth analysis (Step 3) and in the LBB fatigue crack growth demonstration (Step 4) is a semi-elliptical surface flaw with a depth (a) and total length (2c). This flaw is postulated to exist in a highly stressed weld. The size of this reference flaw is based on an envelope of allowable flaws for pre-service examination and in-service inspection. Performance of inspection technologies and accumulated experience are taken into account when defining the size of this reference flaw.

The fatigue crack growth analysis for the reference surface flaw is performed using the normal and upset transient loadings, using the Paris-law fatigue crack growth model (Ref. 7.4) with a conservative fatigue crack growth curve ( $da/dN$  versus  $\Delta K$ ) accounting for environmental effects. The criterion for acceptance is to demonstrate negligible fatigue crack growth of the reference flaw during the course of the projected life of the plant (Step 3 above). Assuming the piping system passes this first level of acceptance, a similar analysis is performed, except an unlimited number of plant lives are assumed. For this case, the acceptance criterion is that if the crack grows through the pipe wall by fatigue, or the ligament tears through the pipe wall, without an instability in the circumferential direction, then the LBB fatigue crack growth condition is demonstrated (Step 4 above). If on the other hand, the crack reaches a critical length before it tears through the wall, then LBB is not demonstrated. For this condition, additional safety measures (e.g., additional in-service inspections) may be incorporated in order to ensure the proof of integrity.

Next, the stability of the end-of-life surface defect, and the stability of the through-wall crack that exists once the reference surface flaw penetrates the pipe wall thickness ( $2c_{Leak}$ ), must be demonstrated for the normal operating plus

maximum accident load condition (e.g., SSE loads), i.e., the resultant leakage size crack ( $2c_{Leak}$ ) must be less than the critical through-wall crack size ( $2c_{crit}$ ) at the normal plus SSE load condition. Frequently, fully plastic limit-load analyses are used for these stability assessments. Given that this end-of-life surface defect and the resultant leaking through-wall crack after surface crack penetration are found to be stable, crack opening area and leak-rate analyses are performed to establish a detectable crack length. The length of this detectable crack ( $2c_{LDS}$ ) is a function of the sensitivity of the leak detection system, as well as the applied loads on the piping system. To demonstrate LBB, this detectable through-wall crack (at normal operating loads) must be smaller than the critical through-wall crack (at normal plus SSE loads), and there must be enough time to detect the leak by the leak detection system before the crack could possibly grow to a critical length, i.e., the growth rate of the through-wall crack is not excessive at the normal operating loads.

In summary, LBB is satisfied if: (1) the leakage crack size ( $2c_{Leak}$ ) after the fatigue crack growth of the reference defect (after unlimited plant lives) is less than the critical crack size ( $2c_{crit}$ ); and, (2) the detectable crack size ( $2c_{LDS}$ ) is less than the critical crack size ( $2c_{crit}$ ); and, (3) the growth of the resultant through-wall crack is slow enough that there is enough time to detect the leak by the leak detection system, see Figure 7.1.

At the time of the publication of Reference 7.2, there were no prescribed safety factors (or margins) on the leakage detection capability or on the leakage or detectable crack to the critical crack size relationship. Discussions had been initiated with the German KTA with the goal of achieving a common understanding on the subject of LBB. One of the main items of these discussions will be establishing prescribed safety factors.

At the time of publication of Reference 7.2, the LBB concept had been applied to a number of Siemens/KWU plants in Germany, as well as in the Netherlands, Brazil, and Argentina. For all of these applications, including the German

applications, the safety factors had been set by Siemens.

### 7.3 Japan

The Japanese LBB procedures are published in the Appendix to Reference 7.5. Reference 7.5 is applicable to reactor coolant pressure boundary (RCPB) piping systems. The basis concept is as follows:

1. A single initial flaw is assumed to exist on the inner surface of the pipe. The size of this initial flaw is based on the ultrasonic testing (UT) detectable limits for pre-service inspection (PSI), with an appropriate margin.
2. A fatigue crack growth analysis for this initial flaw is conducted up to the point when the growing surface flaw penetrates the pipe wall thickness.
3. The length of the resultant through-wall crack at the instant of surface crack penetration is compared with the length of a through-wall crack required to cause a 19 lpm (5 gpm) leak, and the larger of the two cracks is assumed in the crack stability analysis.
4. The stability of the assumed crack is evaluated for Operational Conditions I, II, and III and Operational Conditions I plus an  $S_1$  earthquake.
5. If the resultant through-wall crack from Step 3 is deemed to be stable in Step 4, then LBB is satisfied.

Some of the key details associated with these basic steps outlined above are discussed in the following sections.

**7.3.1 Assumed Initial Surface Flaw** – It is assumed that the integrity of the base pipe materials is ensured by strict quality control and material inspection when taking delivery of the pipes from the mill. Consequently, if a flaw does exist in the piping system under consideration, it would most likely be located in the one of the circumferential girth welds. As such, only circumferentially-oriented flaws in girth welds are considered for evaluation. Further, the presence of a significant flaw in a

weld prior to service need not be considered because of the inspections imposed prior to putting the plant into operation. The depth and length of this assumed initial flaw, based on limits of UT detectability, are  $0.2t$  and  $1.0t$ , respectively, for pipes with wall thicknesses ( $t$ ) greater than 15 mm (0.59 inch). For pipes with wall thicknesses less than 15 mm (0.59 inch),

the assumed flaw length is 3 times 15 mm (0.59 inch). In each case, the flaw shape is assumed to be semi-elliptical.

These assumed, or postulated, initial surface flaws are assumed to exist at locations where the applied stress or cumulative usage factor (CUF) for fatigue are large. For this application, failure

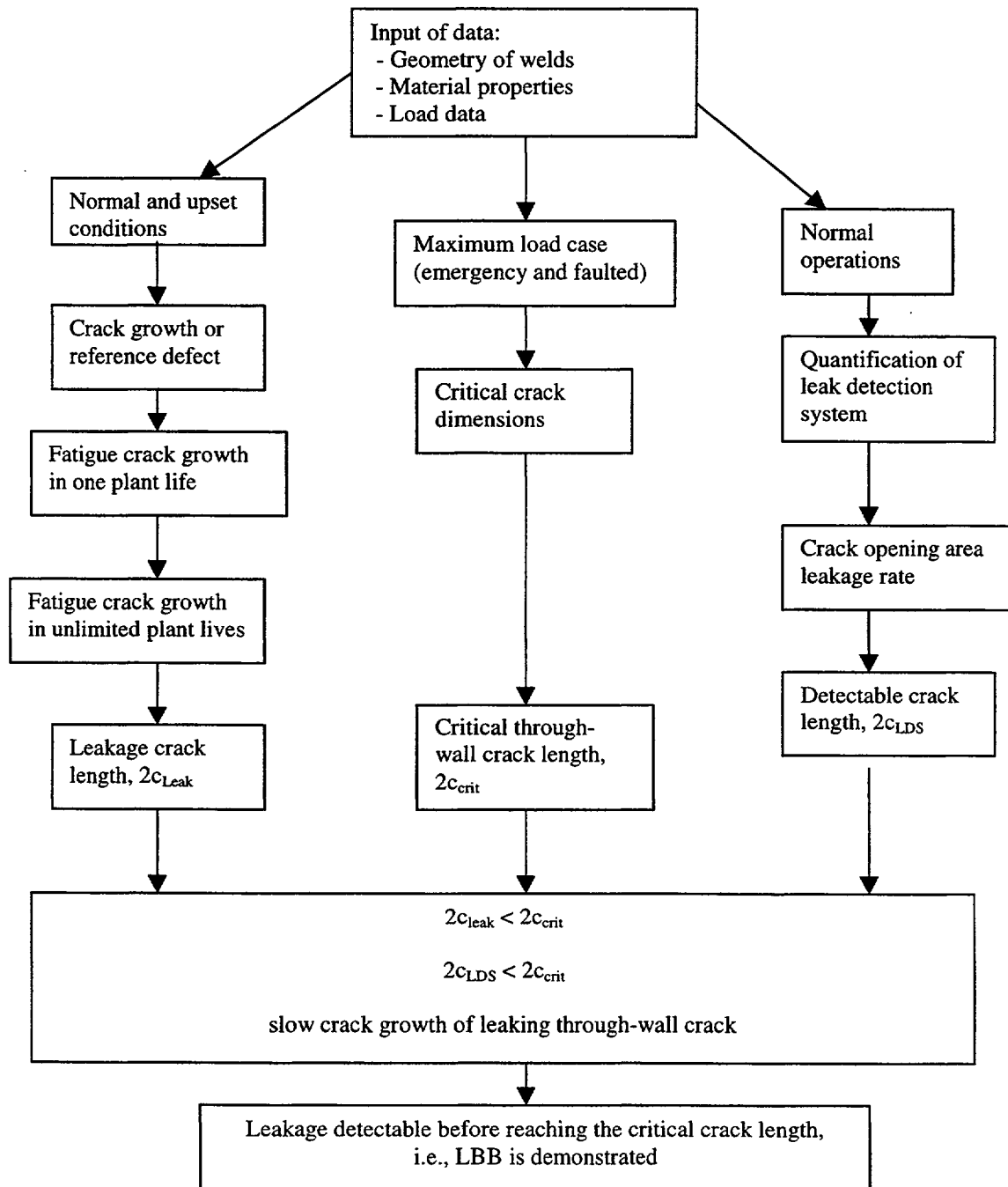


Figure 7.1 Flow diagram for German LBB analysis

is assumed to be foreseeable if the applied stress is greater than  $2.4 S_m$  or if the CUF is greater than 0.1. Moreover, terminal ends are assumed to be places where it is possible that relatively high-applied stresses will exist because of the existence of a structural discontinuity.

### 7.3.2 Applicable Damage Mechanisms

**Considered** – Propagation and failure of a flawed pipe in service is attributed to fatigue. Water quality control has been in sufficient in Japanese plants since some of the original plants were first put into operation such that incidences of stress corrosion cracking have not been observed. Corrosion and erosion/corrosion are not applicable damage mechanisms since these LBB procedures are for RCPB piping made of austenitic stainless steel<sup>26</sup>, and these materials have excellent resistance to general corrosion and erosion/corrosion. As such, incidences of these damage mechanisms have not been observed in the past. Creep is not a concern since the operational temperatures are less than the creep regime, and irradiation embrittlement is not a concern because of the sufficient shielding provided. Finally, water hammer can be excluded from the list of potential damage mechanisms due to precautions taken during design and optimized operational management control measures taken once the plants were placed in operation. As such, through process of elimination, the only known applicable damage mechanism is fatigue.

**7.3.3 Loads Used in Evaluation** – As part of these Japanese LBB procedures, fracture mechanics calculations are made as part of the crack propagation analysis, the crack stability analysis, and the crack-opening-area analysis. The loads assumed for the crack propagation analysis are based on Operational Conditions I and II and 1/3 of the  $S_1$  earthquake load. The loads assumed for the stability analysis are based on Operational Conditions I, II, and III and an Operational Condition I plus an  $S_1$  earthquake. For the crack-opening area analysis, the normal operating loads are used.

<sup>26</sup> The Japanese LBB standards for carbon steel and low-alloy steel piping are under development.

Crack propagation analysis is conducted based on the design stress cycle. However, since it is an onerous task to consider differences in design conditions, pipe configurations, and earthquake resistance conditions for a variety of pipes, stress cycles that are simplified to represent a stress cycle pattern based on the design transient conditions are used. The document provides separate representative stress cycles for BWRs and PWRs, in terms of the design stress intensity ( $S_m$ ). The Operational Conditions I and II and a 1/3  $S_1$  earthquake should be considered when setting the stress cycle for the crack propagation analysis. The number of load, or stress, cycles to be used in the crack propagation analysis is not to be specified, but instead, the crack propagation analysis is carried out until the surface crack penetrates the pipe wall thickness.

For the crack stability analyses, the stresses (or loads) to be considered for analysis are the primary stresses. However, for the sake of safety, the thermal expansion stresses, which are secondary stresses, are also to be considered. Torsional stresses should not be included, only the bending stresses. As far as a method of combining these stresses (or loads), the directional components, or signs, of each of the applicable loads can be considered as a means of superposition. Draft SRP 3.6.3 allows for a similar load combination approach, however, when doing so, the draft SRP plan procedures specify the application of safety factor of 1.4 on load. The draft SRP procedures allow this safety factor for the stability analysis to be decreased to 1.0 if the loads are combined on an individual absolute basis.

**7.3.4 Material Issues** – For the crack propagation analysis, corrosion fatigue crack growth rate data ( $da/dN$  versus  $\Delta K$  data) for a light water reactor environment should be used. The Paris Law (Ref. 7.4) expression, see Equation 7.7, for the fatigue crack growth rate should be used, using the Newman and Raju (Ref. 7.6) K-solution for a flat plate.

$$\frac{da}{dN} = C(\Delta K)^m \quad (7.7)$$

where,

da/dN = fatigue crack growth rate,  
 $\Delta K$  =  $K_{max} - K_{min}$ , and  
C and m = experimentally derived  
fatigue crack growth rate  
constants for a specific  
material and environment.

Values for C and m for austenitic stainless steels in an LWR environment are provided in the Japanese LBB document.

Limit-load analyses are used to predict the stability of the resultant through-wall crack. As such, only strength data are needed; there is no need for fracture toughness data. This is probably an adequate assumption when considering a stainless steel piping system fabricated with higher toughness TIG welds, but some sort of stress multiplier, such as the ASME Z-factors used in Section XI, are needed if the piping system is fabricated from lower toughness SAW or SMAW welds. The strength parameter used is the flow stress, taken to be the average of the Code specified yield and ultimate strengths at the temperature of interest:

$$\sigma_f = \frac{S_y + S_u}{2} \quad (7.8)$$

where,

$\sigma_f$  = flow stress, and  
 $S_y$  and  $S_u$  = Code specified yield and  
ultimate strength values,  
respectively, at the  
temperature of interest.

### 7.3.5 Crack-Opening-Area and Leak-Rate

**Analyses** – As part of the generalized LBB analysis procedures, the length of a through-wall crack that would cause a 19 lpm (5 gpm) leak rate must be calculated. This 19 lpm (5 gpm) leaking through-wall crack is compared with the resultant through-wall crack at the instant of surface-crack penetration, and the longer of the two crack lengths is used as the postulated crack for later use in the crack stability analysis. The basis of this 19 lpm (5 gpm) criterion is the

application of a factor of safety of 5 to the plant's leak-rate detection limit capability of 3.8 lpm (1 gpm). This factor of safety of 5 is half of that specified in the USNRC draft SRP 3.6.3 on LBB.

In Reference 7.5, a rather prescriptive method is provided for calculating this 19 lpm (5 gpm) leakage crack length. The method involves an iterative approach on crack length (c). As part of this methodology, a volumetric flow-rate analysis is conducted to calculate the flow rate per unit area of crack opening. Dividing the prescribed 19 lpm (5 gpm) leak rate by this volumetric flow rate per unit area, one can calculate the necessary crack opening area for a 19 lpm (5 gpm) leak. Two separate models are provided in Reference 7.5 for this mass, or volumetric, flow-rate analysis. A model proposed by Henry is to be used for the case where subcooled water conditions exist, while a model developed by Moody is to be used for the case of saturated water or saturated vapor.

Having established the crack-opening area necessary to sustain a 19 lpm (5 gpm) leak, the crack-opening area (COA) of a through-wall-cracked pipe subjected to the normal operating loads is calculated using the Paris-Tada method (Ref. 7.7). (As shown in Section 5 of this report, the Paris-Tada method is the most conservative of the COA analyses, especially at the higher applied load levels.) The resultant COA, based on the Paris-Tada method, is a function of the pipe geometry (R and t), the applied load or stress ( $\sigma_m$  and  $\sigma_b$ ), and the crack length (c). At this point it is a rather simple matter of iterating on the crack length so that the Paris-Tada calculated COA equals the crack area required to sustain a 19 lpm (5 gpm) leak rate.

One final point with regards to the leak-rate analyses, the prescribed methodology specifies that the inlet losses, acceleration losses and friction losses along the crack flow path be taken into account. The surface roughness value specified is 30  $\mu\text{m}$  (0.0012 inch), which is comparable to the global roughness value of 33.6  $\mu\text{m}$  (0.0013 inch) reported in Table 3.3 of Reference 7.8 for an air fatigue crack in a stainless steel pipe. No data for corrosion

fatigue cracks in stainless steel pipes were reported in Reference 7.8.

## 7.4 Republic of Korea

Leak-Before-Break has been approved in Korea for high energy piping systems inside containment<sup>27</sup> of the recently constructed pressurized water reactors (PWRs). The stated purpose behind the application of LBB for these piping systems is the removal of the dynamic effects associated with the postulated double-ended-guillotine-break from the design basis, as well as the elimination of the need for pipe-whip restraints and jet impingement shields so as to increase access for inspections. Reference 7.9 describes the procedures followed in these applications. These procedures are fundamentally based on the US Nuclear Regulatory Commission (USNRC) requirements as detailed in NUREG-1061 Vol. 3 (Ref. 7.10) and the USNRC draft SRP 3.6.3 (Ref. 7.11). However, in applying LBB for these piping systems, the Koreans imposed a number of additional special requirements and addressed a number of issues of concern not specifically addressed in NUREG-1061 Vol. 3 or the draft SRP 3.6.3. These requirements and concerns are discussed below.

### 7.4.1 Dynamic Fracture Toughness Tests –

For carbon steel piping applications, the Korean regulators required that both static and dynamic fracture toughness tests be performed. This stipulation was added to address the concern that the fracture properties of carbon steel piping materials are known to decrease as the loading rate increases at PWR operating temperatures. This phenomenon has been attributed to dynamic strain aging effects, as discussed previously in Section 5.3.3.3.

### 7.4.2 Thermal Stratification Considerations –

The pressurizer surge line at the Yong Gwang Nuclear Units 3 and 4 (YGN 3&4) barely satisfied the required margin of 2 on crack size when the thermal stratification loads were added

to the normal and faulted loads. As a result, the following additional requirements were stipulated prior to the approval of LBB for the surge lines in these plants:

- The thermal stress due to thermal stratification had to be considered in the piping design stress analysis and had to be considered as a special load in the LBB evaluation.
- The effects of thermal stratification in the surge lines had to be measured during the hot function test of these units to verify the conservatism of the assumptions used in the calculation of the thermal stresses. Intensive measurements of the temperature distribution and piping deflections were made during the start up of YGN Unit 3. The results from these measurements showed that the assumptions used in the thermal stress calculations were indeed conservative.

### 7.4.3 Thermal Striping in the Pressurizer Surge Line –

Because thermal striping in the surge line has the potential to cause fatigue damage, and it was felt that such a crack might go undetected during in-service inspections (ISI), the applicant was required to evaluate the fatigue behavior of a small crack due to thermal striping. The behavior of a crack located in the thermal striping zone in a thermally stratified pipe was numerically investigated. The results of that analysis showed that the behavior of such a crack would depend strongly on the oscillation frequency and the heat transfer coefficient. However, the crack was not expected to grow because the magnitude of the thermal striping stresses is highest on the inside surface and attenuates rapidly through the wall thickness.

### 7.4.4 Water/Steam Hammer in the Main Steam Line –

The applicant of the YGN Units 3 and 4 submitted an application for LBB for the main steam lines. However, that application was not accepted for two main reasons. For one, the required margins could not be satisfied when the water/steam hammer loads were considered. Secondly, for the carbon steel pipe material used for these steam lines, there were a number of uncertainties in the material fracture properties

<sup>27</sup> Primary coolant lines, pressurizer surge lines, safety injection system lines, and shutdown cooling lines

that had to be considered, e.g., dynamic load effects, cyclic load effects, weld/HAZ effects, etc. The necessary data to address each of these concerns did not exist at the time of the application.

#### **7.4.5 Nozzle/Pipe Interface Considerations –**

In some of the LBB analyses considered, the highest stress locations were at the nozzle-to-pipe interface location at the terminal end. At these locations there are asymmetries due to both geometry and material considerations. The concern was that these asymmetries may affect the crack-opening behavior. The effect of asymmetry on the crack-opening behavior, and resultant leak rate, was numerically investigated. The results showed that the traditional simplified finite element model, in which the asymmetry due to geometry and material properties was not considered, still resulted in a conservative assessment when compared with the 3D model in which this asymmetry was considered.

#### **7.4.6 Leak-Rate Detection Limit Capability -**

An additional stipulation on LBB imposed in these applications was that it was not acceptable to use a 1.9 lpm (0.5 gpm) leak-rate detection limit capability with a margin of 10 in order to reduce the size of the postulated leakage crack even though the leak-rate detection system has the detection capability of 1.9 lpm (0.5 gpm). This is more restrictive than the criteria imposed in the draft SRP 3.6.3. Draft SRP 3.6.3 merely stipulates a margin of 10 on leak-rate detection limit capability, regardless of the detection limit capability. Numerous applications have been approved in the US in which the leak-rate detection limit capability was reported to be 1.9 lpm (0.5 gpm).

### **7.5 Russia**

Some of the early generation WWER-440/230 nuclear power plants (NPPs), built in Russia and some of the Eastern Block nations, were designed and built with emergency core cooling systems (ECCS) which were able to cope with only a limited scope of breaks, and were also designed and built without an appropriate containment system. As a result, a large pipe break in some of these plants would result in the

loss of two main safety functions: cooling of the fuel and containment of the radioactive material. Therefore, the applicability of LBB was identified as an issue of major safety significance for their continued operation. Successful application of LBB was a must to justify their continued operation. LBB was considered as the only feasible approach for providing for the reduction of the probability of the primary breaks that these Russian plant designs are not currently able to cope with.

In 1994, the International Atomic Energy Agency (IAEA) published some guidelines for the application of LBB to these types of plants (Ref. 7.12). The LBB guidance/guidelines provided by IAEA are similar in nature to those used in the US. Basically, LBB can be applied to WWER-440 Model 230 type reactors if it can be demonstrated that sufficient margins exist between a through-wall flaw of a size that can be reliably detected by the plants leakage detection systems at normal operating conditions and a through-wall flaw of a critical size at the faulted loading conditions.

As is the case with the US procedures, the IAEA guidelines postulate the existence of leaking through-wall cracks at discrete locations for analysis along the piping system. At these locations, it must be demonstrated that this leaking crack can be detected by the plant's leakage detection systems. Furthermore, if undetected, this leaking through-wall crack would be of such a size that it would not grow in an unstable manner under the faulted loading conditions (SSE loadings) specified for the plant. The IAEA guidelines specify the same margins (i.e., 10 on leak-rate detection limit capability, 2 on crack size, and 1 or 1.4 on loads [depending on the method of load combination] for the crack stability analysis) as incorporated in the draft SRP 3.6.3. In addition, as is the case with the draft SRP, the IAEA guidelines require that it be demonstrated that fatigue, corrosion, and stress corrosion cracking not be active degradation mechanisms for the piping system under consideration.

At about the same time the IAEA was publishing their guidelines for LBB for WWER-

440/230 plants, engineers in Russia were attempting to apply LBB to the main coolant loop piping systems for WWER-1000 plants (Ref. 7.13). Besides the obvious desire for a higher safety level, these engineers were attempting to build a case for the abandonment of a number of the costly protective measures needed to mitigate the consequences of a hypothetical DEGB in a high-energy piping system. The procedures they followed were similar to those advocated by the IAEA (as well as the USNRC), except that they also stipulated the evaluation of a postulated part-through surface crack (0.1t deep and 0.5t long, where "t" is the pipe wall thickness) for fatigue crack growth and surface crack instability analyses. For this particular application, they concluded that the surface crack growth due to fatigue could be neglected, and that the surface crack would not grow unstably (for all crack lengths) as long as the crack depth was less than 50 percent of the pipe wall thickness, and would not grow unstably for cracks less than 90 degrees, as long as the crack depth was less than 75 percent of the pipe wall thickness. Overall, they concluded that LBB could be applied to the main coolant loop piping of WWER-1000 designs.

## 7.6 United Kingdom

In the United Kingdom, Chapter III.II of the R6 document (Ref. 7.14) is one of the documents that deals with the subject of LBB. British Standards document BS7910 and its predecessor PD6493 are two others. The technical details of the LBB procedures in each of these documents are essentially the same. In many instances, the wording is identical. Unlike some of their counterparts in other parts of the world (e.g., the draft SRP 3.6.3 procedures in the United States), the BS7910 and R6 procedures are generic procedures applicable to a variety of industries, not just nuclear. Both BS7910 and R6 set out two alternative methodologies for making an LBB assessment and recommend methods for carrying out each. The first method common to both is a simplified detectable leakage approach based on a postulated through-wall crack, much in the motif of the USNRC draft SRP 3.6.3 procedures. The second method is a full LBB

procedure that sets out a more rigorous approach, that considers the development of a part penetrating defect.

**7.6.1 Detectable Leakage Approach** – The simplified type of LBB argument in both BS7910 and R6 aims to demonstrate that a leaking through-wall crack is detectable long before it grows to a critical length. This type of detectable leakage argument is the type of assessment made in a USNRC NUREG-1061 Vol. 3 or draft SRP 3.6.3 type of LBB analysis. The starting point for this type of assessment is to postulate the existence of a full-penetrating crack, and demonstrating that, should that crack arise, the leakage would be detectable well before the crack grew to a critical length.

While the detectable leakage approach in BS7910 and R6 is fundamentally similar to the USNRC LBB procedures in NUREG-1061 and draft SRP 3.6.3, there are some fundamental differences of note. Because NUREG-1061 is specifically intended for light water reactor piping, some of its recommendations and safety margins are rather specific. On the other hand, in keeping with the basic philosophy of BS7910 and R6, margins are left to the judgment of the user with due regard to the methodology used, the assumptions made, the sensitivity studies conducted, and the specific application.

Implicit in this type of analysis is the assumption that once a through-wall crack develops that results in a leak of size equal to the minimum detectable leakage by the plant's leakage detection systems, that such a leaking crack will be detected almost immediately. However, the authors of BS7910 and R6 recognized the fact that for certain applications, the piping system under consideration is only monitored at set intervals, perhaps by personnel on scheduled inspection tours. As such, these documents stipulate that allowances must be made for any fatigue or creep crack growth that might occur between the instant the crack first penetrates the pressure boundary with a detectable leak rate and the time of the next scheduled inspection.

**7.6.2 Full Leak-Before-Break Approach** – Whereas the starting point for the detectable

leakage approach is a postulated through-wall crack, the starting point for the full LBB approach is usually a surface defect that has yet to break through the pipe or vessel wall. In order to make such an assessment, it is necessary to show that:

- the defect will penetrate the pressure boundary before it can lead to a catastrophic failure; and
- the resulting through-wall crack leaks at a sufficient rate to ensure its detection before it grows to a critical length at which time a catastrophic failure occurs.

In order to carry out such an assessment, several steps are involved. First, the defect must be characterized as a surface crack or through-wall crack, and the mechanisms by which it can grow identified. The next step is to assess the crack shape development as the surface crack grows through the pipe wall in order to calculate the length of the through-wall crack formed as the initial defect penetrates the pressure boundary. Where crack growth occurs by fatigue, methods are provided in the documents to predict the increase in both the depth and length of the defect. Procedures are also provided for the treatment of creep crack growth. The crack length at breakthrough is then in turn compared with the critical crack length of a fully-penetrating crack. Finally, it is necessary to estimate the crack-opening area and the associated leak rate of fluid from the crack, and whether or not the leak will be detected by the plant's leakage detection system before the crack grows to a critical length.

**7.6.3 Crack Opening Area Analyses – R6** provides a relative simple set of closed-form equations for estimating the crack opening area (A) of a through-wall crack in a pipe if through-wall bending stresses are absent or can be ignored, see Equation 7.9.

$$A = \alpha(\lambda) \frac{\pi P_m (2c)^2}{2E} \quad (7.9)$$

where,

$P_m$  = membrane stress,  
 $c$  = half crack length,  
 $E$  = elastic modulus, and  
 $\sigma_f$  = flow stress.

where,

$\alpha$  is a correction factor to account for shell bulging, i.e.,

$$\alpha(\lambda) = 1 + 0.1\lambda + 0.16\lambda^2 \quad (7.10)$$

for axial cracks in cylinders, and

$$\alpha(\lambda) = [1 + 0.117\lambda^2]^{1/2} \quad (7.11)$$

for circumferential cracks in cylinders,

where,

$$\lambda = \text{shell parameter} = [12(1 - \nu^2)]^{1/4} c / (Rt)^{1/2}$$

These expressions were derived using thin-walled, shallow-shell theory, and are strictly valid only for pipes with  $R/t \geq 10$ , and the crack length does not exceed the least radius of curvature of the shell.

These closed-form expressions could be used in a Level 1 type LBB analysis in the prediction of the postulated leakage crack size. On the surface they appear to be somewhat easier to use than the empirically-derived influence functions specified for Level 1 type analyses, see Appendix A. In addition, they may be more theoretically sound due to the fact that they are based on readily recognized shell theory.

These expressions are generally conservative as long as the through-wall bending stresses are negligible. It is recognized in the British documents that through-wall bending stresses can induce crack face rotations that reduce the effective crack opening area. If complete crack closure occurs, a case for LBB cannot be made. In such a case, it may be necessary to invoke a more complicated Level 2 type analysis. Significant through-wall bending stresses may

be associated with thick-walled shells under internal pressure loading, or be associated with weld residual stresses, geometric discontinuities, or thermal gradients. A series of references that may be useful in estimating the elastic crack-face rotations in simple geometries are provided.

It is also recognized that if the crack is close to a significant geometric constraint (e.g., a pipe nozzle intersection), then local effects can influence the amount of crack-opening area. This is the same effect recognized during the IPIRG program referred to as the restraint-of-pressure-induced bending effect on crack-opening displacements. The impact of this effect on LBB analyses is currently being investigated as part of the BINP program. Again, if such a restraint exist, then the user would most likely need to invoke a Level 2 type analysis in lieu of a Level 1 type analysis.

For cracks in complex geometries (such as elbows), reference is made of the need to resort to finite element analyses to obtain an accurate crack-opening-area assessment. Until recently, this was one of the few possible means of estimating the crack opening area of a through-wall crack in an elbow. However, recently, Battelle as part of the USNRC LBB Reg. Guide and BINP programs developed a finite-element based J-estimation scheme that can be used for such assessments. (See Appendix E for a detailed description of this analysis routine.) Also, lots of work in this area has been conducted in India (Refs. 7.15 and 7.16).

Finally, it is recognized in the British documents that off-center loads and crack-face pressure can influence the crack-opening-area predictions. With regards to the crack-face pressure effect, it is recommended that 50 percent of the internal pressure should be added to the membrane stress on the crack face. This value should then be reassessed when undertaking the leakage calculations, and the results iterated, if necessary.

**7.64 Leak-Rate Calculations** – The calculation of the leak rate through a crack is a complex problem involving the crack geometry, flow path length, friction effects, and the thermodynamic

conditions of the fluid through the crack. For two-phase flow, references are made in the British documents to both the PICEP (Ref. 7.17) and SQUIRT (Ref. 7.18) leak-rate codes as being state-of-the-art codes for predicting the leak rate through a crack. These British documents also recognize friction effects, as described by local crack morphology parameters, as being an important consideration in any leak-rate analyses. These parameters vary with the type of cracking mechanism. In addition, at least one of the British documents comments that consideration should be given to the potential for flow reduction mechanisms due to particulate blocking or plugging, but offers no firm advice as how to assess such effects.

## 7.7 Canada

Ontario Hydro has developed an LBB approach for application to the large diameter heat transport piping for the Darlington nuclear generating stations, as an alternative to the provision of pipewhip restraints. This approach, which is described in detail in Reference 7.19, has been applied to pipe sizes that are equal to or greater than 21 inches in diameter. A comprehensive and systematic review of pipe failure mechanisms is considered the first important step in establishing the role and applicability of the LBB concept. The intent, at this first step, is to provide assurance that adequate protection from failures attributable to each relevant potential failure mechanism is provided for, or, that sufficient provisions are incorporated into the program to preclude the occurrence of failures from any mechanism evaluated as being credible. The failure mechanisms assessed included: stress corrosion cracking, corrosion, erosion and erosion-corrosion, cavitation and cavitation accelerated corrosion, conventional and corrosion-assisted fatigue, material aging, external effects (such as fretting, impact, pipewhip, and snubber malfunctions) and excessive loading. Based on this assessment, it was concluded that fatigue was the only mechanism that could be active in these piping systems.

The Ontario Hydro LBB approach incorporates assessments at several levels to provide

assurance against catastrophic rupture. As part of the normal design process for Class 1 nuclear piping, stress analysis are performed to show that the piping system can accommodate the defined service loads with large margins of safety. At a second level, it is further demonstrated that the largest part-through surface flaw that can be detected, will not grow through the pipe wall during its design life, and that such flaws are stable for the maximum credible piping loads. At a third level of assurance, application of elastic-plastic-fracture-mechanics (EPFM) methods are used to show that a postulated leaking through-wall crack will not extend in an unstable manner, and that the leakage rate from that postulated crack is well within the capabilities of the leakage detection systems.

For the evaluation of crack stability, the J-integral/tearing modulus ( $J/T$ ) approach was used. The finite element program ABAQUS was used to perform the EPFM analyses. The analyses were performed not only for circumferentially-oriented cracks at girth welds in straight pipe runs, but also for longitudinally-oriented cracks in fittings, namely, elbows, tees, and branch connections. Extensive material property data were developed from actual large diameter piping, forgings, welds, and heat-affected-zones for the Darlington nuclear generating station.

With respect to leakage, operating policies in place at similar Ontario Hydro facilities require immediate shutdown actions to be initiated upon detection of a 0.5 kg/s (1.1 lbm/s) leak rate from the heat transport system<sup>28</sup>. Based on operating experience, leak rates from the heat transport system significantly less than 0.05 kg/s (0.11 lbm/s) are within the capability of the leakage detection systems in the current design. Thus, there is at least a margin of 10 between detection capability and required action, similar to that in the USNRC draft SRP procedures. A special

---

<sup>28</sup> For the operating pressure assumed in Ontario Hydro's analysis [9.6 MPa (1,400 psi)], this mass leak rate of subcooled water of 0.5 kg/s equates to a volumetric leak rate of 43 lpm (11 gpm).

purpose leak rate code (LEAK RATE) was used to make the leak rate calculations. The crack opening displacements (COD) used in this code are calculated by assuming that only the normal operating pressure in the pipe acts to open the crack, i.e., crack opening due to the bending moments is not accounted for. This approach assures margin on leak rate, and thus provides additional confidence that the overall assessment is conservative. Other crack-opening-displacement aspects that might affect the leak rate calculations that were considered by Ontario Hydro included: crack lipping, surface roughness, and crack face pressure. Crack lipping is a bulging related effect in which the presence of a through-wall crack in a shell structure results in a redistribution of the stresses which results in a relative rotation (lipping) of the two crack faces. The results from studies conducted as part of Reference 7.19, showed that the crack opening area at the outside surface is 50 percent larger than that at the inside surface. Furthermore, it was shown that the leakage rate corresponding to the actual crack geometry was 25 percent larger than when lipping was not accounted for, i.e., when the middle surface crack opening area was used in the analysis. Thus, not accounting for this lipping behavior results in a conservative prediction of the COD from an LBB perspective.

With regards to surface roughness, it was shown as part of Reference 7.19 that the assumed surface roughness can significantly influence the calculated leakage rate. It was shown that an order of magnitude change in surface roughness results in a 50 percent change in the calculated leakage rate.

Finally, Reference 7.19 provides some very useful insights as to the effects of crack face pressure on the crack-opening-displacements, and thus the calculated leakage rates. As stated earlier, the pressure acting on the faces of the through-wall crack will tend to open the crack, which will increase the crack opening area and associated leak rate. Ignoring this effect will result in a conservative assessment of LBB. However, for cases that barely fail to satisfy LBB, accounting for this effect may be all that is needed to successfully demonstrate LBB.

Unfortunately, no concrete means of accounting for this effect have been proposed, until now. However, Reference 7.19 proposes a simple equation to correct for this effect, see Equation 7.12:

$$\frac{COD_{cf}}{COD_{wo}} = \left( 1 + \frac{P_{cf}}{\sigma} \right) \quad (7.12)$$

where,

- COD<sub>cf</sub> = crack opening displacement corrected for the crack face pressure,
- COD<sub>wo</sub> = crack opening displacement not accounting for crack face pressure,
- P<sub>cf</sub> = pressure acting over the crack faces, and
- σ = far field component of the membrane stress perpendicular to the crack plane.

Comparisons were made between this simple correction factor (Equation 7.12) and finite element results, and it was found that Equation 7.12 slightly underpredicted (1 to 7 percent) the finite element calculated corrected COD term. It was also shown that this effect (crack face pressure) could result in an additional 25 to 40 percent in margin on COD, depending on the component geometry (straight pipe versus elbow), crack orientation, and crack size. Consequently, this may be an effect worth considering if LBB cannot be demonstrated using the more conventional LBB methods.

### 7.8 Sweden

In corresponding with Dr. Bjorn Brickstad, the former IPIRG TAG representative from Sweden, SKI (the Swedish Inspectorate) has recently issued a report on the subject of LBB (Report Number SKI-PM 98:39, 2000-03-27, in Swedish). SKI now allows LBB in accordance with the draft SRP 3.6.3 procedures with the following amendments:

- Weld residual stresses should be accounted for when determining the shape of the crack and when evaluating the leak rate.

- There should be strict requirements for leak rate detection and limiting values of detected leak rates above which the plant has to shut down.
- In the fracture mechanics evaluation, the SSE load should be replaced with “the worst emergency faulted load” if such a load exists that is worse than the SSE load.
- The pipe system under consideration for LBB should have been previously subjected to a full volumetric inspection with a qualified procedure, either after construction or later as part of an in-service inspection (ISI).

According to Dr. Brickstad, there are other amendments to consider, but they are of less importance.

### 7.9 References

- 7.1 “A16: Guide for Defect Assessment and Leak Before Break Analysis,” Third Draft Report DMT 96.096, December 1995.
- 7.2 Bartholome, Gunther, “German Leak-Before-Break Concept – Description of German LBB Procedures, Practices, and Applications,” *International Journal of Pressure Vessel and Piping*, Vol. 71, pp 139-146, 1997.
- 7.3 Wellein, R., and Preußer, G., “State of Engineering of the Leak-Before-Break Procedures in Germany,” 7<sup>th</sup> German-Japanese Joint Seminar, MPA-Stuttgart, September 1997.
- 7.4 Paris, P. C., and Erdogan, F., “A Critical Analysis of Crack Propagation Laws,” *Journal of Basic Engineering*, Vol. 85, pp 528-534, 1960.
- 7.5 Kyokai, N., and Bukai, G., “Technical Guidelines for Protection Design Against Postulated Piping Failures in Nuclear Power Plants,” JAEG 4613-1998, December 1998.

7.6 Newman, J. C., and Raju, I. S., "An Empirical Stress-Intensity Factor Equation for the Surface Crack," *Engineering Fracture Mechanics*, Vol. 15, No. 1-2, pp 185-192, 1981.\*

7.7 Paris, P. C., and Tada, H., "The Application of Fracture Proof Design Methods Using Tearing Instability Theory to Nuclear Piping Postulating Circumferential Through-Wall Cracks," NUREG/CR-3464, September 1983.

7.8 Rahman, S., and others, "Probabilistic Pipe Fracture Evaluations for Leak-Rate Detection Applications," NUREG/CR-6004, April 1995.

7.9 Lee, J. B., and Choi, Y. H., "Application of LBB to High Energy Pipings of a Pressurized Water Reactor in Korea," *Nuclear Engineering and Design*, Vol. 190, pp 191-195, 1999.

7.10 "Report of the U. S. Nuclear Regulatory Commission Piping Review Committee – Evaluation of Potential for Pipe Breaks," NUREG-1061, Vol. 3, November 1984.

7.11 "Leak-Before-Break Evaluation Procedures," draft Standard Review Plan 3.6.3, August 1987.

7.12 "Guidance for the Application of the Leak Before Break Concept: Report of the IAEA Extrabudgetary Programme on the Safety of WWER-440 Model 230 Nuclear Power Plants," IAEA-TECDOC-774, November 1994.

7.13 Kiselev, V., A., and others, "Application of Leak-Before-Break Concept to Integrity and Safety of PWR Primary Piping with WWER 1000," *Nuclear Engineering and Design*, Vol. 151, pp 409-424, 1994.

7.14 Milne, I., and others, "Assessment of the Integrity of Structures Containing Defects," Nuclear Electric Report R/H/R6, Revision 3 with updates to June 2000.

7.15 Rastogi, R., Bhasin, V., and Kushwaha, H. S., "Fracture Assessment of Straight Pipes and Elbows with Through-wall Cracks: Using

R-6," Paper G05/5, Division G, *Transactions of the 14<sup>th</sup> International Conference on Structural Mechanics in Reactor Technology*, August 1997.

7.16 Chattopadhyay, J., and others, "Limit-Load Analysis of Straight Pipes and Elbows with Through-Wall Cracks," Paper G05/6, Division G, *Transactions of the 14<sup>th</sup> International Conference on Structural Mechanics in Reactor Technology*, August 1997.

7.17 Norris, D., and others, "PICEP: Pipe Crack Evaluation Program," EPRI Report NP-3596-SR, 1984.

7.18 Paul, D. D., and others, "Evaluation and Refinement of Leak-Rate Estimation Models," NUREG/CR-5128, Rev. 1, June 1994.

7.19 Nathwani, J. S., and others, "Ontario Hydro's Leak Before Break Approach: Application to the Darlington (CANDU) Nuclear Generating Station A," *Nuclear Engineering and Design*, Vol. 111, pp. 85-107, 1989.

## 8 SUMMARY AND CONCLUSIONS

The key outcome of this program was the development of the proposed three-tiered approach to LBB. It is envisioned that this tiered approach will form the basis for the development of a future NRC Regulatory Guide for LBB. In this section, this tiered approach will be summarized along with some of the key conclusions supporting the development of this approach. While this section offers no new revelations from what has been presented in the previous sections, an attempt is made here to synthesize the results and conclusions drawn as part of this program so that the reader has a clearer understanding of how this tiered approach is to be implemented and how it is an improvement over the existing draft SRP 3.6.3 approach. Note, some elements of the overall LBB assessment, e.g., the demonstration of the accuracy of the leak-rate and fracture codes, the definition of the locations for assessment, and the subcritical flaw growth analysis, have not been addressed here. The focus of the tiered approach is on establishing the size of the postulated leaking crack at the normal operating load conditions and the critical crack size analyses at the transient load conditions.

### 8.1 Summary of the Level 1 Approach to LBB

The Level 1 methodology was developed to offer the applicant a simple, yet conservative, methodology by which they could apply for LBB without having to utilize some of the advanced leak-rate or fracture mechanics codes. In lieu of the use of leak-rate codes for predicting the postulated leakage flow size, a series of simple, empirically-derived influence functions were developed for predicting the crack-opening displacements (COD), and in turn the postulated leakage size flow at the normal operating conditions. (Alternatively, a series of simple, closed-form shell-theory based solutions are available for predicting the postulated leakage flow size.) Conservatism has been built into these influence functions through their empirical development and their use of the Paris/Tada COD expressions as their technical

basis. As part of this study, the Paris/Tada COD analysis was found to be the most conservative method for predicting COD from a LBB perspective when compared with finite element analyses. In lieu of the use of some of the advanced fracture mechanics codes (J-estimation schemes, J/T analyses, or finite element analyses) for predicting the critical crack sizes or the crack stability, a simple modified limit-load analysis was used to make the fracture predictions for Level 1.

The Level 1 methodology incorporates Level 1 specific screening criteria to preclude its use outside its realm of applicability. For instance, the Level 1 specific screening criteria precludes the use of Level 1 to piping systems for which the thermodynamic conditions of the water are not subcooled and to small diameter piping for which restraint of pressure-induced bending effects may restrict the amount of crack-opening, thus adversely affecting the postulated leakage crack size analysis from an LBB perspective.

Furthermore, the Level 1 methodology was designed such that piping systems that had readily passed LBB using the existing draft SRP 3.6.3 methodology (e.g., main coolant loop piping in PWRs<sup>29</sup>), would pass the Level 1 criteria as well. As part of the evaluation of the Level 1 method, it was found that the margin on crack size (i.e., critical crack size to postulated leakage crack size) for a cross over leg in a PWR was 2.5 to 3.25 depending on whether one used the empirically-derived influence functions to estimate the postulated critical crack size or the closed-form solutions included in the Level 1 methodology. These values easily exceed the margin of 2 on crack size typically required for an LBB assessment.

---

<sup>29</sup> New LBB applications for main coolant loop piping systems which contain Inconel 82/182 bimetal welds are currently not being approved due to the uncertainties associated with the PWSCC cracking mechanism.

Further details of the Level 1 approach can be found in Chapter 6 and Appendix A of this report.

## 8.2 Summary of Level 2 Approach to LBB

If the piping system fails to satisfy either the Level 1 acceptance criteria or any of the elements of the Level 1 specific screening criteria, the applicant's next logical step would be to try to demonstrate LBB using the proposed Level 2 approach. As an illustrative example, when a Level 1 analysis was applied to an actual surge line (using data gleaned from one of the LBB submittals), it was found that the Level 1 margin on crack size was less than 2.0 (i.e., the critical crack size was less than twice the postulated leakage crack size). As such, this piping system failed to meet one of the acceptance criteria for a Level 1 application<sup>30</sup>. However, when this same piping system was analyzed using the Level 2 criteria, it was found that the resultant margin on crack size was approximately 3, which easily satisfies this element of the existing acceptance criteria.

It is envisioned that the vast majority of future LBB applications will be based on this Level 2 approach to LBB. The Level 2 approach is structured in the motif of the existing draft SRP 3.6.3 procedures, except it will incorporate a number of the recent applicable enhancements in the technology that have arisen from the recent NRC-initiated research. These enhancements include:

- the use of the best leak rate codes, with the most appropriate crack morphology parameters. As part of this study it was shown that the original GE/EPRI COD analysis resulted in a reasonably accurate, yet conservative prediction of the COD from an LBB perspective when compared with finite element analyses. Furthermore, it was shown that the choice of crack morphology

<sup>30</sup> Assuming that the NRC invokes the same, or greater margins of 2 on crack size and 10 on leak rate detection for Level 1 as currently stipulated in the draft SRP 3.6.3 LBB assessment procedures.

parameters could have a significant impact on the postulated leakage crack size. In comparing an applicant's submittal in which they used their own proprietary leak rate code and a relative smooth surface roughness (300 microinches) with analysis conducted as part of this program in which the SQUIRT leak-rate code (using the original GE/EPRI COD analysis) was used with the statistically-determined crack morphology parameters from NUREG/CR-6004 (Ref. 8.1), it was found that the applicant's approach resulted in a postulated leakage crack size that was almost a factor of 2 shorter than that obtained from the analysis conducted as part of this program. In related analyses, it was shown that a significant contributor to this underprediction was their choice of surface roughness. One of the main conclusions drawn as a result of this study was that for a Level 2 approach, the original GE/EPRI COD analyses along with the statistically-determined crack morphology parameters from NUREG/CR-6004 should be used in estimating the postulated leakage size crack.

- the use of most accurate fracture mechanics analyses for predicting the critical crack size at the transient load conditions. For most applications, this implies the use of J-estimation schemes; such as those incorporated in the fracture analysis code NRCPIPE. As part of past studies, it was shown that of these J-estimation schemes, the LBB.ENG2 method tended to be the most accurate when compared with full-scale experimental data, while the GE/EPRI method was slightly more conservative. Either method would be acceptable for use in a Level 2 critical crack size assessment.
- accounting for the increased understanding of the material behavior of nuclear grade pipe steels. Some of the material behavior effects, that have been identified and studied since the initial publication of the draft SRP 3.6.3 on LBB, that need to be considered in a Level 2 assessment include:
  - o load history effects, such as dynamic strain aging effects on ferritic steels at LWR temperatures,

- o aging mechanisms for both cast stainless steels and stainless steel welds,
- o fusion line toughness concerns,
- o bimetallic welds, including the impact of primary water stress corrosion cracking on the LBB behavior for such welds,
- o toughness anisotropy of nuclear grade ferritic pipe steels, and
- o methods for extrapolating J-R curve fracture toughness data from small-scale laboratory specimens.
- accounting for a better understanding of the effects of restraint of pressure induced bending, weld residual stresses, and crack face pressure on the crack opening displacement (COD) predictions used in the postulated leaking crack size analysis.
- accounting for a better understanding of the role of secondary and torsional stresses on the fracture behavior of cracked piping systems. Current practice minimizes the role secondary stresses may play in the fracture process. However, recent research as part of the IPIRG and BINP programs has shown that secondary stresses do contribute to the fracture process, at least for the case where the failure stress is predicted to be less than the yield strength of the material, and should probably be considered like primary stresses. If the failure stress is above yield, secondary stress may also have to be considered, but probably in some nonlinear fashion. In addition, current practice does not explicitly account for torsional stresses. However, torsional stresses are potentially problematic, especially for ferritic piping systems where the low-toughness orientation (due to anisotropy effects) may be aligned with the maximum stress direction in a piping system subjected to high torsional stresses. An analysis method has been developed that accounts for the torsional stresses using an effective bending stress approach in which the torsional stresses are combined with the bending stresses using a Von-Mises type relation.

Further details of this Level 2 approach can be found in Chapter 6 and Appendix B of this report.

If after accounting for all of these enhancements (some which promote LBB and some which are detrimental to LBB) LBB cannot be demonstrated using a Level 2 type analysis, a Level 3 analysis may be used.

### 8.3 Summary of Level 3 Approach to LBB

Level 3 is the most complex and accurate of the three levels of assessment. It is reserved for those cases where one cannot demonstrate LBB using a Level 2 approach. For a Level 3 analysis, the same procedures will be followed as for Level 2 in defining the postulated leakage crack size. The difference between the two levels of assessment rests in the critical crack size analysis for the transient load conditions. Whereas Level 2 analyses use linear elastic stresses, possibly extracted from a design stress report, the Level 3 analyses attempt to take benefit of the inherent margins one might realize by using a nonlinear analysis. The inherent margin comes from the fact that linear elastic calculated stresses are used in the Level 1 and 2 methodologies with nonlinear fracture mechanics analysis. The nonlinear stress analysis for Level 3 reduces the applied moments and provides additional damping for seismic loading, as well as possible reductions of secondary stresses. It is envisioned that this nonlinear analysis can take one of three forms.

- o an uncracked nonlinear pipe analysis,
- o a linear pipe analysis with nonlinear crack behavior, and
- o a nonlinear pipe analysis with nonlinear crack behavior.

As part of this program, a test case analysis of a surge line was conducted in which an additional 20 to 30 percent in crack size margin was realized by incorporating nonlinear pipe analysis with nonlinear crack behavior.

Further details of this Level 3 approach can be found in Chapter 6 and Appendix C of this report.

#### **8.4 Margins to be Used in the Tiered Approach to LBB**

One critical element of any LBB assessment that has not been addressed in this report is that of applied margins. The margins in the existing draft SRP 3.6.3 are 2 on crack size or  $\sqrt{2}$  on stress<sup>31</sup> and 10 on leak rate detection capability. For the Level 1 approach, which does not include many of the recent enhancements in the technology, these same margins of 10 on leak rate and 2 on crack size or  $\sqrt{2}$  on stress may be used. However, for the Levels 2 and 3 approaches, which do include these recent enhancements, it may be possible to apply different margins. However, this decision rests with the NRC staff, with possible input from its contractors, and will resolve itself during the publication of the future Regulatory Guide on LBB. At this time it is premature to speculate as to what applied margins may be used.

#### **8.5 References**

8.1 Rahman, S., and others, "Probabilistic Pipe Fracture Evaluations for Leak-Rate-Detection Applications," NUREG/CR-6004, April 1995.

---

<sup>31</sup> In draft SRP 3.6.3, for stress components combined in an absolute manor, the safety factor on stress can be reduced from  $\sqrt{2}$  to 1.0.

## APPENDIX A

### LEVEL 1 LBB PROCEDURES

The Level 1 Leak-Before-Break (LBB) procedures will be the simplest of the three levels of LBB procedures, requiring the least amount of information/data to apply. The margins associated with the Level 1 LBB procedure may be different than those prescribed for the Level 2 or 3 procedures. The Level 1 approach was developed such that piping systems that easily passed LBB using the draft SRP 3.6.3 procedure should be able to pass this Level 1 LBB procedure. If a piping system fails to pass the Level 1 LBB procedure, the applicant can apply either a Level 2 or 3 LBB procedure in order to demonstrate LBB.

Whereas a Level 2 or 3 LBB procedure may require the use of a detailed leak-rate code for estimating the postulated leakage size crack and a detailed fracture mechanics code or finite element analyses for calculating the allowable moments or stresses, the Level 1 LBB procedure employs a series of simple algebraic equations to predict:

- the leakage area for a prescribed leak rate,
- the crack-opening displacement,
- the crack length, and
- the allowable moment or stress.

The key elements of the Level 1 LBB procedure are described next.

#### A.1 Key Elements of Level 1 LBB Procedure

Upfront of all three LBB procedures will be a general screening criteria to eliminate those piping systems for which LBB is not applicable,

e.g., piping systems susceptible to high undefined stresses (i.e., water hammer), or susceptible to cracking mechanisms causing long surface cracks (e.g., stress corrosion cracking). If a piping system passes this general screening criterion, then the user may elect to apply this Level 1 LBB procedure. The key elements of this Level 1 LBB procedure are:

- Data input requirements,
- Definition of critical locations for analysis,
- Prescribed safety factors,
- Simple algebraic equations for calculating the postulated leakage crack length,
- Level 1 specific screening criteria,
- Level 1 fracture analysis, and
- Level 1 LBB assessment.

Each of these elements is described in more detail in the subsequent sections.

#### A.1.1 Data Input Requirements

The data typically required to apply a Level 1 LBB procedure are shown in Table A.1. As a point of reference, Table A.1 also includes some of the typical data requirements for a Level 2 or 3 LBB procedure. Comparing the data requirements, the relative simplicity of the Level 1 approach is apparent when compared with either the Level 2 or 3 LBB procedure.

### A.1.2 Definition of Critical Locations for Analysis

In applying a Level 1 LBB analysis to a subject piping system it will be necessary to make the necessary assessments at a number of critical locations along the piping system. At a minimum, each of the following locations should be considered in a Level 1 LBB analysis:

- (a) the location with the highest normal operating stresses (this is the location where a crack is more likely to occur),
- (b) the location with the highest safe shutdown earthquake (SSE), or transient, stresses,
- (c) the location with the highest ratio of normal operating plus SSE stress (N+SSE) to normal operating stresses (N),
- (d) any other locations that have a material toughness with a J-R curve that is less than 75 percent of the J-R curve for the above material locations.

Normally, weld joint locations are selected as locations to be explicitly evaluated. Both the material properties of the weld material and the base material should be evaluated at these locations (particularly where cast stainless steel pieces are used). Also, it is important to consider the case where the high stress occurs at a low toughness location.

### A.1.3 Prescribed Margins

With any of the three levels of LBB procedures there are certain values that must be prescribed by the NRC, most notably factors of safety on crack size and leak-rate detection capability. For the existing criterion in draft SRP 3.6.3, these prescribed factors of safety are typically 10 on leak rate and 2 on crack length (Ref. A.1). The actual factors of safety of all three levels of assessment will need to be set by the NRC during the preparation of the Regulatory Guide on LBB.

### A.1.4 Postulated Leaking Crack Length Determination

The determination of the maximum postulated leaking crack length for the Level 1 LBB procedure is one of the major differences between the Level 1 LBB procedure and the Level 2 and 3 LBB procedures. (The other major differences are the fracture analysis used and potentially the factors of safety applied.) Instead of employing detailed computer codes for calculating crack-opening areas, crack-opening displacements, and postulated leakage crack lengths (as might be the case for a Level 2 or 3 analysis), the Level 1 LBB procedure employs a series of simple algebraic equations, that incorporate pre-established influence functions, to make these types of assessments. These influence functions have been established empirically through a series of sensitivity calculations in which each of the parameters that may have influenced the postulated leakage crack length were systematically varied while holding the other parameters constant.

In order to determine a postulated leakage crack length for the Level 1 analysis, one needs to calculate a leakage area (A) and a crack-opening displacement (COD). Then assuming an elliptical crack shape, one can calculate the total postulated leakage crack length (2c) using the expression:

$$2c = (4/\pi) \times (A/COD) \quad (A.1)$$

For the Level 1 analysis, the postulated leakage area (A) is calculated by dividing the piping system's leak-rate detection limit capability (LR), with an appropriate safety factor applied (LR w/SF), by the estimated flow rate per unit area (FR):

$$A = (LR \text{ w/SF})/FR \quad (A.2)$$

The flow rate per unit area (FR) is a function of the thermo-hydraulic conditions of the water (i.e., temperature (T) and pressure (P), the surface roughness of the crack (SR), and the wall thickness of the pipe (t). Mathematically it

**Table A.1 Typical data requirements for a Level 1 analysis, with typical requirements for a Level 2 or 3 analysis shown for comparison**

Level 1 requirements	Level 2 requirements	Level 3 requirements
Physical dimensions - Pipe diameter - Wall thickness	Same as Level 1	Same as Level 1
Thermohydraulic conditions - Temperature - Pressure	Same as Level 1	Same as Level 1
Material property data - Code or actual yield and ultimate strength values	Material property data - Code or actual yield and ultimate strength values - Stress-strain data - J-R curve data - Leakage flaw type (e.g., fatigue crack) - Surface roughness - Number of turns	Same as Level 2
Specialized computer codes required - None	Specialized computer codes required - Leak rate code, e.g. SQUIRT or PICEP - Fracture mechanics code, e.g., NRCPIPE or FEM analyses	Same as Level 2, except also need a finite element code for dynamic pipe system evaluations, e.g., ANSYS, ABAQUS, etc.
Stresses - Elastically calculated normal operating and transient stresses (i.e., SSE or transient thermal expansion stresses) from stress report	Same as Level 1	Stresses - Nonlinear finite element analysis
Fracture analysis - Simplified procedures (modified limit load)	Fracture analysis - J-estimation scheme - FEM analyses	Same as Level 2

was found that for fatigue-type cracks, the flow rate per unit area could be expressed as a baseline value of FR ( $FR_{baseline}$ ) times a series of influence functions that account for the effects of temperature, pressure, and wall thickness, see Equation A.3.

$$FR = (t_f)(T_f)(P_f)(FR_{baseline}) \quad (A.3)$$

The influence functions for wall thickness ( $t_f$ ), temperature ( $T_f$ ), and pressure ( $P_f$ ) were empirically established through a series of sensitivity calculations using the SQUIRT leak-rate computer code (Version 2.4). The SQUIRT2 module was used to make these calculations. (Note, Equation A.3 is only valid for two-phase flow conditions through the crack.) In Equation A.3, the baseline value of

the flow rate per unit area ( $FR_{baseline}$ ) is 1.47 lpm/mm<sup>2</sup> (250 gpm/inch<sup>2</sup>).

The pipe wall thickness influence function ( $t_f$ ) was found to be:

$$t_f = 1.0 - (t-25.4) \times 0.0071 \quad \text{for } t > 25.4 \text{ mm}$$

$$t_f = 1.0 - (t-1.0) \times 0.18 \quad \text{for } t > 1.0 \text{ inch}$$

or (A.4)

$$t_f = 1.0 - (t-25.4) \times 0.024 \quad \text{for } t < 25.4 \text{ mm}$$

$$t_f = 1.0 - (t-1.0) \times 0.6 \quad \text{for } t < 1.0 \text{ inch}$$

The water temperature influence function ( $T_f$ ) was found to be:

$$T_f = 1.0 - ((T - 288)/288) \times 2.37 \quad \text{for } T > 288 \text{ C}$$

$$T_f = 1.0 - ((T - 550)/550) \times 2.5 \quad \text{for } T > 550 \text{ F}$$

or (A.5)

$$T_f = 1.0 - ((T - 288)/288) \times 0.95 \quad \text{for } T < 288 \text{ C}$$

$$T_f = 1.0 - (T - 550)/550 \quad \text{for } T < 550 \text{ F}$$

The pipe system pressure influence function ( $P_f$ ) was found to be:

$$P_f = 1.0 + ((P - 15.5)/15.5) \times 1.1 \quad \text{where pressure (P) is in terms of Mpa}$$

or (A.6)

$$P_f = 1.0 + ((P - 2,250)/2,250) \times 1.1 \quad \text{where pressure (P) is in terms of psi.}$$

Using the above influence functions, one can easily calculate the flow rate per unit area (FR). Knowing the flow rate per unit area (FR) and the leak-rate detection limit capability (with Safety Factor), i.e., LR w/SF, one can then calculate the leakage area (A) using Equation A.2. Then to calculate the postulated leakage crack length ( $2c$  or  $2\theta$ ) using Equation A.1, one only needs to be able to estimate the crack-opening displacement (COD).

For this Level 1 methodology, the crack-opening displacements are estimated using the Paris-Tada approach (Ref. A.2). As part of the leak-rate code sensitivity study conducted as part of this program, it was found that the Paris-Tada method resulted in the most conservative predictions of COD, i.e., the Paris-Tada approach predicted relative smaller COD values for austenitic steels which resulted in relatively large crack lengths for the same leak rate/crack opening area.

The crack-opening displacements (COD) based on the Paris-Tada approach can be estimated using Equation A.7:

$$\text{COD} = 2R_m^2 I_T(\theta_e) [\sigma_B(3 + \cos(\theta_e)/4 + \sigma_T)]/cE \quad (\text{A.7})$$

where,

$R_m$  = mean pipe radius,  
 $I_T(\theta_e)$  = the tensile compliance function as defined in Reference A.2,

$\theta_e$  = effective half crack angle accounting for the plastic-zone size,  
 $c$  = half crack length,  
 $E$  = elastic modulus,  
 $\sigma_B$  = nominal bending stress =  $M/(\pi R_m^2 t)$ ,  
 $\sigma_T$  = nominal tensile stress =  $F_x/(2\pi R_m t)$ ,  
 and  
 $F_x$  = axial load on the pipe.

The effective half crack angle is:

$$\theta_e = \theta + [K_I/\sigma_y]^2 / (\beta_1 \pi R_m) \quad (\text{A.8})$$

$\theta$  = half the total crack angle,  
 $K_I$  = stress intensity factor,  
 $\sigma_y$  = yield strength, and  
 $\beta_1$  = plastic-zone size parameter.

The estimate of the plastic-zone size in Equation A.8 is only accurate for a small-plastic zone. In order to estimate J throughout the entire range between elastic and fully plastic conditions, Paris-Tada developed a method to interpolate between elastic and fully plastic conditions. This interpolation method amounted to modifying the  $\beta_1$  term in Equation A.8. Therefore  $\beta_1$  has to be determined in somewhat of a complicated fashion that depends on the current load as detailed in Reference A.2.

Comparisons of the Paris-Tada elastic-plastic COD values (using  $\theta_e$  as defined in Equation A.8) were made with the linear elastic COD values (where  $\theta_e = \theta$ ) to see how much of an effect this plastic-zone size correction had on the COD values. What was found was that in the range of load values typical of normal operating conditions for LBB, the difference was insignificant. Furthermore, even at the higher load levels (~75 percent of yield of the uncracked pipe), the differences were only on the order of 10 to 15 percent. In addition, the error was such that one would end up with a more conservative assessment of COD and crack length if the effect was ignored. As a result in order to simplify the Level 1 approach, the plastic-zone size correction was ignored, and

$$\theta_e = \theta \quad (\text{A.9})$$

Consequently, using the empirically derived influence functions for flow rate per unit area (FR) and the Paris-Tada equations for crack-opening displacement, one can estimate the postulated leakage size crack ( $2c$  or  $2\theta$ ) using Equations A.1 through A.9. This requires an iterative approach on crack length ( $2c$ ) that is handled most efficiently using a spreadsheet.

Alternatively, one can make an estimate of the Level 1 leakage crack size using the expression

$$A = \alpha(\lambda) \left[ \frac{\pi P_m (2c)^2}{2E} \right] \quad (\text{A.10})$$

that is a shell-theory based equation used in the LBB procedures incorporated in the R6 document. It provides a conservative estimate of the crack opening area ( $A$ ) as long as the through-wall bending stresses can be ignored.

In Equation A.10,

$\lambda$  = a shell parameter =  $[12(1 - \nu^2)]^{0.25}(c/(Rt)^{0.5})$ ,  
 $c$  = half crack length,  
 $R$  = shell radius,  
 $t$  = shell thickness,  
 $\nu$  = Poisson's ratio,  
 $P_m$  = membrane stress,  
 $E$  = elastic modulus, and  
 $\alpha(\lambda)$  = a correction factor to account for bulging which is a function of the shell parameter ( $\lambda$ ),

where,

$\alpha(\lambda) = (1 + 0.117\lambda^2)^{0.25}$  for circumferential cracks in cylinders.

One can rearrange Equation A.10 so that all of the terms which are a function of crack length ( $2c$ ) are on one side of the equation and all of the known terms are on the other, such that

$$(2c)^2 \alpha(\lambda) = \frac{2EA}{\pi P_m} \quad (\text{A.11})$$

The value of the crack opening area ( $A$ ) is established using Equations A.2 through A.6. Then, Equation A.11 can be solved iteratively

for the crack length ( $2c$ ) using a simple spreadsheet.

As will be shown in Appendix D, the level of conservatism associated with this shell-based approach is about 30 percent greater than it is using the Level 1 influence expressions from Equations A.1 through A.9.

Consequently, the applicant has 2 options for calculating the leakage crack size to use in the LBB assessment. However, before proceeding to the fracture analysis/critical flaw size analysis, it is necessary to invoke the Level 1 LBB screening criteria to establish the appropriateness of employing a Level 1 LBB procedure.

### A.1.5 Level 1 Specific Screening Criteria

Before proceeding further with the Level 1 LBB procedure, it is now time to check the values calculated up to this point to check the appropriateness of the assumptions invoked in a Level 1 LBB procedure. The four elements of the Level 1 specific screening criteria are:

1. Check the ratio of the COD to the surface roughness. If this ratio is less than approximately 2.5 (Ref. A.3), then the validity of the analysis is questionable when using the standard crack morphology model from Reference A.4. For this standard crack morphology model, the surface roughness is approximately  $40.5 \mu\text{m}$  ( $0.00159$  inches) for corrosion fatigue cracks. The empirically derived influence functions discussed above were developed using the standard crack morphology model in SQUIRT. If the ratio of COD to the surface roughness is less than 2.5 (i.e., COD less than  $0.10$  mm ( $0.004$  inches) for corrosion fatigue cracks), then one needs to go on to the Level 2 or Level 3 LBB procedure, and possibly invoke the COD-dependent crack morphology model from Reference A.4.
2. Check the thermo-hydraulic conditions of the water. The influence functions used to estimate the leakage area, which in turn are used to estimate the leakage size flaw, are based on SQUIRT calculations that are only

valid for two-phase flow from subcooled water. If the temperature and pressure are such that subcooled water conditions do not exist, then a more rigorous leak-rate analysis, using a code such as PICEP, will be required. This will involve a Level 2 LBB analysis.

3. Check the ratio of the postulated crack length to the pipe circumference. If this ratio is greater than approximately one-eighth of the pipe circumference, then there is the possibility that there may be restraint of the COD from the pipe system boundary conditions that need to be considered. (The exact definition of this predetermined value will be established as part of the Battelle Integrity of Nuclear Piping (BINP) program.) If this ratio is greater than one-eighth of the pipe circumference, then one needs to go on to a Level 2 analysis, which will account for these effects.
4. Ascertain whether or not the piping system welds have been stress relieved or not. If not, then one needs to make an assessment as to whether or not weld residual stresses will impact the crack-opening displacements. For "thick-wall" piping the effects of weld residual stresses on the crack-opening displacements are probably minor. For "thin-wall" piping, the effects of weld residual stresses could be significant, and one will need to go on to a Level 2 analysis. The determination as to what is a "thick-wall" piping system and what is a "thin-wall" piping system still needs to be addressed as part of the BINP program.

### A.1.6 Level 1 Fracture Analysis

The Level 1 fracture analysis is a simple limit-load analysis for which the allowable bending stress ( $S$ ) is a function of flow stress ( $\sigma_f$ ), and postulated crack length ( $2\theta$ ), see Equation A.12. A factor of safety is applied to the postulated crack length. For convenience, this postulated total crack length with safety factor will be referred herein to as  $2\theta_1$ .

$$S = 2\sigma_f [2\sin(\beta) - \sin(\theta_1)]/\pi \quad (\text{A.12})$$

where,

$$\beta = [(\pi - \theta_1) - \pi P_m/\sigma_f]/2 \quad (\text{A.13})$$

where, the flow stress ( $\sigma_f$ ) can be defined either in terms of Code properties ( $S_y$  and  $S_u$ ) or actual material data ( $\sigma_y$  and  $\sigma_u$ ), if available. The flow stress can be defined as either:

$$\begin{aligned} \sigma_f &= (S_y + S_u)/2 \\ &\text{or} \\ \sigma_f &= (\sigma_y + \sigma_u)/2 \end{aligned} \quad (\text{A.14})$$

depending on whether actual material data are available. Typically for the leak-rate analysis used to estimate the postulated crack length, average data are used. Conversely, for the stability analysis, minimum values are typically used.

The allowable stress index ( $SI_{\text{allowable}}$ ) can be found by adding the combined membrane stress ( $P_m$ ) due to internal pipe pressure, deadweight, and seismic to the allowable bending stress ( $S$ ).

$$SI_{\text{allowable}} = S + M P_m \quad (\text{A.15})$$

where,

$M$  = margin associated with the load combination method selected for analysis (i.e., for absolute [ $M = 1.0$ ] or for algebraic [ $M = 1.4$ ]).

This allowable stress index is then compared with the applied stress index ( $SI_{\text{applied}}$ ) for the normal operating plus safe shutdown earthquake stresses (N+SSE) from the stress report to determine whether the piping system passes the Level 1 type analysis. If the applied stress index at the faulted conditions (see Equation A.16) is greater than the allowable stress index (see Equation A.15), then the piping system fails to satisfy the Level 1 criteria and one would need to move on to a Level 2 or 3 analysis.

$$SI_{\text{applied}} = M(P_m + P_b + P_e)Z \quad (\text{A.16})$$

where,

$P_b$  = combined primary bending stresses, including deadweight and seismic components,  
 $P_e$  = combined thermal expansion stresses at normal operating conditions and seismic anchor motion<sup>1</sup>.

For lower toughness materials, e.g., ferritic steels and lower toughness austenitic flux welds, one will need to apply a stress multiplier factor to the calculated allowable stress value. It is envisioned that this stress multiplier factor may resemble the Z-factors incorporated in the ASME Section XI pipe flaw evaluation criteria.

### **A.1.7 Level 1 LBB Acceptability Assessment**

A piping system would pass the Level 1 LBB criteria if the applied stress index ( $SI_{\text{applied}}$ ) at the faulted conditions is less than the allowable stress index ( $SI_{\text{allowable}}$ ) for a flaw twice as long as the postulated leakage crack size at normal operating conditions. If the applied stress index is greater than the allowable, then one needs to go on to a Level 2 or Level 3 analysis in order to demonstrate LBB.

## **A.2 References**

A.1 Solicitations for public comment on "Standard Review Plan 3.6.3 LEAK-BEFORE-BREAK EVALUATION PROCEDURES," *Federal Register*, Vol. 52, No. 167, Friday, August 28, 1987, Notices, pp 32626 to 32633.

A.2 Paris, P. and Tada, H., "The Application of Fracture Proof Design Methods Using Tearing Instability Theory to Nuclear Piping Postulating Circumferential Through Wall Cracks," NUREG/CR-3464, September 1983.

---

<sup>1</sup> If the applicant wishes to exclude secondary stresses from their Level 1 stability analysis for certain situations, e.g. large diameter primary piping analyses, they may do so subject the approval of the NRC. For large diameter piping systems, the postulated leakage size crack will most likely be a small percentage of the pipe circumference, such that the failure stress for the stability analysis will most likely be above the yield strength of the material, such that the role of secondary stresses is less important from a fracture viewpoint.

A.3 Ghadiali, N., and others, "Deterministic and Probabilistic Evaluations for Uncertainty in Pipe Fracture Parameters in Leak-Before-Break and In-Service Flaw Evaluations," NUREG/CR-6443, June 1996.

A.4 Rahman, S., and others, "Probabilistic Pipe Fracture Evaluations for Leak-Rate-Detection Applications," NUREG/CR-6004, April 1995.

**APPENDIX B**

**LEVEL 2 LBB PROCEDURES**

The Level 2 LBB procedures involve a more detailed analysis than the Level 1 LBB procedures in this document or the draft SRP 3.6.3 Leak-Before-Break (LBB) procedures. The factors of safety associated with the Level 2 LBB procedures may be less than the Level 1 LBB procedures. The Level 2 LBB procedures were developed to incorporate improvements to the draft SRP 3.6.3 LBB procedures (Ref. B.1), using the technologies from the various NRC and international programs developed since the introduction of draft SRP 3.6.3 (Ref. B.2). If a piping system fails to pass the Level 2 LBB procedures, then the applicant can apply the Level 3 LBB procedures in order to demonstrate LBB or choose to evoke certain options within the Level 2 LBB procedures.

The key elements of the Level 2 procedures are described next.

### **B.1 Key Elements of Level 2 Procedure**

An initial requirement for all three LBB procedures is a general screening criterion to determine if LBB can be applied to the piping system. Piping systems not eligible for LBB are those where there may be large unknown stresses (e.g., water hammer) or where long surface flaws could occur (e.g., stress-corrosion cracking). The fatigue usage factor shall be below 1.0 for the life of the plant using design stresses and any service encountered stress

cycles that have become known prior to the LBB application. Since the forces from a steam-hammer event can be calculated, lines susceptible to steam hammer can be considered for LBB. If a piping system passes this general screening criterion, then the user may elect to apply these Level 2 LBB procedures. The key elements of the Level 2 LBB procedures are:

- Data input requirements,
- Determination of critical locations for assessment,
- Applied safety factors,
- Procedures to calculate the postulated crack length for the acceptable leak rate, (some screening criteria are provided to circumvent unnecessary steps),
- Level 2 fracture analysis, and
- Level 2 LBB assessment.

Each of these elements is described in more detail in the subsequent sections.

#### **B.1.1 Data Input Requirements**

The data typically required for a Level 2 LBB assessment are shown in Table B.1. All of the input data are also needed for a Level 3 LBB assessment.

**Table B.1 Typical data requirements for a Level 2 LBB assessment, with typical requirements for Level 1 and 3 LBB procedures shown for comparison**

<b>Level 1 requirements</b>	<b>Level 2 requirements</b>	<b>Level 3 requirements</b>
Physical dimensions - Pipe diameter - Wall thickness	Same as Level 1	Same as Level 2
Thermohydraulic conditions - Temperature - Pressure	Same as Level 1	Same as Level 2
Material property data - Code or actual yield and ultimate strength values	Material property data - Code or actual yield and ultimate strength values - Stress-strain data - J-R curve data - Leakage flaw type (e.g., fatigue crack) - Surface roughness - Number of turns	Same as Level 2
Specialized computer codes required - None	Specialized computer codes required - Leak-rate code, e.g., SQUIRT, PICEP, - Fracture mechanics code, e.g., NRCPIPE or FEM analyses	Same as Level 2, except also need a finite element code for dynamic pipe system evaluations, e.g., ANSYS, ABAQUS, etc.
Stresses - Elastically calculated normal operating and transient stresses (i.e., SSE or transient thermal expansion) from the stress report	Same as Level 1	Stresses - Nonlinear finite element analysis
Fracture analysis - Simplified procedures (modified limit load)	Elastic-plastic fracture analysis - J-estimation schemes, or - FEM analyses	- Same as Level 2

### **B.1.2 Critical Location Determination**

In applying a Level 2 LBB procedure to a subject piping system it is necessary to make assessments at a number of critical locations along the piping system. At a minimum, each of the following locations shall be considered in a Level 2 LBB procedure:

- (a) The location with the highest normal operating stresses (this is the location where a crack is more likely to start),
- (b) The location with the highest transient stresses, i.e., safe shutdown earthquake (SSE) or transient thermal expansion stresses at start-up or shut-down,
- (c) The location with the highest ratio of normal operating plus SSE stresses (N+SSE) to normal operating stresses (N),
- (d) The next three highest stress locations with ratios of the normal operating plus transient stresses to the normal operating stresses (N) being greater than 80 percent of the location with the highest ratio, and
- (e) Any other location that has a material toughness with a J-R curve that is less

than 75 percent of the J-R curve for the above material locations.

Postulated cracks can be in the straight pipes, girth welds, and fittings. For fittings, the most common type of fitting to develop cracks is an elbow. Elbow cracks can be either circumferential cracks on the extrados (closing moment applied), or axial cracks on the flank of the elbow.

### **B.1.3 Physical Dimensions**

The entire pipe system, from anchor to anchor, needs to be included in the LBB evaluation. A detailed sketch with the pipe-system geometry (including pipe hanger locations, snubbers locations, etc.) shall be included in the submittal. The pipe nominal diameters, thicknesses, and materials throughout the pipe system shall be identified. Actual thickness values can be used. If a weld location is considered as a critical location for an LBB application, then the thickness used in the evaluation shall be the minimum design or minimum actual thickness, i.e., the actual thickness at a counterbore without the weld crown.

### **B.1.4 Prescribed Safety Factors**

With any of the three levels of LBB analyses, safety factors need to be prescribed by the NRC, typically on crack size and leak-rate detection capability. For the existing draft SRP 3.6.3 criteria, these prescribed safety factors are typically 10 on leak rate and 2 on crack length (Ref. B.1). For the Level 2 LBB procedures, the safety factor on leak-rate could be decreased since the leak-rate analyses are more detailed than in draft SRP 3.6.3. The safety factor for the fracture analyses will be on crack length only, not on stress level. The actual factors of safety for all three levels of assessment will need to be established by the NRC during the preparation of the Regulatory Guide for LBB.

### **B.1.5 Postulated Leaking Crack Length Determination**

The determination of the postulated maximum leaking crack length for the Level 2 LBB

procedure is one of the major differences between the Level 2 LBB procedure and the existing draft SRP 3.6.3.

In order to determine a postulated crack length for the Level 2 LBB procedure, one needs to first know the leak-rate detection capability with some safety factor. For instance, a leak detection capability of a PWR system is typically 1 gpm, and the safety factor of 10 has been typically applied. This would give a target 10-gpm leak rate for crack-size determination. The crack-opening displacement is then calculated for an initial crack length at the normal operating stresses, and then the leak-rate is determined. An iterative procedure is used until the crack length corresponding to the target leak rate is determined.

This is the basic step in this part of the Level 2 LBB procedures that is consistent with the draft SRP 3.6.3 approach. The additional requirements are:

1. The acceptable COD-analyses procedures are specified,
2. The effects of restraint on the COD from the pipe-system boundary conditions need to be included if simplified COD methods from Step 1 are used,
3. Crack-face pressure effects on COD can be included if desired by the applicant,
4. The COD-dependant crack-morphology parameters (surface roughness and number of turns) to be used in the leak-rate analyses are specified,
5. The effects of residual stresses need to be considered for certain cases, and
6. The acceptable leak-rate analyses and computer codes are given.

**B.1.5.1 Acceptable COD Analyses:** The acceptable COD analyses are either the Tada-Paris analysis (Ref. B.3), the original GE/EPRI method (Ref. B.4), or by finite element analyses (Ref. B.5 gives results from numerous FEM COD analyses). The original GE/EPRI solutions for combined bending-and-pressure loading in both the PICEP (Ref. B.6), SQUIRT (Ref. B.7) and NRCPIPE (Ref. B.8) codes have been found to give comparable results to finite

element analyses (Ref. B.5). The Tada-Paris method in the NRCPIPE code has also been benchmarked against finite element results in Reference B.5. Other COD estimation schemes can be used if appropriately benchmarked and documented in the submittal. These analyses consider that the pipe is a simple endcapped vessel, and hence do not account for pipe-system boundary conditions on restraining the induced bending from the axial stresses. For these analyses, a correction factor from Section B.1.5.2 of this appendix is needed.

Finite element solutions can involve relatively simple straight-pipe models that use end capped pipe boundary conditions as in Reference B.5, or could attempt to model the whole pipe system with the crack and the boundary conditions that might restrain the induced bending from axial tension loads. If a simple straight-pipe FE model is used, then the correction factor for pipe-system boundary conditions needs to be used.

**B.1.5.2 Reduction of Axial Tension COD Due to Pipe-System Restraint:** The COD estimation scheme analyses for combined loading typically consider that the pipe is free to rotate from the axial stresses applied. FEM analyses may also model only a straight section of pipe rather than the whole pipe system with the actual system boundary conditions for COD analyses. In a real pipe system, pipe anchors (such as vessel nozzles or nozzles to much larger pipes) will restrain the rotation that comes from the eccentricity of the crack section under axial tension loading. It is envisioned, based on some efforts being undertaken as part of the BINP program that the following procedure may be used to determine the reduction of the axial tension COD component. The axial tension stresses could be from pressure or other loads. This correction is only for the COD due to axial tension stress. This analysis step can be skipped if the following normal operating conditions can be met:

- If the axial tension stress is less than some percent<sup>1</sup> of the total stress, then there are negligible effects from the pipe-system boundary conditions,
- If the crack length is less than 1/8 of the pipe circumference, then this effect is negligible, or
- If the crack plane is more than 10 pipe diameters from an anchor or elbow in either direction and the crack length is less than 1/4 of the pipe circumference, then these effects can be ignored.

If these conditions cannot be met and the entire pipe system with the crack was not considered in the FEM model for COD analyses, then the following steps may be able to be used to estimate the effect of the restraint on the COD predictions.

1. Start with an estimated initial crack length and calculate the COD for combined bending and axial tension (pressure) forces using an estimation scheme like the GE/EPRI estimation scheme in PICEP, SQUIRT, or NRCPIPE<sup>2</sup>,
2. Calculate the bending only COD for the same crack length using the same COD estimation scheme,
3. Subtract the bending only COD (in Step 2) from the total COD (in Step 1). This gives the unrestrained axial tension COD component,
4. Using the following equation<sup>3</sup>, calculate the restrained axial tension component of the COD (COD<sub>restrained</sub>);

$$COD_{restrained} = COD_{unrestrained} * fcn(R_m/t, \theta/\pi, L_1/D, L_2/D) \quad (B.1)$$

where,

<sup>1</sup> To be determined from future BINP program efforts.

<sup>2</sup> Use the original GE/EPRI estimation scheme without plastic-zone correction in the elastic term in the NRCPIPE code. Do not use the Battelle-modified GE/EPRI estimation scheme method in the NRCPIPE code.

<sup>3</sup> Exact form of the adjustment factor (fcn) is to be determined from future BINP work.

- $R_m$  = pipe mean radius,
  - $t$  = pipe thickness,
  - $\theta$  = half crack angle, radians,
  - $L_1$  = distance from crack plane to closest nozzle, pipe elbow, or pipe hanger on one side of the crack plane,
  - $L_2$  = distance from crack plane to farthest nozzle, pipe elbow, or pipe hanger on the other side of the crack plane, and
  - $D$  = mean pipe diameter.
  - $fcn$  = functional closed form adjustment factor
5. Add the  $COD_{restrained}$  axial tension component to the bending only COD component from Step 2,
  6. Calculate the leak rate using PICEP or SQUIRT with the crack morphology parameters given in Section B.1.5.4, and
  7. Iterate on the crack length until the target leak rate is determined.

**B.1.5.3 Effects of Crack-Face Pressure on COD:** The effect of the pressure on the crack faces is to open up the crack further than if it was ignored. This effect should make it easier to meet LBB conditions, hence the applicant can ignore it and still be acceptable from a regulatory sense<sup>4</sup>. This effect is probably only significant if the crack length is longer than a prescribed percent of the pipe circumference<sup>5</sup>. This effect may compensate for some of the restraint of pressure-induced bending effects required in Section B.1.5.2. The following steps are acceptable for this analysis:

1. From the leak-rate calculations in Section B.1.5.2, determine the exit plane fluid pressure (Pressure at throat in

- PICEP or exit plane pressure in SQUIRT).
2. Assume the pressure distribution is linear through the thickness from the inside pressure to the exit plane (outside diameter).
  3. Calculate the applied bending moment and axial tension forces on the pipe by integrating the pressure along the crack faces.
  4. Add those moments and axial tension forces to the applied normal operating loads in Step 1 of Section B.1.5.2. Calculate the new leak rate. Check the pressure distribution through the thickness from the leak-rate code and iterate until there is convergence for that crack length.
  5. Change the crack length and iterate through Step 1 of this section until the target leak rate is determined.

**B.1.5.4 Crack Morphology Parameters:** To maintain consistency with different LBB applications, specified crack morphology parameters shall be used. These parameters are the surface roughness and number of turns. As a crack opens up, then the number of turns decreases, and the surface roughness decreases. Hence, these parameters depend on the COD value. By having a COD-dependant roughness and number of turns, problems with the friction factor relationships in these leak-rate codes for tight cracks can be circumvented. The roughness and number of turns was chosen from the statistical evaluation of corrosion-fatigue cracks and thermal fatigue cracks found in service. The mean values are to be used, see Table B.2.

---

<sup>4</sup> While crack face pressure may result in a beneficial effect on the postulated leakage crack size, the impact of this effect on the crack driving force for the critical crack size assessment is unknown and should be assessed prior to one taking credit for its effect on the leakage crack size.

<sup>5</sup> Prescribed value could be determined from additional proposed work in this program.

**Table B.2 Mean and standard deviation of crack morphology parameters**

Crack morphology variable	Corrosion fatigue or thermal fatigue cracks	
	mean	standard deviation
$\mu_L, \mu\text{m} (\mu\text{inch})$	8.814 (347)	2.972 (117)
$\mu_G, \mu\text{m} (\mu\text{inch})$	40.513 (1,595)	17.653 (695)
$n_{tL}, \text{mm}^{-1} (\text{inch}^{-1})$	6.73 (171)	8.07 (205)

In Reference B.9, the following equations were established using engineering judgment. For the surface roughness ( $\mu$ ), the following equation should be used as a function of the center crack-opening displacement ( $\delta$ ).

$$\mu = \begin{cases} \mu_L, & 0.0 < \frac{\delta}{\mu_G} < 0.1 \\ \mu_L + \frac{\mu_G - \mu_L}{9.9} \left[ \frac{\delta}{\mu_G} - 0.1 \right], & 0.1 < \frac{\delta}{\mu_G} < 10 \\ \mu_G, & \frac{\delta}{\mu_G} > 10 \end{cases} \quad (\text{B.2})$$

For the number of turns ( $n_t$ ), the following equation should be used as a function of the center crack-opening displacement ( $\delta$ ).

$$n_t = \begin{cases} n_{tL}, & 0.0 < \frac{\delta}{\mu_G} < 0.1 \\ n_{tL} - \frac{n_{tL}}{11} \left[ \frac{\delta}{\mu_G} - 0.1 \right], & 0.1 < \frac{\delta}{\mu_G} < 10 \\ 0.1n_{tL}, & \frac{\delta}{\mu_G} > 10 \end{cases} \quad (\text{B.3})$$

#### B.1.5.5 Effect of Residual Stresses on Leak

**Rate:** Weld residual stresses have been investigated and determined that they could possibly affect the leak rate under certain conditions. These conditions are being explored in the BINP program. What is now known about weld residual effects on crack opening and leak rates is summarized below.

1. Weld residual stresses can be either tension-compression through the thickness for a "thin-walled" weld or

tension-compression-tension for a "thick-walled" weld, respectively.

2. The effect of weld residual stresses on the COD is to rotate the crack faces. Hence "thin-walled" welds (with tension-compression stresses through the thickness) will rotate the crack faces more than "thick-walled" welds.
3. If the applied normal operating loads give a COD that is much larger than the change in the COD due to the rotation of the crack faces from the residual stresses, then the weld residual stress effect can be ignored. The effect of the elliptical crack-opening shape should be considered in this evaluation.
4. Because of low crack-face rotations, the effect of residual stresses can be considered negligible for a "thick-walled" weld. The definition of a "thin-walled" versus "thick-walled" weld needs to be established.
5. Stress relieved welds can be considered exempt from weld residual stress effects on the COD.

At this time, based on preliminary results from the BINP program, it is envisioned that a correction factor to the GE/EPRI V-function, used to estimate the COD, will be developed as part of BINP to address the effect of weld residual stress effects on COD predictions for LBB analysis.

#### B.1.5.6 Acceptable Leak-Rate Codes:

Computer codes that are acceptable for leak-rate analyses are PICEP and SQUIRT. Other codes that have been benchmarked against similar

leak-rate data sets can be used if documentation is provided.

In these codes, an elliptical crack-opening shape shall be used.

The SQUIRT code should only be used for two-phase flow conditions. Only the original GE/EPRI COD analyses should be used in SQUIRT for COD analyses. Alternatively, the Tada-Paris COD analysis procedure or FEM COD values could be determined, and then used with only the thermohydraulic options in SQUIRT (SQUIRT2 module) or PICEP (pick leakage only option). In the PICEP code, the GE/EPRI solution is the only option to use.

For single-phase flow through the cracks (either all-water or 100-percent quality steam lines), benchmarking of leak rates in this flow regime is desired for whatever computer code is used.

The surface roughness and number of turns used shall be those in Section B.1.5.4 in this report.

### B.1.6 Level 2 Fracture Analysis

The Level 2 fracture analysis involves an elastic-plastic fracture analysis. Cracks could be either in straight pipes or in fittings. Based on service history, circumferential cracks are more likely to occur in straight pipes and in particular at girth welds near terminal ends or near fittings.

Circumferential through-wall cracks in straight pipes and at girth welds to fittings can be analyzed using the same analyses. Based on comparisons with full-scale pipe test data in Reference B.10 and B.11, the acceptable analyses for combined pressure and bending of a circumferential through-wall crack in a straight pipe are;

- ASME Section XI Z-factor equations (Refs. B.12 and B.13),
- Original GE/EPRI analysis (Ref. B.4 and in the PICEP, SQUIRT and NRCPIPE Codes),
- LBB.ENG2 analysis (Ref. B.10 and in the NRCPIPE Code),

- LBB.NRC analysis (Ref. B.14 and in the NRCPIPE Code), and
- Dimensionless Plastic-Zone Parameter (DPZP) analysis (Refs. B.2 and B.15).

For axial cracks in straight pipes, the analysis in Reference B.15 could be used.

The most common type of fitting where cracks have occurred is in elbows. Appendix E summarizes work from the BINP program in which methods to evaluate axial and circumferential through-wall flaws in elbows were developed. Alternatively, one could use a finite element analysis for cracks in elbows or other fittings.

There are many common input parameters for these analyses. The following input parameters can be used.

**B.1.6.1 Yield, Ultimate, Flow Stress, and Stress-Strain Curves:** These properties should be determined for the operating condition of interest (temperatures may be different for normal operating versus transient loading conditions), and can be for quasi-static loading rates.

The yield and ultimate strength can be either the ASME Section II Code values ( $S_y$  and  $S_u$ ) at the service temperature of interest, actual values at that service temperature ( $\sigma_y$  and  $\sigma_u$ ), or reasonable bounding values<sup>6</sup> from a database at the service temperature of interest.

The flow stress ( $\sigma_f$ ) shall be defined by

$$\begin{aligned} \sigma_f &= (S_y + S_u)/2 \\ \text{or} \\ \sigma_f &= (\sigma_y + \sigma_u)/2 \end{aligned} \quad (\text{B.4})$$

For weld metals, only the weld metal or HAZ toughness is needed. The weld metal strength is not needed. Some analyses<sup>7</sup> allow the weld

<sup>6</sup> Mean minus one standard deviation value is considered a reasonable lower bound value.

<sup>7</sup> FEM analyses including the weld geometry, or the LBB.ENG3 J-estimation scheme (Reference B.11) using base and weld metal stress-strain curves.

metal strength to be incorporated in them, but these analyses are not required.

Typically, for the crack-opening analysis used to estimate the postulated crack length at normal operating conditions, the average strength data are used. Conversely, for the stability analysis, minimum values or reasonable lower-bound values<sup>5</sup> are typically used. Furthermore, for the stability and critical flaw size analyses, the strength parameters should be defined at conditions consistent with the occurrence of the stresses, e.g., for a surge line during heatup, the analysis may not be for the surge line at normal operating temperature.

The stress-strain curve in these fracture analyses are typically represented by a Ramberg-Osgood curve, see Equation B.5.

$$\epsilon/\epsilon_0 = (\sigma/\sigma_0) + \alpha(\sigma/\sigma_0)^n \quad (\text{B.5})$$

In this equation, it is required that

$$\sigma_0/\epsilon_0 = E \quad (\text{B.6})$$

where,

- E = elastic modulus from Section II of ASME Code
- $\epsilon_0$  = reference strain
- $\sigma$  = any stress value
- $\sigma_0$  = reference stress
- $\alpha$  = parameter from curve fitting of data
- n = strain-hardening exponent

$\sigma_0$  is typically the yield strength, but could be any other value as long as Equation B.6 is satisfied and  $\alpha$  and n are determined with this value. If a plastic-zone correction is used in the GE/EPRI analysis, then  $\sigma_0$  should be taken as the yield strength.

The Ramberg-Osgood curve fit shall be obtained using the engineering stress-strain curve and fitting the data from 0.1-percent strain to the strain corresponding to 80-percent of the ultimate strength, Ref. B.2.

**B.1.6.2 Fracture Toughness: Specimen orientation** - The fracture toughness can be from actual test data, or representative lower-bound data<sup>5</sup>. For a circumferential through-wall flaw, the data should be from specimens machined in the L-C orientation<sup>8</sup>. For axial flaw evaluations, the data should be for specimens machined in the C-L orientation.

For crack locations at welds, the postulated crack location is in the center of the weld metal as well as in the HAZ and fusion lines. The HAZ/fusion line crack should be put in fracture specimens (i.e., bend-bar or C(T) specimens) fabricated so that the crack and HAZ/fusion line is normal to the specimen surface. Typically more specimens are needed for HAZ/fusion line testing than for base metal or weld centerline testing (Ref. B.17). It is suggested that five specimens be tested for HAZ/fusion line testing, and the lowest J-R curve from those five specimens should be used.

In the absence of such data, one possible means of accounting for cracks in the HAZ and along the fusion line is to use the weld metal J-R curve up to some prescribed value and then assume a flat J-R curve for the remainder of the J-R curve, see Figure 5.28.

**Loading rate** - Data for austenitic base metals and weld metals can be at quasi-static loading rates.

If seismic loading or other dynamic loading is part of the transient loading condition for the fracture evaluation, then due to dynamic strain aging effects, the fracture toughness data for ferritic steels at temperatures greater than 149 C (300 F) should be tested at a dynamic loading rate comparable to the transient loading rate (Refs. B.2 and B.18). Steels with ultimate strengths at temperature that are greater than the ultimate strength at room temperature are susceptible to dynamic strain aging and should be tested at higher loading rates.

<sup>8</sup> See Reference B.16 for specimen orientation definition.

For a dynamic event, the loading rate should correspond to the time to reach crack initiation in one-quarter of the period of the first natural frequency of the piping system (Ref. B.2). The experimental time to crack initiation can be a factor of  $\pm 25\%$  of the time corresponding to one-quarter of the period of the first natural frequency of the piping system.

In the absence of dynamic data, one could assume a factor of safety of 2 on the quasi-static data based on a review of past quasi-static and dynamic data developed at Battelle and in Korea.

Cyclic loading effects on toughness – Cyclic loading effects can also be detrimental to the toughness of the material.

Bimetallic welds - For bimetallic welds involving a stainless steel weld to a carbon steel pipe, the J-R curve of the HAZ/fusion line of the stainless steel weldment to the carbon steel (or low alloy steel) material should be considered in determining where the lowest toughness region is. For Inconel welds or welds using Inconel buttering on the low alloy or carbon steel materials, then the toughness of the Inconel weld or the carbon steel/low alloy steel can be used for the toughness of the bimetallic weld (Ref. B.19). Note, however, for bimetal welds made with Inconel 82/182 weld metal, the issue of primary water stress corrosion cracking (PWSCC) must be considered.

Thermal aging - Thermal aging needs to be accounted for in cast stainless steel base metals. Trend curves with ferritic number or chemistry can be used to project the end-of-life toughness properties.

Thermal aging can also affect stainless steel welds. In cast stainless piping, the aged base metal properties may govern the toughness considerations over the weld metal. However, the thermal aging effects on the weld metal should also be considered for wrought stainless steel piping systems.

Extrapolation of J-R curves - Data for crack growth of up to 30-percent of the initial ligament

of the fracture specimen can be used to establish the J-R curve. A significant amount of research results have shown that it is conservative to make a power-law extrapolation of the deformation theory J-R curve (Ref. B.20).

It has also been shown that the Modified J-R curve ( $J_M$ ) gives good predictions for large crack growth in estimations schemes such as those mentioned at the beginning of Section B.1.6 (Ref. B.2). The  $J_M$ -R curve can only be used in cases where the slope of the J-R curve is linear, i.e.,  $J_M$ -R curve should not be used if they exhibit an upward hooking behavior (power-law coefficient greater than 1.0).

**B.1.6.3 Stress Definitions:** For fracture analyses, the applied stresses from the plant stress report can be used to calculate a crack size that corresponds to that load-controlled instability. That is, the crack length can be increased so that maximum load is achieved at the transient loads (typically the N+SSE load). The stress components to be used in this evaluation are as follows:

1. Global secondary stresses and primary stresses shall be combined as an algebraic sum. A global secondary stress includes thermal expansion stresses and seismic anchor motion stresses. Primary stresses are dead-weight, pressure and inertial stresses. If the predicted failure stress for the flaw in question is less than the yield strength of the material then the secondary stresses and primary stresses should be considered equally from a fracture perspective. If the failure stress is predicted to be greater than yield, then the secondary stress should be combined with the primary stress, but in some reduced nonlinear manner<sup>9</sup>.
2. Weld residual stresses and through-thickness thermal stresses can be

---

<sup>9</sup> One possible nonlinear correction for Level 2 is to combine the secondary stresses with the primary stresses in some strain-based nonlinear manner in which the NRC provides some upper bound stress-strain curve for this adjustment.

ignored if ductile fracture behavior is demonstrated in the J-R curve tests for the material at the temperatures of interest.

3. An equivalent bending moment ( $M_{eq}$ ) shall be determined from a combination of the moments and torsion in the different directions using a Von Mises combination of these loads (Ref. B.21), i.e.,

$$M_{eq} = \{M_b^2 + [(3^{0.5}/2)*T^2]\}^{0.5} \quad (B.7)$$

where

$$M_b = (M_x^2 + M_y^2)^{0.5}$$

$M_x$  = Bending moment in one plane

$M_y$  = Bending moment in the other plane

T = Torsion in x-y plane

**B.1.6.4 Fracture Calculations:** The critical crack lengths shall be calculated for the different postulated LBB locations. The critical crack length is the crack length at the maximum load (a load-controlled instability analysis). It is possible that some systems may not result in a double-ended guillotine break for applied displacements (from secondary stresses) that could go beyond the maximum load, but post maximum-load stability will be kept as an additional reserve margin.

The critical crack lengths shall be calculated for the service transient load (e.g., N+SSE or possibly startup/shutdown for the surge line) using the guidance in Section B.1.6 of this appendix.

### B.1.7 Level 2 LBB Acceptance Criterion

A piping system would pass the Level 2 LBB acceptance criterion if the calculated critical crack length from Section B.1.6.4 is equal to or greater than the leakage crack length from Section B.1.5, with some margin applied as defined by the NRC and the leakage size crack is stable at the N+SSE loads with some margin as defined by the NRC. If it does not pass, then several of the options in the Level 2 LBB

procedure can be invoked, or a Level 3 LBB procedure can be employed.

## B.2 References

B.1 Solicitations for public comment on "Standard Review Plan 3.6.3 LEAK-BEFORE-BREAK EVALUATION PROCEDURES," *Federal Register*, Vol. 52, No. 167, Friday, August 28, 1987, Notices, pp 32626 to 32633.

B.2 Wilkowski, G. M., Olson, R. J., and Scott, P. M., "State-of-the-Art Report on Piping Fracture Mechanics," U.S. Nuclear Regulatory Commission report NUREG/CR-6540, BMI-2196, February 1998.

B.3 Paris, P. C., and Tada, H., "Application of Fracture Proof Methods Using Tearing Instability Theory to Nuclear Piping Postulating Circumferential Through Wall Cracks," NUREG/CR-3464, September 1983.

B.4 Kumar, V. and German, M., "Elastic-Plastic Fracture Analysis of Through-Wall and Surface Flaws in Cylinders," EPRI Report NP-5596, January 1986.

B.5 Rudland, D. Wang, Y. Y. and Wilkowski, G. M. "Comparison Of Estimation Schemes and FEM Analysis Predictions of Crack-Opening Displacement For LBB Applications," 2000 ASME PVP Conference.

B.6 Norris, D., and others, "PICEP: Pipe Crack Evaluation Program," EPRI Report NP-3596-SR, 1984.

B.7 Ghadiali, N., and others, "SQUIRT Computer Code - DOS Version 2.4 - User's Manual," Battelle report to the U.S. NRC April 30, 1996.

B.8 Ghadiali, N., and others, "NRCPIPE - Windows Version 3.0 - User's Guide," Battelle report to the U.S. NRC April 30, 1996.

B.9 Rahman, S., and others, "Probabilistic Pipe Fracture Evaluations for Leak-Rate-Detection Applications," NUREG/CR-6004, pp 3-11 to 3-12, April 1995.

B.10 Brust, F. W., "Approximate Methods for Fracture Analyses of Through-Wall Cracked Pipes," NRC Topical Report by Battelle Columbus Division, NUREG/CR-4853, February 1987.

B.11 Brust, F. W., and others, "Assessment of Short Through-Wall Circumferential Cracks in Pipes," NUREG/CR-6235, April 1995.

B.12 ASME Boiler and Pressure Vessel Code, Section XI, "Rules for In-service Inspection of Nuclear Power Plant Components," 1995 Edition, July 1995, Appendix C.

B.13 ASME Boiler and Pressure Vessel Code, Section XI, "Rules for In-service Inspection of Nuclear Power Plant Components", 1995 Edition, July 1995, Appendix H.

B.14 Klecker, R., and others, "NRC Leak-Before-Break (LBB.NRC) Analysis Method for Circumferentially Through-Wall Cracked Pipes Under Axial Plus Bending Loads," NUREG/CR-4572, May 1986.

B.15 G. M. Wilkowski, and P. M. Scott, "A Statistical Based Circumferentially Cracked Pipe Fracture Mechanics Analysis for Design on Code Implementation," Nuclear Engineering and Design, Vol. III, 1989, pp 173-187.

B.16 "Standard Terminology Relating to Fatigue and Fracture Testing," ASTM E1823-96, 1999 Annual Book of ASTM Standards, Volume 03.01, 1999.

B.17 Rosenfield, A. R., and others, "Stainless Steel Submerged Arc Weld Fusion Line Toughness," NUREG/CR-6251, April 1995.

B.18 Marschall, C. W., Mohan, R., Krishnaswamy, P., and Wilkowski, G. M., "Effect of Dynamic Strain Aging on the Strength and Toughness of Nuclear Ferritic Piping at LWR Temperatures," NUREG/CR-6226, October 1994.

B.19 Scott, P. M., and others, "Fracture Evaluations of Fusion Line Cracks in Nuclear

Pipe Bimetallic Welds," NUREG/CR-6297, April 1995.

B.20 G. M. Wilkowski, C. W. Marschall, and M. Landow, "Extrapolations of C(T) Specimens J-R Curves for Use in Pipe Flaw Evaluations," ASTM STP 1074, 1990, pp 56-84.

B.21 Mohan, R., and others, "Effects of Toughness Anisotropy and Combined Tension, Torsion, and Bending Loads on Fracture Behavior of Ferritic Nuclear Pipe," NUREG/CR-6299, April 1995.

**APPENDIX C**

**LEVEL 3 LBB PROCEDURES**

The Level 3 LBB procedure is the last option available to an applicant for demonstrating LBB in a piping system, and should only be considered as a last resort. Building upon the foundation of the Level 2 analysis, the Level 3 analysis looks for additional margin in the nonlinearity of the crack, the piping system, or both. Because such nonlinearities consume energy, this energy is not available for driving the crack. Thus, there may not be a large enough crack driving force to reach the critical crack load and hence, LBB is satisfied.

The key elements of the Level 3 procedure are described next.

### **C.1 Key Elements of Level 3 Procedures**

Level 3 builds directly upon the Level 2. Thus, Level 3 has all of the same requirements for data inputs, applied safety factors and procedures to calculate the postulated crack length as listed in Appendix B. All of the screening criteria and exclusions of Level 2 apply. Where Level 3 differs from Level 2 is that a nonlinear stress analysis is performed in place of a pseudo-static, response spectrum, or dynamic linear analysis.

### **C.2 Nonlinear Stress Analysis Data Input Requirements**

The data typically required for a Level 3 LBB assessment are as follows:

1. A piping system that qualifies for a Level 2 analysis but that does not meet the Level 2 LBB fracture margin requirement,
2. A finite element model of the piping run from anchor to anchor containing the hypothesized flaw,
3. A complete characterization of the loading in the time domain,
4. A load-displacement description of the crack behavior,
5. An assumed flaw orientation,
6. The stress-strain behavior of the pipe at the operating temperature, and
7. A nonlinear finite element analysis program.

### **C.2.1 Qualified Piping System**

In applying a Level 3 LBB procedure to a piping system, all of the basic requirements for a Level 2 analysis must be met, except for demonstration of an adequate fracture margin from the Level 2 analysis. If any piping system is disqualified from consideration for LBB in Level 2 due to a violation of one of the Level 2 screening criteria stipulations, it is automatically disqualified from consideration for LBB in Level 3.

### **C.2.2 Finite Element Model**

The entire pipe system, from anchor to anchor, needs to be included in the Level 3 model. A detailed sketch with the pipe-system geometry (including pipe hanger locations, snubbers locations, etc.) shall be included in the submittal. The pipe nominal diameters, thicknesses, and materials throughout the pipe system shall be identified. Actual thickness values can be used. The characteristics of all supports (stiffness and damping properties) must be known.

### **C.2.3 Loading**

All loads on the pipe system during the SSE event (pressure, dead weight, thermal expansion, cold springing, seismic anchor motion, inertial loading, etc.) must be known as a function of time. It is anticipated that the dead weight, pressure, and thermal expansion loads will be constant with time. The SSE loading, both the seismic anchor motion and inertial loading, will be time varying and must be known in three orthogonal directions. As appropriate, loads such as thermal stratification must be considered in combination with the SSE loading.

The three orthogonal directions of the SSE time history loading (seismic anchor motion and inertial loading) must be known at a sufficiently small time increment that the nonlinear analysis will converge. In the event that the analysis fails to converge because the time step is too coarse, a finer time step must be used.

#### **C.2.4 Postulated Crack Description**

The hypothesized crack must be characterized in terms of a load-displacement behavior as part of the nonlinear analysis. For a circumferential crack, the crack behavior is generally given in moment-rotation coordinates. For axial cracks, a COD versus hoop load would be appropriate. The crack characterization must include the effects of all applicable loading (bending, pressure, tension) and unloading behavior and crack closure must be included.

In general, the required load-displacement characterization of the crack will come from the Level 2 leakage size crack calculations. A suitable factor of safety as defined by the NRC must be applied to this Level 2 leakage crack size. J-estimation scheme or finite element analyses of some sort will then be used to define the crack behavior. The effect of yielding of the crack on unloading can be modeled. Crack closure must be included if the possibility of the crack faces touching exists. Because the LBB assessment is only concerned with whether or not the applied load is sufficient to reach the maximum moment of the crack, the crack load-displacement characterization is only needed up to the predicted maximum moment.

#### **C.2.5 Crack Orientation**

An orientation for the crack must be chosen for the Level 3 analysis. Unlike a Level 1 or 2 analysis, where there is a known applied load from the stress report that is given independent of direction, the Level 3 crack is fixed in a given orientation in the finite element model and will respond only to loads that will open/close the crack. Thus, if a Level 3 crack is oriented vertically and all of the loads are applied horizontally, LBB will be satisfied because the crack will not experience any crack-opening load.

It is important to correctly orient the crack so that a true LBB assessment is made. A conservative Level 3 LBB analysis would consider the largest possible leakage size flaw based on the normal operating loads, but oriented in the direction of the largest possible

SSE loading in the nonlinear analysis. A less conservative, but technically defensible option would be to orient the crack for the time history finite element analysis solely based on the direction of the largest normal operating loads, since it would be the normal operating loads that would cause the crack in the first place. In this case, if the SSE loads were in a different direction from the crack orientation, LBB would be satisfied.

#### **C.2.6 Remote Piping Material Properties**

One of the possible sources of nonlinearity in a piping system that could contribute to LBB being satisfied is plasticity remote from the crack. In order to consider this possibility, the stress-strain characteristics of the pipe materials at all locations in the piping system at the appropriate temperature must be known. In general, true stress-true strain data are required. In the event that plasticity remote from the crack is not to be considered, modulus and Poisson's ratio at the operating temperature is all that is needed.

#### **C.2.7 Nonlinear Finite Element Analysis Program**

In order to successfully complete a Level 3 LBB analysis, a nonlinear finite element analysis program is required. In addition to having the standard features of a piping stress analysis program, the program must have:

- Time-history loading
- Option 1: A means to implement a nonlinear model of the crack
- Option 2: Means to conduct an analysis considering plasticity in all of the piping system.

The time history capability is needed because the crack/piping nonlinearities are load-path dependent. The nonlinear crack model is the finite element implementation of the postulated crack, see Figure C.1. In the event that the contribution of plasticity remote from the crack is to be considered in order to demonstrate that LBB is satisfied, the finite element program must have piping elements that permit yielding.

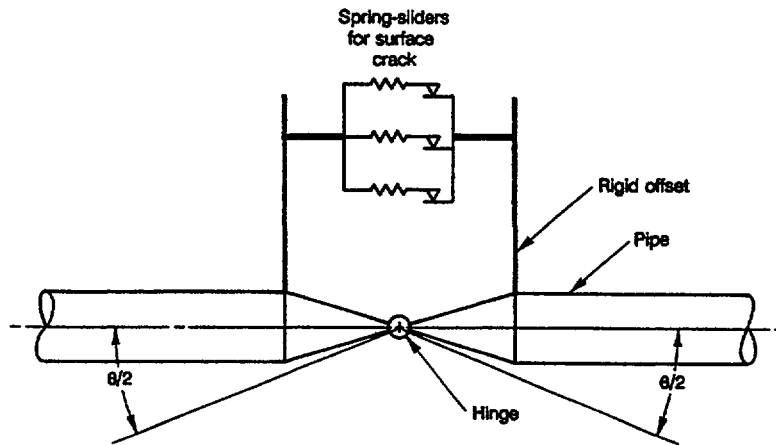


**Figure C.1 Spring-slider model of a surface crack (or through-wall crack)**

For analysis of circumferential cracks, standard pipe (beam) elements can be used for the bulk of the model. Shell elements can also be used for the circumferential crack analyses. For axial cracks, shell elements or beam elements with extra shell hoop behavior modes will be required since most beam-based pipe elements only consider beam bending behavior.

### C.3 Level 3 LBB Acceptance Criterion

A piping system would pass the Level 3 LBB acceptance criterion if the load applied in the finite element analysis to the postulated leaking crack (with the prescribed safety factor applied to the crack size), is less than the maximum load carrying capacity of the crack as calculated in Section C.2.4. The postulated leaking crack in this Level 3 analysis is the same leakage crack size calculated during the Level 2 analysis.

### C.4 Level 3 Analysis Procedures

The procedures for conducting a Level 3 analysis are as follows:

#### General Set-Up

1. Make sure that the piping system meets all of the qualifications of the Level 2 analysis except for the fracture margin.

2. Build the basic piping finite element model including all boundary conditions (supports and anchors, snubbers, etc.). If the time history of loading is seismic anchor motion and inertial loads, the model only needs to consider the piping system from anchor to anchor. If the time history of loading is ground acceleration, the model must include a representation of the building foundation, the building, and the relevant members inside the building that affect the motion of the anchors of the pipe system. The piping model can be built from beam-type elements or shell elements. The building/foundation model, if needed, can be built from any number of different elements, so long as the correct interface to the pipe model is made. Structural damping, as appropriate to the type of system and construction should be included in the model.
3. Define the static loading – pressure, dead weight, thermal loading, etc. As appropriate, positionally varying loads, such as thermal gradients (thermal stratification), must be considered.
4. Define the SSE loading as a time history at a suitably fine time step. Defining the loading at a fine enough time step may

require interpolation. The interpolation should be done in the frequency domain (Ref. C.1) to preserve the spectral content of the interpolated signal. Failure to perform the interpolation in the frequency domain can introduce discontinuities in response, particularly if displacements (seismic anchor motions) are interpolated.

#### Analysis Considering Crack Nonlinear Behavior

5. Define the crack load-displacement behavior. In general, the crack behavior will come directly from the Level 2 analysis and will be given in moment-rotation or hoop load-COD coordinates.
6. Convert the crack load-displacement behavior into a finite element representation. For circumferential cracks, the load-displacement behavior can be converted to finite elements using a hinge with nonlinear springs across the hinge (Ref. C.2). Special considerations must be given to cracks when they unload. For axial cracks, the crack can be modeled as a shell with nonlinear properties over part of the circumference. Line-spring elements in a shell model can be used to model either circumferential or axial cracks. The effect of crack closure can be modeled as very stiff springs with a gap that comes into play when the crack displacements go negative.
7. Put the finite elements representing the crack into the piping system model. The crack must be oriented in a direction that can be technically justified.

#### Analysis Considering Plasticity Remote from the Crack

8. Define the true stress-true strain behavior of the piping system materials.
9. Invoke the necessary plastic analysis procedures in the finite element analysis.

#### Finite Element Runs

10. Run the finite element time history analysis, ensuring that convergence has been met. Depending on the severity of the plasticity that the loading invokes, the time step increment may need to be reduced to a very small value (some small fraction of a millisecond) in order to have a successful run.
11. Extract the relevant applied load response data (load or moment) from the finite element time history at the crack location.

#### LBB Assessment

12. If the applied load in the nonlinear finite element analysis is less than the maximum load capacity of the postulated leakage crack (with the prescribed safety factor on crack size applied), then LBB is satisfied.

The Level 3 analysis considers all of the loads applied to the crack and correctly phased. Thus, there is no need to be concerned about how the various components of load are combined (algebraic, absolute sum, etc.) because they are always automatically summed algebraically.

It may be necessary to consider multiple nonlinear analyses to assure LBB because of the non-deterministic nature of the SSE loading. Experience has shown that multiple seismic time histories derived from the same response spectrum can have very different time history effects on a crack (Ref. C.3). A single time history can be used, provided that it meets certain duration, spectrum enveloping, frequency density, and PSD specifications (Ref. C.4).

#### C.5 References

C.1 Smith, Strether, "Filling in the Gaps: Interpolation of Sparse Time-History Data", *Sensors Magazine*, September 1994, pp. 62-71.

C.2 Olson, R.J., Wolterman, R.L., Wilkowski, G.M., and Kot, C.A., "Validation of Analysis Methods for Assessing Flawed Piping Subjected

to Dynamic Loading”, NUREG/CR-6234,  
August 1994.

C.3 Rahman, S., Olson, R., Rosenfield, A., and  
Wilkowski, G., “Summary of Results from the  
IPIRG-2 Round-Robin Analyses”, NUREG/CR-  
6337, February 1996.

C.4 US NRC, “Seismic Design Parameters”,  
Standard Review Plan 3.7.1- Revision 2, August  
1989.

**APPENDIX D**

**EVALUATION OF THE TIERED APPROACH TO LBB**

In evaluating the various levels of the tiered approach to LBB, a number of actual piping systems from nuclear power plants were evaluated. The details of these piping systems were gleaned from actual LBB submittals provided to Battelle and Engineering Mechanics Corporation of Columbus (Emc<sup>2</sup>) by the NRC as part of Task 2 of this program. For the Level 1 evaluations, five different piping systems were considered. For one of these piping systems, multiple load cases were considered. Due to the added complexity associated with the Level 2 and 3 approaches, only two piping systems (with multiple load cases) were considered during the Level 2 analyses and only a single piping system/load case was considered as part of the Level 3 analyses. Table D.1 provides a summary of the piping systems and load cases used in the evaluation of the various levels of the proposed tiered approach for LBB. Tables D.2 and D.3 provide a summary of the material data used in these evaluations. Table D.2 summarizes the data used in the leakage crack size analyses (i.e., mean data) and Table D.3 summarizes the data used in the critical crack size analyses (i.e., lower bound data). Table D.4 summarizes the load cases evaluated in the analyses of the one of the surge lines considered, i.e., Test Cases 1 and 2.

For the evaluation of the Level 2 methodology, only a surge line and a 6-inch diameter safety injection system (SIS) line were considered. For the surge line, two different load cases were considered. In addition, two different leak rate detection limit capabilities were assumed during the Level 2 analysis of both of these piping systems. Furthermore, for the Level 2 analyses, four different sets of boundary conditions were considered for each test case. The four sets of boundary conditions, representing different assumed degrees of restraint of pressure induced bending effects, are:

- unrestrained axial tension (typical of past LBB analyses),
- restrained axial tension with symmetric restraint lengths ( $L_1/D = L_2/D = 1$ ), where the restraint lengths  $L_1$  and  $L_2$  are the distances from the postulated crack plane to the nearest restraint on each

- side of the crack plane, e.g., hanger, nozzle, etc., and  $D$  is the pipe diameter,
- restrained axial tension with unsymmetric restraint lengths ( $L_1/D = 1$  and  $L_2/D = 10$ ), and
- restrained axial tension with unsymmetric restraint lengths ( $L_1/D = 1$  and  $L_2/D = 20$ ).

For the Level 3 analyses, only one analysis was conducted. It was a modified surge line analysis where the maximum moment for the faulted condition (Load Case E) was arbitrarily increased such that the piping system would not pass Level 2. Thus, if this piping system passed Level 3 for this modified load case, this would demonstrate the benefit of invoking a Level 3 type analysis. The moment-rotation curve used for the postulated crack length for this Level 3 analysis was based on the unrestrained axial tension case (typical of past LBB analyses) for Load Case B, for the case of a 1.9 lpm (0.5 gpm) leak rate detection limit capability for the postulated crack location where the surge line joins to the pressurizer. No Level 3 analyses were made for the restrained axial tension cases.

In addition to evaluating each of the above piping systems using the proposed three-tiered approach for LBB, in some cases, LBB results from the actual LBB submittals provided to Battelle and Emc<sup>2</sup> by the NRC were available as a baseline comparison. By comparing the results from the various levels of the three-tiered approach with these baseline results, it is possible to ascertain the level of conservatism associated with each of the proposed levels of analyses.

Table D.5 shows the postulated leakage size cracks from the proposed three-tiered approach. Table D.5 also shows the postulated leakage size cracks as reported in the applicant's LBB submittals supplied to Battelle and Emc<sup>2</sup> by the NRC. Table D.6 presents the calculated critical flaw sizes based on the draft SRP 3.6.3 procedures and the LBB.ENG2 J-estimation scheme approach. The reported critical flaw sizes from the applicant's LBB submittals are also provided in Table D.6 for comparison.

In comparing the postulated leakage size cracks in Table D.5 from the various analysis methods, it can be seen that the Level 1 method tends to result in the most conservative assessment of the leakage size cracks, i.e., the longest postulated cracks. Furthermore, the Level 1 leakage crack sizes using the shell-theory based equations are on average approximately 35 percent longer than the Level 1 leakage crack sizes calculated using the Level 1 influence functions. The only minor exception to this is the RHR line (Test Case 7) where the Level 1 leakage crack (based on the influence functions) is slightly shorter than the leakage crack extracted from the applicant's LBB submittal.

Of further note from Table D.5 is the fact that the effect of axial tension restraint (pressure induced bending effects) is insignificant for the 14-inch diameter surge line. However, for the smaller 6-inch nominal diameter safety injection system (SIS) line, the effect is much larger, especially for the case of symmetric restraint where the restraints are near the crack plane (i.e.,  $L_1/D = L_2/D = 1$ ). For this particular piping system, the postulated leakage size crack for the restrained case is 25 to 40 percent longer than for the unrestrained case.

Finally, it is of note from Table D.5 that the leakage size cracks extracted from the actual LBB submittals tended to be significantly shorter than the calculated leakage size cracks calculated using the proposed tiered approach for LBB. This is possibly an artifact of the applicant's use of a proprietary leak rate code with lower bound surface roughness values. As part of the COD/leak rate code sensitivity study conducted as part of this program, it was shown that the use of their approach was nonconservative with respect to the practices recommended for a Level 2 type analysis.

One point of note from Table D.6 is the comparison of the calculated critical flaw sizes based on the draft SRP 3.6.3 procedures with reported values from the actual LBB submittals supplied by the NRC. The draft SRP 3.6.3 procedure for calculating the critical crack lengths is basically an ASME Section XI Appendix C approach in which the crack length

is incrementally increased until the allowable stresses for that crack size equal the applied stresses at the transient faulted condition. In comparing the calculated critical crack sizes from the draft SRP procedures with the reported values from the LBB submittals, it can be seen that the reported values tend to be 10 to 20 percent longer than draft SRP calculated values.

**Table D.1 Input parameters for piping system test cases used to evaluate the different levels of the proposed LBB methodology**

Test Case	Piping System	Outside Diameter, inch	Wall Thickness, mm (inch)	Pressure, MPa (psi)	Normal Operating Temperature, C (F)	Moment at Normal Operating Conditions, kN-m (in-kips)	Normal Operating Stress, MPa (ksi)	Temperature at Faulted Conditions, C (F)	Moment at Faulted Conditions, kN-m (in-kips)	Faulted N+SSE Stress, MPa (ksi)	Leak Rate Detection Capability, lpm (gpm)
1	Surge Line (B/E Load)	14	35.7 (1.406)	16.0 (2,327)	345 (653)	199.5 (1,766.2)	105.4 (15.28)	345 (653)	241.6 (2,138.3)	122.5 (17.76)	1.9 & 3.8 (0.5 & 1.0)
2	Surge Line (B/F Load)	14	35.7 (1.406)	16.0 (2,327)	345 (653)	174.6 (1,545.8)	94.2 (13.66)	96 (205)	370.9 (3,282.8)	148.6 (21.55)	1.9 & 3.8 (0.5 & 1.0)
3	SIS Cold Leg C	6.625	18.2 (0.718)	16.0 (2,327)	41 (105)	15.4 (136.5)	77.8 (11.28)	41 (105)	18.2 (161.1)	88.5 (12.84)	0.95 & 1.9 (0.25 & 0.5)
4	Cross Over Leg	37.5	80.0 (3.15)	15.2 (2,200)	283 (542)	1559.7 (13,805)	67.7 (9.82)	283 (542)	3487.0 (30,864)	114.3 (16.58)	3.8 (1.0)
5	Surge Line (B/G Load)	10.75	22.2 (0.875)	15.5 (2,250)	345 (653)	46.2 (408.5)	81.2 (11.78)	235 (455)	194.8 (1724.4)	201.1 (29.16)	3.8 (1.0)
6	RCS Bypass	8.625	23.0 (0.906)	16.0 (2,327)	285-323 (545-613)	21.7 (192.2)	60.8 (8.82)	285-323 (545 to 613)	24.4 (215.7)	66.7 (9.67)	1.9 (0.5)
7	RHR	12.75	33.3 (1.312)	16.0 (2,327)	323 (613)	14.6 (129.3)	34.5 (5.00)	323 (613)	77.6 (686.5)	67.1 (9.72)	1.9 (0.5)
8	Level 3 Test Case <sup>(1)</sup>	14	35.7 (1.406)	16.0 (2,327)	345 (653)	199.5 (1,766.2)	105.4 (15.28)	345 (653)	361.5 (3,200)	168.3 (24.41)	3.8 (1.0)

(1) Test Case 1 assuming a 1.9 lpm (0.5 gpm) leak rate detection capability, except the moment at the faulted condition was increased to demonstrate the benefits of applying a Level 3 type analysis.

**Table D.2 Mean material property data used for leakage flaw size analyses**

Test Case	Piping System	Mat'l	Yield Strength, MPa (ksi)	Ultimate Strength, MPa (ksi)	Elastic Modulus, GPa (ksi)	$\epsilon_0$	$\alpha$	n
1, 2	Surge Line (Load Cases B/E and B/F)	TP304	154.8 (22.45)	442.4 (64.16)	179 (26,000)	0.000863	6.5	3.8
3	SIS Cold Leg C	TP316	262 (38.0)	558 (81.0)	193 (28,000)	0.001357	5.58	4.77
4	Cross Over Leg	CF8A	192 (27.8)	450 (65.2)	179 (26,000)	0.001069	-	-
5	Surge Line (Load Case B/G)	TP316	188 (27.3)	-	173 (25,030)	0.001090	-	-
6	RCS Bypass	TP304	185 (26.8)	456 (66.2)	176 (25,500)	0.001051	3.25	7.31
7	RHR	TP316	169 (24.5)	469 (68.0)	176 (25,500)	0.000961	3.75	4.82
8	Level 3 Test Case	TP304	154.8 (22.45)	442.4 (64.16)	179 (26,000)	0.000863	6.5	3.8

**Table D.3 Lower bound material property data used for critical crack size stability analyses**

Test Case	Piping System	Yield Strength, MPa (ksi)	Ultimate Strength, MPa (ksi)	Elastic Modulus, GPa (ksi)	$\epsilon_0$	$\alpha$	n	J-R Curve
1	Surge Line (B/E)	130 (18.8)	379 (55.0)	179 (26,000)	0.000723	9.12	3.8	Figure D.1
2	Surge Line (B/F)	237 (34.4)	525 (76.1)	190 (27,600)	0.001246	-	-	Figure D.1
3	SIS Cold Leg C	207 (30.0)	517 (75.0)	-	-	-	-	Figure D.1
4	Cross Over Leg	153 (22.2)	450 (65.2)	179 (26,000)	0.000854	NA	NA	Figure D.1
5	Surge Line (B/G)	150 (21.8)	498 (72.2)	180 (26,100)	0.000835	NA	NA	Figure D.1
6	RCS Bypass	163 (23.7)	427 (61.9)	176 (25,500)	0.000929	7.3	8.9	Figure D.1
7	RHR	163 (23.7)	427 (61.9)	176 (25,500)	0.000929	7.3	8.9	Figure D.1
8	Level 3 Test Case	130 (18.8)	379 (55.0)	179 (26,000)	0.000723	9.12	3.8	Figure D.1

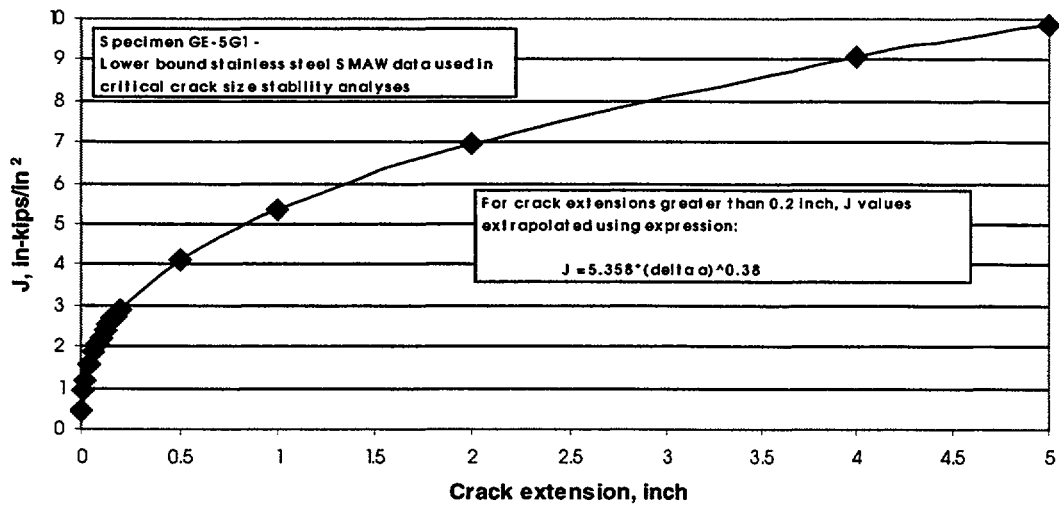


**Figure D.1 Lower bound stainless steel SMAW J-R curve used in critical crack size/crack stability analyses**

**Table D.4 Description of normal operating and faulted load cases considered in the evaluation of three-tiered LBB analysis of one of the surge lines considered, i.e., Test Cases 1 and 2**

Load Case	Description of Load Case	Normal Operating or Faulted Condition <sup>(1)</sup>
A	Normal operating case at 345C (653F) consisting of the algebraic sum of the loading components due to P, DW, and TH <sup>(2)</sup> .	Normal Operating
B	Normal operating case at 345C (653F) consisting of algebraic sum of the loading components due to P, DW, and ST <sub>345/20</sub> .	Normal Operating
C	Heatup/cooldown case at temperatures between 60C (140F) and 235C (455F) with stratification consisting of the algebraic sum of the load components due to P, DW, and ST <sub>235/175</sub> .	Normal Operating
D	Faulted operating case at 345C (653F) consisting of the absolute sum (every component of load is taken as positive) of P, DW, TH, and SSE.	Faulted
E	Faulted operating case at 345C (653F) consisting of the absolute sum of P, DW, ST <sub>653/36</sub> , and SSE.	Faulted
E'	Variant of Load Case E used in Level 3 analysis with a larger SSE load which would cause postulated crack from Load Case B (with safety factor of 2.0 applied) to fail.	Faulted
F	Forced cooldown case at temperatures between 96C (205F) and 235C (455F) with stratification consisting of the absolute sum of P, DW, and ST <sub>235/139</sub> .	Faulted
G	Faulted heatup/cooldown case at temperature between 60C (140F) and 235C (455F) with stratification consisting of the absolute sum of P, DW, ST <sub>235/175</sub> , and SSE <sup>(3)</sup> .	Faulted

(1) Normal operating loads used in postulated leakage size crack analysis while faulted load cases used in critical flaw size analysis.

(2) P = pressure, DW = dead weight, TH = thermal, ST<sub>345/20</sub> = stratification stress due to normal operating temperature of 345C (653F) and stratification  $\Delta T = 20C$  (36F), and SSE = safe shutdown earthquake stress.

(3) Very low probability event during which earthquake occurs while on hold during a heatup or cooldown with stratification ( $\Delta T = 175C$  [315F]). Typically not considered by NRC during LBB assessment.

**Table D.5 Postulated leakage size cracks from the proposed three-tiered approach plus reported values from an applicant's actual LBB submittals**

Test Case	Piping System	Leak Rate Detection Capability, lpm (gpm)	Postulated Leakage Size Cracks, mm (inches)							
			Level 1 using influence functions	Level 1 using shell-theory based equation	Level 2 Unrestrained Axial Tension	Level 2 Restrained Axial Tension L <sub>1</sub> /D = 1, L <sub>2</sub> /D = 1	Level 2 Restrained Axial Tension L <sub>1</sub> /D = 1, L <sub>2</sub> /D = 10	Level 2 Restrained Axial Tension L <sub>1</sub> /D = 1, L <sub>2</sub> /D = 20	Level 3 Unrestrained Axial Tension	From Applicant's LBB Submittal
1	Surge Line (Load Case B/E)	1.9 (0.5)	159 (6.25)	262 (10.3)	89.7 (3.53)	98.0 (3.86)	92.2 (3.63)	90.9 (3.58)	-	71.1 (2.80)
1	Surge Line (Load Case B/E)	3.8 (1.0)	210 (8.25)	340 (13.4)	114 (4.47)	125 (4.91)	117 (4.60)	115 (4.54)	-	-
2	Surge Line (Load Case B/F) <sup>1</sup>	1.9 (0.5)	166 (6.55)	262 (10.3)	99.1 (3.90)	109 (4.28)	102 (4.01)	101 (3.96)	-	78.7 (3.10)
2	Surge Line (Load Case B/F) <sup>1</sup>	3.8 (1.0)	218 (8.60)	340 (13.4)	125 (4.91)	137 (5.40)	128 (5.05)	127 (4.99)	-	-
3	SIS Cold Leg C	0.95 (0.25)	-	-	101 (3.96)	124 (4.89)	107 (4.22)	103 (4.06)	-	-
3	SIS Cold Leg C	1.9 (0.5)	-	-	116 (4.57)	164 (6.47)	130 (5.13)	122 (4.82)	-	108 (4.26)
4	Cross Over Leg	3.8 (1.0)	271 (10.65)	348 (13.7)	-	-	-	-	-	173 (6.80)
5	Surge Line (Load Case B/G)	3.8 (1.0)	203 (8.00)	272 (10.7)	-	-	-	-	-	109 (4.30)
6	RCS Coolant Bypass Line	1.9 (0.5)	151 (5.95)	204 (8.05)	-	-	-	-	-	144 (5.67)
7	RHR	1.9 (0.5)	210 (8.28)	230 (9.05)	-	-	-	-	-	212 (8.36)
8	Level 3 Test Case (B/E')	1.9 (0.5)	-	-	-	-	-	-	89.7 (3.53) <sup>2</sup>	-

(1) Differences in postulated crack lengths for Test Cases 1 and 2 are due to differences in the location of the postulated cracks even though the evaluations were made for the same load case (i.e., Load Case B). Postulated crack location for Test Case 1 was at the location where the surge line joins the pressurizer while for Test Case 2 the postulated crack location was at the location where the surge line joins the hot leg.

(2) Same postulated leakage size crack as for Test Case 1, Level 2 analysis (unrestrained axial tension) for 1.9 lpm (0.5 gpm) leakage detection capability.

**Table D.6 Calculated critical flaw sizes based on draft SRP 3.6.3 procedures and the LBB.ENG2 J-estimation scheme plus reported values from LBB submittals supplied by the NRC**

Test Case	Piping System	Critical Flaw Size Based on Draft SRP 3.6.3 Procedures, mm (inch)	Critical Flaw Size Based on LBB.ENG2 J-estimation Scheme Procedures, mm (inch)	Reported Critical Crack Size from Applicant's LBB Submittal, mm (inch)
1	Surge Line (Load Case B/E)	328 (12.9)	262 (10.3)	427 (16.8)
2	Surge Line (Load Case B/F)	396 (15.6)	-	404 (15.9)
3	SIS Cold Leg C	244 (9.60)	-	273 (10.74)
4	Cross Over Leg	879 (34.6)	-	Not Reported
5	Surge Line (Load Case B/G)	196 (7.70)	-	202 (7.95)
6	RCS Coolant Bypass Line	320 (12.6)	272 (10.7)	379 (14.91)
7	RHR	462 (18.2)	395 (15.55)	641 (25.25)
8	Level 3 Test Case – straight linear analysis (Load Case E'); $M_{max} = 345.9$ kN-m (3,061.7 in-kips)	-	179 (7.06)	-
8	Level 3 Test Case – nonlinear crack plus linear pipe beam elements (Load Case E'); $M_{max} = 291.1$ kN-m (2,576.5 in-kips)	-	214 (8.41)	-
8	Level 3 Test Case – nonlinear crack plus nonlinear pipe beam elements (Load Case E'); $M_{max} = 267.9$ kN-m (2,371.4 in-kips)	-	231 (9.11)	-

**Table D.7 Comparison of ratios of critical crack sizes to leakage crack sizes using proposed three-tiered approach plus values reported in an applicant's actual LBB submittals**

Test Case	Piping System	Leak Rate Detection Capability, lpm (gpm)	Ratio of Critical Crack sizes to Postulated Leakage Crack Sizes							From Applicant's LBB Submittal
			Level 1 using influence functions	Level 1 using shell-theory based equations	Level 2 Unrestrained Axial Tension	Level 2 Restrained Axial Tension $L_1/D = 1, L_2/D = 1$	Level 2 Restrained Axial Tension $L_1/D = 1, L_2/D = 10$	Level 2 Restrained Axial Tension $L_1/D = 1, L_2/D = 20$	Level 3 Unrestrained Axial Tension	
1	Surge Line (Load Case B/E)	1.9 (0.5)	2.06 (1.65) <sup>1</sup>	1.25 (1.00)	3.65 (2.92)	3.34 (2.67)	3.55 (2.84)	3.60 (2.88)	-	6.0
1	Surge Line (Load Case B/E)	3.8 (1.0)	1.56 (1.25)	0.96 (0.77)	2.89 (2.30)	2.63 (2.10)	2.80 (2.24)	2.84 (2.27)	-	-
2	Surge Line (Load Case B/F)	1.9 (0.5)	2.38	1.51	4.08	3.64	3.89	3.94	-	5.13
2	Surge Line (Load Case B/F)	3.8 (1.0)	1.81	1.16	3.17	2.89	3.09	3.13	-	-
3	SIS Cold Leg C	0.95 (0.25)	-	-	2.42	1.96	2.27	2.36	-	-
3	SIS Cold Leg C	1.9 (0.5)	-	-	2.10	1.48	1.87	1.99	-	-
4	Cross Over Leg	3.8 (1.0)	3.25	2.53	-	-	-	-	-	-
5	Surge Line (Load Case B/G) <sup>2</sup>	3.8 (1.0)	0.96	0.72	-	-	-	-	-	1.85
6	RCS Coolant Bypass Line	1.9 (0.5)	2.12	1.57	-	-	-	-	-	2.63
7	RHR	1.9 (0.5)	2.20	2.01	-	-	-	-	-	3.02
8	Level 3 Test Case (Load Case E')	1.9 (0.5)	-	-	2.00 <sup>3</sup>	-	-	-	2.38 <sup>4</sup> 2.58 <sup>5</sup>	-

- (1) Numbers without parentheses are based on calculating the critical crack sizes using the draft SRP 3.6.3 procedures while numbers in parentheses are based on calculating the critical crack sizes using the LBB.ENG2 J-estimation scheme analysis method.
- (2) Consideration of load case "G" is beyond the scope of what is currently considered for a surge line LBB analysis by the USNRC due to the very low probability of such an event occurring.
- (3) Straight linear finite element analysis used in calculation of critical crack length
- (4) Nonlinear crack plus linear pipe elements used in calculation of critical crack length
- (5) Nonlinear crack plus nonlinear pipe elements used in calculation of critical crack length

Table D.7 shows a comparison of the ratios of the critical crack sizes (Table D.6) to the postulated leakage crack sizes (Table D.5). For a piping system to pass LBB, this ratio of the critical crack length to the leakage crack length should be greater than 2.0.<sup>1</sup> Table D.7 shows these ratios for each of the piping systems and load cases from Table D.1 for all three levels of the tiered approach. In addition, the ratios of the critical crack sizes to the leakage size cracks as reported in the actual LBB submittals supplied by the NRC are also shown.

Of particular note from Table D.7 are the results from the Level 3 analysis of one of the surge lines considered, Test Case 8. For this analysis, a factor of safety of 2.0 was applied to the postulated leakage size crack (89.7 mm [3.53 inches]) from the Level 2 analysis for Load Case B for the case of the 1.9 lpm (0.5 gpm) leakage detection limit capability. An LBB.ENG2 analysis was then conducted using this crack size (with safety factor of 2) to estimate the maximum moment capacity of the cracked pipe section. The maximum moment from this LBB.ENG2 analysis was 345.9 kN-m (3,061.7 in-kips).

Next, a scaled version (Load Case E') of the Load Case E seismic load history was applied to a straight linear analysis of the surge line, i.e., an uncracked analysis. The magnitude of the load history was scaled such that the maximum moment obtained was 345.9 kN-m (3,061.7 in-kips). This scaled load history ended up being a 0.657 g seismic event. The next analysis conducted was another finite element analysis of the surge line, using the same scaled forcing function, except the nonlinear characteristics of the crack were introduced at the location where the surge line joins to the pressurizer. The remainder of the piping system was still model with linear pipe elements. The maximum moment obtained at the postulated crack location (surge line/pressurizer weld) for this analysis was 291.1 kN-m (2,576.5 in-kips). The

---

<sup>1</sup> Assuming the new NRC Regulatory Guide for LBB specifies the same factor of safety of 2 on crack size as now incorporated in draft SRP 3.6.3.

final finite element analysis conducted was another nonlinear analysis, except this time the pipe elements were allowed to undergo nonlinear behavior in addition to the crack section. The maximum moment at the postulated crack location for this fully nonlinear analysis was 267.9 (2,371.4 in-kips).

The LBB.ENG2 J-estimation scheme within NRCPIPE was then again exercised to determine the critical crack lengths for these two nonlinear analyses, i.e., the crack lengths that corresponded to the maximum moments from the two nonlinear finite element analyses. The results of those calculations are shown in Table D.6.

From Table D.7, it can be seen that ratios of the critical crack lengths to the postulated leakage crack size (3.53 inches) for these three levels of analyses were:

- 2.0 for the straight linear analysis (i.e., a Level 2 analysis),
- 2.38 for the Level 3 analysis in which nonlinearity was only introduced at the crack, and
- 2.58 for the Level 3 analysis in which nonlinearity was introduced both at the crack and in the rest of the piping system.

Consequently, invoking a Level 3 type analysis in this application resulted in an additional margin on crack length of 20 to 30 percent depending on the extent of nonlinearity introduced into the analysis.

**APPENDIX E**

**THE DEVELOPMENT OF A J-ESTIMATION SCHEME FOR  
CIRCUMFERENTIAL AND AXIAL  
THROUGH-WALL CRACKED ELBOWS**

## **E.1 Introduction**

Leak before break (LBB) considerations for pipe fittings such as tee joints and elbows have not been investigated in detail to date. Reference E.1 presented the development of a surface crack estimation scheme for elbows. These solutions were then used to investigate the possibility of using simple influence functions, based on ASME Section III stress indices, along with existing straight pipe solutions, to predict the fracture response of a surface-cracked elbow. The use of this small database of influence functions, combined with existing straight pipe J-estimation methods showed promise in predicting the fracture response of the surface-cracked elbows.

However, in order to perform LBB sensitivity studies on fittings, such as elbows, TWC solutions must be available. With the TWC elbow solutions available, one can investigate the feasibility of using influence functions and straight pipe TWC solutions to predict the LBB behavior of fittings. The main purpose of this effort is to provide a new J-estimation scheme for TWC elbows. Both circumferential and axial cracks are considered. In addition, crack-opening displacements can be estimated so that LBB considerations can be assessed.

## **E.2 Background on Piping J-Estimation Schemes**

The nuclear industry has traditionally taken the lead in the development of J-estimation schemes to allow engineers to make estimates of the fracture behavior of nuclear piping components. These J-estimation schemes have permitted engineers to make simple fracture assessments of planar component geometries (Ref. E.2), through-wall-cracked (TWC) pipes (Ref. E.3), as well as surface-cracked (SC) pipe (Ref. E.4). This early work sometimes had inaccuracies implicit within the solutions, in part due to the fact that the finite element methods used at that time were not quite fully developed, nor as robust as today's numerical tools.

Corrections and improvements to pipe fracture J-estimation schemes were made subsequent to

this original work. References E.5 and E.6 represent the development of alternative J-estimation schemes for TWC pipe which are not based on the compilation of a series of numerical solutions; rather these solutions were developed from making certain geometric assumptions. References E.7 and E.8 are similar non-finite element based J-estimation schemes for surface cracked pipe. References E.9 and E.10 represent the improvements and corrections to the original numerical solutions using improved numerical finite element techniques (compared with the original solutions) and permitted pipes with "small" cracks to be more accurately modeled. In addition, some of these methods were specifically developed to account for cracks in welds (Refs. E.8 and E.11). References E.8 to E.12, and many references cited therein, summarize many of these methods, both numerical and engineering based, and compare predictions to full-scale experimental test data.

The J-estimation schemes discussed above were appropriate for cracked pipe. Fracture estimates for more complicated geometries, such as pipe fittings, had to be performed on a case-by-case basis using finite element analysis. These analyses are time consuming, often requiring significant resources, and the results are only appropriate for the specific geometry and material considered. As such, the development of more general J-estimation schemes for pipe fittings, such as elbows and Tee joints, has begun. A surface crack estimation scheme for axial and circumferential cracked elbows was developed in Reference E.1.

The purpose of this effort is to develop a J-estimation scheme for axial and circumferential through-wall cracks in elbows. Solutions are compiled for the pure pressure, combined pressure and bending, and pure bending cases. However, before presenting these solutions, it is first instructive to discuss some unique features associated with fracture of elbows, which are not necessarily intuitive based on experience with straight pipe. Many of these anomalies are associated with the way that elbows ovalize.

### E.3 General Overview of Deformation and Fracture Response of Elbows

**E.3.1 Geometry** - The geometry of the cracked elbows considered here is illustrated in Figure E.1. We are interested in estimating J and crack opening displacement (COD) for both circumferential and axial 'flank' cracks. The ratio of  $R_{el}/R_m = 3$  here represents a long radius elbow. The loading cases considered are pure pressure, pure bending, and combined pressure and bending. The pressure loading turns out to be very important consideration for elbows. Note that the outer length of the elbow [i.e.  $(R_{el} + R_m/2) * \psi$ ] is greater than the inner length of the elbow [i.e.  $(R_{el} - R_m/2) * \psi$ ]. From the free body diagram alone, this means that the

integrated pressure along the outer length of the elbow is greater than that along the inside of the elbow, i.e., there is a net outward force that must be equilibrated by the end cap pressure T (see Figure E.1). This means that, due to pressure alone, the elbow wants to straighten out. Therefore, for the cases of pressure and combined pressure and bending, both the pressure and end cap tension must be applied. This is not the case for a straight pipe, where the pressure can be neglected when developing J-estimation schemes for circumferential cracks. It turns out that the effect of pressure also has an important effect on the ovalization of the elbow, which in turn, affects the J- and COD- solutions.

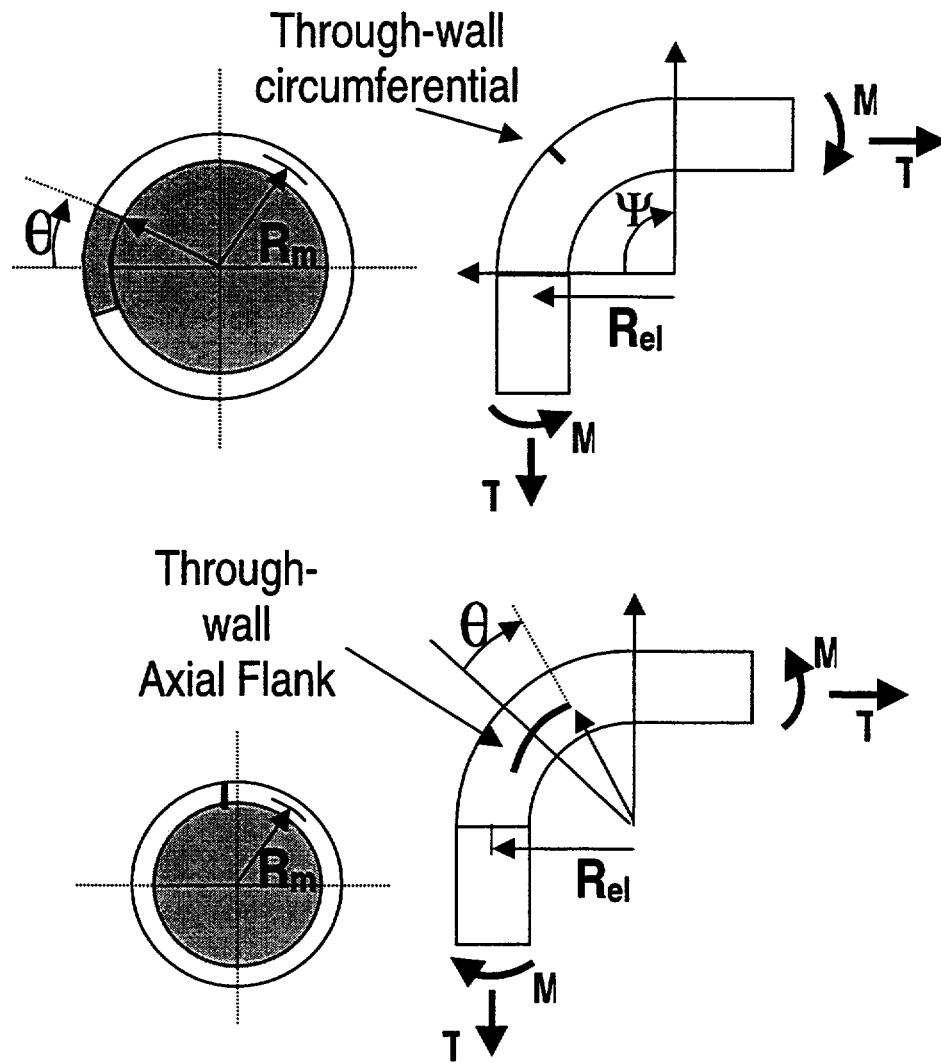
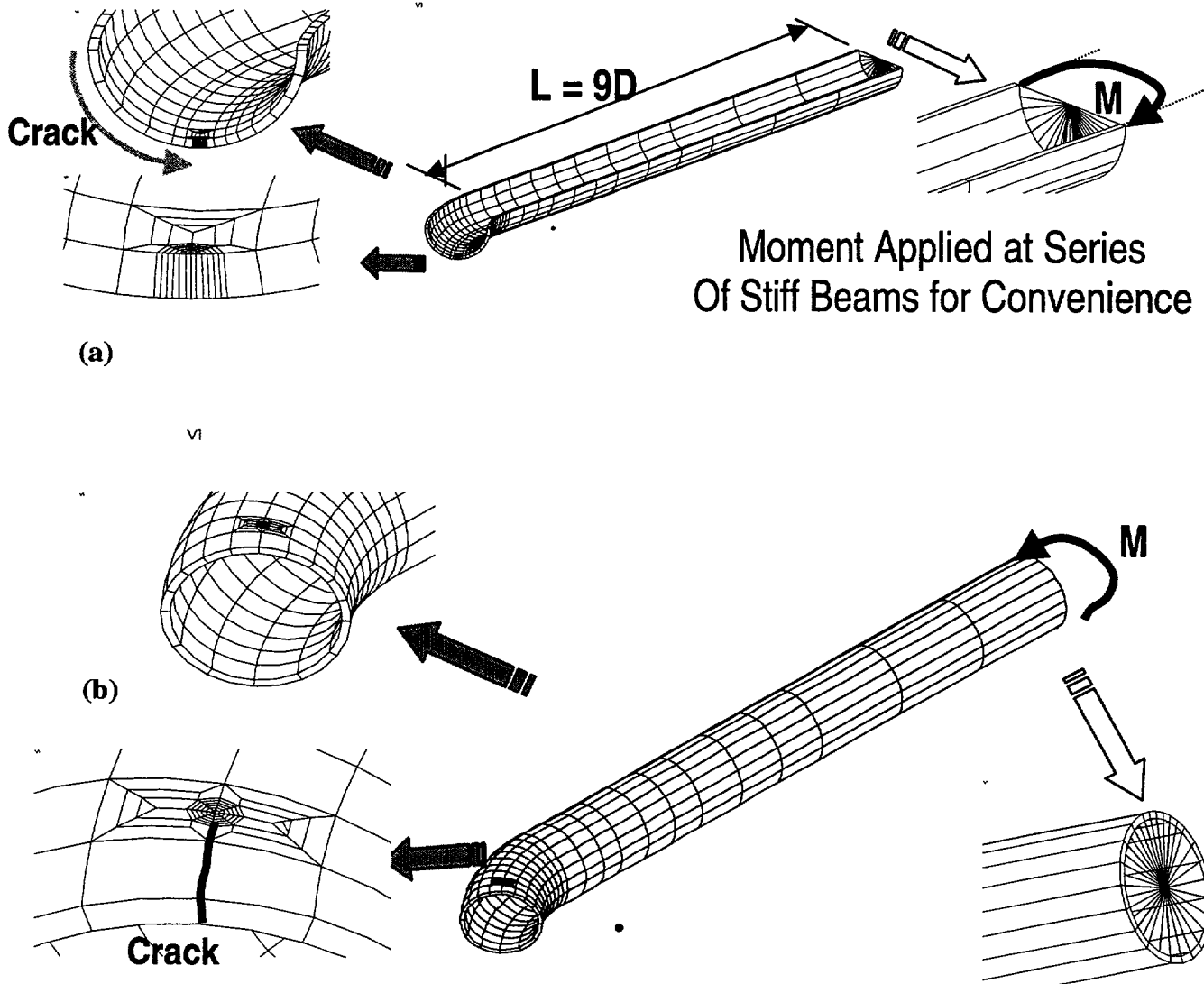


Figure E.1 Crack geometries considered for elbows

**E.3.2 Solution Procedure** - Figure E.2 shows a typical finite element mesh that was used for the analyses. Figure E.2(a) shows an example of a 90-degree circumferential crack in an elbow. A quarter model, with symmetry about the plane of the crack and a symmetry plane about the half crack length,  $\theta$ , was used to simplify the analyses. As seen in Figure E.2, a long length of straight pipe, equal to  $L = 9D$  (with  $D$  the diameter), was included in the model. At the end of the length of pipe, a series of very stiff beams were attached to the pipe, which met at a point node at the center of the pipe. The

bending moment,  $M$ , was applied at this node. The length,  $9D$ , was determined by performing a series of mesh sensitivity studies. This technique simplified the analysis procedure, the reduction of data, and assured that the elbow solutions were not distorted by end effects. Figure E.2(b) shows a typical mesh for a 15-degree axial crack. For the axial cracks, half symmetry models were used. For both circumferential and axial cracks, pressure along the entire inside pipe and elbow surfaces were included along with end cap pressure at the end of the long length of straight pipe.



**Figure E.2 Typical finite element mesh and model geometry for (a) a 90-degree circumferential crack and (b) a 15-degree axial flank crack**

The ABAQUS commercial finite element package was used for all analyses. The 20-node isoparametric brick element was used for all solutions. A deformation theory plasticity model was used, although, as will be seen later, flow theory was used for some of validation studies. Because the ABAQUS deformation solution procedure includes the elastic strains, each solution was monitored and considered complete (i.e., fully plastic) when the plastic

strain at each integration point became greater than ten times the elastic strain. As an independent check on the adequacy of the fully plastic solution, the h-functions (see next section), were plotted as a function of load at each load step in the analysis. Typically, h reached a constant, converged value long before the analysis was automatically completed using the criteria discussed above. The compilations of h-functions were performed using one element through the thickness, as illustrated in

Figure E.3. However, as seen in Figure E.3(b) several solutions were performed using a mesh with four elements through the thickness. The average J-integral, and COD, solutions for the four elements through the thickness mesh compared well with the results for the one element mesh. It is noted that there is a variation of J through the thickness, especially for the axial flank cracks, but the use of one, average value for J, is adequate for engineering estimation purposes. An extensive mesh sensitivity study was performed to ensure adequate solution convergence. The procedure was also validated by comparing results for known straight pipe solutions. Because of the use of parabolic elements, the values of J for the one element through the thickness meshes (Figure E.3(a)) were calculated using:

$$J_{AVG} = J_I + 4J_M + J_O,$$

where  $J_I$  is the value of J at the inner surface node at the crack,  $J_M$  is J at the mid side node, and  $J_O$  is J at the outside node.

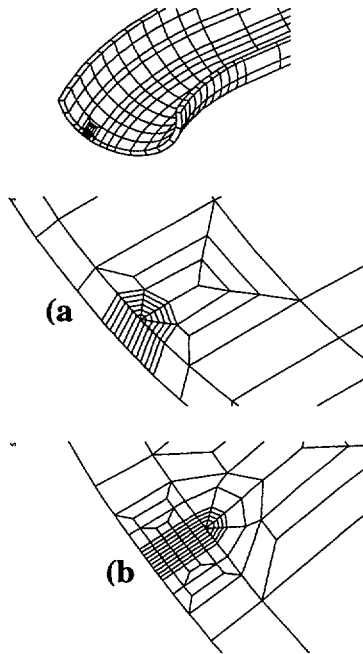


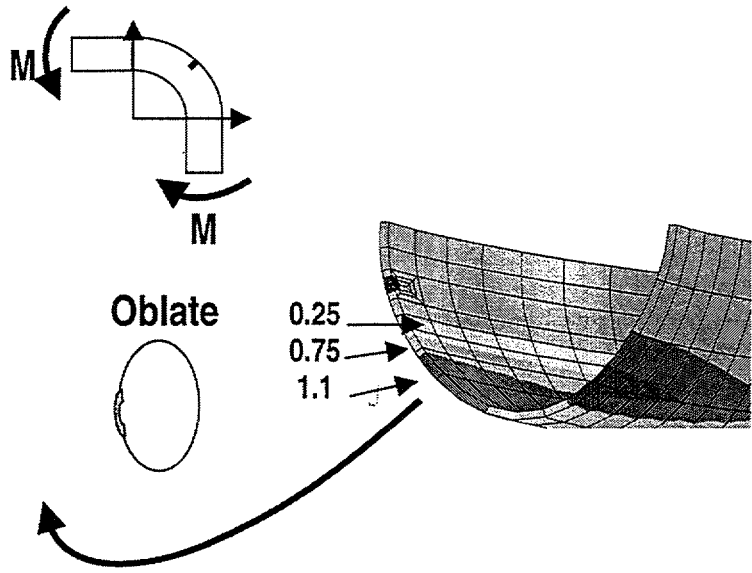
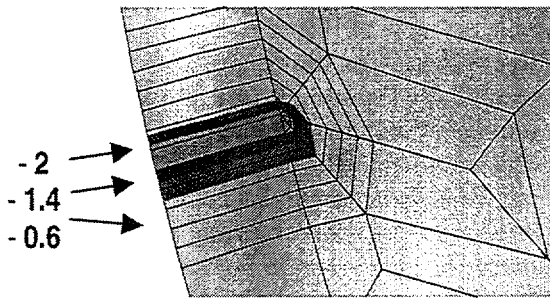
**Figure E.3. Typical mesh (circumferential crack, 45-degree crack) (a) one element through thickness (b) four elements**

## E.4 Ovalization Effects on Elbow Fracture

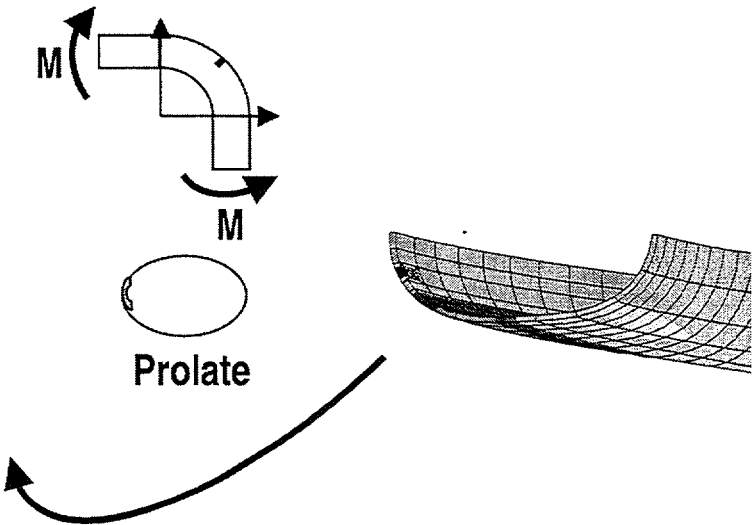
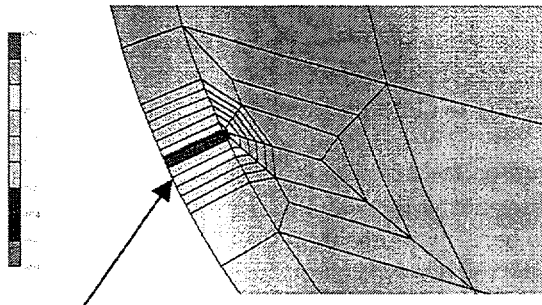
### E.4.1 Circumferential Cracks - The ovalizations induced in elbows that are subjected to bending loads turns out to have an important effect on the predicted J-integral, crack opening displacements, and fracture response. Consider the simple example of Figure E.4. In the upper plot (Figure E.4(a)), an illustration of a circumferentially cracked elbow subjected to a closing moment is shown. Intuitively, an elbow closing moment would be expected to open the crack, similar to what occurs in a straight length of pipe subjected to a crack opening moment. The illustration to the right in Figure E.4(a) shows a deformed plot caused by the applied moment. The shaded areas represent contour plots of the crack opening stress and the numbers represent normalized stress (normalized with yield stress). For this elastic case, the magnitude of the stresses is not important. Notice that the stresses are negative ahead of the crack. For the illustration in Figure E.4b, the moment was applied in the opposite direction, i.e., an elbow opening moment. For this case, a low level of tension exists ahead of the crack tip despite the fact that the moment is attempting to close the crack faces.

The reason for this somewhat surprising behavior lies in the way that the elbow ovalizes due to bending moment. As seen, the closing moment ovalizes the elbow cross section into the shape of an oblate spheroid while the elbow opening moment causes a prolate spheroid deformed shape. The case illustrated in Figure E.4 represents a radius to thickness ratio,  $R/t = 20$ . The same behavior occurs for  $R/t = 5$ , i.e. the stiffer case. In fact, for the un-cracked case, an elbow closing moment results in compressive stresses that develop up to an angle of between 20 and 25 degrees at the toe of the elbow, depending on the  $R/t$  ratio.

(a) Elbow Closing Moment

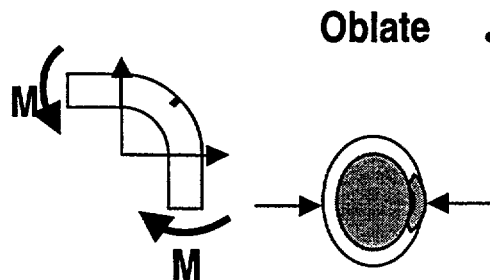


(b) Elbow Opening Moment



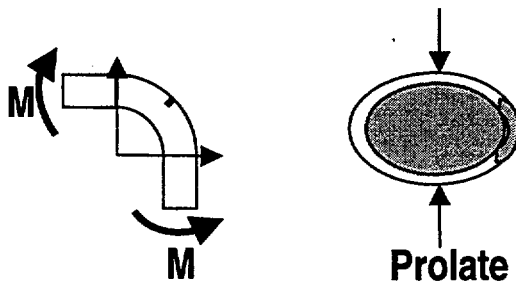
Tension (0.5)  
(Low Level)

Figure E.4 Illustration of ovalization effects on stresses near the crack tip (Numbers represent crack opening stresses normalized with yield strength)



### • Closing Moment

- Additional Compression at Crack
  - $R/t = 20$  (Full Closing)
  - $R/t = 10$  (OD Closing)
  - $R/t = 5$  (Opening - Reduced K or J)



### • Opening Moment

- Additional Tension at Crack

**Figure E.5 Summary of ovalization effects on crack opening response of circumferential cracks in elbows subjected to bending**

This response is further summarized in Figure E.5. The top illustration summarizes the response to an elbow closing moment. As illustrated, this results in an oblate spheroid type ovalization. As illustrated, one can think of this ovalization as being caused by 'pinching' forces applied along a plane at the center of the crack. This type of ovalization will induce a compressive contribution to the stress state in this region. Hence, there is a competition between the crack closing caused by ovalization, and the opening caused by the global bending load. It turns out that this competition is won by the ovalization component for crack sizes less than 20 to 25 degrees, depending on  $R/t$  ratio. For an elbow opening (or straightening) moment, bottom illustration in Figure E.5, the opposite occurs. The prolate type ovalization component causes crack opening while the

global moment closes the crack. This leads to a modest crack opening for smaller crack sizes. Because of this, **circumferential cracks are not expected to develop at the knee of the elbow.** Rather, they are expected to develop for crack size angles on the order of 45 to 90 degrees. The solutions tabulated below are compiled for crack sizes of 45 and 90 degrees. For these larger crack sizes, the cracks are open along the entire length.

**E.4.2 Axial Cracks** - For the axial flank cracks the ovalization effect on crack opening is even more important. Figure E.6 illustrates the response of an axial flank crack, with total crack size angle of 15-degrees, subjected to bending. An elbow straightening moment causes tensile opening stresses in the crack region (this is also an elastic case).

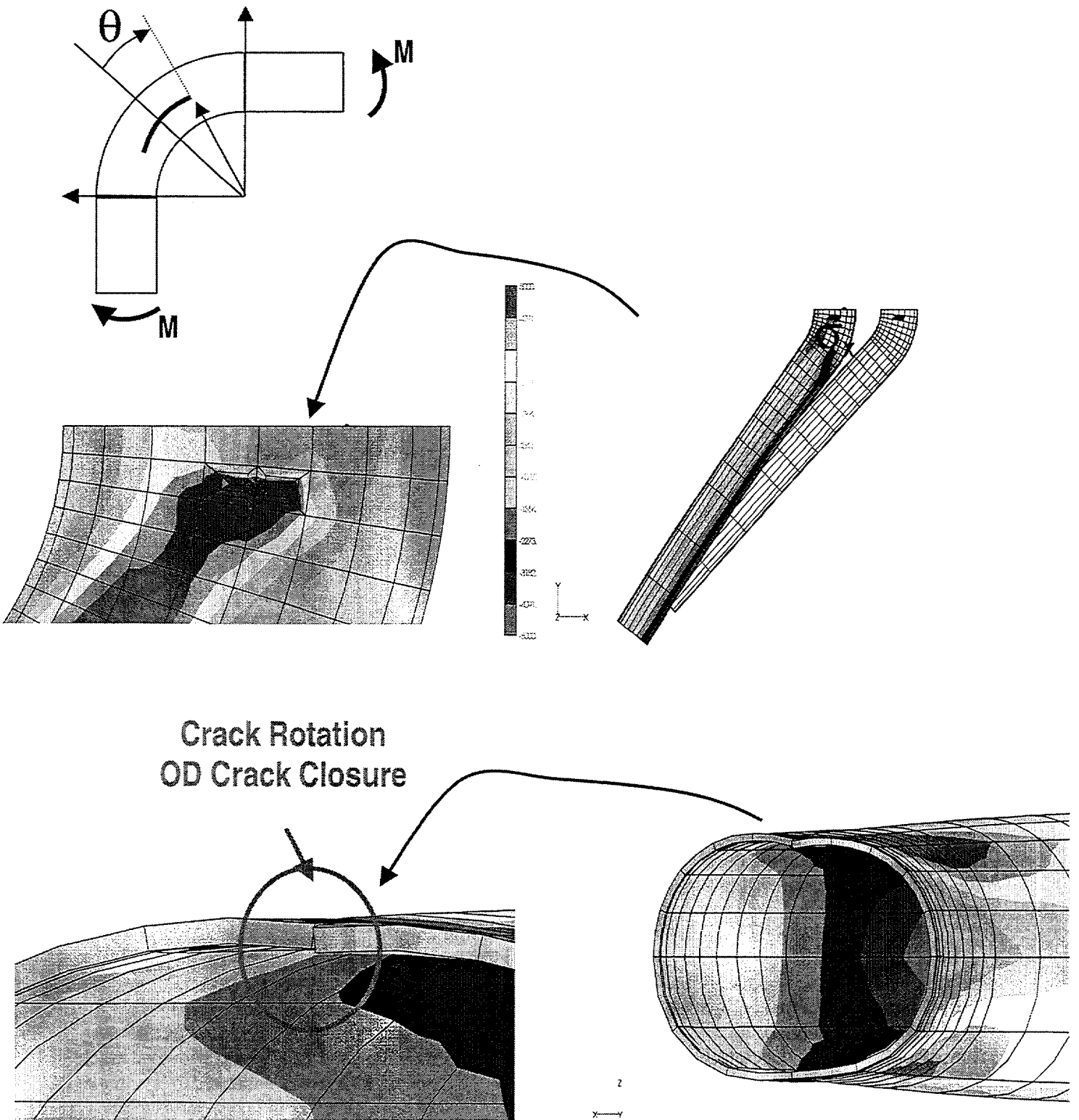


**Figure E.6 Illustration of ovalization effects for 15-degree axial flank crack**

The shaded contours on these plots represent the opening stress,  $\sigma_x$ , and all stress contours in the crack region are tensile. This means that the crack should open. However, it is also seen that the 'oblate' spheroid ovalization causes the crack faces to rotate, with the inner crack opening greater than the outer diameter opening. The example illustrated in Figure E.6 is for the large  $R/t$  ratio case of 20. This same behavior occurs for the stiffer  $R/t = 5$  case. In fact, for the 15-degree crack, the outer diameter region of the crack actually closes. Because of this crack face rotation, the crack opening functions were compiled for both the inner and outer surfaces. This 'pinching' of the crack opening along the outer surface should impede leaking, and hence LBB considerations. Hence, for LBB predictions one should account for crack face rotation in the leak rate models.

Figure E.7 illustrates this effect further. Crack opening profile plots are illustrated for the outer diameter (OD), middle surface (MS), and along the inner diameter (ID) for an axial crack subjected to bending alone. In Figure E.7(a), which is for a 15-degree (total) crack angle (i.e.

$2\theta = 15$ -degrees – see Figure E.1), the OD predicts negative crack opening. Of course, the negative crack openings are physically impossible, but it means that the crack faces will be closed and contacting each other at the OD. This will impede fluid leakage and affect leak rate calculations. Figure E.7(b) shows similar results for a 30-degree total crack angle. While the closure is not as severe as for the smaller crack, some crack face contact will occur along the OD. The predicted values in Figure E.7 are made assuming an elliptic crack opening shape. It is seen that elliptic profile is still a good approximation for the opening even if the crack faces rotate.

In an actual elbow, which is subjected to combined tension and pressure, the competition between the pressure, which causes opening COD's at both the ID and OD, and the bending, which closes the crack at the OD, will ultimately determine the service opening profile. However, the ovalization induced from elbow bending must be considered in the COD predictions which are then used in leak rate calculations for LBB considerations.

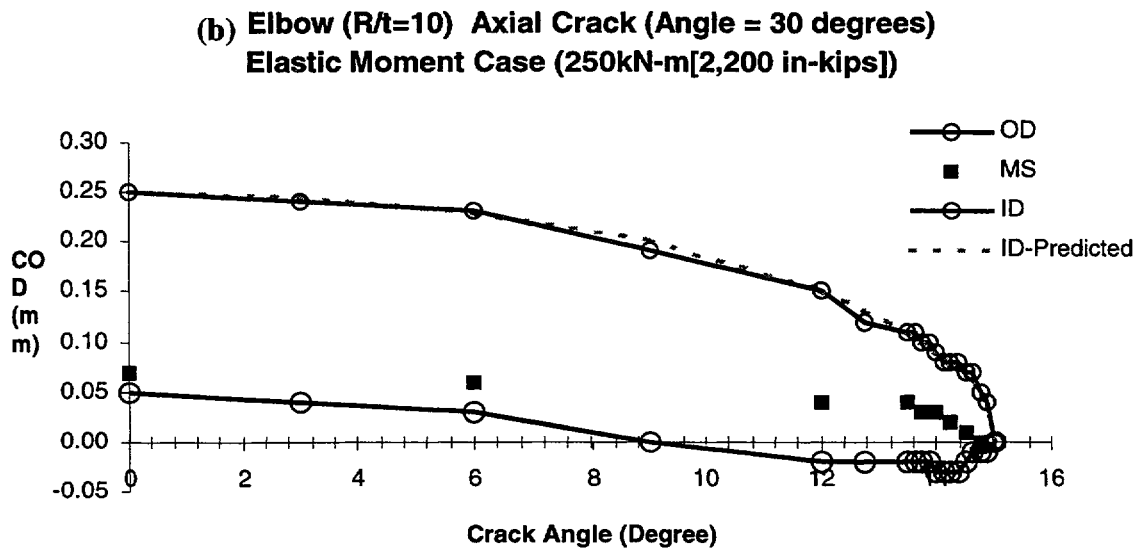
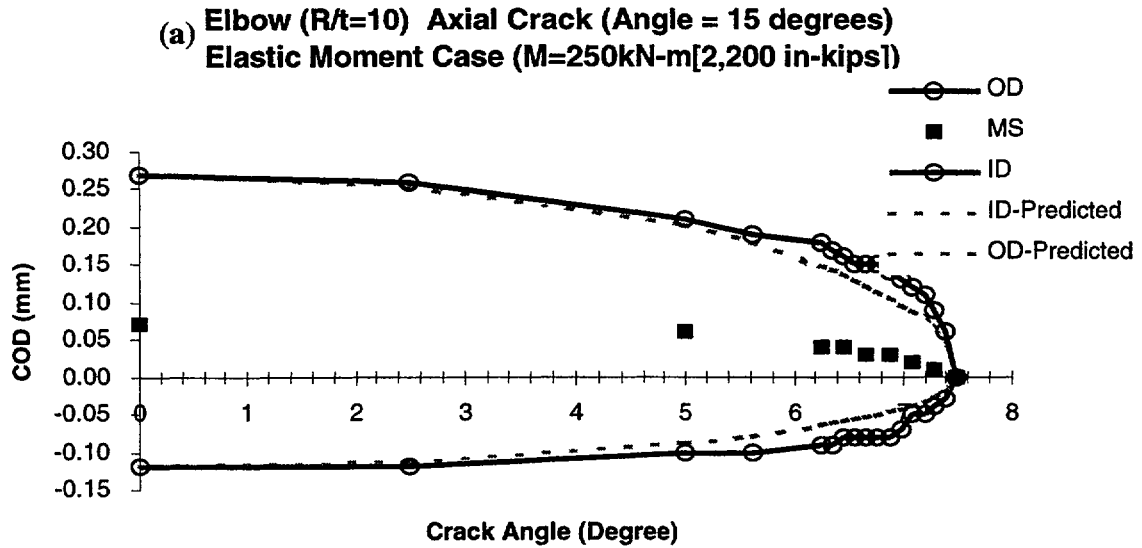


Figure E.7 Crack opening plots for axial cracked elbows – bending.

### E.5 Estimation Schemes

Elastic-plastic estimations schemes are based on the concept of proportional loading. If a cracked body is loaded in a proportional manner, such that the constitutive response is adequately modeled via deformation theory plasticity, then Il'yushin has shown that deformations, stresses,

and energies (e.g. J-integral) are proportional to a load parameter, material parameters, and geometric quantities. This concept has been overviewed extensively in the fracture mechanics literature (see for instance References E.1 through E.6).

For a cracked structure that obeys an elastic/power law constitutive relation, the stress/strain response follows:

$$\varepsilon = \varepsilon^e + \varepsilon^p = \frac{\sigma}{E} + k(\sigma)^n \quad (\text{E.1})$$

In Equation E.1,  $\varepsilon^e$  and  $\varepsilon^p$  are the elastic and plastic strains,  $E$  is the elastic modulus, and  $k$  and  $n$  are fitted material constants. This constitutive law leads to a violation of Illyushin's theorem since an elastic term is present (only the second term in Equation E.1 should be present). However, it has been observed that developing elastic-plastic estimation schemes using the separate elastic and plastic components provides a reasonable estimate for engineering purposes. It is common practice to write the constitutive relationship in the following form:

$$\frac{\varepsilon}{\varepsilon_0} = \frac{\sigma}{\sigma_0} + \alpha \left( \frac{\sigma}{\sigma_0} \right)^n, \quad (\text{E.2})$$

where  $\sigma_0$  is a reference stress,  $\varepsilon_0 = \sigma_0 / E$ ,  $n$  is the fitted material parameter, and  $\alpha$  is a material parameter related to  $k$ . The approximate solutions are determined by adding the contributions from an elastic and plastic part, as discussed next.

**E.5.1 Estimating J and Crack Opening Displacement (COD)** - The estimation scheme for  $J$  is written as:

$$J = J^e + J^p. \quad (\text{E.3})$$

In Equation E.3,  $J$  represents the total estimated value for  $J$ , and  $J^e$  and  $J^p$  are the elastic and plastic components of  $J$ , respectively.

The estimation scheme for crack opening displacement is written as:

$$\delta_T = \delta^e + \delta^p. \quad (\text{E.4})$$

In Equation E.4,  $\delta_T$  is the total crack opening displacement at the mouth (i.e. displacement at the center of the crack), while  $\delta^e$  and  $\delta^p$  are the elastic and plastic contributions to the total COD, respectively.

### E.5.2 Elastic Component J-Integral

The elastic component of  $J$  is estimated by superimposing the component contributions from the pressure (designated 'T' for 'Tension') and bending (designated 'B' for 'Bending'). This can be written as:

$$J^e = J_T^e + J_B^e = \frac{[F_T \sigma_T \sqrt{\pi a}]^2}{E} + \frac{[F_B \sigma_B \sqrt{\pi a}]^2}{E} = \frac{K_T^2 + K_B^2}{E} \quad (\text{E.5})$$

In Equation E.5, 'a' is crack size and  $F_T$  and  $F_B$  have been compiled in Tables E.1 to E.4 for the through-wall cracked elbow cases. The  $F_T$  functions were compiled by performing elastic solutions for the pure pressure case (with end cap tension present), and  $F_B$  functions were compiled for pure bending.  $\sigma_T$  and  $\sigma_B$  are calculated as nominal stresses using:

**For Circumferential Cracks**

$$\sigma_T = \frac{p(\pi R_i^2)}{\pi(R_o^2 - R_i^2)} \quad (\text{E.6})$$

**For Axial Cracks**

$$\sigma_T \equiv \sigma_H = \frac{2p(\pi R_i^2)}{\pi(R_o^2 - R_i^2)} \quad (\text{E.7})$$

**Bending**

$$\sigma_B = \frac{M(R_m)}{\frac{\pi}{4}(R_o^4 - R_i^4)} \quad (\text{E.8})$$

Here,  $p$  is the internal elbow pressure,  $R_i$  is inner radius,  $R_o$  is outer radius,  $R_m$  is mean radius, and  $M$  is the applied bending moment. The denominator in the bending stress definition is the moment of inertia. Notice that for the axial cracks,  $\sigma_T$  is defined as twice that for the circumferential crack, or a nominal  $\sigma_H$  since it is more like a 'hoop' stress that opens the axial cracks.

**E.5.3 Elastic Component COD** - Likewise, the elastic component of COD is estimated by superimposing the pressure (tension) and bending components of COD.

$$\delta_e = \delta_e^T + \delta_e^B \quad (\text{E.9})$$

where  $\delta_e^T$  is the elastic COD contribution from pressure alone and  $\delta_e^B$  is the elastic COD component for bending alone, and are written as:

$$\delta_e^T = \frac{4\sigma_T a}{E} V_1(T) \quad (\text{E.10})$$

$$\delta_e^B = \frac{4\sigma_B a}{E} V_1(B) \quad (\text{E.11})$$

The same definitions of the stress for the pressure loading apply, i.e. Equation E.6 is the tensile stress for circumferential cracks and Equation E.7 is the hoop stress used for axial cracks.

The functions  $V_1(T)$  and  $V_1(B)$  are compiled in Tables E.1 and E.2 for the circumferential crack cases and Tables E.3 and E.4 for the axial cracks. Notice from Tables E.3 and E.4 that  $V_1(T)$  and  $V_1(B)$  are tabulated for both the ID and OD. Hence, the user can estimate the COD angle that occurs through the elbow wall as discussed in Section E.4. Figure E.8 illustrates this effect. The rotation through the elbow wall remains nearly linear, even when five parabolic elements are used to model the wall thickness.

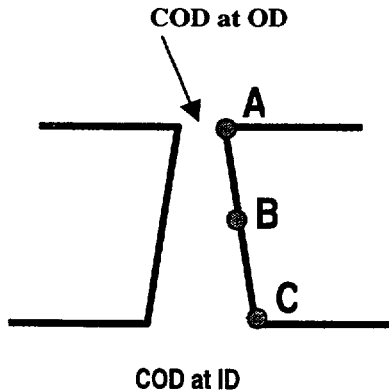


**Figure E.8. Crack opening profile for axial cracks.**

**E.5.4 Plastic Components of J** - The plastic component of J is estimated as:

$$J^P = \alpha \sigma_0 \epsilon_0 a (1 - \theta/\pi) h_1 (P/P_0')^{n+1} \quad (\text{E.12})$$

Everything has been previously defined in Equation E.12 except  $P_0'$ , which is defined as:

$$P_0' = \frac{1}{2} \left[ \frac{-\lambda P_0^2 R_m}{M_0} + \sqrt{\left\{ \frac{\lambda P_0^2 R_m}{M_0} \right\}^2 + 4P_0^2} \right] \quad (\text{E.13})$$

In Equation E.13,  $\lambda$  is the load ratio defined as:

$$\lambda = \frac{M}{PR_m} \quad (\text{E.14})$$

P in Equations E.12 and E.14 is defined as:

$$P = \sigma_T \pi (R_o^2 - R_i^2) \quad (\text{E.15})$$

It is emphasized that the  $h_1$  functions from Equation E.12 have a strong dependence on load ratio,  $\lambda$ . Again as described above,  $\sigma_T$  is defined using Equation E.6 for circumferential cracks and using Equation E.7 for axial cracks. The two as yet undefined parameters in Equation E.13,  $M_0$  and  $P_0$ , are:

$$M_0 = 4\sigma_0 R_m^2 t [\cos(\theta/2) - 0.5 \sin(\theta)] \quad (\text{E.16})$$

**For Circumferential Cracks**

$$P_0 = 2\sigma_0 R_m t [\pi - \theta - 2 \sin^{-1}(0.5 \sin \theta)] \quad (\text{E.17a})$$

## For Axial Cracks

$$P_o = (1)\sigma_o R_m t [\pi - \theta - 2 \sin^{-1}(0.5 \sin \theta)] \quad (\text{E.17b})$$

Notice that, for the axial cracks the value of  $P_o$  (Equation E.17b) is one half that for circumferential cracks. This is because hoop stresses dominate the failure for axial cracks, and hence  $P_o$  should be smaller. Equation E.17a represents the standard limit load estimate for a circumferential crack in a pipe subjected to pressure. These definitions of  $P_o$  lead to reasonable values for the h-functions that are easily interpolated to provide very accurate estimates between the values tabulated in Tables E.1 to E.4.

The values of  $h_1$  are tabulated in Tables E.1 and E.2 for circumferential cracks and Tables E.3 and E.4 for axial cracks. They have been tabulated for values of  $\lambda = [0, 0.5, 1.0, 2.0, 4.0, 8.0, \text{ and } \text{infinity}]$ . The case  $\lambda = 0$  corresponds to the pure pressure case without bending, while  $\lambda = \text{infinity}$  corresponds to the pure bending solution.

For typical nuclear piping LBB applications, the pipe experiences uniform or constant pressure the entire time while the moment is applied. As such, for a given crack size and material, the only quantity that changes in the estimate for J in Equation E.12 is  $\lambda$  which continually increases as the moment increases, while P in Equation E.14 remains constant. The values of  $\lambda$  for which  $h_1$  were tabulated are quite sufficient for practical nuclear applications. In fact, for practical purposes, a  $\lambda$  value of 18 should be used for interpolation when  $\lambda$  is between 8 and infinity. Most practical nuclear fracture assessments for pressurized elbows rarely find  $\lambda$  greater than about 6.

The compilations in Tables E.1 to E.4 represent 336 full nonlinear finite element solutions. These were compiled by proportionally applying the pressure and moment simultaneously. However, as will be seen in the validation section, solutions where pressure is applied first,

followed by moment compare very well with the estimation scheme.

It is recommended that the plastic zone correction applied to the elastic solution be neglected. In general, as discussed in References E.1 to E.6, these type of J-estimation solutions have fundamental errors associated with them in the transition region between elastic and fully plastic solution ranges. However, we have found the plastic zone corrections to be unnecessary for most of the numerous validation cases that were performed (to be summarized later) here. However, the user can assure conservative solutions by including the form of the plastic zone correction procedure summarized on page 2-4 in Reference E.4. The user might want to use the plastic zone correction procedure for large 'n' values in cases where the elastic contribution to J is large (large crack size in high (R / t) elbow)

**E.5.5 Plastic Components of COD** - The plastic contribution to the crack opening displacement can be calculated using:

$$\delta^p = \alpha \epsilon_o a h_2 (P/P_o')^n \quad (\text{E.18})$$

The  $h_2$ -function is tabulated in Tables E.1 and E.2 for circumferential cracks and Tables E.3 and E.4 for axial cracks. The functions for the axial cracks are tabulated for both the ID and OD so the user can estimate the variation of COD through the elbow thickness. As discussed above, the usual assumption of an elliptic crack opening shape works well for elbows even when the opening varies through the thickness. P in Equation E.18 is defined in Equations E.6 and E.15 for circumferential cracked elbows, and Equations E.7 and E.15 for axial cracks.  $P_o$  is defined in Equation E.17a for circumferential cracks and Equation E.17b for axial cracks.

## E.6 Estimation Scheme for Pure Bending of Elbows ( $\lambda = \text{infinity}$ )

For the  $\lambda = \text{infinity}$  case, a bending moment only was applied. For this case, one can design the estimation scheme based on an alternative approach. The total estimate for J still uses Equation E.3 and Equation E.5, for the elastic

estimate remains the same. Likewise, the total estimate for COD (Equation E.4) remains the same with Equations E.9 to E.11 providing the estimate for the elastic values. However, the estimates for  $J^P$  (Equation E.12) and  $\delta^P$  (Equation E.18) can be replaced by:

$$J^P = \alpha \sigma_0 \epsilon_0 a (1 - \theta/\pi) h_1^M (M/M_0)^{n+1} \quad (E.19)$$

$$\delta^P = \alpha \epsilon_0 a h_2^M (M/M_0) \quad (E.20)$$

The compilations for  $h_1^M$  and  $h_2^M$  are provided in Tables E.5 and E.6. These can be compared directly with similar compilations for straight pipe to observe the differences.

Alternatively, all of the h-functions could have been based on formulas (Equations E.19 and E.20). It is instructive to investigate the choice made here to use Equations E.12 and E.18 rather than Equations E.19 and E.20. It will be seen that, in theory, one will obtain the same prediction of the plastic components of J and COD using either normalizing parameters, the choice made here results in much more accurate interpolation within the tables for predictions made for cases not directly tabulated.

First of all, from Figure E.9 the nature of the convergence of the  $h_1^M$  functions can be observed. The dashed horizontal line represents the converged solution of  $h_1^M = 1.3$ . This is for  $R/t = 10$ . The curve with the filled circles represents the convergence of the h-function versus load for a pure bending case (no internal pressure). The analyses were all performed using ABAQUS and the constitutive law represented by Equation E.2. Typically, the solution is monitored until the plastic strains become greater than ten times the elastic strains at every Gauss point in the body that is monitored. It is seen that it converges to the correct value at an  $M/M_0$  value of about 5. Here, the monitoring procedure kept the analysis

going until  $M/M_0 = 15$ . This was clearly adequate. In fact, convergence was assured for every value listed in Tables E.1 to E.4 in this fashion.

Also shown in Figure E.9 is a curve designated with solid diamonds. This was a case where a pressure of 10 MPa (typical operating pressure) was applied first, and then the bending moment was applied until it converged to the pure bending solution. With the definition of lambda ( $\lambda = M/(PR)$ ), since PR remains constant for this case (constant pressure), it is clearly seen that  $h_1^M$  depends on  $\lambda$ . As  $\lambda$  approaches infinity, the pure bending solution is obtained. This convergence to the pure bending solution occurs at large values of  $M/M_0$  approaching 35. The h-functions published in Reference E.1 were developed in this way – pressure applied and held while the moment was applied. As such, the h-functions really are those for the pure bending case. Unfortunately, the h-functions obtained in this way are non-conservative and one will typically under predict the value of J – sometimes significantly, depending on  $\lambda$ .

Figure E.10 compares the h-functions calculated using Equations E.12 and E.19. The value of h based on Equation E.19 is very large for smaller values of  $\lambda$  (for instance,  $h_1 = 3450$  for  $\lambda = 0.5$ ). It is seen that the h-values based on Equation E.12 have much more uniform values. It should be clear that the interpolation between values in the tables will be much more stable using the normalization based on Equation E.12 versus Equation E.19.

## E.7 Validation Examples

This next section illustrates independent validation of the estimation schemes developed here. Before presenting the validation examples, it is useful to discuss the Ramberg-Osgood representation of material stress-strain data versus actual data. Figure E.11 illustrates a typical relationship. The bottom plot shows an example of idealized data that are to be fit with a Ramberg-Osgood equation. The ‘flow-2’ curve has an elastic slope and a yield stress of 200 MPa (29 ksi) in this case. The Ramberg-Osgood

curve (Equation E.2) permits plastic strains to occur throughout the deformation. It is seen that, over the entire strain range, there is negligible difference between a Ramberg-Osgood and 'flow' representation (upper curve, Figure E.11). However, in the small strain regime, there are some small differences which manifest themselves as slight differences in predicted displacements, and J-Integral values. It will be seen that the representation in Figure E.11 results in a slightly conservative prediction of J-integral values in the following results. It is useful for the user of the estimation schemes to keep this in mind when making engineering predictions of fracture. How one fits a Ramberg-Osgood relation to actual test data can have an influence on predictions. See References E.5 and E.6 for more details.

In addition to the consistency checks on solution accuracy discussed above (see Figures E.9 and E.10), additional quality control was maintained by performing independent analyses. For each crack type and size, an independent analysis was performed for at least one set of material parameters and often for several sets. These validation analyses were performed as follows: pressure was applied first followed by bending. This violates the formal definition of a deformation theory solution. However, it is an excellent independent check on the accuracy of the solution procedure since, in actual nuclear piping, pressure is typically present, at constant value, and then bending is applied. It will be seen that this results in slight differences between the flow theory solutions (which are strictly required for this set of loading

conditions), and deformation theory solutions. For the examples which follow, the pressure applied was 5 MPa (0.75 ksi) for  $R/t = 20$ , 10 MPa (1.5 ksi) for  $R/t = 10$ , and 20 MPa (2.9 ksi) for the  $R/t = 5$  cases. After the solution for pressure was complete, bending was applied. Solutions obtained in this manner are then directly compared to predictions using the estimation schemes developed here. The plastic-zone correction to the elastic solution are not included in the following.

**E.7.1 Axial Cracks** - Figures E.12 to E.14 illustrate the validation for some of the axial crack cases. It is clearly seen that the estimation scheme is quite accurate, even for the flow theory cases. Notice that the crack opening displacement (COD) begins at a non zero value which corresponds the pressure case before applying a moment. Note also that the outer diameter (OD) COD's are typically much smaller than the ID cases. In fact, crack closure (Figure E.13) occurs for some cases.

**E.7.2 Circumferential Cracks** - Figures E.15 to E.17 illustrate the validation for some of the circumferential crack cases. Again, the estimation scheme performs very well. It is seen that there are some small differences between the deformation and flow theory solutions. However, in general, the deformation theory solution is more conservative and the estimation scheme typically falls between the two solutions.

Circumferential Crack (Theta = 90, n=5)

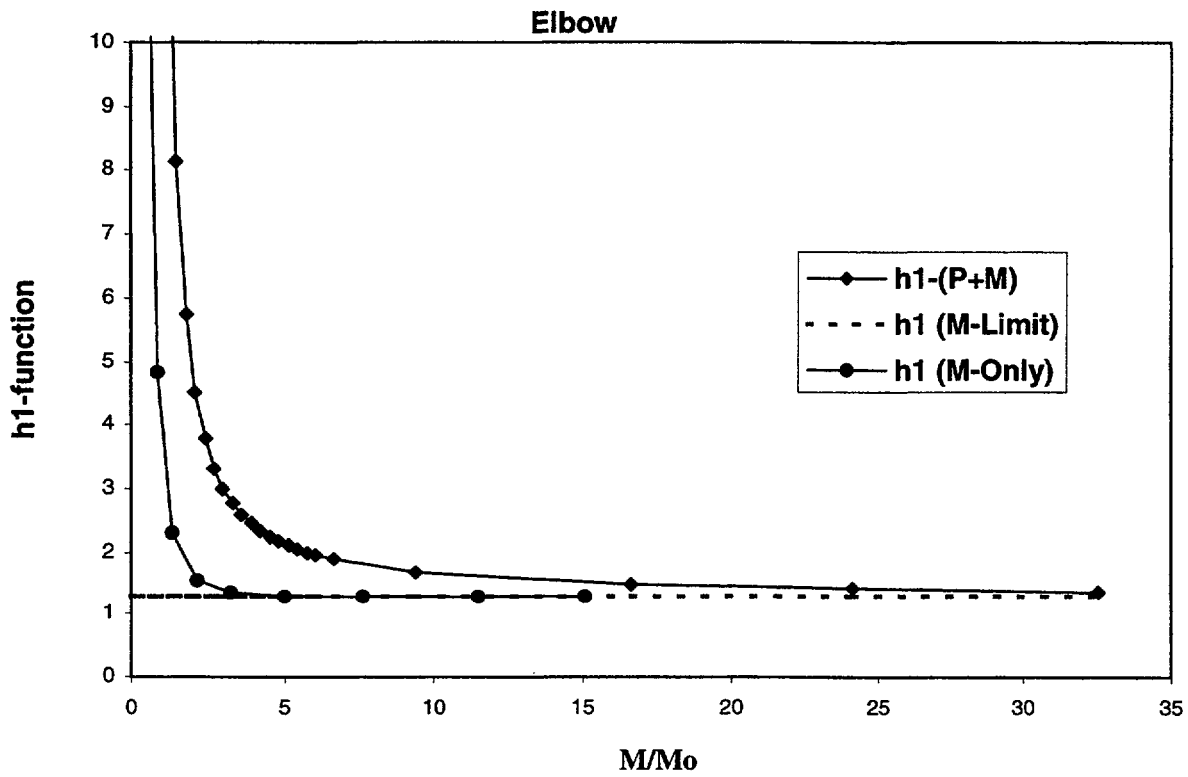


Figure E.9 Convergence of h-functions versus applied load

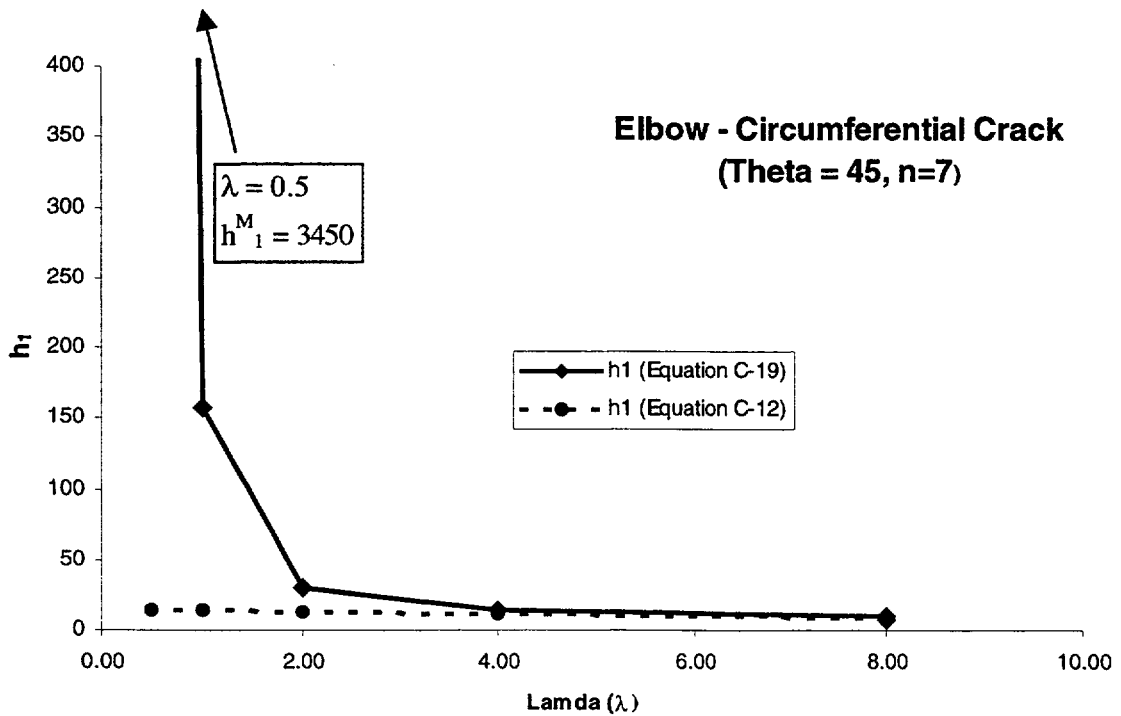
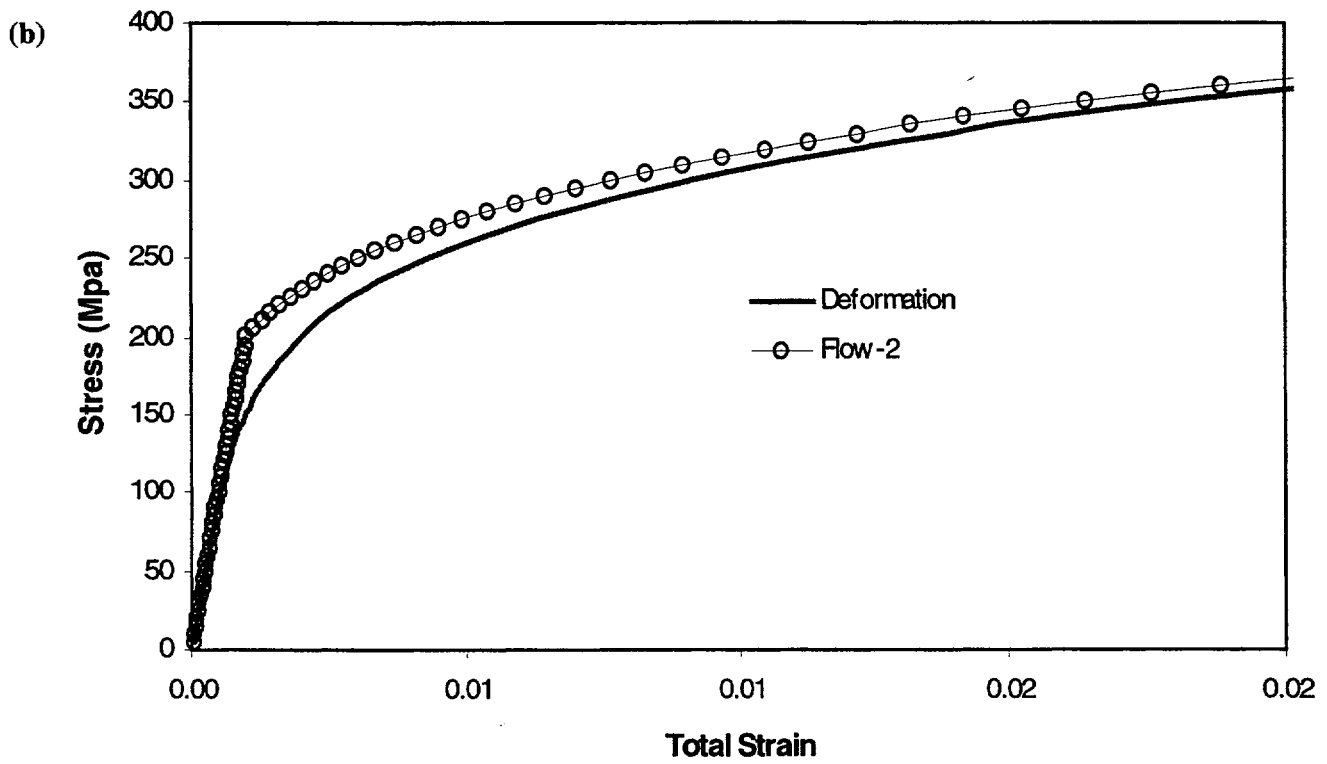
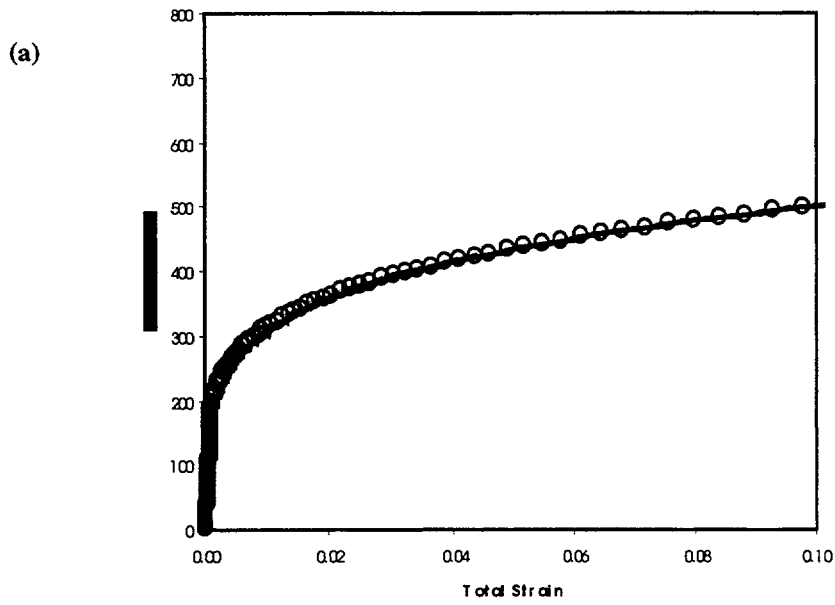
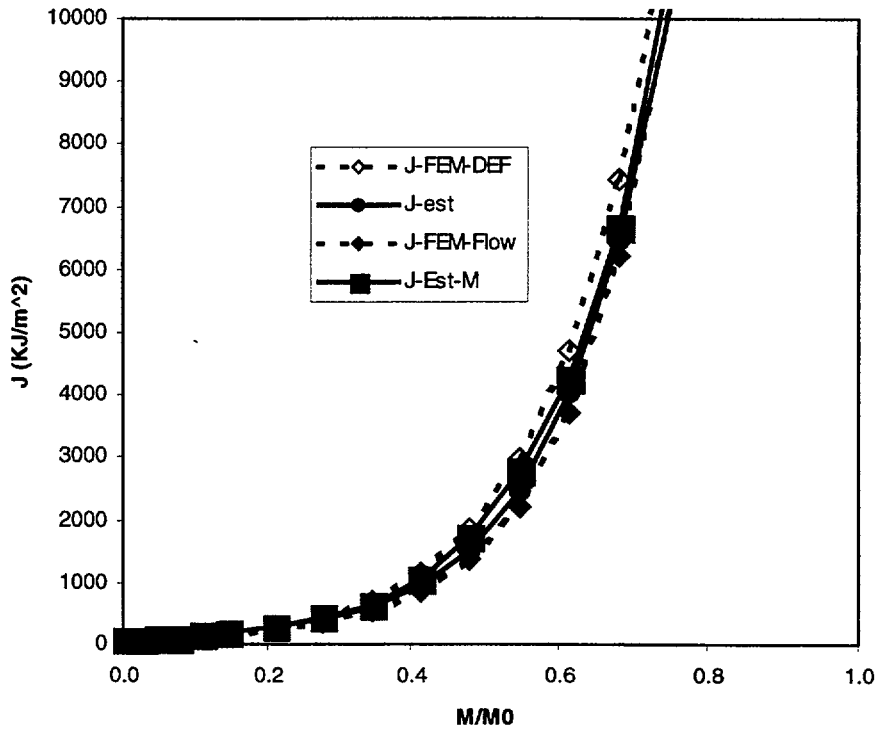


Figure E.10 Convergence of h-functions versus Lamda



**Figure E.11 Comparison between Ramberg-Osgood relationship and a typical flow theory representation**

Elbow - Axial Crack (Theta = 15, n=5, R/t=20)



Elbow - Axial Crack (Theta = 15, n=5, R/t=20)

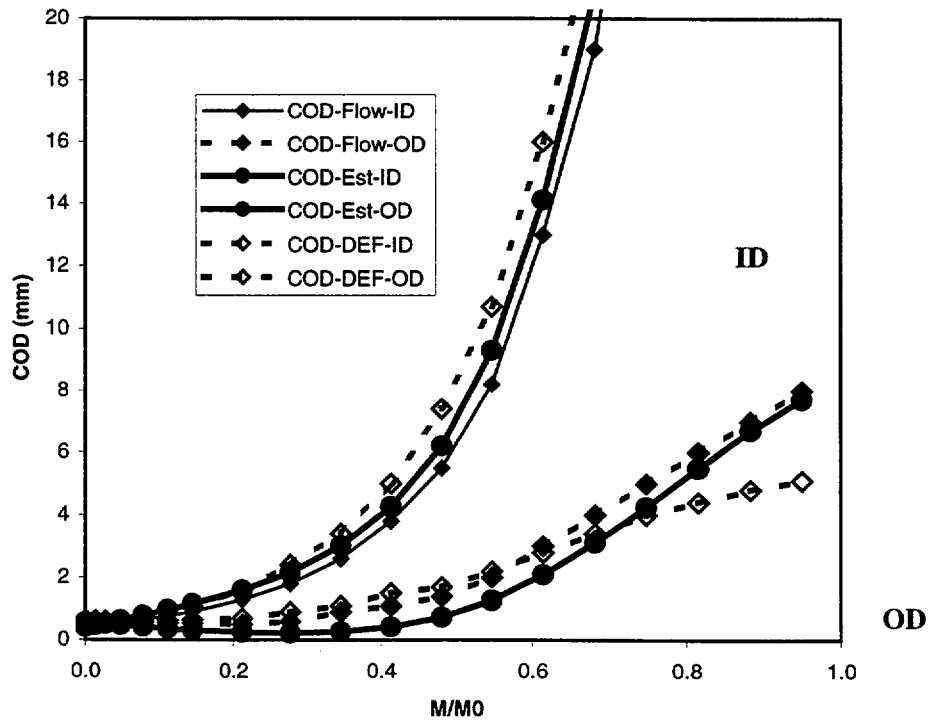
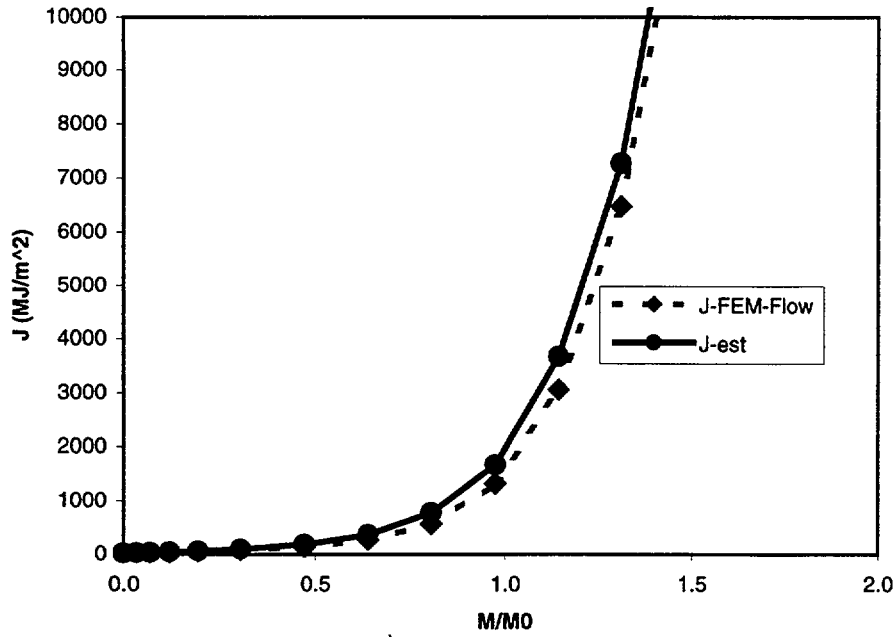


Figure E.12 Validation check (R/t = 20, axial crack 2θ = 15, n = 5)

Elbow - Axial Crack (Theta = 15, n=5, R/t=5)



Elbow - Axial Crack (Theta = 15, n=5, R/t=5)

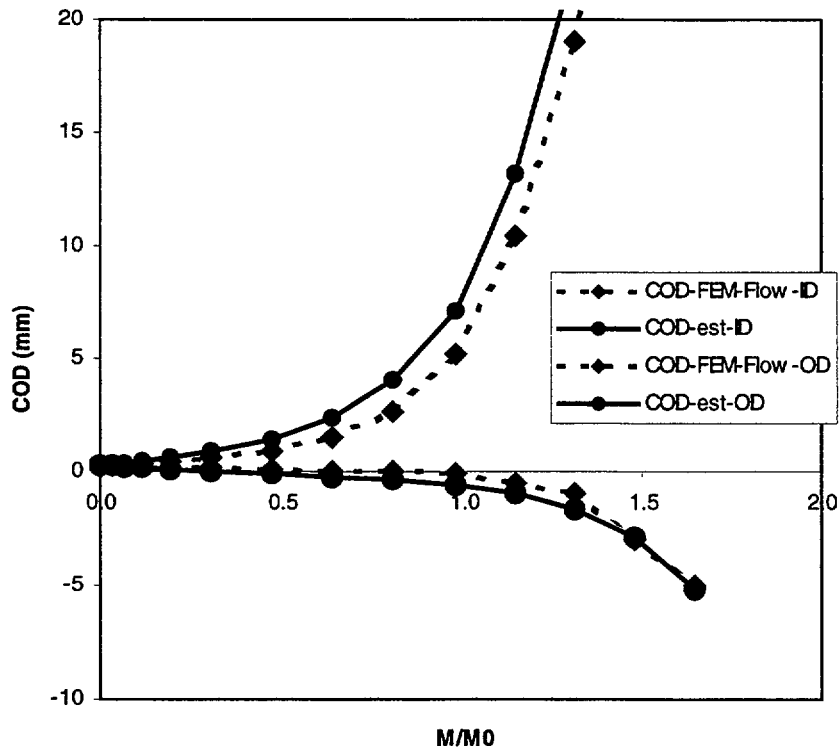


Figure E.13 Validation check (R/t = 5, axial crack, 2θ = 15, n = 5)

Elbow - Axial Crack (Theta = 30, n=5, R/t=5)

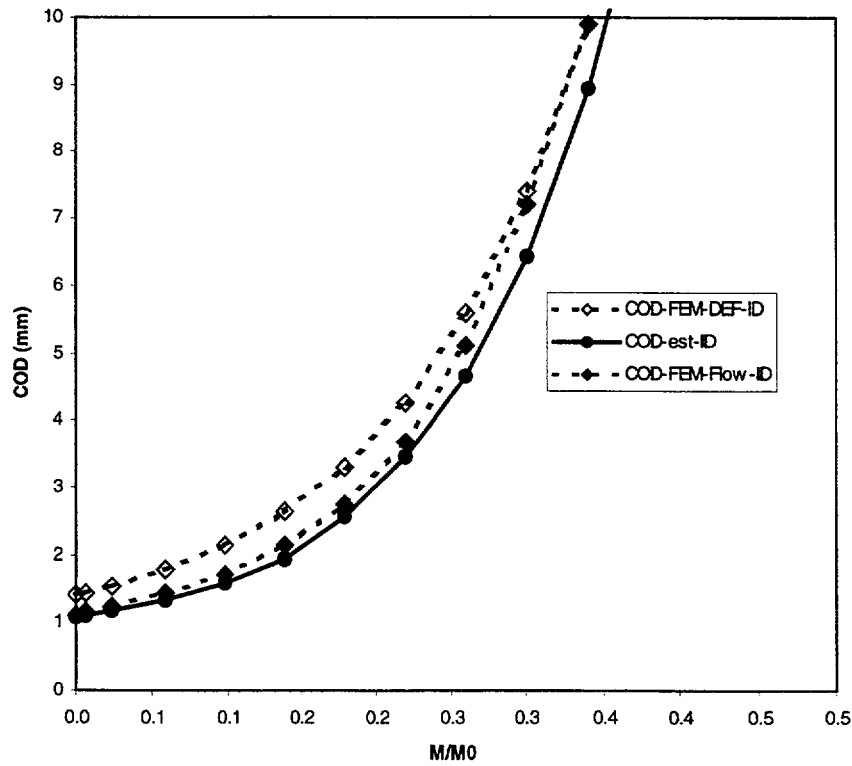
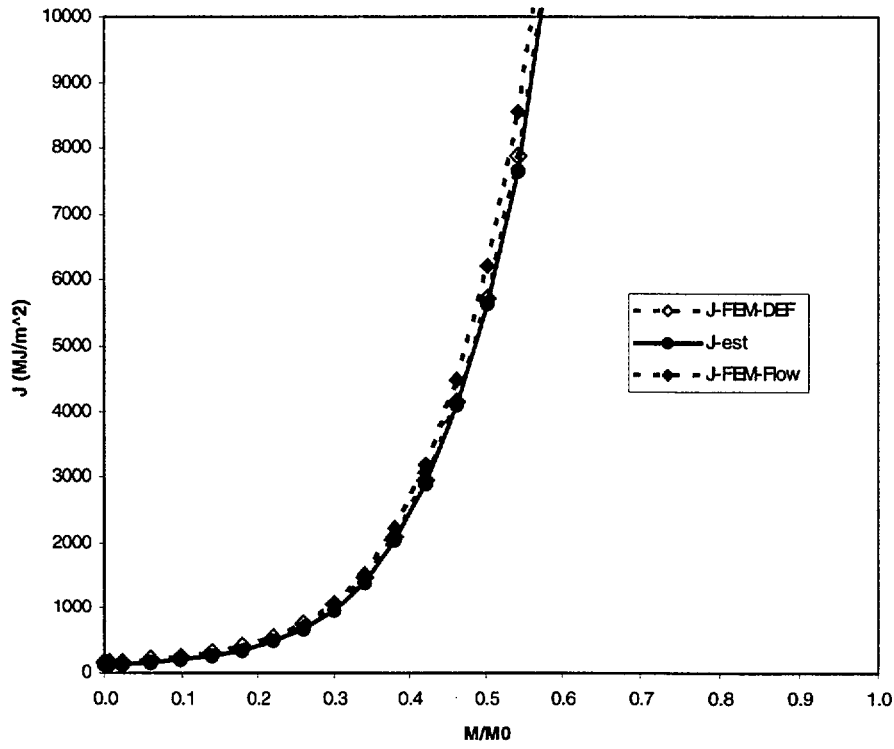


Figure E.14 Validation check (R/t = 5, axial crack, 2θ = 30, n = 5)

Elbow - Circumferential Crack (Theta = 45, n=5, R/t=5)

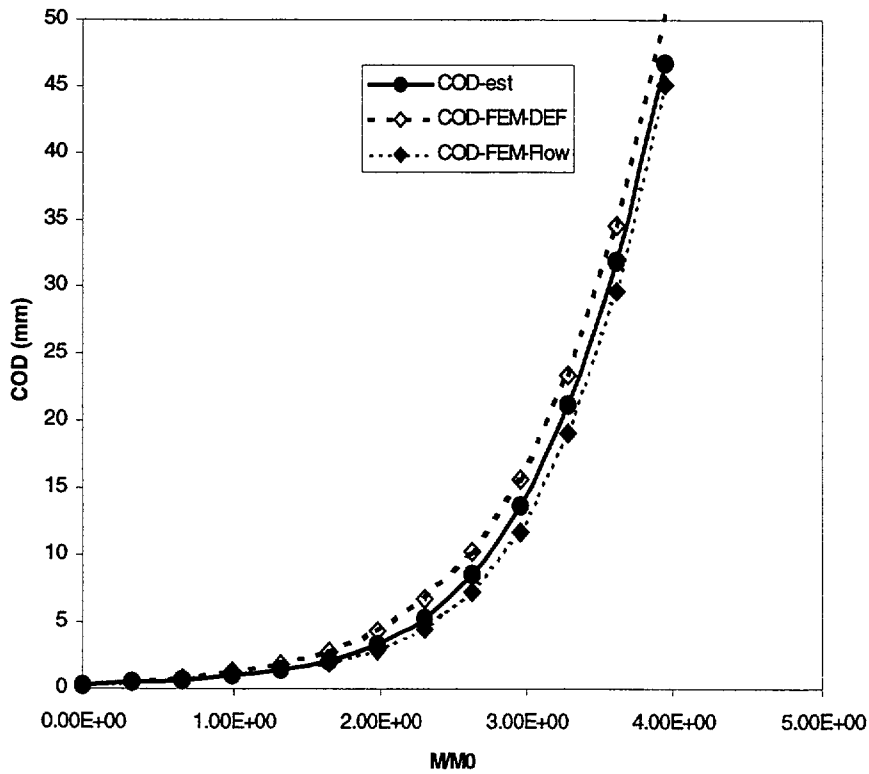
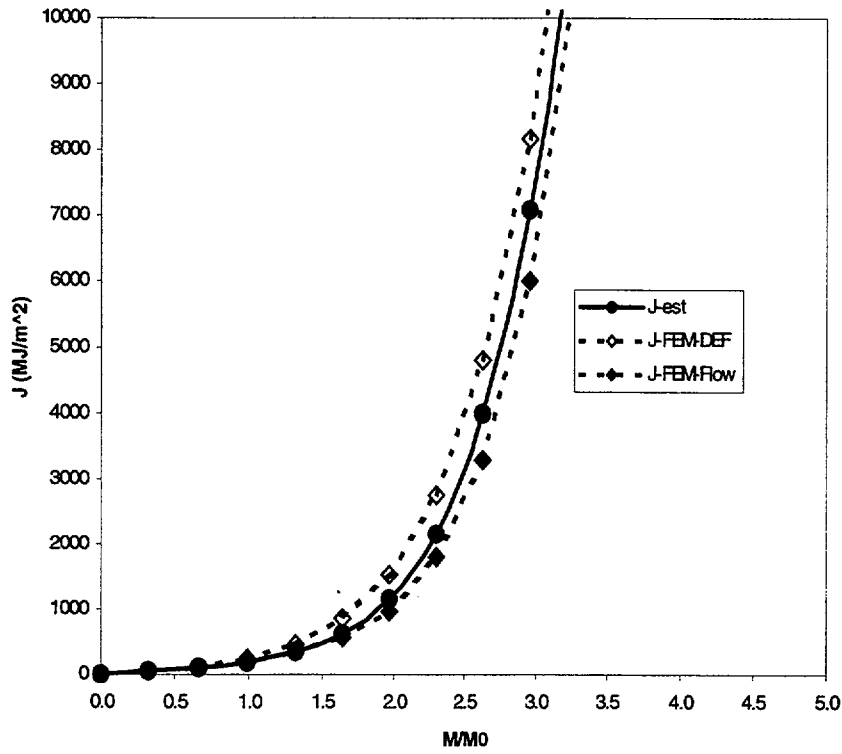


Figure E.15 Validation check (R/t = 5, circumferential crack, 2θ = 90, n = 5)

Elbow - Circumferential Crack (Theta = 45, n=5, R/t=20)

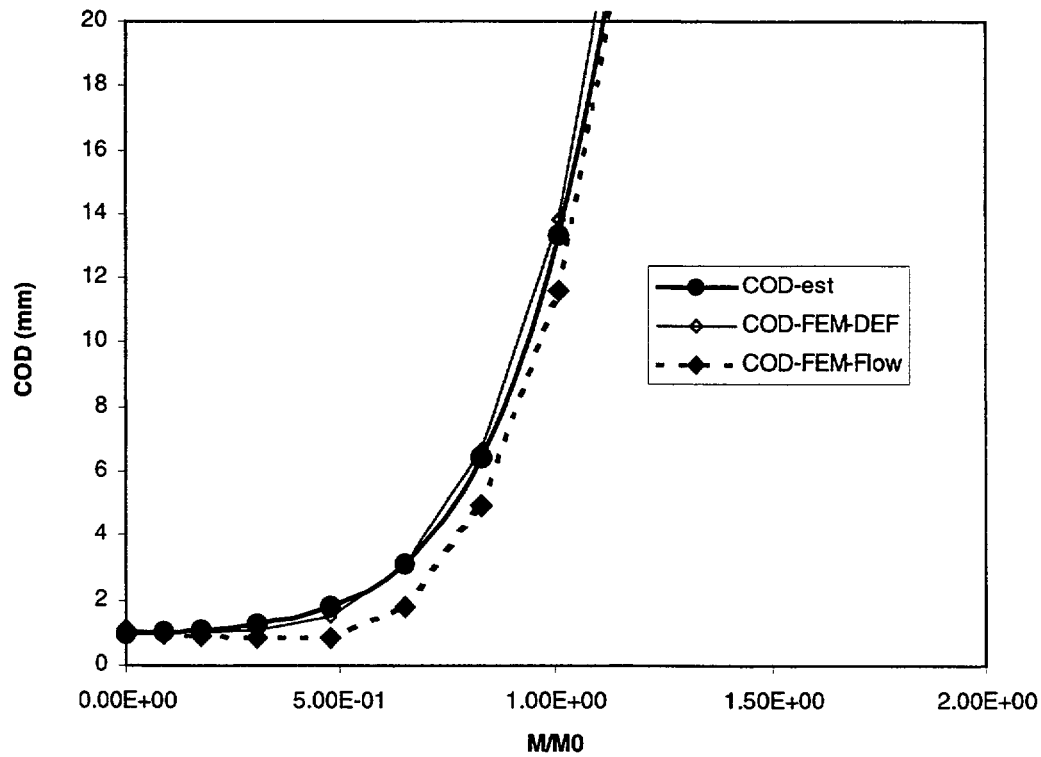
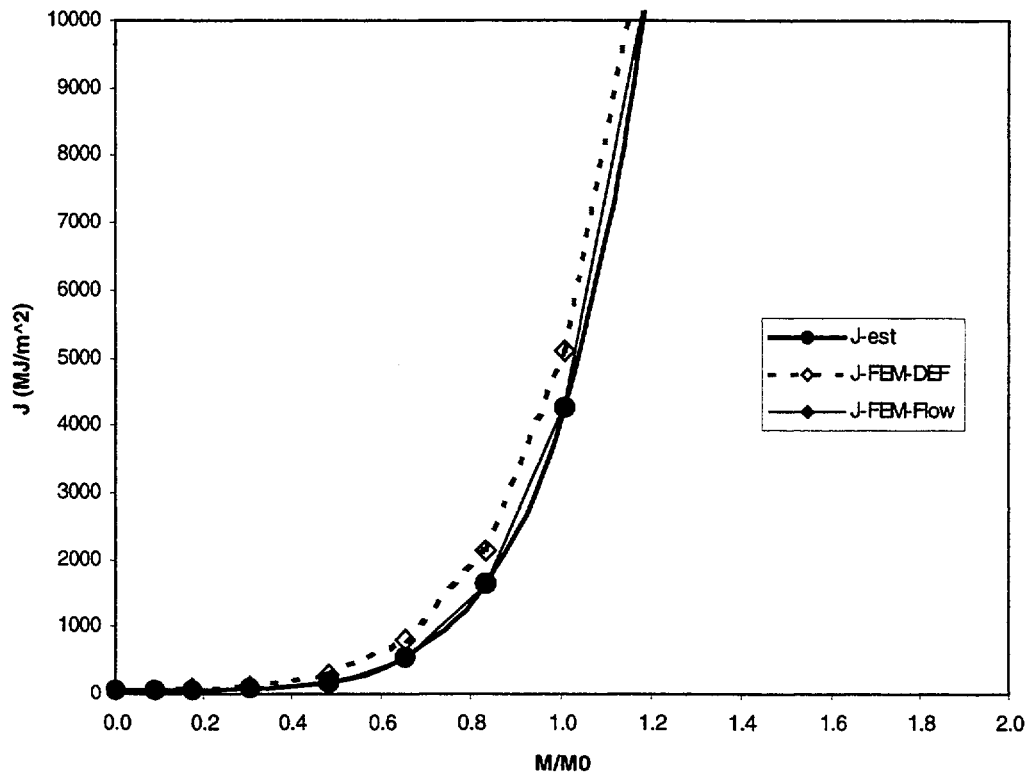
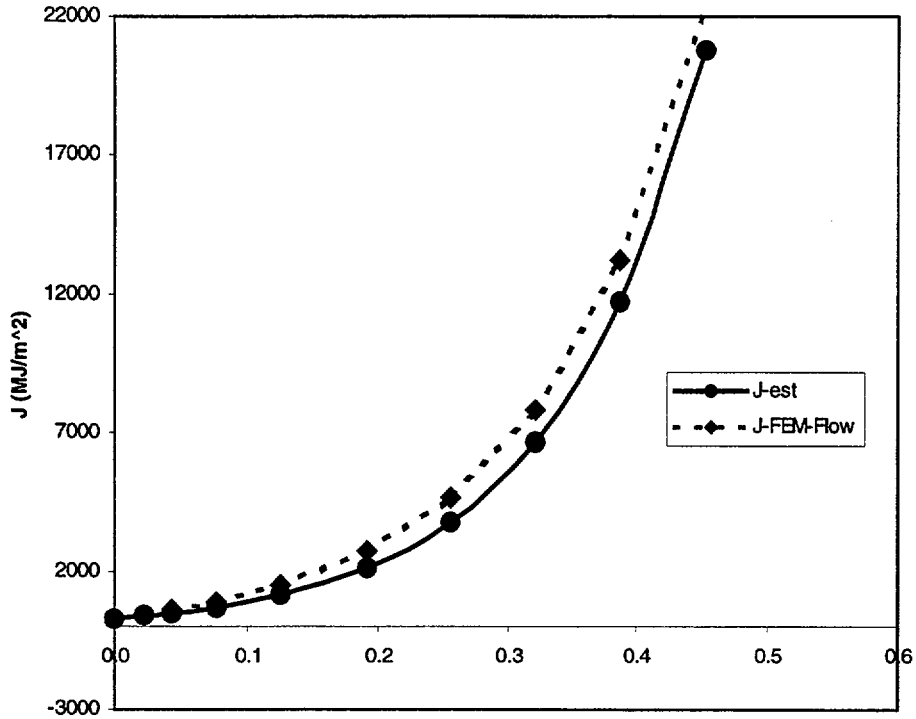


Figure E.16 Validation check ( $R/t = 20$ , circumferential crack,  $2\theta = 90$ ,  $n = 5$ )

Elbow - Circumferential Crack (Theta = 90, n=5, R/t=20)



Elbow - Circumferential Crack (Theta = 90, n=5, R/t=20)

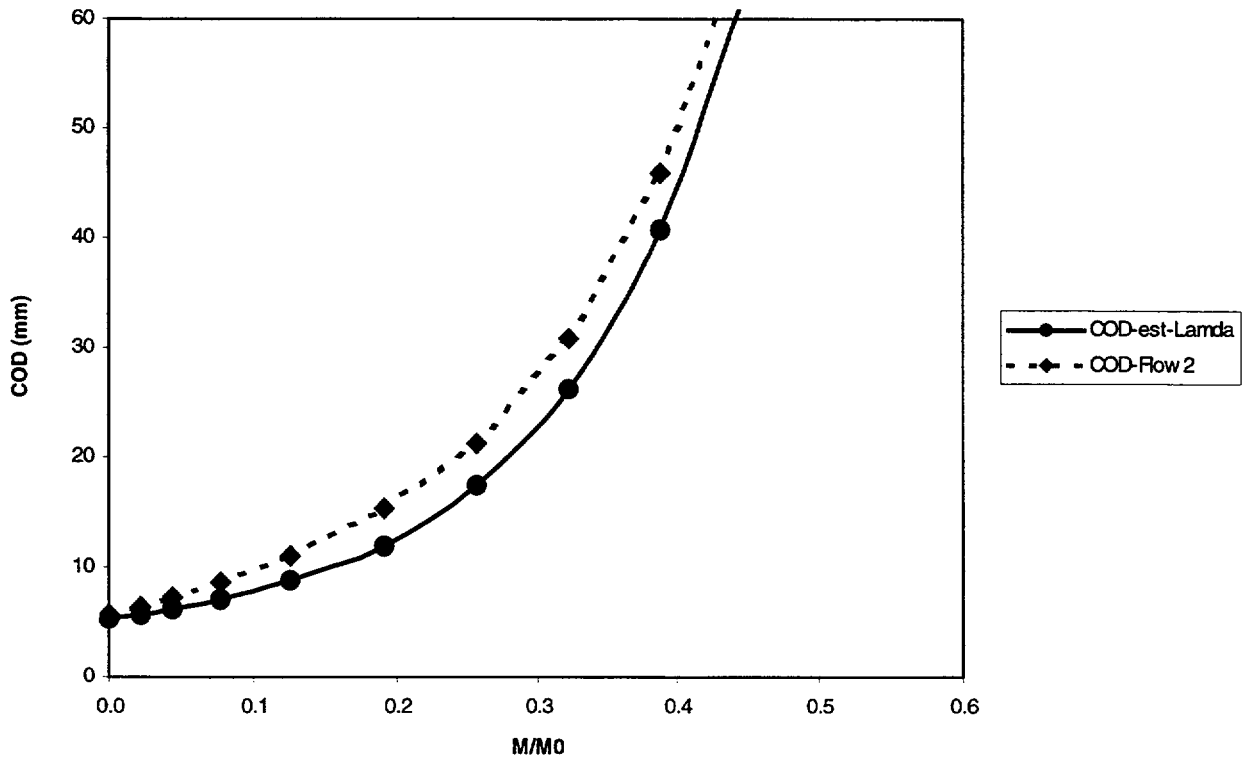


Figure E.17 Validation check (R/t = 20, circumferential crack, 2θ = 180, n = 5)

**Table E.1(a) Elbow with circumferential crack – combined pressure and bending compilation ( $R/t = 5, \theta = 45^\circ$ )**

F-(T)	F-(B)	Lamda	n = 3	n = 5	n = 7	n = 10
			$h_1$	$h_1$	$h_1$	$h_1$
1.69	1.11	0.0	6.23	10.67	17.47	34.68
		0.5	6.39	8.04	9.75	12.42
		1.0	5.92	6.55	6.92	7.34
		2.0	5.23	5.10	4.78	4.25
		4.0	4.46	4.05	3.47	2.58
		8.0	3.91	3.43	2.79	2.01
		inf (=18)	3.17	2.76	2.11	1.36
V-1 (T)	V-1 (B)	Lamda	$h_2$	$h_2$	$h_2$	$h_2$
2.04	1.19	0.0	8.59	14.87	24.65	49.31
		0.5	6.56	7.99	9.56	12.05
		1.0	5.70	6.17	6.45	6.78
		2.0	5.09	4.92	4.61	4.08
		4.0	4.59	4.17	3.57	2.67
		8.0	4.24	3.71	3.04	2.20
		inf (=18)	3.72	3.13	2.46	1.60

**Table E.1(b) Elbow with circumferential crack – combined pressure and bending compilation ( $R/t = 10, \theta = 45^\circ$ )**

F-(T)	F-(B)	Lamda	n = 3	n = 5	n = 7	n = 10
			$h_1$	$h_1$	$h_1$	$h_1$
2.16	0.87	0.0	10.55	17.79	28.26	53.93
		0.5	8.75	11.96	14.42	18.32
		1.0	8.46	11.86	13.60	16.54
		2.0	7.91	10.47	12.80	15.27
		4.0	6.83	9.06	10.76	12.08
		8.0	5.85	7.82	8.99	10.76
		inf (=18)	4.47	6.06	6.89	7.87
V-1 (T)	V-1 (B)	Lamda	$h_2$	$h_2$	$h_2$	$h_2$
3.39	0.67	0.0	15.04	27.26	45.21	90.60
		0.5	9.17	12.29	14.89	19.01
		1.0	7.92	10.28	12.24	14.88
		2.0	7.45	9.61	11.60	13.82
		4.0	6.83	8.93	10.48	11.75
		8.0	6.18	8.21	9.37	11.09
		inf (=18)	5.07	6.89	8.06	8.86

**Table E.1(c) Elbow with circumferential crack – combined pressure and bending compilation ( $R/t = 20, \theta = 45^\circ$ )**

F-(T)	F-(B)	Lamda	n = 3	n = 5	n = 7	n = 10
			$h_1$	$h_1$	$h_1$	$h_1$
3.01	0.25	0.0	21.04	33.34	46.65	61.68
		0.5	15.57	27.30	41.30	72.98
		1.0	13.48	26.87	44.95	88.46
		2.0	11.14	26.02	49.25	113.49
		4.0	7.82	21.81	44.90	115.15
		8.0	5.66	17.59	38.84	96.94
		inf (=18)	3.22	11.07	25.92	66.57
V-1 (T)	V-1 (B)	Lamda	$h_2$	$h_2$	$h_2$	$h_2$
6.30	0.66	0.0	33.70	54.86	81.83	112.34
		0.5	19.23	34.59	54.73	100.90
		1.0	14.06	26.80	44.28	86.08
		2.0	11.75	25.37	45.85	102.22
		4.0	8.95	24.18	47.14	114.72
		8.0	6.43	21.00	45.08	108.47
		inf (=18)	2.99	14.08	33.69	86.77

**Table E.2(a) Elbow with circumferential crack – combined pressure and bending compilation ( $R/t = 5, \theta = 90^\circ$ )**

F-(T)	F-(B)	Lamda	n = 3	n = 5	n = 7	n = 10
			$h_1$	$h_1$	$h_1$	$h_1$
4.04	2.52	0.0	1.33	0.82	0.53	0.31
		0.5	2.30	1.77	1.53	1.29
		1.0	2.67	2.26	2.05	1.99
		2.0	2.59	2.08	1.82	1.64
		4.0	2.12	1.56	1.20	0.90
		8.0	1.75	1.14	0.79	0.50
		inf (=18)	1.26	0.69	0.41	0.20
V-1 (T)	V-1 (B)	Lamda	$h_2$	$h_2$	$h_2$	$h_2$
6.52	4.46	0.0	2.11	1.14	0.70	0.38
		0.5	2.92	2.08	1.72	1.42
		1.0	3.26	2.55	2.26	2.14
		2.0	3.21	2.43	2.07	1.83
		4.0	2.83	1.95	1.47	1.08
		8.0	2.49	1.53	1.04	0.65

**Table E.2(b) Elbow with circumferential crack – combined pressure and bending compilation ( $R/t = 10, \theta = 90^\circ$ )**

F-(T)	F-(B)	Lamda	n = 3	n = 5	n = 7	n = 10
			h <sub>1</sub>	h <sub>1</sub>	h <sub>1</sub>	h <sub>1</sub>
4.16	3.24	0.0	1.99	1.00	0.62	0.36
		0.5	3.28	2.45	2.02	1.69
		1.0	4.04	3.23	2.88	2.68
		2.0	4.12	3.19	2.72	2.46
		4.0	3.53	2.46	1.88	1.38
		8.0	2.98	1.88	1.33	0.82
		inf (=18)	2.24	1.22	0.71	0.35
		<hr/>				
V-1 (T)	V-1 (B)	Lamda	h <sub>2</sub>	h <sub>2</sub>	h <sub>2</sub>	h <sub>2</sub>
9.66	5.93	0.0	2.99	1.51	0.86	0.47
		0.5	4.25	2.92	2.30	1.85
		1.0	4.91	3.72	3.19	2.58
		2.0	5.05	3.78	3.12	2.74
		4.0	4.59	3.15	2.34	1.67
		8.0	4.09	2.57	1.77	1.06
		inf (=18)	3.35	1.84	1.06	0.50

**Table E.2(c) Elbow with circumferential crack – combined pressure and bending compilation ( $R/t = 20, \theta = 90^\circ$ )**

F-(T)	F-(B)	Lamda	n = 3	n = 5	n = 7	n = 10
			h <sub>1</sub>	h <sub>1</sub>	h <sub>1</sub>	h <sub>1</sub>
5.00	4.56	0.0	2.87	1.75	1.13	0.62
		0.5	6.27	4.93	4.21	3.36
		1.0	8.43	7.34	6.69	6.31
		2.0	9.35	8.28	7.64	6.90
		4.0	8.60	7.13	5.99	4.57
		8.0	7.59	5.58	4.52	3.21
		inf (=18)	5.95	3.96	2.69	1.55
		<hr/>				
F-(T)	F-(B)	Lamda	h <sub>1</sub>	h <sub>1</sub>	h <sub>1</sub>	h <sub>1</sub>
17.08	7.94	0.0	5.83	3.26	1.95	0.99
		0.5	8.27	6.31	5.22	4.03
		1.0	9.94	8.69	7.85	7.26
		2.0	10.72	9.85	9.16	8.25
		4.0	10.09	8.95	7.69	5.93
		8.0	9.13	7.32	6.12	4.44
		inf (=18)	7.57	5.57	3.96	2.35

**Table E.3(a) Elbow with axial crack – combined pressure and bending  
 compilation ( $R/t = 5$ ,  $\theta = 15^\circ$ )**

			n = 3	n = 5	n = 7	n = 10
<b>F-(T)</b>	<b>F-(B)</b>	<b>Lamda</b>	<b>h<sub>1</sub></b>	<b>h<sub>1</sub></b>	<b>h<sub>1</sub></b>	<b>h<sub>1</sub></b>
1.57	0.81	0.0	1.01	0.49	0.22	0.07
		0.5	0.73	0.28	0.10	0.02
		1.0	0.65	0.25	0.09	0.02
		2.0	0.59	0.24	0.09	0.02
		4.0	0.53	0.22	0.09	0.02
		8.0	0.46	0.19	0.07	0.02
		inf (=18)	0.33	0.12	0.04	0.01
<b>Inner</b>	<b>Diameter</b>					
<b>V-1 (T)</b>	<b>V-1 (B)</b>	<b>Lamda</b>	<b>h<sub>2</sub></b>	<b>h<sub>2</sub></b>	<b>h<sub>2</sub></b>	<b>h<sub>2</sub></b>
1.45	1.20	0.0	1.42	0.70	0.32	0.10
		0.5	1.49	0.59	0.21	0.04
		1.0	1.61	0.62	0.22	0.04
		2.0	1.76	0.73	0.27	0.06
		4.0	1.81	0.78	0.31	0.07
		8.0	1.68	0.72	0.29	0.07
		inf (=18)	1.30	0.51	0.19	0.04
<b>Outer</b>	<b>Diameter</b>					
<b>V-1 (T)</b>	<b>V-1 (B)</b>	<b>Lamda</b>	<b>h<sub>2</sub></b>	<b>h<sub>2</sub></b>	<b>h<sub>2</sub></b>	<b>h<sub>2</sub></b>
2.04	-0.45	0.0	2.40	1.22	0.58	0.18
		0.5	1.42	0.60	0.23	0.05
		1.0	0.96	0.41	0.16	0.03
		2.0	0.48	0.22	0.09	0.02
		4.0	0.09	0.06	0.03	0.01
		8.0	-0.15	-0.03	-0.01	-0.01
		inf (=18)	-0.37	-0.11	-0.04	-0.01

**Table E.3(b) Elbow with axial crack – combined pressure and bending  
 compilation ( $R/t = 10, \theta = 15^\circ$ )**

			<b>n = 3</b>	<b>n = 5</b>	<b>n = 7</b>	<b>n = 10</b>
<b>F-(T)</b>	<b>F-(B)</b>	<b>Lamda</b>	<b>h<sub>1</sub></b>	<b>h<sub>1</sub></b>	<b>h<sub>1</sub></b>	<b>h<sub>1</sub></b>
1.79	1.26	0.0	1.44	0.78	0.41	0.15
		0.5	1.16	0.49	0.19	0.04
		1.0	1.20	0.56	0.23	0.06
		2.0	1.39	0.77	0.39	0.14
		4.0	1.56	0.97	0.57	0.25
		8.0	1.57	0.92	0.58	0.27
		inf (=18)	1.25	0.73	0.39	0.17
<b>Inner</b>	<b>Diameter</b>					
<b>V-1 (T)</b>	<b>V-1 (B)</b>	<b>Lamda</b>	<b>h<sub>2</sub></b>	<b>h<sub>2</sub></b>	<b>h<sub>2</sub></b>	<b>h<sub>2</sub></b>
1.83	1.73	0.0	2.08	1.18	0.63	0.24
		0.5	2.28	0.99	0.39	0.08
		1.0	2.73	1.30	0.55	0.14
		2.0	3.53	2.06	1.08	0.40
		4.0	4.10	2.77	1.68	0.79
		8.0	4.15	2.76	1.81	0.89
		inf (=18)	3.39	2.23	1.28	0.59
<b>Outer</b>	<b>Diameter</b>					
<b>V-1 (T)</b>	<b>V-1 (B)</b>	<b>Lamda</b>	<b>h<sub>2</sub></b>	<b>h<sub>2</sub></b>	<b>h<sub>2</sub></b>	<b>h<sub>2</sub></b>
2.59	-0.77	0.0	3.50	2.05	1.13	0.43
		0.5	2.28	1.12	0.48	0.11
		1.0	1.73	0.96	0.45	0.13
		2.0	0.98	0.70	0.41	0.17
		4.0	0.11	0.22	0.18	0.10
		8.0	-0.59	-0.21	-0.09	-0.03
		inf (=18)	-1.25	-0.64	-0.32	-0.13

**Table E.3(c) Elbow with axial crack – combined pressure and bending  
 compilation ( $R/t = 20, \theta = 15^\circ$ )**

			<b>n = 3</b>	<b>n = 5</b>	<b>n = 7</b>	<b>n = 10</b>
<b>F-(T)</b>	<b>F-(B)</b>	<b>Lamda</b>	<b>h<sub>1</sub></b>	<b>h<sub>1</sub></b>	<b>h<sub>1</sub></b>	<b>h<sub>1</sub></b>
2.18	1.94	0.0	2.89	2.19	1.60	1.02
		0.5	2.46	1.37	0.67	0.22
		1.0	2.95	1.96	1.16	0.58
		2.0	4.21	3.59	2.87	2.04
		4.0	5.39	5.34	5.14	5.39
		8.0	5.60	5.82	6.44	6.91
		inf (=18)	4.71	4.81	4.54	4.59
<b>Inner</b>	<b>Diameter</b>					
<b>V-1 (T)</b>	<b>V-1 (B)</b>	<b>Lamda</b>	<b>h<sub>2</sub></b>	<b>h<sub>2</sub></b>	<b>h<sub>2</sub></b>	<b>h<sub>2</sub></b>
2.68	2.64	0.0	4.47	3.65	2.78	1.90
		0.5	4.70	2.75	1.40	0.48
		1.0	4.72	4.25	2.61	1.31
		2.0	8.76	8.16	6.85	5.04
		4.0	11.00	12.27	12.62	13.66
		8.0	11.10	13.35	15.64	17.76
		inf (=18)	9.13	10.76	11.17	12.03
<b>Outer</b>	<b>Diameter</b>					
<b>V-1 (T)</b>	<b>V-1 (B)</b>	<b>Lamda</b>	<b>h<sub>2</sub></b>	<b>h<sub>2</sub></b>	<b>h<sub>2</sub></b>	<b>h<sub>2</sub></b>
3.72	-1.04	0.0	7.08	3.91	4.65	3.15
		0.5	4.98	3.35	1.85	0.69
		1.0	4.33	3.57	2.40	1.30
		2.0	3.18	3.62	3.37	2.71
		4.0	1.11	3.00	2.58	3.10
		8.0	-0.95	-0.14	0.26	0.78
		inf (=18)	-3.14	-2.88	-2.62	-2.46

**Table E.4 (a) Elbow with axial crack – combined pressure and bending compilation ( $R/t = 5, \theta = 30^\circ$ )**

<b>F-(T)</b>	<b>F-(B)</b>	<b>Lamda</b>	<b>n = 3</b> <b>h<sub>1</sub></b>	<b>n = 5</b> <b>h<sub>1</sub></b>	<b>n = 7</b> <b>h<sub>1</sub></b>	<b>n = 10</b> <b>h<sub>1</sub></b>
2.18	0.79	0.0	2.32	1.67	1.20	0.83
		0.5	1.45	0.72	0.35	0.13
		1.0	1.07	0.45	0.18	0.05
		2.0	0.79	0.32	0.12	0.03
		4.0	0.56	0.22	0.08	0.02
		8.0	0.40	0.15	0.05	0.01
		inf (=18)	0.22	0.07	0.02	0.00

<b>Inner</b> <b>V-1 (T)</b>	<b>Diameter</b> <b>V-1 (B)</b>	<b>Lamda</b>	<b>h<sub>2</sub></b>	<b>h<sub>2</sub></b>	<b>h<sub>2</sub></b>	<b>h<sub>2</sub></b>
2.67	1.24	0.5	3.78	2.93	2.23	1.58
		1.0	2.80	1.49	0.76	0.29
		2.0	2.34	1.05	0.44	0.12
		4.0	2.01	0.85	0.33	0.08
		8.0	1.68	0.69	0.26	0.06
		inf (=18)	1.41	0.55	0.20	0.04
		inf (=18)	0.96	0.33	0.11	0.02

<b>Outer</b> <b>V-1 (T)</b>	<b>Diameter</b> <b>V-1 (B)</b>	<b>Lamda</b>	<b>h<sub>2</sub></b>	<b>h<sub>2</sub></b>	<b>h<sub>2</sub></b>	<b>h<sub>2</sub></b>
3.87	0.16	0.0	6.35	4.90	4.03	2.91
		0.5	4.05	2.33	1.25	0.49
		1.0	2.90	1.38	0.60	0.16
		2.0	1.95	0.89	0.35	0.08
		4.0	1.21	0.52	0.21	0.05
		8.0	0.73	0.31	0.12	0.03
		inf (=18)	0.25	0.10	0.04	0.01

**Table E.4(b) Elbow with axial crack – combined pressure and bending  
 compilation ( $R/t = 10$ ,  $\theta = 30^\circ$ )**

			<b>n = 3</b>	<b>n = 5</b>	<b>n = 7</b>	<b>n = 10</b>
<b>F-(T)</b>	<b>F-(B)</b>	<b>Lamda</b>	<b>h<sub>1</sub></b>	<b>h<sub>1</sub></b>	<b>h<sub>1</sub></b>	<b>h<sub>1</sub></b>
2.58	1.22	0.0	4.26	4.35	4.70	5.88
		0.5	2.64	1.73	1.22	0.80
		1.0	2.18	1.16	0.62	0.24
		2.0	1.95	1.11	0.59	0.22
		4.0	1.67	0.99	0.57	0.24
		8.0	1.37	0.80	0.19	0.20
		inf (=18)	0.88	0.47	0.24	0.09
<b>Inner</b>	<b>Diameter</b>					
<b>V-1 (T)</b>	<b>V-1 (B)</b>	<b>Lamda</b>	<b>h<sub>2</sub></b>	<b>h<sub>2</sub></b>	<b>h<sub>2</sub></b>	<b>h<sub>2</sub></b>
4.13	2.01	0.0	8.48	9.81	11.35	14.96
		0.5	5.99	4.48	3.41	2.40
		1.0	5.21	3.12	1.78	0.67
		2.0	4.93	3.03	1.68	0.65
		4.0	4.61	2.91	1.75	0.76
		8.0	4.05	2.54	1.52	0.69
		inf (=18)	2.91	1.68	0.90	0.34
<b>Outer</b>	<b>Diameter</b>					
<b>V-1 (T)</b>	<b>V-1 (B)</b>	<b>Lamda</b>	<b>h<sub>2</sub></b>	<b>h<sub>2</sub></b>	<b>h<sub>2</sub></b>	<b>h<sub>2</sub></b>
5.64	0.40	0.0	12.92	15.37	18.03	23.83
		0.5	8.21	6.59	5.20	3.16
		1.0	6.27	4.01	2.38	0.87
		2.0	4.81	3.12	1.77	0.70
		4.0	3.48	2.34	1.87	0.64
		8.0	2.39	1.64	1.02	0.48
		inf (=18)	1.00	0.67	0.38	0.15

**Table E.4(c) Elbow with axial crack – combined pressure and bending  
 compilation ( $R/t = 20, \theta = 30^\circ$ )**

			<b>n = 3</b>	<b>n = 5</b>	<b>n = 7</b>	<b>n = 10</b>
<b>F-(T)</b>	<b>F-(B)</b>	<b>Lamda</b>	<b>h<sub>1</sub></b>	<b>h<sub>1</sub></b>	<b>h<sub>1</sub></b>	<b>h<sub>1</sub></b>
3.13	1.91	0.0	9.38	15.32	27.79	79.02
		0.5	5.87	5.83	6.71	9.57
		1.0	5.51	4.46	3.55	2.68
		2.0	5.96	5.13	4.35	3.43
		4.0	5.96	6.14	6.07	2.95
		8.0	5.33	5.61	5.89	5.68
		inf (=18)	3.64	3.47	3.23	3.03
<b>Inner</b>	<b>Diameter</b>					
<b>V-1 (T)</b>	<b>V-1 (B)</b>	<b>Lamda</b>	<b>h<sub>2</sub></b>	<b>h<sub>2</sub></b>	<b>h<sub>2</sub></b>	<b>h<sub>2</sub></b>
6.78	3.64	0.5	22.16	41.11	79.18	233.37
		1.0	15.12	17.82	22.37	16.14
		2.0	14.03	13.13	11.61	9.62
		4.0	14.72	14.20	12.74	10.53
		8.0	14.96	16.90	17.65	17.73
		inf (=18)	13.76	16.00	17.75	18.10
		inf (=18)	9.95	10.57	10.48	10.29
<b>Outer</b>	<b>Diameter</b>					
<b>V-1 (T)</b>	<b>V-1 (B)</b>	<b>Lamda</b>	<b>h<sub>2</sub></b>	<b>h<sub>2</sub></b>	<b>h<sub>2</sub></b>	<b>h<sub>2</sub></b>
8.71	1.36	0.0	28.07	57.82	111.73	329.87
		0.5	19.34	24.05	30.95	15.74
		1.0	16.16	15.95	14.60	12.49
		2.0	14.43	14.48	13.25	11.15
		4.0	12.42	14.78	15.70	16.00
		8.0	9.74	12.18	13.97	14.47
		inf (=18)	5.20	6.03	6.20	6.29

**Table E.5 Elbow with circumferential crack – pure bending compilation**  
 ( $\theta = 45, 90^\circ$ ) for use with Equations E.19 and E.20.

(a)  $R/t = 5$ , (b)  $R/t = 10$ , (c)  $R/t = 20$

(a)

	<b>n = 3</b>	<b>n = 5</b>	<b>n = 7</b>	<b>n = 10</b>
$\theta$	<b><math>h_1</math></b>	<b><math>h_1</math></b>	<b><math>h_1</math></b>	<b><math>h_1</math></b>
45.0	3.27	2.89	2.24	1.47
90.0	1.31	0.73	0.44	0.22
$\theta$	<b><math>h_2</math></b>	<b><math>h_2</math></b>	<b><math>h_2</math></b>	<b><math>h_2</math></b>
45.0	3.81	3.25	2.60	1.72
90.0	2.05	1.08	0.64	0.32

(b)

	<b>n = 3</b>	<b>n = 5</b>	<b>n = 7</b>	<b>n = 10</b>
$\theta$	<b><math>h_1</math></b>	<b><math>h_1</math></b>	<b><math>h_1</math></b>	<b><math>h_1</math></b>
45.0	4.61	6.34	7.32	8.55
90.0	2.32	1.29	0.77	0.38
$\theta$	<b><math>h_2</math></b>	<b><math>h_2</math></b>	<b><math>h_2</math></b>	<b><math>h_2</math></b>
45.0	5.18	7.16	8.49	9.55
90.0	3.45	1.93	1.13	0.55

(c)

	<b>n = 3</b>	<b>n = 5</b>	<b>n = 7</b>	<b>n = 10</b>
$\theta$	<b><math>h_1</math></b>	<b><math>h_1</math></b>	<b><math>h_1</math></b>	<b><math>h_1</math></b>
45.0	3.32	11.58	27.53	72.32
90.0	6.18	4.20	2.91	1.72
$\theta$	<b><math>h_2</math></b>	<b><math>h_2</math></b>	<b><math>h_2</math></b>	<b><math>h_2</math></b>
45.0	3.06	14.62	35.51	93.56
90.0	7.79	5.84	4.24	2.58

**Table E.6 Elbow with axial crack – pure bending compilation ( $\theta = 15, 30^\circ$ ) for use with Equations E.19 and E.20.**

(a)  $R/t = 5$ , (b)  $R/t = 10$ , (c)  $R/t = 20$

(a)

		$n = 3$	$n = 5$	$n = 7$	$n = 10$
<b>Inner Diameter</b>	$\theta$	$h_1$	$h_1$	$h_1$	$h_1$
	15.0	5.8	9.1	13.6	22.8
	30.0	4.0	5.6	7.5	11.4
<b>Inner Diameter</b>	$\theta$	$h_2$	$h_2$	$h_2$	$h_2$
	15.0	11.2	18.5	28.4	49.4
	30.0	8.3	12.0	16.5	25.8
<b>Inner Diameter</b>	$\theta$	$h_2$	$h_2$	$h_2$	$h_2$
	15.0	-3.2	-4.1	-5.6	-8.7
	30.0	2.1	3.6	5.4	9.0

(b)

		$n = 3$	$n = 5$	$n = 7$	$n = 10$
<b>Inner Diameter</b>	$\theta$	$h_1$	$h_1$	$h_1$	$h_1$
	15.0	22.1	54.6	123.0	467.5
	30.0	15.5	35.4	76.5	240.1
<b>Inner Diameter</b>	$\theta$	$h_2$	$h_2$	$h_2$	$h_2$
	15.0	29.2	80.8	195.8	777.9
	30.0	25.1	61.3	138.6	457.0
<b>Inner Diameter</b>	$\theta$	$h_2$	$h_2$	$h_2$	$h_2$
	15.0	-10.8	-23.1	-49.5	-176.3
	30.0	8.7	24.5	58.8	205.6

(c)

		$n = 3$	$n = 5$	$n = 7$	$n = 10$
<b>Inner Diameter</b>	$\theta$	$h_1$	$h_1$	$h_1$	$h_1$
	15.0	83.4	358.0	1422.8	12395.0
	30.0	64.6	259.4	1017.9	8254.8
<b>Inner Diameter</b>	$\theta$	$h_2$	$h_2$	$h_2$	$h_2$
	15.0	78.8	390.7	1705.8	15853.2
	30.0	86.1	385.3	1609.4	13664.0
<b>Inner Diameter</b>	$\theta$	$h_2$	$h_2$	$h_2$	$h_2$
	15.0	-27.1	-104.5	-400.8	-3240.7
	30.0	45.0	219.7	951.6	8350.6

## E.8 Simplified Analysis for Through-Wall Cracks in Elbows

To establish a more complete Regulatory Guide for Leak-Before-Break, an evaluation procedure for through-wall cracks in elbows was desired. Finite element solutions for elbows with axial and circumferential cracks under combined pressure and bending have been developed as discussed above. This effort was somewhat similar to the work done for surface cracks in NUREG/CR-6444, "Fracture Behavior of Circumferentially Surface-Cracked Elbows" that was done for the IPIRG-2 program, Ref. E.14.

The recent through-wall-cracked elbow work developed a limited number of finite element solutions and a J-estimation scheme with h-function fits through these solutions. As with the case of the prior surface-cracked elbow work, it was desirable to see if a simplified solution could be developed from these results and be applicable over a wider range of through-wall cracks in elbows.

**E.8.1 Finite element analyses** - As discussed above, numerous 3-D finite element analyses were developed for the intent of developing a J-estimation scheme analyses. In developing these analyses, there were a limited number of analyses that could be conducted. The analyses conducted were for:

- Axial (flank) cracks with two crack lengths,
- Circumferential (extrados) cracks with two crack lengths,
- Elbows with two different cross-sectional radius-to-thickness (R/t) ratios,
- 90-degree, long-radius elbows,
- Materials with several different strain-hardening exponents, and
- Combined internal pressure and bending.

The initial finite element analyses were made with a constant pressure and varying the bending moment. For the estimation scheme developed, additional analyses were conducted where the pressure was varied in proportion to the bending

moment. In the constant pressure cases, the pressure was fixed so that the hoop stress corresponded to the average design stress ( $S_m$ ) of nuclear pipe materials. From NUREG/CR-6445, this  $S_m$  value was estimated to be 122.5 MPa (17.7 ksi), Ref. E.1.

For the purpose of evaluating an estimation procedure, the constant pressure elbow finite element results were used directly, rather than using the estimation procedure.

The cases chosen to evaluate were:

- The longest and shortest crack lengths,
- Both axial and circumferential crack orientations, and
- The largest and smallest cross-sectional R/t ratios.

Since most nuclear pipe materials have strain-hardening exponents of about 5, only that case was examined. Thus, eight cracked elbow cases were examined.

**E.8.2 Simplified Procedures** - In NUREG/CR-6444, a simplified procedure was developed for surface cracks in elbows, Ref. E.14. This involved comparing the elbow results to those for a circumferential surface crack in a pipe of the same dimensions and with the same material properties.

From that report, it was found that the ratio of the pipe to the elbow moments at the same J value was constant as the J value increased. This constant ratio between the elbow and pipe moment values for a particular case was found to be theoretically correct when comparing the general equations for fully plastic solutions for straight pipes and elbows as given below.

$$J^{\text{pipe}} = \alpha \sigma_o \epsilon_o b h_1^{\text{pipe}} (M^{\text{pipe}} / M_o^{\text{pipe}})^{n+1} \quad (\text{E.21a})$$

$$J^{\text{elbow}} = \alpha \sigma_o \epsilon_o b [R_m / (\lambda_1 t)] h_1^{\text{elbow}} (M^{\text{elbow}} / M_o^{\text{elbow}})^{n+1} \quad (\text{E.21b})$$

Where,

$\alpha, \sigma_o, \epsilon_o, n$  = Ramberg-Osgood parameters

$h_1^{pipe}, h_1^{elbow}$	= FEM determined geometric parameters relating moment to J
$M_o^{pipe}, M_o^{elbow}$	= reference moments at a stress of $\sigma_o$
b	= t-a
t	= thickness
$\lambda_1$	= an elbow parameter = $R_{el}t/R_m^2$
$R_{el}$	= bend radius of the elbow
$R_m$	= mean radius of pipe and elbow

Considering the case where  $J^{pipe} = J^{elbow}$ , for the same material, pipe size, and crack size gives

$$h_1^{pipe} (M_o^{pipe}/M_o^{elbow})^{n+1} |J = h_1^{elbow} [R_m/(\lambda_1 t)] (M_o^{elbow}/M_o^{elbow})^{n+1} |J \quad (E.22)$$

Rearranging Equation E.22 gives

$$(M_o^{pipe}/M_o^{elbow}) |J = [(h_1^{elbow}/h_1^{pipe})^{1/(n+1)} [R_m/(\lambda_1 t)]^{1/(n+1)} (M_o^{elbow}/M_o^{elbow}) |J] |J \quad (E.23)$$

For a given material, pipe, and elbow geometry and similar crack size, the right-hand side of Equation E.23 is a constant and independent of the J value, and hence  $(M_o^{pipe}/M_o^{elbow}) |J$  is a constant. The plastic part of J dominates the moment ratio for  $J_{applied}$  values of generally greater than  $100 \text{ kJ/m}^2$  ( $570 \text{ in-lb/in}^2$ ), which bounds the toughness range of typical nuclear piping materials, except perhaps some aged CF8M steels. It was then found that the constant value for the particular crack-size/pipe radius-to-thickness geometry/material case varied linearly with the elbow stress indices,  $B_2$ . This same simplified approach was examined for through-wall cracks in elbows as part of this effort.

**E.8.2.1 Straight-Pipe Solutions** - For the relative comparison of the moment versus J solutions of the straight pipe to the elbow cases, two different circumferential through-wall-cracked straight-pipe solutions were used. These were the LBB.ENG2 and original GE/EPRI methods in Version 3.0 of NRCPIPE.

The LBB.ENG2 method was used since it was the most accurate in predicting the maximum

moment for through-wall-cracked straight-pipe experiments, Ref. E.9. However, the LBB.ENG2 analysis requires an additional parameter that was not used in the FE solutions, that is, the ultimate strength of the material. For this analysis procedure it was assumed that the yield to-ultimate strength ratio was 0.85.

The GE/EPRI solution does not need the ultimate strength of the material, so it was also used. However, it was experimentally found that the GE/EPRI analysis was the most conservative analysis in predicting the full-scale straight-pipe experiments, i.e., it overpredicted the crack-driving force, Ref. E.9.

All analyses were for 410-mm (16.14-inch) outside diameter pipe. Additionally, all analyses were conducted with non-growing cracks.

### E.8.2.2 Comparison of Circumferential Extradors Through-Wall-Cracked Elbow and Straight-Pipe Solutions

- To make this comparison, the J versus moment curves from both the straight pipe and elbow solutions were first compared. Figures E.18 and E.19 show the results for the circumferential crack case with an R/t of 20 and total crack lengths of 90 and 180 degrees. Note in Figure E.18 that there is also a curve for an elbow curve-fit equation. This was done since the pipe and elbow solutions did not have values at exactly the same J values. The elbow curve-fit equation (as shown in Figure E.18) was used to compare the moments of the elbow to the straight pipe at the same J values, i.e., for  $(M_o^{pipe}/M_o^{elbow}) |J$ .

Figure E.18 shows that the curve fit is a very close approximation of the FE data points. Also, there is a difference in the two straight-pipe solutions, with the GE/EPRI solution giving higher J-values as was expected.

In Figure E.19, it is interesting to note that the elbow and LBB.ENG2 straight-pipe analyses give similar results, whereas the GE/EPRI solution for the straight pipe gives much higher J values. After these analyses were completed, it was recalled that the 180-degree crack R/t=20 analysis in the GE/EPRI solution in NRCPIPE

was found to be in error, so that in this case only the LBB.ENG2 analysis should be used.

The results for the  $R/t = 5$  case are shown in Figures E.20 and E.21.

The next step was to compare the ratio of the moments at the same  $J$  value. A graph of the  $J$  value versus the moment ratio is given for each case in Figures E.22 to E.25.

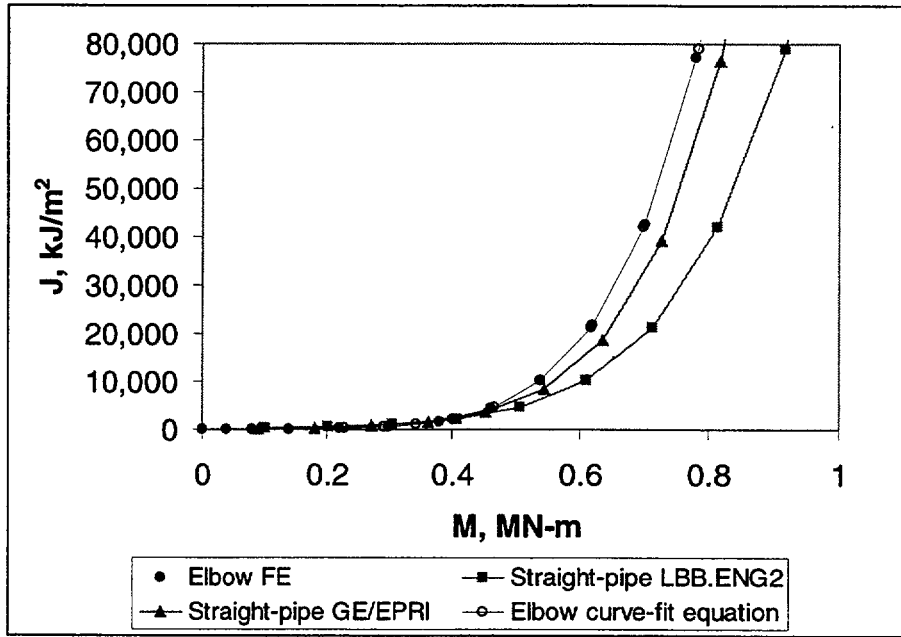


Figure E.18 Comparison of  $J$  versus moment curves for a circumferential through-wall crack in a straight pipe and centered on the extrados of an elbow with an  $R/t = 20$  and  $2\theta = 90$  degrees

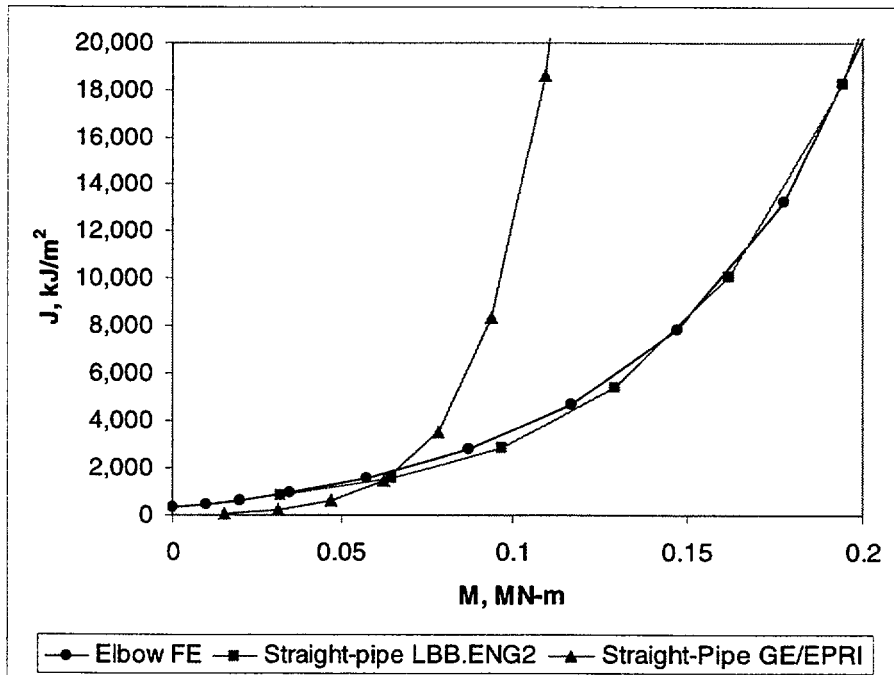


Figure E.19 Comparison of  $J$  versus moment curves for a circumferential through-wall crack in a straight pipe and centered on the extrados of an elbow with an  $R/t = 20$  and  $2\theta = 180$  degrees

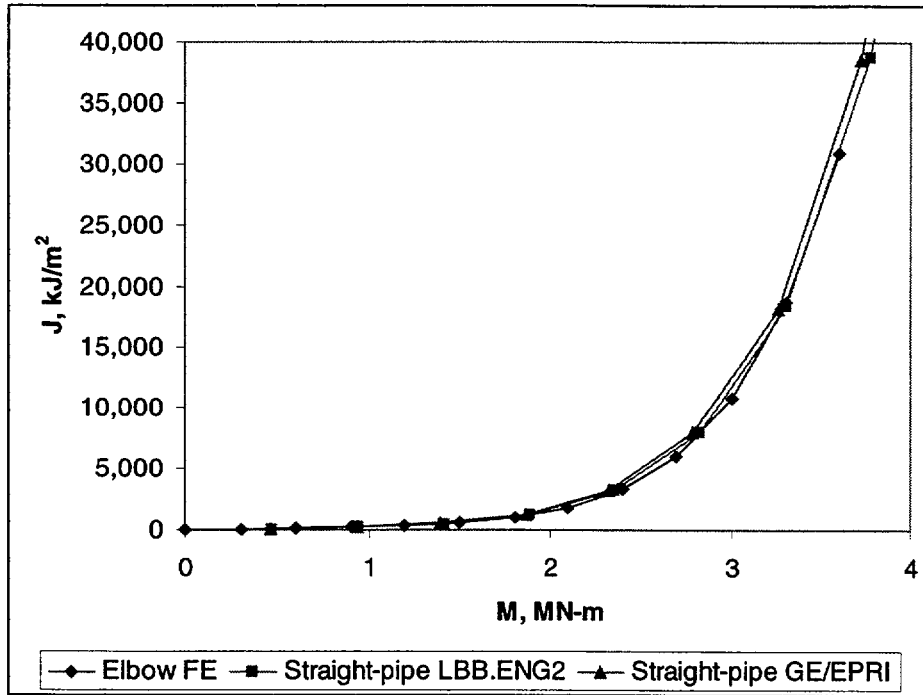


Figure E.20 Comparison of J versus moment curves for a circumferential through-wall crack in a straight pipe and centered on the extrados of an elbow with an  $R/t = 5$  and  $2\theta=90$  degrees

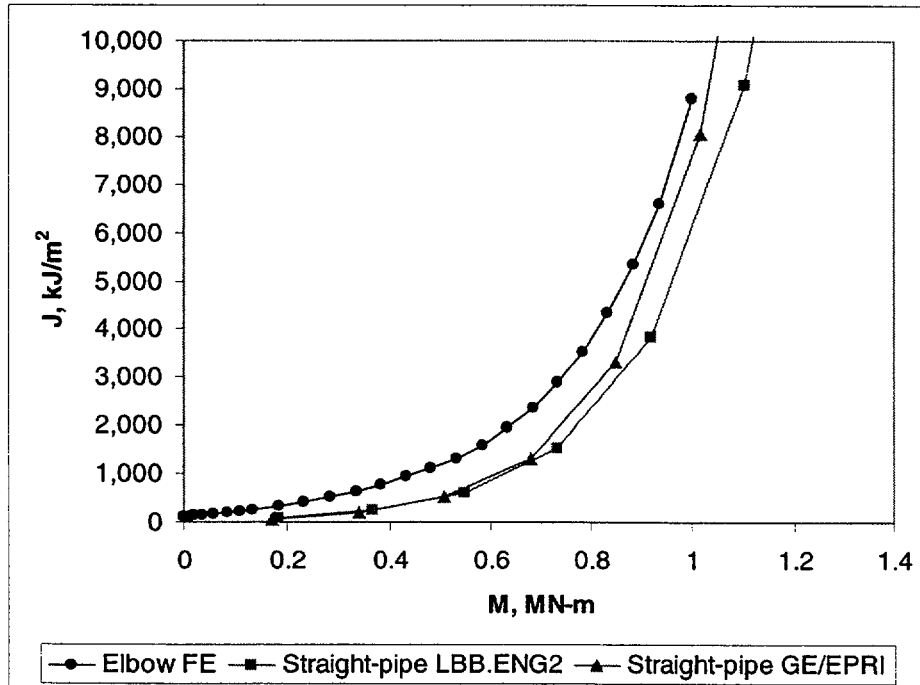


Figure E.21 Comparison of J versus moment curves for a circumferential through-wall crack in a straight pipe and centered on the extrados of an elbow with an  $R/t = 5$  and  $2\theta=180$  degrees

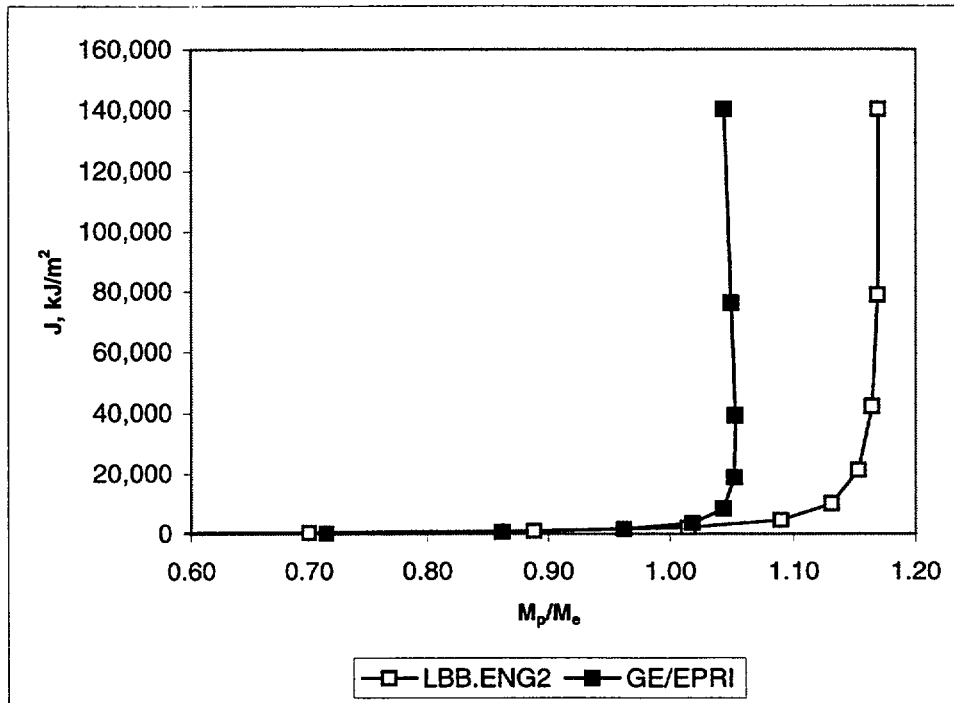


Figure E.22 Comparison of J versus moment ratios for a circumferential through-wall crack in a straight pipe and centered on the extrados of an elbow with an  $R/t = 20$  and  $2\theta=90$  degrees

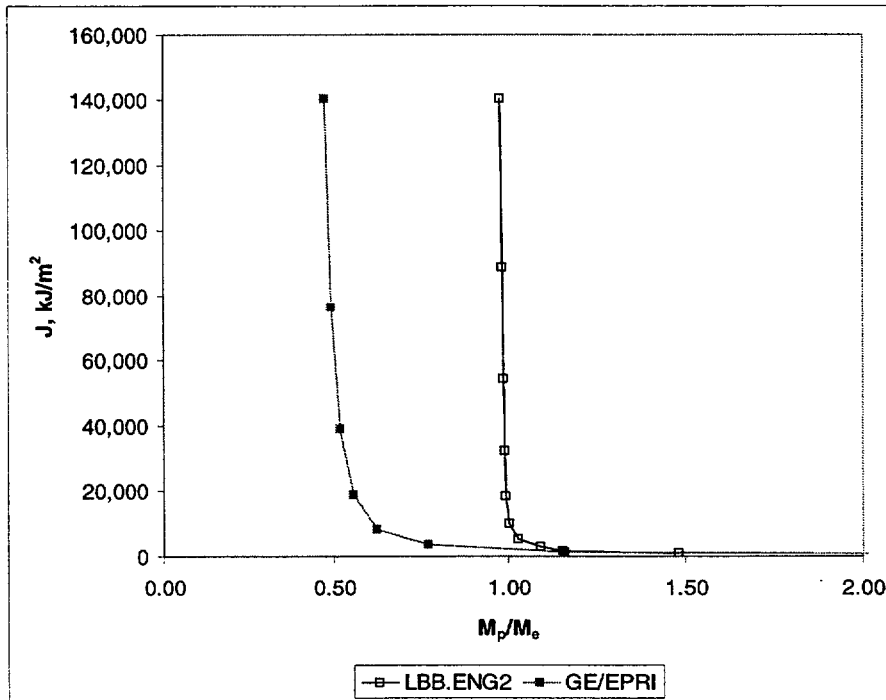


Figure E.23 Comparison of J versus moment ratios for a circumferential through-wall crack in a straight pipe and centered on the extrados of an elbow with an  $R/t = 20$  and  $2\theta=180$  degrees

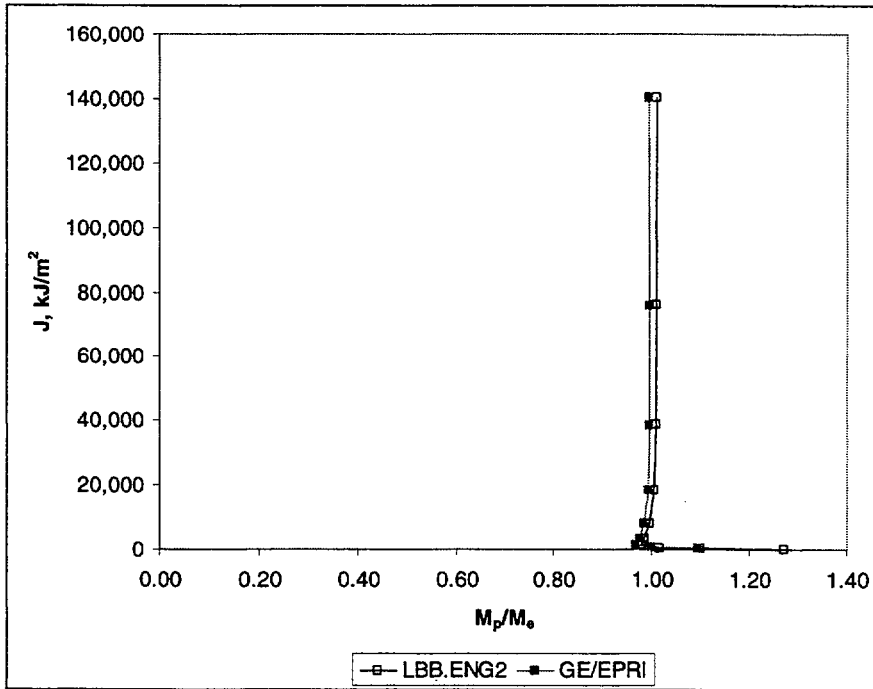


Figure E.24 Comparison of J versus moment ratios for a circumferential through-wall crack in a straight pipe and centered on the extrados of an elbow with an  $R/t = 5$  and  $2\theta=90$  degrees

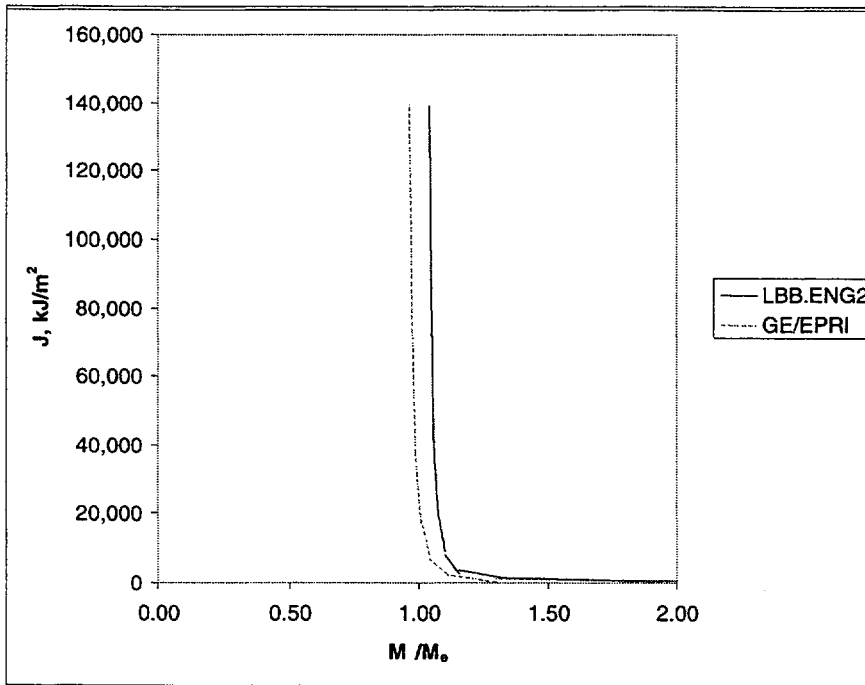


Figure E.25 Comparison of J versus moment ratios for a circumferential through-wall crack in a straight pipe and centered on the extrados of an elbow with an  $R/t = 5$  and  $2\theta=180$  degrees

The final step was to compare the constant moment ratio values from Figures E.22 to E.25 to the stress indices for the elbows. Since the elbow was under bending, the ASME  $B_2$  index was used. The  $B_2$  index is for primary bending stresses to avoid failure by collapse (using the design stress analysis definition of limit load). It should be noted that the elbow stress indices essentially gives a stress multiplier for the location in the piping product where the stresses are the highest. For the case of an elbow under bending, the stresses are the highest along the flank of the elbow normal to the axial direction. Equations E.24 and E.25 define the  $B_2$  stress index from Section III, Article NB-3683.7 of the ASME Boiler and Pressure Vessel Code.

$$B_2 = 1.3/h^{2/3}, B_2 \geq 1.0 \quad (\text{E.24})$$

Where,

$$h = tR_{cf}/R_m^2 \quad (\text{E.25})$$

These equations assume the elbows have a perfectly circular cross-section, which was a condition in the development of the FE elbow results.

The results of this comparison are shown in Figure E.26. If there is essentially no effect of the elbow curvature on the fracture behavior, then the moment ratios should be close to 1.0 for all  $B_2$  values. On the other hand, if there was a strong effect of the elbow curvature, then the moment ratios should be close to the 45-degree line in Figure E.26. As can be seen in Figure E.26, the values are all close to 1.0 indicating that for a circumferential through-wall flaw in an elbow that the straight-pipe solution could be used.

There was one data point that gave an  $M_{\text{pipe}}/M_{\text{elbow}}$  value of about 0.5. This was when the GE/EPRI solution was used for the case of a 180-degree flaw in pipe with an  $R/t$  of 20. However, we know that the solution in this case is not correct in NRCPIPE so that this data point can be disregarded. Consequently, the circumferential through-wall-flaw straight-pipe solution could be used in the new LBB Regulatory Guide for the fracture analyses of the case of a circumferential through-wall flaw in an elbow.

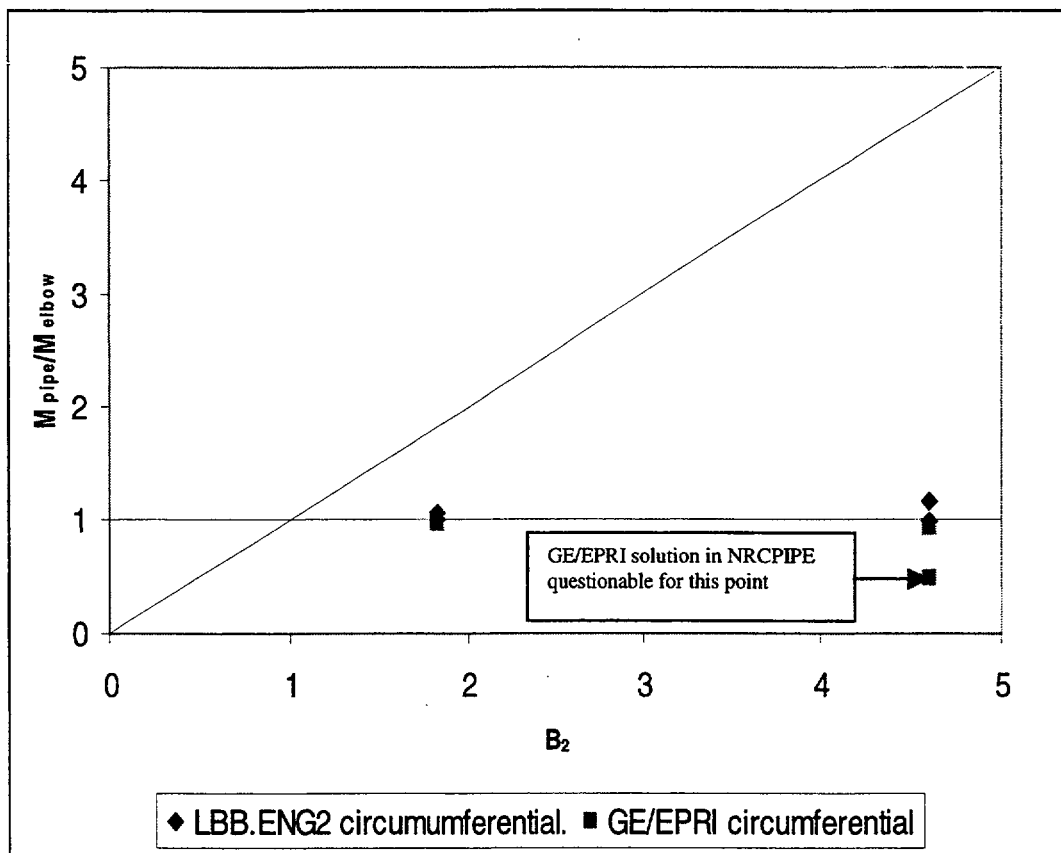


**Figure E.26 Ratio of circumferentially through-wall-cracked pipe-to-elbow moments for constant applied J values versus the ASME B<sub>2</sub> index for the elbow**

### E.8.2.3 Comparison of Axial Flank Through-Wall-Cracked Elbow and Straight-Pipe Solutions

To make this comparison, the J versus moment curves from both the straight-pipe and elbow solutions were compared in a similar manner as was done for the elbow circumferential crack case. Figures E.27 and E.28 show the results for the axial flank crack case with an R/t of 20 and total crack lengths of 15 and 30 degrees. Figures E.29 and E.30 show the results for the axial flank crack case with an R/t of 5 and total crack lengths (2θ) of 15 and 30 degrees.

In Figures E.27 to E.30, it can be seen that the elbow solutions give higher J values than the straight pipe solutions for the same moment. The GE/EPRI solution always gives a higher crack-driving force than the LBB.ENG2 analysis for the two straight-pipe solutions. This is consistent with past experience. The crack lengths are much shorter in these analyses than what was used in the circumferential cracked

elbows analysis, so that there was no problem with either straight-pipe solution in the NRCPIPE code.

The next step was to compare the ratio of the moments at the same J value. A graph of the moment ratio versus the J value is given for each case in Figures E.31 to E.34. Again note how the moment ratio reaches a constant value as the plastic solution of J dominates.

The final step was to compare the constant moment ratio values from Figures E.31 to E.34 to the B<sub>2</sub> stress indices for the elbows.

The results of this comparison are shown in Figure E.35. If there is essentially no effect of the elbow curvature on the fracture behavior, then the moment ratios should be close to 1.0 for all B<sub>2</sub> values. On the other hand, if there was a strong effect of the elbow curvature, then the moment ratios should be close to the 45-degree line in Figure E.35.

As can be seen in Figure E.35, the moment ratio values show that there is an effect of the elbow curvature on the crack-driving force for an axial through-wall crack on the flank of an elbow. A conservative option would be to divide the circumferential through-wall straight-pipe moment by the elbow  $B_2$  value for an axial through-wall flaw on the flank of the elbow. Alternatively, a linear correction such as

suggested by the lines in Figure E.35 could be used. Consequently, the moment from a circumferential through-wall-flaw straight-pipe solution (under pressure and bending) divided by the elbow  $B_2$  stress index could be used in the new LBB Regulatory Guide for the fracture analyses for the axial flank through-wall flaw case in an elbow.

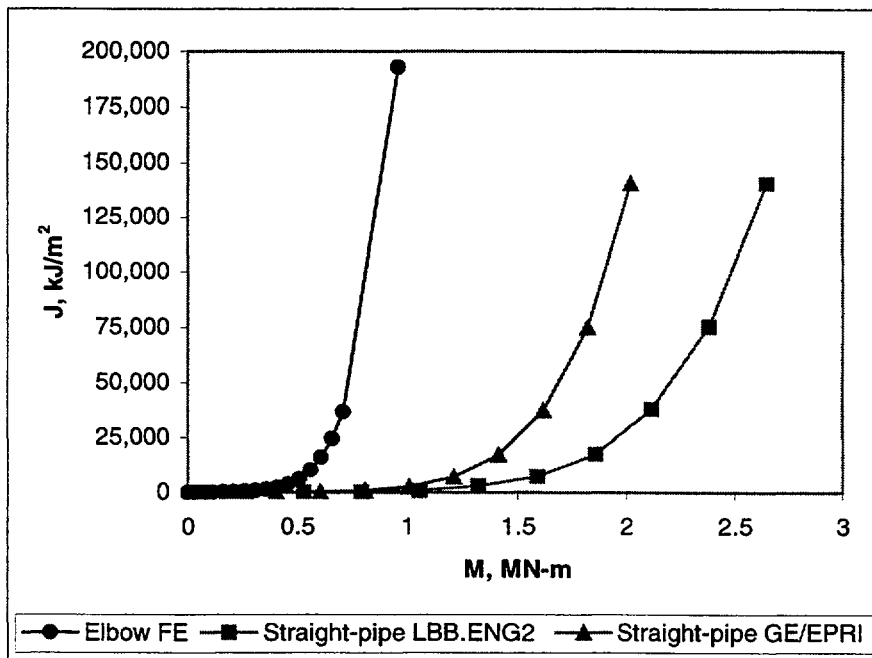


Figure E.27 Comparison of J versus moment curves for an axial through-wall crack in a straight pipe and an axial through-wall crack on the flank of an elbow with an  $R/t = 20$  and  $2\theta = 15$  degrees

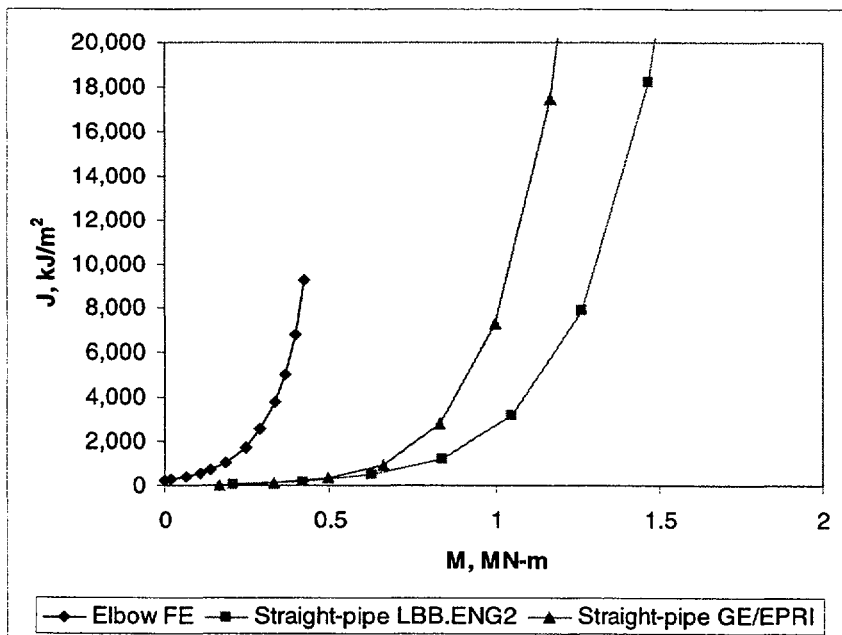


Figure E.28 Comparison of J versus moment curves for an axial through-wall crack in a straight pipe and an axial through-wall crack on the flank of an elbow with an  $R/t = 20$  and  $2\theta = 30$  degrees

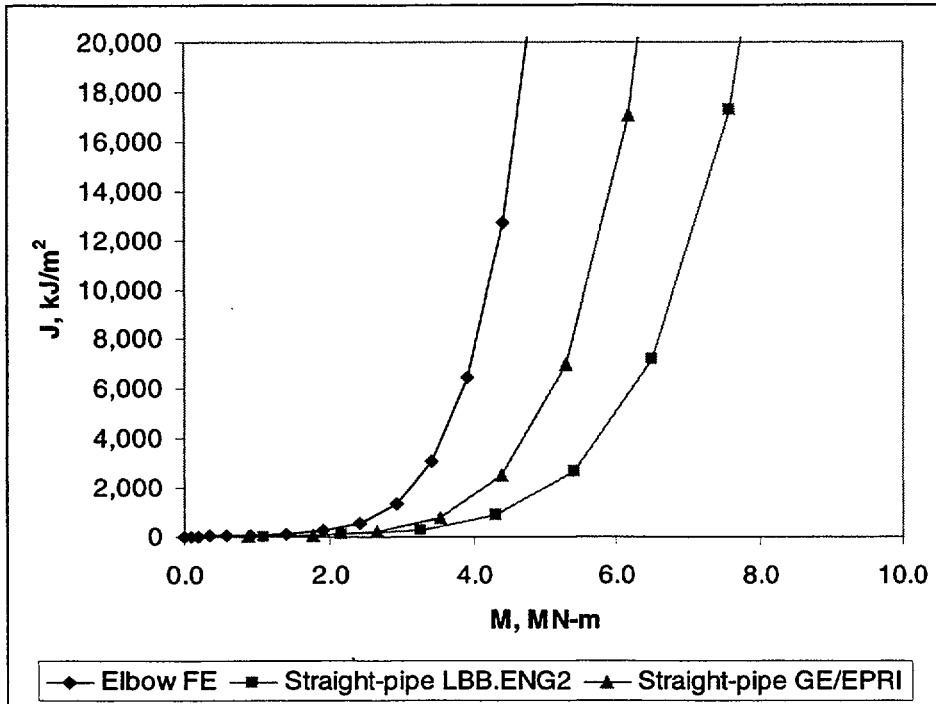


Figure E.29 Comparison of J versus moment curves for an axial through-wall crack in a straight pipe and an axial through-wall crack on the flank of an elbow with an  $R/t = 5$  and  $2\theta = 15$  degrees

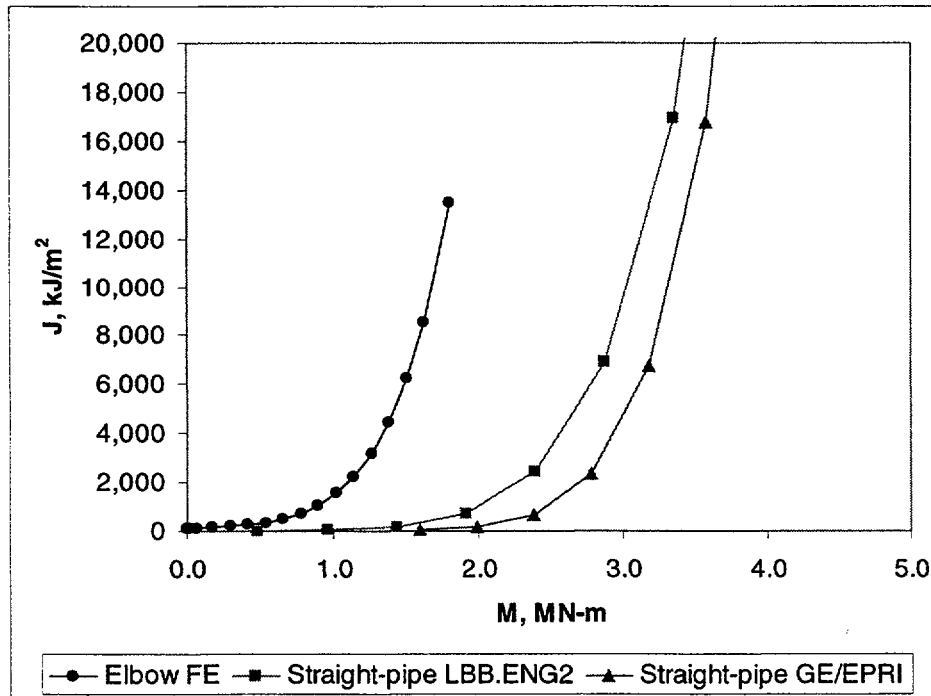
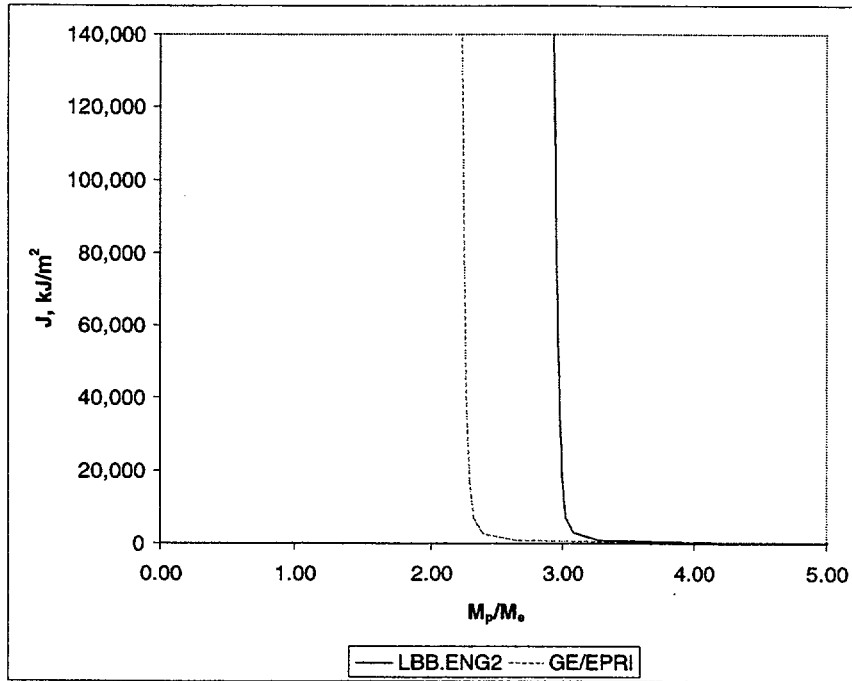
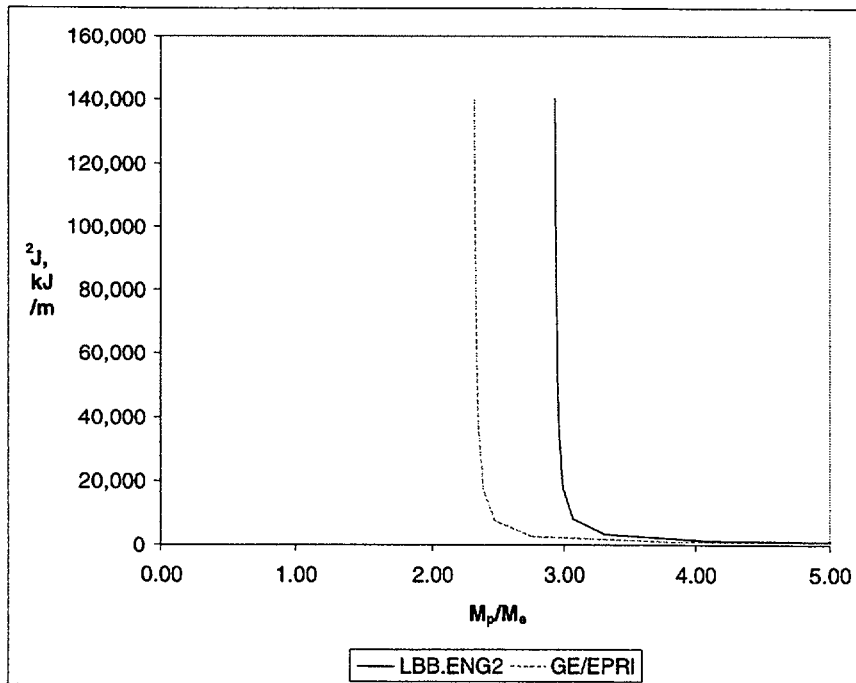


Figure E.30 Comparison of J versus moment curves for an axial through-wall crack in a straight pipe and an axial through-wall crack on the flank of an elbow with an  $R/t = 5$  and  $2\theta = 30$  degrees



**Figure E.31** Comparison of  $J$  versus moment ratios for an axial through-wall crack in a straight pipe and an axial through-wall crack on the flank of an elbow with an  $R/t = 20$  and  $2\theta = 15$  degrees



**Figure E.32** Comparison of  $J$  versus moment ratios for an axial through-wall crack in a straight pipe and an axial through-wall crack on the flank of an elbow with an  $R/t = 20$  and  $2\theta = 30$  degrees

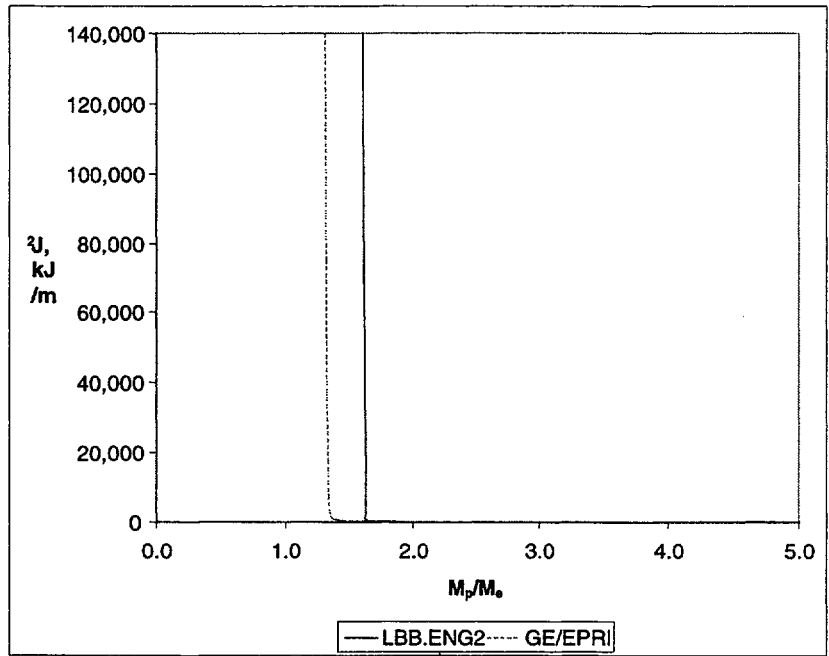


**Figure E.33** Comparison of J versus moment ratios for an axial through-wall crack in a straight pipe and an axial through-wall crack on the flank of an elbow with an  $R/t = 5$  and  $2\theta = 15$  degrees

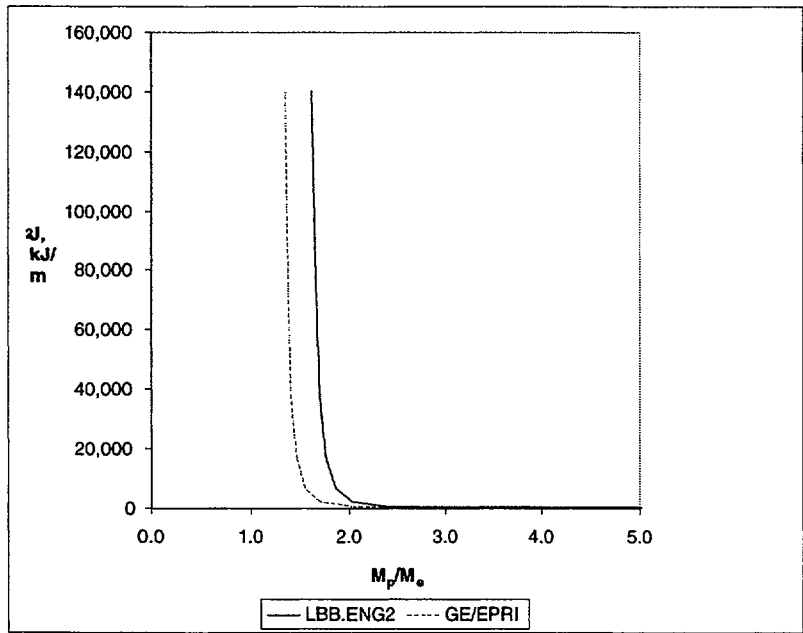


**Figure E.34** Comparison of J versus moment ratios for an axial through-wall crack in a straight pipe and an axial through-wall crack on the flank of an elbow with an  $R/t = 5$  and  $2\theta = 30$  degrees

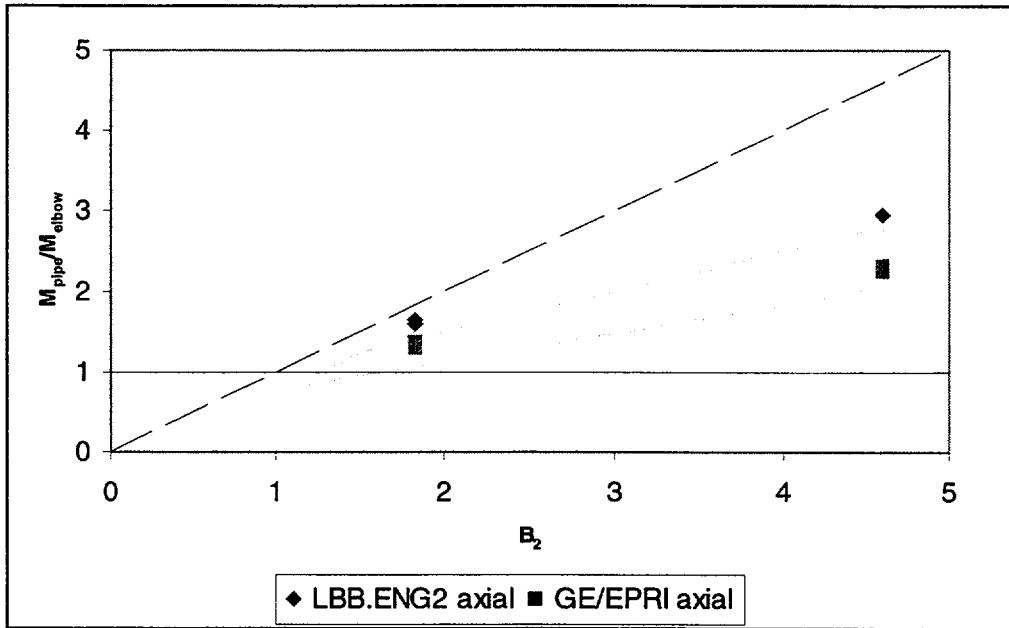


**Figure E.35** Ratio of axially through-wall-cracked pipe-to-elbow moments for constant applied J values versus the ASME B<sub>2</sub> index for the elbow

#### E.8.2.4 Comments on Crack-Opening

**Displacement** - The analyses conducted in Sections E.8.2.2 and E.8.2.3 for circumferential and axial through-wall cracks in elbows, respectively, were for determining the crack-driving force when plasticity occurs. This would be valid for the LBB fracture assessment under normal plus SSE loads. The crack-opening displacement, however, occurs under more elastic loading conditions. It was beyond the scope of this effort to make those comparisons, and using the same B<sub>2</sub> correction approach should be used with caution with the COD analysis.

**E.8.3 Summary and Conclusions** - The objective of this evaluation was to determine if a more simplified analysis could be established for axial and circumferential through-wall cracks in elbows under combined pressure and bending. This was assessed by using the elbow finite element analyses developed as part of this effort with a hoop stress loading of 1.0 S<sub>m</sub> for typical nuclear piping steels. The approach undertaken was to compare the ratio of the moments for the same size crack in an elbow and straight-pipe at the same applied J values. This was similar to efforts done for circumferential surface flaws in

elbows in the IPIRG-2 program. The following conclusions came from this analysis.

- The results of the analysis showed that a circumferential crack centered on the extrados of an elbow had the same crack-driving force under plastic conditions as a circumferential through-wall crack in a straight pipe. Hence, for the new LBB Reg. Guide, the simple straight-pipe solutions could be used for the fracture analysis of a circumferential through-wall crack in an elbow.
- The results of the analysis showed that an axial crack on the flank of an elbow had a higher crack-driving force under plastic conditions than a circumferential through-wall crack in a straight pipe. A conservative approach would be to use the straight-pipe solution, but divide the straight-pipe moment by the elbow B<sub>2</sub> index. This could readily be done in the new LBB Reg. Guide Level 1 or 2 analyses for the fracture analysis of an axial flank through-wall crack in an elbow.
- The COD evaluations were not conducted in this effort. Caution should be used in applying this same approach for the COD

values since the COD should be for elastic loading where the constant moment ratio that occurs under plastic conditions does not exist.

## E.9 References

- E.1 Mohan, R., Brust, F. W., Ghadiali, N. D., and Wilkowski, G. M., "Development of a J-Estimation Scheme for Internal Circumferential and Axial Surface Cracks in Elbows", NUREG/CR 6445, June, 1996.
- E.2 Kumar, V., German, M., and Shih, E., "An Engineering Approach for Elastic-Plastic Fracture Analysis", EPRI Report No. NP-1931, July 1981.
- E.3 Kumar, V., German, M., Wilkening, Andrews, W., deLorenzi, H., and Mowbray, D., "Advances in Elastic-Plastic Analysis" EPRI Final Report NP-3607, August 1984.
- E.4 Kumar, V., and German, M. D., "Elastic-Plastic Fracture Analysis of Through-Wall and Surface Flaws in Cylinders", EPRI Final Report NP-5596, January, 1988.
- E.5 P. Gilles and F. W. Brust, "Approximate Fracture Methods for Pipes, Part I, Theory", Nuclear Engineering and Design, Vol. 127, pp. 1-17, 1991.
- E.6 P. Gilles, K. S. Chao, and F. W. Brust, "Approximate Fracture Methods for Pipes, Part II, Applications," Nuclear Engineering and Design , Vol. 127, pp. 19-31, 1991.
- E.7 Scott, P. M., and Ahmad, J., "Experimental and Analytical Assessment of Bending Circumferentially Surface-Cracked Pipes Under Bending", NUREG/CR-4872, April 1987.
- E.8 Rahman, S. and Brust, F. W., "Approximate Methods for Predicting J-integral of a Circumferentially Surface-Cracked Pipe Subject to Bending," International Journal of Fracture, Vol. 85, No. 2, October 1997, pp. 111-130.
- E.9 Brust, F., Scott, P., Rahman, S., Ghadiali, N., Kilinski, T., Francini. R., Krishnaswamy, P., and Wilkowski, G., "Assessment of Short Through-Wall Cracks in Pipes - Experiments and Analyses," Topical Report, NUREG/CR-6235, U. S. Nuclear Regulatory Commission, Washington, DC, April 1995
- E.10 Krishnaswamy, P., Scott, P., Choi, Y., Mohan, R., Rahman, S., Brust, F., and Wilkowski, G., "Fracture Behavior of Short Circumferentially Surface-Cracked Pipe," Topical Report, NUREG/CR-6298, U. S. Nuclear Regulatory Commission, Washington, DC, November 1995.
- E.11 Rahman, S., and Brust, F. W., "Elastic-Plastic Fracture of Circumferential Through-Wall Cracked Pipe Welds Subject to Bending", ASME Journal of Pressure Vessel Technology, Vol. 114, pp 410-416, November, 1992.
- E.12 Mohan, R., Krishna, A., Brust, F. W., and Wilkowski, G., "J-estimation Scheme for Internal Circumferential and Axial Surface Cracks in Pipe Elbows," ASME J. of Pressure Vessel Technology, Vol. 120, Nov. 1998.
- E.13 Kilinski, T., and others, "Fracture Behavior of Circumferentially Surface-Cracked Elbows," NUREG/CR-6444, December 1996.

**BIBLIOGRAPHIC DATA SHEET**

(See instructions on the reverse)

1. REPORT NUMBER  
(Assigned by NRC, Add Vol., Supp., Rev.,  
and Addendum Numbers, if any.)

NUREG/CR-6765

2. TITLE AND SUBTITLE

Development of Technical Basis for Leak-Before-Break Evaluation Procedures

3. DATE REPORT PUBLISHED

MONTH | YEAR

May | 2002

4. FIN OR GRANT NUMBER

W6854

5. AUTHOR(S)

P.M. Scott(1), R.J. Olson(1), G.M. Wilkowski(2)

6. TYPE OF REPORT

7. PERIOD COVERED (Inclusive Dates)

12/97 - 2/02

8. PERFORMING ORGANIZATION - NAME AND ADDRESS (If NRC, provide Division, Office or Region, U.S. Nuclear Regulatory Commission, and mailing address; if contractor, provide name and mailing address.)

(1) Battelle  
505 King Avenue  
Columbus, OH 43201

(2) Engineering Mechanics Corporation of Columbus  
3518 Riverside Drive, Suite 202  
Columbus, OH 43221

9. SPONSORING ORGANIZATION - NAME AND ADDRESS (If NRC, type "Same as above"; if contractor, provide NRC Division, Office or Region, U.S. Nuclear Regulatory Commission, and mailing address.)

Division of Engineering Technology  
Office of Nuclear Regulatory Research  
US Nuclear Regulatory Commission  
Washington DC 20555-0001

10. SUPPLEMENTARY NOTES

C. Santos, NRC Project Manager

11. ABSTRACT (200 words or less)

In the mid 1980's the USNRC began to accept LBB for large-diameter, high quality piping systems as a means of enhancing safety. To aide NRC staff in evaluating LBB submittals, a draft Standard Review Plan (SRP) entitled "Leak-Before-Break Evaluation Procedures" was published in 1987. Because of ongoing research, this draft SRP was never published in final form. Now that research is nearly complete, the NRC has decided to develop and issue a LBB Regulatory Guide. A final version of SRP 3.6.3 will follow publication of the Regulatory Guide. These documents will address updated, acceptable LBB analyses. Consequently, in 1997 the NRC contracted with Battelle to conduct a study entitled "Technical Support for Regulatory Guide on LBB Evaluation Procedures". During this study, a three-tiered approach to LBB was developed. Level 1 is the simplest level of assessment, designed to provide a conservative LBB evaluation. Level 2 is similar to the draft SRP procedures, except that it incorporates enhancements in technology that have resulted from recent research. Level 3 is the most complex level of assessment, where nonlinear stress analyses are used to take advantage of margins that exist when one invokes elastic analysis on a nonlinear problem. Case studies of actual piping systems were conducted to ascertain the relative conservatism of the three levels of assessment.

12. KEY WORDS/DESCRIPTORS (List words or phrases that will assist researchers in locating the report.)

Pipe, Fracture Mechanics, Leak-Before-Break

13. AVAILABILITY STATEMENT

unlimited

14. SECURITY CLASSIFICATION

(This Page)

unclassified

(This Report)

unclassified

15. NUMBER OF PAGES

16. PRICE



Federal Recycling Program

**UNITED STATES  
NUCLEAR REGULATORY COMMISSION  
WASHINGTON, DC 20555-0001**

---

**OFFICIAL BUSINESS  
PENALTY FOR PRIVATE USE, \$300**